DETAILED NON-NEWTONIAN FLOW BEHAVIOUR MEASUREMENTS USING A PULSED ULTRASOUND VELOCIMETRY METHOD: EVALUATION, OPTIMISATION & APPLICATION

REINHARDT KOTZÉ

CAPE PENINSULA UNIVERSITY OF TECHNOLOGY

NOVEMBER 2011

DETAILED NON-NEWTONIAN FLOW BEHAVIOUR MEASUREMENTS USING A PULSED ULTRASOUND VELOCIMETRY METHOD: EVALUATION, OPTIMISATION & APPLICATION

by

REINHARDT KOTZÉ

Thesis submitted in fulfilment of the requirements for the degree

Doctor of Technology: Electrical Engineering

in the Faculty of Engineering

at the Cape Peninsula University of Technology

Supervisor: Prof Rainer Haldenwang
Co-supervisors: Dr Johan Wiklund & Prof Richardt Wilkinson

Cape Town
November 2011

DECLARATION

I, Reinhardt Kotzé, declare that the contents of this thesis represent my own unaided work, and that the thesis has not previously been submitted for academic examination towards any qualification. Furthermore, it represents my own opinions and not necessarily those of the Cape Peninsula University of Technology.

Signed **Date**

DETAILED NON-NEWTONIAN FLOW BEHAVIOUR MEASUREMENTS USING A PULSED ULTRASOUND VELOCIMETRY METHOD: EVALUATION, OPTIMISATION & APPLICATION

Reinhardt Kotzé

ABSTRACT

Ultrasonic Velocity Profiling (UVP) is both a method and a device to measure an instantaneous one-dimensional velocity profile along a measurement axis by using Doppler echography. UVP is an ideal technique since it is non-invasive, works with opaque systems, inexpensive, portable and easy to implement relative to other velocity profile measurement methods. Studies have suggested that the accuracy of the measured velocity gradient close to wall interfaces need to be improved. The reason for this is due to, depending on the installation method, distortion caused by cavities situated in front of ultrasonic transducers, measurement volumes overlapping wall interfaces, refraction of the ultrasonic wave as well as sound velocity variations. A new ultrasonic transducer, which incorporates a delay line material optimised for beam forming could reduce these problems (Wiklund, 2007). If these could be addressed, UVP could be used for the measurement of velocity profiles in complex geometries (e.g. contractions, valves, bends and other pipe fittings) where the shape of the velocity profile is critical to derive models for estimating fluid momentum and kinetic energy for energy efficient designs.

The objective of this research work was to optimise the UVP system for accurate complex flow measurements by evaluating a specially designed delay line transducer and implementing advanced signal processing techniques.

The experimental work was conducted at the Material Science and Technology (MST) group at the Cape Peninsula University of Technology (CPUT). This work also formed part of a collaborative project with SIK – The Swedish Institute for Food and Biotechnology. Acoustic characterisation of the ultrasonic transducers using an advanced robotic setup was done at SIK. Different concentrations of the following non-Newtonian fluids exhibiting different rheological characteristics were used for testing: carboxymethyl cellulose (CMC) solutions, kaolin and bentonite suspensions. Water was used for calibration purposes.

A specially designed delay line transducer (Signal Processing SA, Switzerland) was acoustically characterised and evaluated. Velocity profiles measured using the delay line transducer, were initially distorted due to the effect of finite sample volume characteristics and propagation through the delay line material boundary layers. These negative effects were overcome by measuring physical properties of the ultrasonic beam and implementing a newly developed deconvolution procedure. Furthermore, custom velocity estimation algorithms were developed, which improved the time resolution and penetration depth of the UVP system.

The optimised UVP system was evaluated and compared to standard transducers in three straight pipes (16, 22.5 & 52.8 mm) and two complex geometries (50% open diaphragm valve and 300 mm rectangular open channel). Velocity data obtained using the optimised UVP system showed significant improvement close to wall interfaces where the velocity gradients are high. The new transducer technology and signal processing techniques reduced previously mentioned problems and are now more suitable for industrial process monitoring and control.

A new non-intrusive method (UVP-FD) for determining the rheology of a fluid flowing in a flume has also been developed. By using UVP in combination with a Flow Depth (FD) measurement the complete flow curve can be obtained in-line from a single measurement. In-line rheological characterisation can however also be achieved in a straight pipe by using the UVP and Pressure Difference (UVP-PD) method. The optimised UVP system made it possible to obtain accurate rheology by ensuring a fixed wall interface position. Results were compared with data obtained from conventional off-line rheometry and in-line tube viscometry and results were within 15% of each other. The combination of the signal processing techniques and new transducer design has shown significant potential in the development of a new in-line rheometer that can be used for quality and process control in a wide range of industrial applications.

ACKNOWLEDGEMENTS

I wish to thank:

- **Prof Rainer Haldenwang and Dr Johan Wiklund, my supervisors, who guided me through the whole research process with much encouragement, wisdom and enthusiasm;**
- **Richard du Toit, Material Science and Technology (MST) laboratory manager, is acknowledged for his support with all the laboratory equipment and setup needed for this research;**
- **Dr Jean-Claude Willemetz, founder of Signal Processing SA, the specially designed and manufactured ultrasonic transducers formed the basis of this research project;**
- **Magnus Holmbom, for his assistance with experimental tests at the Flow Process Research Centre (FRPC);**
- **Naziem George, for his support on rotary viscometry;**
- **Dr Veruscha Fester, for her assistance with non-Newtonian flow in diaphragm valves;**
- **Andre du Plessis, for the many hours spent on the 3D design of the diaphragm valves and ultrasonic transducer housing ports;**
- **The Adaptronics Advanced Manufacturing Technology Laboratory (AMTL) at Cape Peninsula University of Technology (CPUT) is acknowledged for manufacturing and installation of the diaphragm valve;**
- **Joachim Macke is acknowledged for the design and construction of the ultrasound flow adapters and pressure adapters;**
- **The Material Science and Technology (MST) group at the Cape Peninsula University of Technology (CPUT) where I was given the opportunity to conduct the research;**
- **The Centre for Instrumentation Research (CIR), for their assistance with electronic instrumentation;**
- **SIK - The Swedish Institute for Food and Biotechnology is gratefully acknowledged for scientific collaboration;**
- **Wi-Ka Mekaniska are acknowledged for assistance with design and manufacturing of the flow cells;**
- **Anders Petterson, for assistance with the high precision robotic set-up at SIK - The Swedish Institute for Food and Biotechnology;**
- **The Cape Peninsula University of Technology (CPUT) and Vetenskapsrådet – The Swedish Research Council, Research Links, for funding;**
- **My parents for their continuous support during all these years. Their love and belief in me helped me not to give up at the difficult moments.**
- **My girlfriend, for her love and support; and**
- **My colleagues and everybody who somehow contributed to this work are also acknowledged.**

The financial assistance of the National Research Foundation towards the research is acknowledged. Opinions expressed in this thesis and the conclusions arrived at are those of the author and are not necessarily to be attributed to the National Research Foundation.

DEDICATION

To my father, my inspiration and my teacher

To my mother, always supportive and understanding

To my eldest brother, who always makes me laugh

To my only sister, the angel of our family

To my three youngest brothers, the joy of our family

With love to all of you

The ideal engineer is a composite ... He is not a physicist, he is not a mathematician, he is not a sociologist or a writer; but he may use the knowledge and techniques of any or all of these disciplines in solving engineering problems.

N.W. DOUGHERTY

Vertrou op die Here met alles wat jy het. Moenie staat maak op jou eie insigte nie. Vra na die wil van God in alles wat jy doen. Hy sal die regte pad vir jou wys.

SPREUKE 3:5-6

With men things are possible
With God all things are possible

NOMENCLATURE

Symbol	*Description*	*Unit*
A	cross sectional area	m^2
A_{max}	wave amplitude	mm
c	sound velocity	m/s
c_c	propagation speed in medium	m/s
D	internal pipe diameter	m
Δd	moving distance along US beam or measuring line	mm
$\mathcal{F}$	Fourier Transform	
$\mathcal{F}^{-1}$	inverse Fourier transform	
f	fanning friction factor	
f_d	Doppler shift frequency	Hz
f_e, f_o	frequency of emitted ultrasound wave	Hz
f_r	frequency of reflected ultrasound wave	Hz
f_0	resonant frequency	Hz
G	pseudo shear rate	1/s
g	gravitational acceleration	m/s^2
H	flow depth / distance between two transducers	m
h	flume flow depth	m
h_f	frictional head	m
I	US intensity	W/cm^2
I	in-phase echo data	
i	sample volume intensity function	

K	fluid consistency index	Pa.s
k	(angular) wave number	
k	inverse of spatial coordinate r	
k	pipe roughness	m
L	pipe length, characteristic length	m
L_c	thickness of piezoelectric crystal	m
N	number of area segments / error quantities	
N_f	near-field distance of US transducer	m
n	flow behaviour index	
P, p	pressure, acoustic pressure	Pa
PRF	Pulse Repetition Frequency	Hz
Q	volumetric flow rate	m^3/s
Q	quadrature echo data	
R	pipe radius (inner)	m
R_1, R_2	maximum and minimum radius of hyperbolic contraction	m
R_h	hydraulic radius	m
R_{plug}	plug radius	m
Re	Reynolds number	
r	radial position	m
S	power spectrum	
Δs	moving distance along mainstream direction	mm
T	Temperature	°C
T, t	Time	s
T_{prf}	time between two US emissions	s
t_d	time delay	s

u, v	point velocity	m/s
V	average velocity	m/s
V_n	velocity across area segment	m/s
V_{Tr}	target velocity	mm/s
V_t	velocity in direction of US beam or measuring line	mm/s
V_m	measured velocity profile as function of k	
V_z	velocity distribution across flume flow depth	m/s
v_m	measured velocity profile	m/s
v_t	true velocity profile	m/s
x	distance	m
z	on-axis co-ordinate of US beam	m
z	specific acoustic impedance	$\mathrm{gr/(cm^2 s)}$

Greek Symbols

α_0	spatial attenuation coefficient	dB/cm
$\dot{\gamma}$	shear rate	s^{-1}
$\dot{\gamma}_{wN}$	pseudo wall shear rate	s^{-1}
γ_0	US beam divergence half-angle	degrees
Δ	increment	
δ_0	temporal attenuation coefficient	1/s
θ	incline, Doppler angle	degrees
κ	adiabatic compressibility	
λ	wavelength	m
μ	Newtonian or apparent viscosity	Pa.s
ρ	material, fluid or slurry density	$kg.m^{-3}$
p_0	reference acoustic pressure of US sensor	Pa
τ	shear stress	Pa
τ_w, τ_o	wall shear stress	Pa
τ_y	yield stress	Pa
ω	velocity function, angular velocity, angular frequency	$rad.s^{-1}$

Subscripts

MAX, max	maximum
x, y, z	Cartesian / spatial coordinates
0	state of the medium at rest, mean value

ABBREVIATIONS AND ACRONYMS

ActiveX Library:	3rd Party software for communication with UVP-DUO
ADC:	Analog-to-Digital Converter
AToM:	Acoustic Time of Flight Measurement
CFD:	Computational Fluid Dynamics
CMC:	Carboxymethyl cellulose
DMEA:	Demodulated Echo Amplitude (commonly known as I-Q data)
DSP:	Digital Signal Processor
ERT:	Electrical Resistance Tomography
FFT:	Fast Fourier Transform
FD:	Frequency Domain
LDA/LDV:	Laser Doppler Anemometry / Velocimetry
MRI:	Magnetic Resonance Imaging
MST:	Material Science and Technology group, Cape Town, South Africa
PC:	Personal Computer
PD:	Pressure Difference
PRF:	Pulse Repetition Frequency
SIK:	The Swedish Institute for Food and Biotechnology, Gothenburg, Sweden
SNR:	Signal-to-Noise Ratio
SPSA:	Signal Processing SA, Lausanne, Switzerland
TD:	Time Domain
TGC:	Time Gain Control
US:	Ultrasound
UVP-DUO:	UVP monitor supplied by Met-Flow SA, Lausanne, Switzerland
UVP:	Ultrasonic Velocity Profiling
UVP-PD:	Ultrasonic Velocity Profiling with Pressure Difference – A methodology for in-line rheometry

TERMS AND CONCEPTS CITED

Acoustic impedance: The ratio of acoustic excess pressure to the particle velocity. It is defined as $z = \rho \cdot c$.

Aliasing: Artifact that occurs when the measured Doppler-induced frequency shift exceeds one half of the UVP instrument's pulse repetition frequency (PRF).

Doppler effect: The apparent change in frequency and wavelength of a wave that is perceived by an observer moving relative to the source of the waves.

Doppler angle: In this research work the Doppler angle is defined as the physical angle between the ultrasonic beam axis and one-dimensional direction of the fluid flow.

Friction factor: There are two kinds of friction factors: The fanning friction factor is proportional to shear stress at pipe/conduit wall as number of velocity heads and is used in momentum transfer in general and turbulent flow calculations, in particular. It is equivalent to (1/4) the Darcy friction factor.

Laminar flow: Non turbulent streamline flow in parallel layers.

Turbulent flow: Flow in which the velocity at any point varies erratically.

Newtonian fluid: Any fluid that has a directly proportional relationship between shear stress and shear rate. Water is an example of a Newtonian fluid.

Non-Newtonian fluid: Any fluid whose flow properties differ in any way from those of Newtonian fluids. Most commonly the viscosity of non-Newtonian fluids is not independent of shear rate or shear rate history.

Pseudoplastic fluid: Any fluid which shows a decrease in apparent viscosity with increasing shear rate; also known as a shear-thinning fluid.

Reynolds number: The ratio between viscous and inertial forces is proportional to the Reynolds number. The number is expressed in terms of the density, velocity, characteristic length and the viscosity of the fluid. This number is also used to define whether a fluid is laminar or turbulent.

Shear Stress: Shear stress is a stress state where the shape of a material tends to change (usually by "sliding" forces – torque by transversely-acting forces) without particular volume change.

Spatial Resolution: Distance between the center of adjacent measuring volumes or channels inside a measuring window.

Transducer: A device that converts one type of energy to another, or responds to a physical parameter. A transducer is, in its fundamental form, a passive component. If the component is electrical, it generally has two electrical terminals.

Transition: The region or process acting between the laminar and turbulent flow regimes.

Time Resolution: Sampling time of one velocity profile measurement, which is directly influenced by the number of pulse repetitions per profile.

Viscosity: A measure of the resistance to flow of a fluid under an applied force.

TABLE OF CONTENTS

APPENDIX B

LIST OF FIGURES

LIST OF TABLES

CHAPTER ONE

INTRODUCTION

CHAPTER ONE

INTRODUCTION

1.1 BACKGROUND

Flow through complex geometries are important problems in fluid engineering because they are integral parts and occur frequently in pipeline systems. In order to derive models for estimating fluid momentum and kinetic energy in complex geometries, the shape of the velocity profile is critical in determining accurate quantities. In some applications, such as flow through pipe fittings, abrupt contractions and enlargements, theoretical velocity profiles in combination with mathematical models have thus far been used to determine fluid momentum, kinetic energy and loss coefficients. From these models and depending on the application, design equations are produced for practical implementation within the industry, but are not very accurate for highly-concentrated, non-Newtonian fluids. Computational Fluid Dynamics (CFD) is a tool for developing theoretical velocity profiles and models within complex geometries. However, the only way to verify the accuracy of these theoretical models is to physically measure velocity profiles in these complex geometries and compare results to theoretical predictions.

The fact that the fluids or slurries used in industry are normally highly-concentrated and opaque, effectively narrows down the variety of velocity profile measurement techniques, as these instruments are normally based on laser or visible light methods, such as Laser Doppler Anemometry (LDA). Magnetic Resonance Imaging (MRI) is a highly accurate and versatile technique, but the experimental apparatus are expensive, difficult to implement in industry and require highly trained staff to effectively utilise the technique in order to study complex flow patterns. Ultrasonic Velocity Profiling (UVP) is an ideal technique since it is non-invasive (to a certain extent) and it is easy to implement relative to MRI and LDA.

The rheological characterisation of fluids is an important issue that has a direct effect on the effectiveness of flow predictions. In-line rheological characterisation is often achieved by using tube viscometry where the volumetric flow rate and the pressure drop are measured and used to calculate the viscosity at a single shear rate, i.e. a

point-wise measurement. In-line rheological characterisation can however also be achieved by using Ultrasonic Velocity Profiling (UVP) in combination with Pressure Difference (PD) measurements to obtain the complete flow curve from a single measurement. A complete methodology for UVP-PD in-line measurements have recently been proposed and described e.g. by Birkhofer (2007), Wiklund (2007), Wiklund *et al.* (2007), Birkhofer *et al.* (2008), Wiklund and Stading (2008); and Wiklund *et al.* (2010). Recently, Kotzé *et al.* (2008) investigated the capabilities and limitations of this method for different concentrations of non-transparent, highly concentrated non-Newtonian model mining slurries and found that this methodology can be used effectively for in-line measurement of rheological parameters. However, the accuracy of these parameters is largely dependent on the shape and magnitude of measured velocity profiles, especially close to pipe wall interfaces, where the velocity gradient is usually high. More work is thus needed, especially on the ultrasonic transducer side, in order to improve the in-line rheometric method for future industrial applications.

This thesis focuses on the capabilities and limitations of the UVP system for measurement of detailed non-Newtonian flow behaviour in different geometries and on improving the accuracy of UVP measurements by using new generation ultrasonic transducers as well as advanced signal processing techniques.

1.2 STATEMENT OF THE PROBLEM

In pulsed ultrasound velocimetry, attenuation, absorption and multiple scattering of ultrasound can lead to reduced penetration depth and errors near pipe walls. The main problem with reduced penetration depth is the loss of spatial resolution when trying to increase the measurement distance. In order to reduce the effect of attenuation, ultrasonic transducers are often installed with direct contact to the fluid. To avoid measurements within the near field the transducers are often pulled back a few millimetres into a small cavity within the pipe wall. The cavity in the pipe in front of the transducer thus leads to additional errors close to the pipe wall, which influences the shape of the measured velocity profile.

The magnitude of estimated velocities using ultrasound Doppler based methods are largely dependent on the angle of observation or Doppler angle. When non-invasive measurements are considered, ultrasonic propagation at the boundary between two materials must be analysed. At each wall interface the ultrasonic beam will reflect and diffract, depending on the acoustic properties of the layer material. Thus the direction of the ultrasonic beam or measurement axis has changed according to Snell's law and therefore a significant error is introduced in the estimation of radial point velocities. Also, when the ultrasonic wave crosses wall interfaces of different acoustic properties, the physical beam shape will also change, which further influences the detection of an accurate velocity distribution along the measurement axis. The velocity of sound parameter in the fluid of interest is equally important for accurate measurement of velocity profiles. Distances between transducers need to be calibrated accurately and can become very complicated when measuring through different materials. Flow adapter setups with transducers installed in direct contact with the test fluid may fail due to particle build up inside the cavities which contain the near-field distance. This can lead to density changes and as a result inaccurate velocity of sound measurements.

In pulsed ultrasound systems, returning echo is sampled at specific time intervals corresponding to a certain depth from the transducer, which are commonly known as channels or gates. The sample volume size or area where the velocity distribution is detected, is an important parameter. Any flow particles passing through this region produce ultrasonic echoes (signals) which are detected by the receiver. The received signal is a spectrum of frequencies containing Doppler shifts of passing particles. The three-dimensional sample volume geometry and intensity are important as they influence the spectral content of the back-scattered signal and thus the accuracy of velocity estimation. Also, when considering velocity profile measurements in complex geometries, knowledge of the physical ultrasonic beam geometry and acoustic pressure distribution is important as it may cross wall interfaces which will introduce significant errors in velocity estimation at those particular points.

1.3 OBJECTIVES

The main objective of this research project was to improve the capabilities and limitations of the UVP system for accurate measurement of velocity profiles in complex geometries. This was achieved by implementing newly designed ultrasonic transducers and advanced signal processing techniques. Further objectives were to optimise the UVP-PD in-line rheometric technique using the improved UVP system and verify results with that obtained from conventional tube and rotational viscometry.

1.4 METHODOLOGY AND THESIS OUTLINE

To reach the objectives, the following research methodology was followed. A UVP technique was used to measure velocity profiles of non-Newtonian fluids in various complex geometries during this research. The Met-Flow SA UVP-DUO monitor (supplied by the MST group) from Met-Flow SA, Lausanne, Switzerland was used in this research. Newly designed ultrasonic transducers by Signal Processing SA, Switzerland were tested and compared against commercial transducers (Imasonic, Bensecon, France) with emitting frequency of 4 MHz. The new transducers incorporate a special material for ultrasonic beam forming (called a delay line, discussed in Chapter 3), which is in flush with the pipe wall and was used to improve the accuracy of near pipe wall measurements. A collaborative project with SIK – The Swedish Institute for Food and Biotechnology, Gothenburg, Sweden, was established between January 2009 and December 2011. This is since SIK is equipped with an advanced robotic set-up for acoustic characterisation of ultrasound transducers including Doppler needle and string phantoms as well as various UVP-PD flow loops. Some of the experimental work was thus conducted at SIK.

Furthermore, the UVP technique was used in combination with a pressure difference method (PD) to establish rheological parameters of the non-Newtonian fluids used. Conventional methods such as off-line rotary viscometry and tube viscometry were used to verify results determined by the UVP-PD method. The UVP-PD methodology was fitted to a tube viscometer so that the fluids tested can be analysed simultaneously for accurate readings. Different concentrations of the following non-Newtonian fluids were used for testing: carboxymethyl cellulose (CMC) solutions, characterised as a power-law / pseudoplastic fluid; kaolin suspensions characterised as a Herschel-Bulkley / yield-pseudoplastic fluid and bentonite suspensions characterised as a

Bingham plastic fluid. Water was used for calibration purposes. The experimental work was conducted at the Material Science and Technology (MST) group at the Cape Peninsula University of Technology (CPUT) in Cape Town.

The overall approach is displayed in flow-chart format in Figure 1.1.

1.4.1 Literature review (Chapter 2)

The literature review is divided into three parts. Firstly, the basic physics of ultrasound and concepts such as the Doppler effect are described. PUV is discussed in detail followed with velocity estimation and signal processing techniques. Flow in complex geometries is discussed in the next sub-section which describes available flow measuring techniques, flow simulation (CFD) and previous work done. Lastly, the methodology of the UVP-PD technique as well as latest work and current problems are discussed. A brief description of fluid rheology, theoretical models and rheological characterisation methods is also included.

1.4.2 Methods of investigation and apparatus (Chapter 3)

Various flow loops were designed and constructed for this research project. MST constructed three UVP-PD flow loops, each fitted with extra pipes and instrumentation for in-line viscometric measurements. A 300 mm rectangular open channel fitted with six ports for ultrasonic transducer installation was already available at the MST.

The Adaptronics Advanced Manufacturing Technology Laboratory (AMTL) at the Cape Peninsula University of Technology (CPUT) specially designed and manufactured several 50% open diaphragm valves fitted with transducer housing ports for complex flow measurements. A hyperbolic contraction flow loop was constructed at SIK, which was installed next to a high precision robotic arm setup (described in detail in Chapter 3) for ultrasonic transducer movement during tests. The same robotic setup was used for acoustic characterisation of different ultrasonic transducers at SIK. Three rheologically different non-Newtonian fluids were tested over a wide range of laminar flow rates.

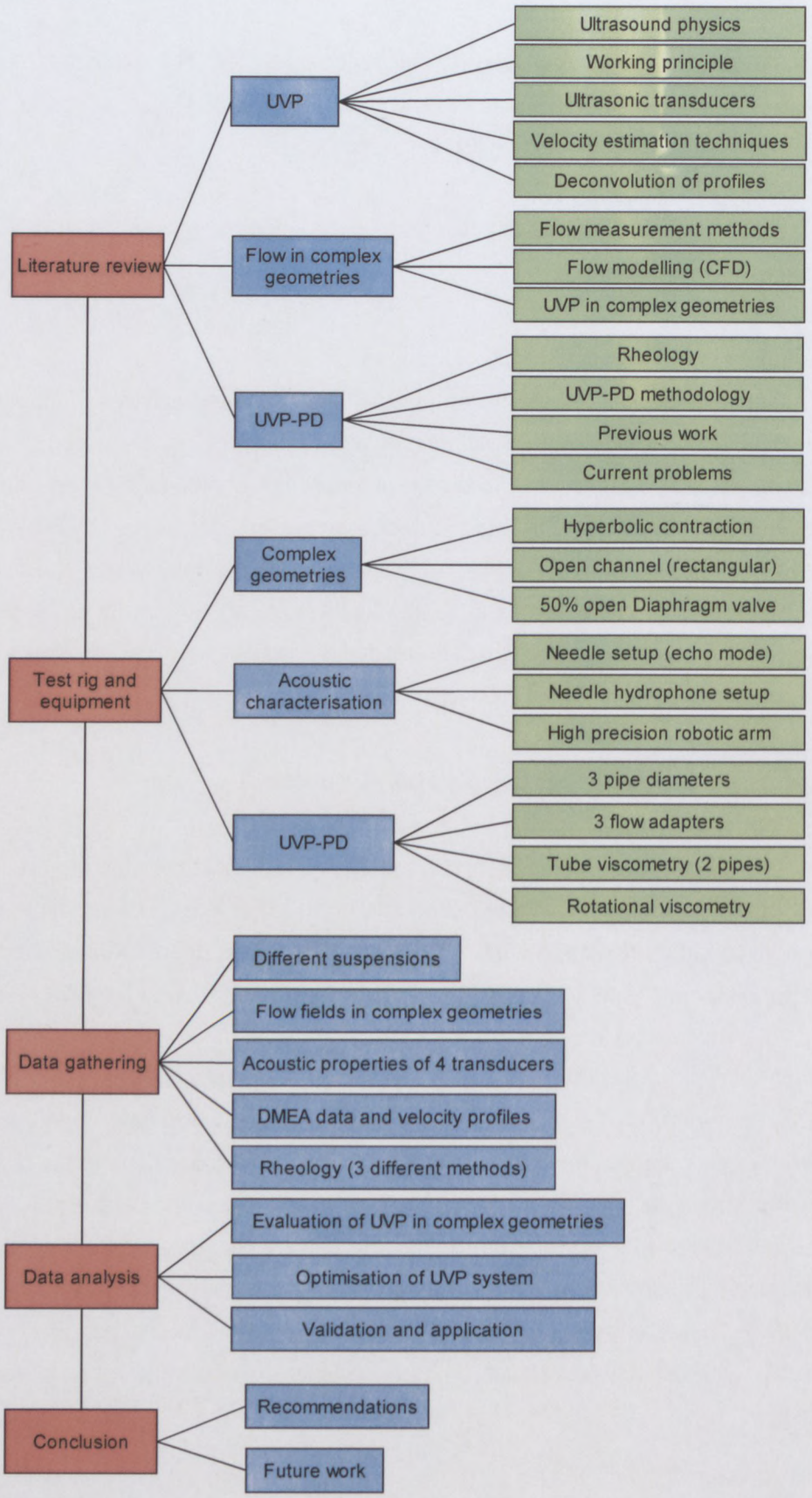

Figure 1.1: Flow chart of research approach

1.4.3 Experimental evaluation of UVP for complex flow measurements (Chapter 4)

In this chapter UVP is evaluated in three geometries: hyperbolic contraction, artificial open channel and 50% open diaphragm valve. Commercial ultrasonic transducers and conventional installation and measuring techniques were used during these preliminary measurements of complex non-Newtonian flow. The rate of fluid flow was calculated and compared to flow rates obtained from electromagnetic flow meters installed in the flow loops.

1.4.4 Optimisation of pulsed ultrasound measurements (Chapter 5)

The pulsed ultrasound velocity profile measurement methodology was optimised using special delay line ultrasonic transducers (described in Chapter 3) as well as advanced signal processing techniques. Commercial and specially designed transducers were acoustically characterised and results were compared. Erroneous velocity data close to wall interfaces were corrected by using a deconvolution procedure (algorithm described in Chapter 3). Furthermore, custom velocity estimation algorithms were written using ActiveX Demodulated Echo Amplitude (DMEA) data and calculated velocity profiles were compared with that obtained using commercial UVP Version 3 software from Met-Flow SA, Switzerland.

1.4.5 Application and validation of optimised UVP system (Chapter 6)

Velocity profiles were measured inside a 50% open diaphragm valve and 300 mm rectangular open channel using commercially available as well as special delay line ultrasonic transducers combined with a deconvolution procedure. Flow rates were calculated using a triangulation as well as integration method and results were compared with a reference electromagnetic flow meter. The optimised UVP system was also used for in-line rheological measurements using the UVP-PD methodology and results were compared with that obtained from in-line tube viscometry as well as off-line rotational rheometry.

1.4.6 Summary, contributions, recommendations and conclusions (Chapter 7)

The significant contributions of this research are summarised in this chapter, as well as conclusions drawn from experimental work. Limitations of the optimised methodology for pulsed ultrasound measurements are discussed and recommendations are made for future research in this field.

1.5 DELINEATION

This research work is strictly based on the testing of Doppler devices such as the commercially available UVP systems. Other methods such as EIT, LDA and MRI were not considered.

Immersion type, pulsed ultrasonic transducers (emitting frequency 4 MHz), which operate in transmitting and receiving mode, were used during this work. Only transducers manufactured by Imasonic, France, and Signal Processing SA, Switzerland were evaluated.

Further focus was to compare the accurate measurement of the rheology of different concentrations of non-Newtonian fluids using only a tube viscometer and the UVP-PD method. Only rotary viscometers were used for further off-line comparison.

CHAPTER TWO

THEORY AND LITERATURE REVIEW

CHAPTER TWO

THEORY AND LITERATURE REVIEW

2.1 INTRODUCTION

The theory and literature on Ultrasonic Velocity Profiling (UVP), flow in complex geometries, rheology and the UVP-PD methodology are presented in this chapter. Basic ultrasound transducer design and physics are introduced in Section 2.2.2 followed by the working principle of UVP. This section explains how UVP is used to obtain velocity profiles in fluid flow using different techniques. Previous work regarding deconvolution procedures of measured velocity profiles in the medical industry is discussed in the last sub-section. Finally, the UVP-PD methodology is discussed and it is shown how this method can be used to obtain rheological parameters of different types of fluids, including model and industrial suspensions, followed by a description of current problems associated with the in-line rheometric method.

2.2 ULTRASONIC VELOCITY PROFILING (UVP)

2.2.1 Introduction

UVP is a technique originally developed for studying blood flow in humans. This method was extended in the mid 1980's to include measurements in general fluids and has since become an important tool within academia and industry (Takeda, 1986, 1991, 1995, 1999). UVP is both a method and a device to measure an instantaneous velocity profile in a liquid flow by echography. The technique detects the Doppler shift frequency information contained in the ultrasound echoed by particles contained in the fluid as a function of time. The measurement is one-dimensional providing a velocity profile projected along the probing axis. Since the majority of the small scattering particles are assumed to travel at a velocity equal to that of the continuous phase, the true velocity distribution along the probing axis is obtained. UVP is an ideal technique since it is non-invasive, works with opaque systems, inexpensive, portable and easy to implement relative to other velocity profile measurement methods (Teufel

et al., 1992; Powell, 2008; Shirai *et al.*, 2008). This method in some cases is also the only feasible way of determining process parameters (Povey, 1997; Wiklund, 2007).

2.2.2 Ultrasound and acoustic properties

The region of acoustical phenomena that are not accessible to human perception because of the high frequencies involved is characterised as ultrasound. Thus ultrasound can be thought of as analogous to ultraviolet light (Kuttruff, 1991). Ultrasound can penetrate optically opaque materials and can provide high-quality information in a rapid and non-invasive manner. The measurement of acoustic parameters of particulate suspensions has been investigated by many researchers in the past decades. Acoustic properties relevant to the research work are discussed in the next sub-sections.

2.2.2.1 Propagation and sound velocity

Ultrasound is a mechanical vibration of matter with frequencies above 20 kHz (audible range). Ultrasonic waves propagate through a material as a disturbance of particles in the medium supporting the wave. Particles oscillate around there mean positions due to the presence of the ultrasonic wave and the oscillation is along the direction of the propagating wave, making it a longitudinal wave (Jensen, 1996). No mass is transported and thus the ultrasonic wave acts as a mere disturbance in the medium. The velocity of this disturbance is dependent on the medium and is given by:

$$c = \sqrt{\frac{1}{\rho_0 \kappa}}, \tag{2.1}$$

where ρ_0 is the mean density and κ is the adiabatic compressibility (Urick, 1947). The measurement of the velocity of sound can be done quickly and accurately. Many different measurement techniques are described in literature, the most common known as 'Acoustic Time of Flight Measurement' (AToM). Detailed descriptions of possible errors associated with sound velocity measurements can be found in Povey (1997). More information on parameters such as temperature, solids concentrations and fluid viscosity that influence ultrasonic propagation can also be found in Shutilov (1980) and Povey (1997).

2.2.2.2 Attenuation

The ultrasonic wave propagation in the medium will be attenuated due to absorption and scattering. Absorption is the conversion of the sound energy to other forms of energy. Scattering is the reflection of sound energy in directions other than its original direction of propagation. Many different scattering theories have been formulated over the past years. For detailed scattering theory analysis and experimental validation, see Povey (1997). The attenuation of an ultrasound wave propagating in a fluid can be expressed as a function of the wave amplitude to the propagating distance. The *spatial attenuation coefficient* α_0 characterises the damping of an ultrasound wave with distance in space (Shutilov, 1980). This coefficient is defined by:

$$\alpha_0 = \left(\frac{-1}{A_{MAX}}\right)\left(\frac{dA_{MAX}}{dx}\right). \tag{2.2}$$

A_{MAX} is the wave amplitude of the transmitted ultrasound wave. Figure 2.1 shows how the amplitude of an ultrasound wave reduces with the distance x, according to the exponential law given in Equation 2.3.

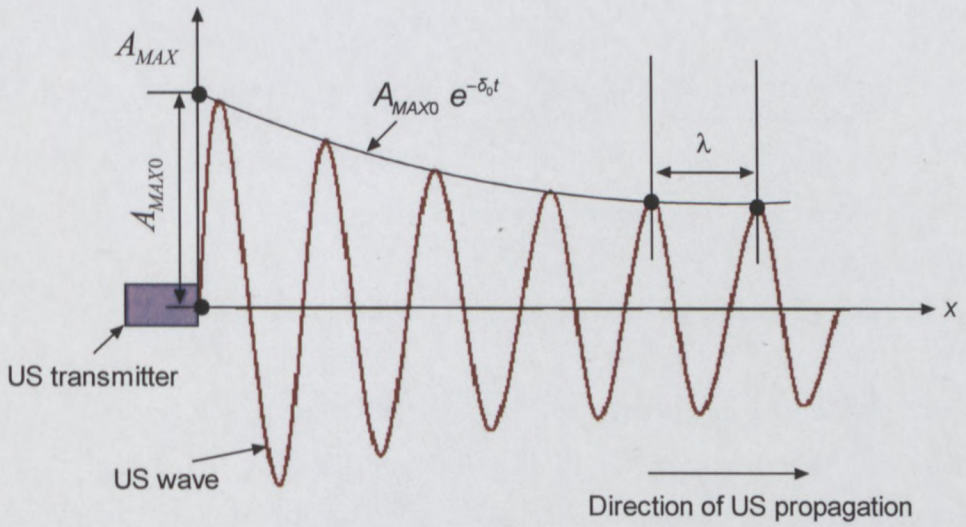

Figure 2.1: Attenuation of an ultrasonic wave (Ouriev, 2000)

Within the time delay t, the sound wave propagates with a sound velocity across a distance x. Substituting the expression $x = ct$ in Equation 2.3 gives a general law of ultrasound wave attenuation in a sample fluid, namely:

$$A_{MAX} = A_{MAX0} e^{-\alpha_0 ct} \ . \tag{2.3}$$

The attenuation coefficient depends on the material, ultrasound frequency, temperature and other possible parameters. For measurements through a pipe wall or material layer, it is very important to optimise the choice of the wall material so that one does not use a wall material with a high attenuation coefficient.

2.2.2.3 Reflection and refraction

According to Shutilov (1980), the following analysis is made for the description of ultrasound wave propagation at the boundary between two materials. Figure 2.2 shows that two material layers are taken into consideration.

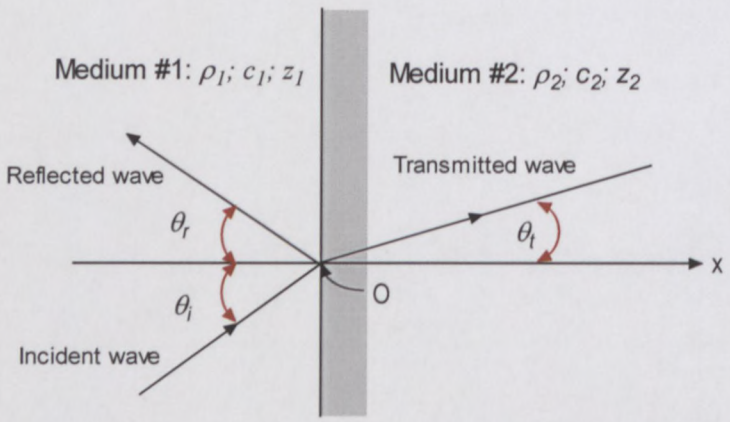

Figure 2.2: Ultrasound wave propagating between two materials

The first medium #1 has a specific acoustic impedance $z1 = \rho_1 c_1$, where ρ_1 is the material layer density and c_1 is the sound velocity in the material (subscript 1 denotes parameters related to medium #1). Equal definition can be used for medium #2. The ultrasound wave propagates in medium #1 with the inclination angle θ_i to the x-axis. At each boundary surface or interface the ultrasound wave will reflect and diffract. Thus, depending on the acoustic properties of the layer material, the direction of the ultrasound propagation will be changed from layer #1 to layer #2. As shown in Figure

2.2, the angle changes at the interface between two different materials to another angle θ_t. The following law holds for the angle θ_t of refraction:

$$\frac{sin\theta_t}{sin\theta_i} = \frac{c_2}{c_1} . \tag{2.4}$$

Equation 2.4 is known in optics as 'Snell's law' and θ_i is the beam angle of the incident ultrasound wave. According to Snell's law, the following conclusion can be drawn: the higher the sound velocity of medium #2, the larger the transmitted beam angle θ_t will be. If the Doppler method is used (see Section 2.2.4), the beam angle is an important factor in interpreting the correct velocity information measured along the ultrasonic beam. More information on acoustic intensity, transmission and reflection analysis as well as impedance matching can be found in Kuttruff (1991), Jensen (1996) and Ouriev (2000).

2.2.3 Ultrasonic transducers and their properties

The history of ultrasound over a long period coincides with the history of general acoustics. However, two important discoveries which were of crucial importance for the future development of ultrasound technology took place in the 19th century: the discovery of magnetostriction by J. P. Joule in 1847, and that of piezoelectric effect by the brothers J. and P. Curie in 1880 (Kuttruff, 1991). Today the active element of most acoustic transducers is a piezoelectric ceramic, which can be cut in various ways to produce different wave modes.

2.2.3.1 Transducer design

There are many different types of transducers optimised for each particular application ranging from the medical industry to high power non-destructive testing. Examples of transducer type configurations are contact, immersion, focusing, dual-element, phased array and high temperature transducers. In this research, plain-wave immersion type ultrasonic transducers, which operate in transmitting and receiving mode, were used. A more detailed description of different transducer configurations can be found in Jensen (1996) and Met-Flow SA (2002). An ultrasonic transducer is made out of three main

components: the active element, the backing layer and the wear plate or matching layer. A schematic of a single element transducer is shown in Figure 2.3.

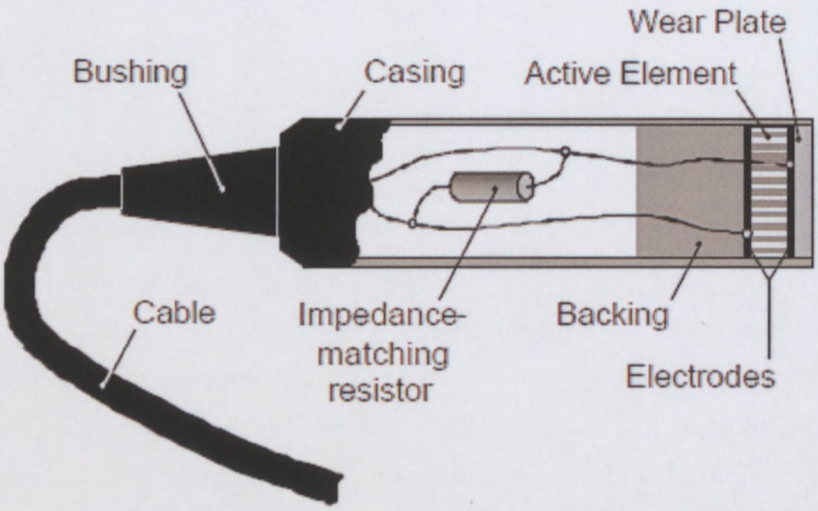

Figure 2.3: Construction of a single element ultrasonic transducer (Met-Flow, 2002)

The active element, usually made from a piezoelectric crystal, converts electrical energy into ultrasonic energy and vice versa. The crystal thickness is designed at half a wavelength, making the resonance frequency equal to

$$f_0 = \frac{c_c}{2L_c}, \tag{2.5}$$

where c_c is the propagation speed in the material and L_c is the thickness of the crystal (Jensen, 1996). An impedance matching layer is inserted in front of the crystal in order to protect it from the external environment and to ensure maximum energy transfer. The matching layer can have different shapes for ultrasonic beam focusing. A damping or backing layer is also inserted to dampen the oscillation of the crystal. The purpose of the backing layer is to absorb acoustic energy radiating from the back face of the crystal or active element. Depending on the application, the bandwidth or energy output of the transducer can be optimised by using an impedance mismatch or matching backing layer. Air will give maximum ultrasonic reflections and maximum the energy output, but will not dampen the crystal oscillation and thus a longer pulse and narrow frequency band is obtained due to transducer ringing. On the other hand, a very heavy damping layer will absorb energy radiated toward the back and ensure a short, broad

band pulse. In pulsed ultrasound systems, fast switching between transmission and reception of ultrasonic energy as well as spatial resolution across the measuring axis is of great importance and thus transducers with impedance-matched backing are used for good dynamic characteristics (Jensen, 1996).

2.2.3.2 Radiated fields of ultrasonic transducers

In order to choose the correct ultrasonic transducer for a particular application, the physical ultrasound beam properties and characteristics have to be considered. The following equation expresses the relative acoustic pressure distribution along the transducer axis:

$$p = \frac{2\pi\, p_0}{k} \sqrt{2 - 2\cos\left(k\sqrt{\frac{\alpha^2}{2} + z^2} - k\,z\right)}, \tag{2.6}$$

where p is the acoustic pressure, p_o the reference acoustic pressure on the transducer and z the on-axis co-ordinate of the ultrasound beam (Wiklund, 2003). The generated ultrasound beam can be divided into two main regions called the "near-field" (Fresnel zone) and the "far-field" (Fraunhofer zone). Figure 2.4 shows the sound field generated by an ultrasonic transducer.

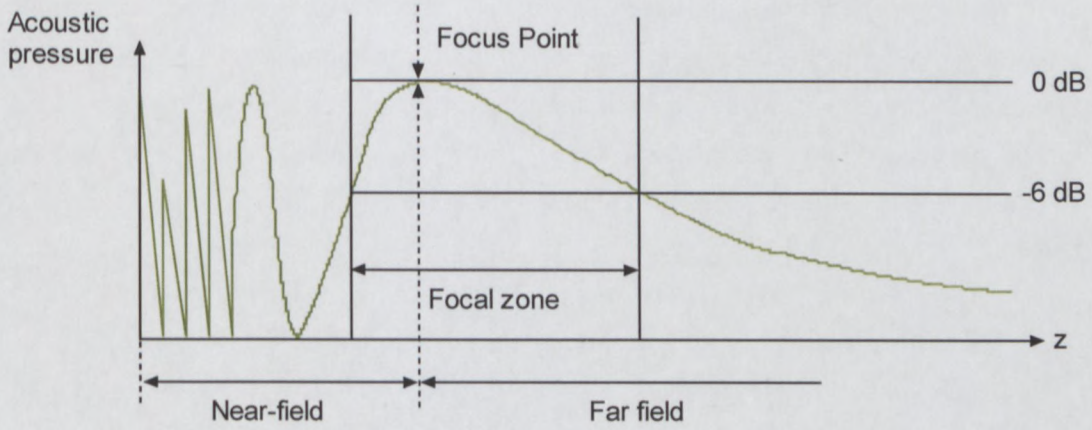

Figure 2.4: Sound field generated by an ultrasonic transducer

In the near-field region, the intensity oscillates along the axis of the transducer and starts at the transducer's front surface. The distance N_f is called the "near-field distance" and can be estimated by Equation 2.7:

$$N_f = \frac{\alpha^2 f_0}{4\,c}. \tag{2.7}$$

The near-field zone is avoided when practical velocity measurements are conducted due to the unstable nature of the ultrasonic beam in this region. Transducer housing ports and special flow adapters were specifically designed so that the transducers could be pulled back in order to have the far-field region of the ultrasonic beam within the flow area. Transducer installation methods are described in more detail in Chapter 3.

The far-field starts from the focus point of the transducer and in this region the intensity of the acoustic field varies as the inverse square of the distance from the transducer, z. The sound beam also diverges at a constant angle for a given pressure amplitude drop. The beam divergence half-angle, γ_0, is defined as the half-width (-6 dB) of the sound pressure and can be expressed by (Metflow, 2002):

$$\gamma_0 = \sin^{-1}\left(0.51\frac{\lambda}{\alpha}\right). \tag{2.8}$$

In pulsed Doppler ultrasound, an emitter (ultrasonic transducer) periodically emits a short ultrasonic burst and a receiver continuously collects echoes issued from targets or particles that may be present in the path of the ultrasonic pulse. The region where the ultrasonic energy is scattered back due to flowing particles is called the measuring or sample volume (Jorgensen *et al.*, 1973). The lateral dimensions of the measuring volumes depend on their position along the ultrasonic beam, as shown in Figure 2.5 below.

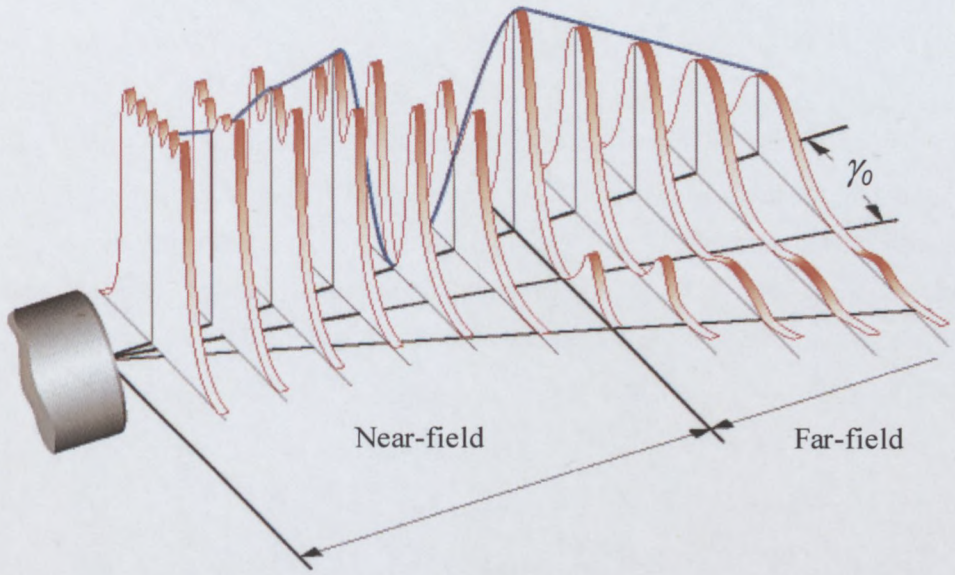

Figure 2.5: Lateral dimensions of measuring volumes versus position along US beam (Signal Processing SA, 2007)

The sample volumes increase according to the active beam diameter and the beam divergence half-angle. Thus the amount of target particles passing through the sample volumes increases which produce a broad Doppler frequency spectrum. Due to the larger number of moving particles, averaging effects occur and the accuracy of velocity determination within the measuring volumes consequently decreases (Birkhofer, 2007). As a result, distortion of the measured velocity profile occurs with increasing spatial depth, due to wider measuring volumes as well as attenuation of the ultrasonic beam.

2.2.4 The Doppler effect and working principle

The Doppler effect is the apparent change in frequency and wavelength of a wave that is perceived by an observer moving towards or away from the source of the wave. This effect was proposed by the Austrian physicist Johann Christian Doppler, who first noticed it in sound waves in 1842 (Halliday, Resnick & Walker, 1993). The Doppler effect may result from either motion of the source or motion of the observer and holds for electromagnetic waves, including microwaves, radio waves as well as visible light.

The link between the emitted ultrasonic wave frequency f_e, sound velocity and wavelength is given by:

$$f_e = \frac{c}{\lambda}\,, \tag{2.9}$$

where c is the sound velocity in the fluid sample and λ the wavelength (see Figure 2.1) of the emitted ultrasonic wave. The fundamental Doppler equation expresses the frequency shift of acoustic energy scattered from a target particle moving at a certain velocity in terms of the frequency of the emitted wave, the speed of sound in the propagation medium, and the angle between the direction of fluid flow and ultrasonic beam propagation as

$$f_d = 2f_e\left(\frac{v}{c}\right)cos\theta\,, \tag{2.10}$$

where f_d is the Doppler frequency shift, v the target particle velocity and θ the angle between the ultrasonic beam and direction of flow, also known as the Doppler angle (Barber *et al.,* 1985). Rearranging Equation 2.10, the velocities of the moving reflectors in the fluid medium of interest can therefore be expressed as

$$v = \frac{c\,f_d}{2\,f_e\,\cos\theta}, \tag{2.11}$$

where f_e is the emitting frequency and $f_d = f_e - f_r$ is the difference between the emitted frequency and the received frequency. It must be emphasised that the Doppler effect is only an artefact in the UVP system. Pulsed ultrasonic systems are often called Doppler systems, which is misleading because it does not use the Doppler effect. This is because it is not the Doppler shift frequency that is measured, but the time shift or time delay of the received signals. The time shift is then compared to the received preceding signal frequencies, depending on the scatter motion. In other words, it is the shift of position of the signals between pulses that is employed, and thus the classical Doppler effect plays a minor role (Jensen, 1996).

In order to obtain spatial velocity information along the ultrasonic beam, the measuring window is divided into segments or channels, as depicted in Figure 2.6. Each channel in fact is a measuring or sample volume by which the velocity of the target particle is calculated (see Section 2.2.3.2, Figure 2.5). A transducer transmits a short ultrasonic pulse that travels along the measurement axis. When the ultrasonic pulse hits small

moving particles suspended in the liquid, part of the energy scatter and echo back to the transducer. The transducer is switched to receiving mode directly after transmitting and the time interval between successive pulses is available for echo reception since the pulses are separated by a fixed Pulse Repetition Frequency (PRF). A target particle that has moved a distance Δs in the flow direction and by Δd in the measuring direction, is shown inside a magnified sample volume in Figure 2.6.

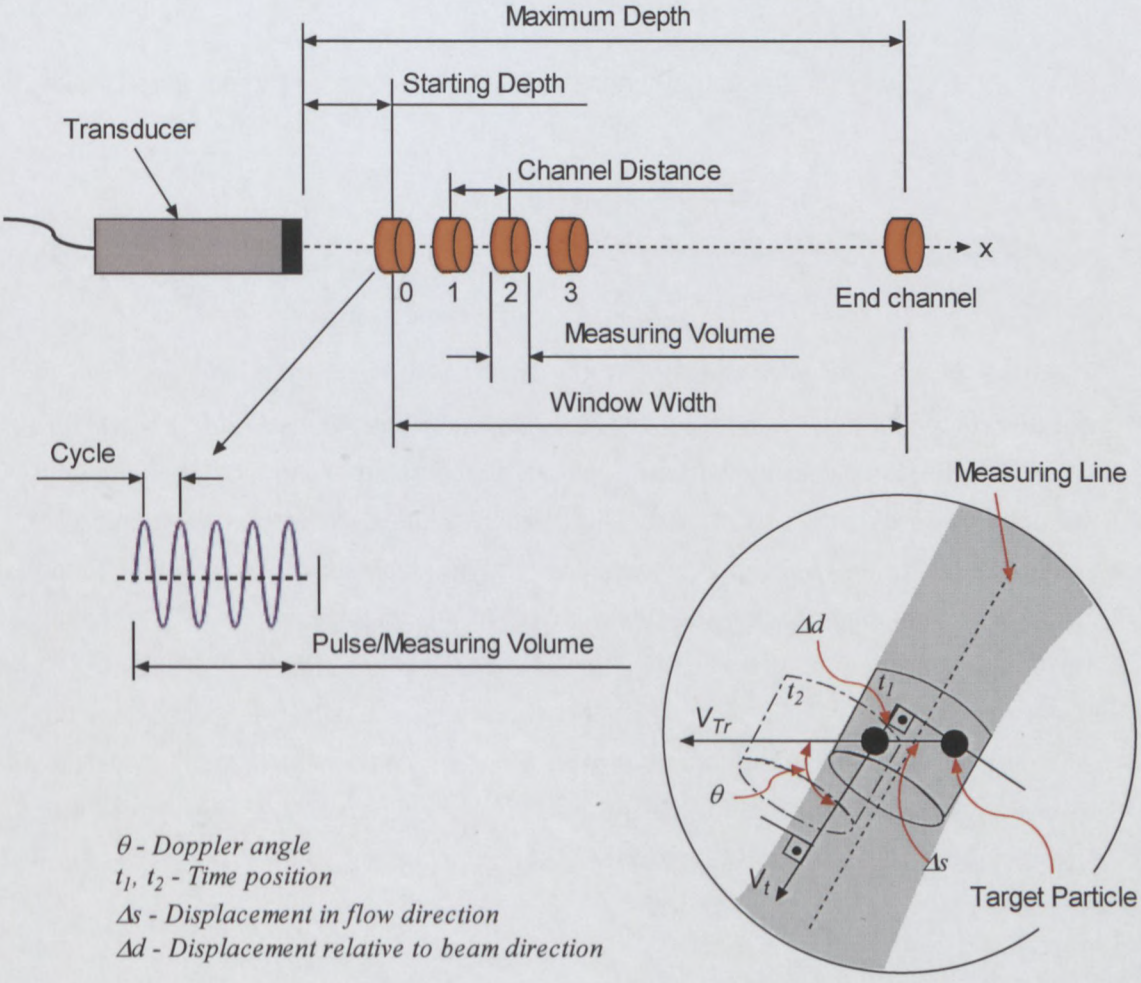

Figure 2.6: Schematic of UVP working principle (adapted from Ouriev, 2000)

Within the time delay $\Delta t = t_2 - t_1$, a particle suspended in a fluid has moved over the distance Δd along the ultrasonic beam or measuring axis. This distance is written as

$$\Delta d = \frac{(t_2 - t_1)\, c}{2}, \tag{2.12}$$

where c is the sound velocity in the fluid suspension (Ouriev, 2000). In order to calculate the velocity in the flow direction, the velocity obtained along the ultrasonic beam is corrected with the Doppler angle θ as:

$$\Delta s = \frac{\Delta d}{cos\,\theta} = \frac{(t_2 - t_1)\, c}{2\ cos\,\theta}. \tag{2.13}$$

Finally, the velocity of the target particle is calculated according to the following expression:

$$V_{Tr} = \frac{\Delta d}{T_{PRF}} = \frac{(t_2 - t_1)\, c}{2\, T_{PRF}\ \cos(90° - \theta)} = \frac{V_t}{\cos(90° - \theta)}, \tag{2.14}$$

where V_{Tr} is the velocity component in the direction of the mainstream and V_t is the velocity component in the direction of the measuring line (Ouriev, 2000). From this information the local velocity in many separate space points along the measuring axis (window width) can be constructed. The channel width depends on the number of cycles per pulse as well as the wavelength of the ultrasonic wave. The channel distance is the distance between two adjacent measuring volumes. The spatial resolution thus depends on a combination of these two parameters (Wiklund, 2007). Parameter setting values, limitations and practical measurement considerations regarding this type of instrument can also be found in Met-Flow SA (2002). A detailed description and working principle of the pulsed ultrasonic technique can be found in Takeda (1986, 1991, 1995, 1999), Kutruff (1991) and Jensen (1996).

2.2.5 Signal processing and velocity estimation techniques

There are many publications on different algorithms for estimating the velocity from the returning / sampled echo signals. The first instruments employed a full analog system for frequency estimation of the baseband signal. Later the baseband signal was digitised which opened many new possibilities and methods for velocity estimation (Birkhofer, 2007). Figure 2.7 shows a conventional analog quadrature demodulation scheme in block diagram format. Noise is removed by using a lowpass filter after the mixing process followed by a sample and hold circuit. The signal is then digitised for processing using different velocity estimation algorithms (Jensen, 1996). Algorithms used for detecting the Doppler shift frequency or time delay (Equation 2.10) can be divided into spectral (FFT) and time domain algorithms.

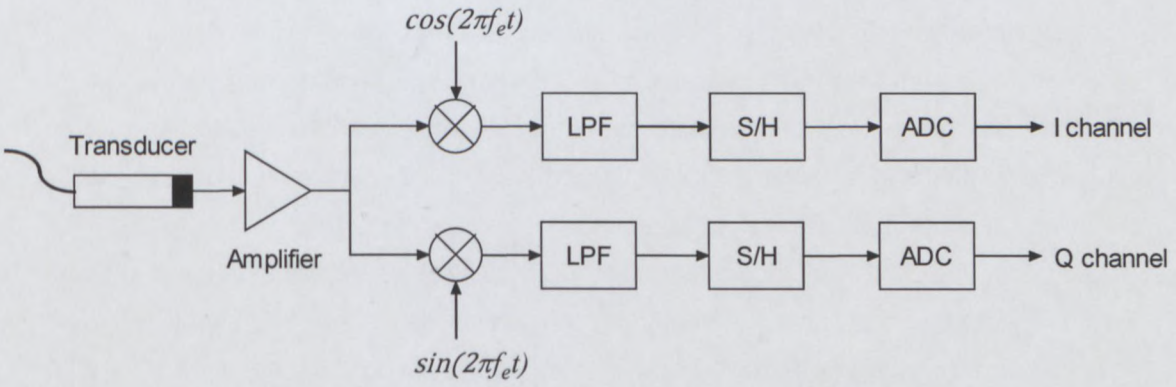

Figure 2.7: Conventional analog demodulation of baseband signal (Jensen, 1996)

In spectral signal processing the mean Doppler frequency is derived from the power spectrum of the returning I and Q signals. Many different frequency domain processing techniques have been published where several different spectral estimation methods have been compared (Abdel-Azim & Hottinger, 1982; Barber *et al.*, 1985; Nowicki *et al.*, 1985; Mo *et al.*, 1988; Tortoli *et al.*, 1996). Markou and Ku (1991) also compared four different signal analysis techniques (zero crossing detector, FFT, Burg autoregressive and minimum variance) for velocity measurements of an aqueous glycerin solution in pipe flow with Reynolds numbers ranging between 500 and 8000. Guidi *et al.* (2000) compared the Burg algorithm with the complex FFT method and concluded that the Burg algorithm (autoregressive method) provides a power spectrum with less variance (more precision in Doppler frequency estimation). However, it was also concluded that when the full spectral profile is considered it is ideal to have access

to both methods, since the FFT can be used for detailed spectral analysis of the Doppler signals. Several spectral estimation techniques were also reviewed by Vaitkus and Cobbold (1988). Techniques included the moving average model, autoregressive models such as the Yule-Walker method, Burg algorithm, least squares algorithm and the Capon method as well as different autoregressive-moving average models (extended Yule-Walker equations, Singular Value Decomposition (SVD) and moving average coefficient estimation). Aydin *et al.* (1994) and Aydin and Evans (1994) compared and implemented four different quadrature to directional velocity estimation methods (time and frequency domain) including a phasing-filter technique, the extended Weaver receiver technique, Hilbert transform in the frequency domain and the complex FFT.

Determining the correct Doppler frequency from a signal with a broad spectral spread and low signal-to-noise ratio can be extremely complicated and thus scientists are always interested in alternative signal processing techniques. Time domain signal processing techniques have been found to perform well in a wide range of signal-to-noise ratios than when compared to standard FFT methods. Implementation of time domain algorithms is usually straightforward and can be implemented quite easily (Barber *et al.,* 1985). Time domain algorithms can be separated into (i) phase-shift estimators that employ autocorrelation techniques of the baseband signal and (ii) time shift estimators that use frequently cross-correlation of the RF signal to track movement of scatterers in the fluid medium. Barber *et al.* (1985), Kasai *et al.* (1985), Kristoffersen (1988) and Feng *et al.* (2006) developed new time domain signal processing methods based on autocorrelation techniques of the baseband signal for velocity estimation. More information on signal processing, anti-aliasing, Doppler spectral broadening and signal-to-noise ratio can be found in Birkhofer (2007).

2.2.6 Deconvolution of velocity profiles

Velocity profiles are generally not known with sufficient accuracy as a result of the effect of the finite sample volume characteristics and propagating through solid boundaries or wall material layers (Jorgensen & Garbini, 1974; Flaud *et al.,* 1997). The influence of the sample volume geometry and intensity has been thoroughly investigated by Jorgensen *et al.* (1973) and Jorgensen and Garbini (1974). Some authors describe the sample volume to be cylindrical with the pulse length and ultrasonic beam diameter (Wunderlich & Brunn, 2000; Nowak, 2002; Kikura *et al.,*

2004). However, the sample volume actually has a drop shaped geometry, as described in Figure 2.8. For a short driving pulse the ultrasonic wave intensity increases exponentially until the end of the electrical pulse followed by a gradual decay due to the transducer ringing phase (exponential decay of stored energy). Sound field characteristics of the sample volume are determined by the ultrasonic transducer focal properties, the sound scatterers in the flow medium and the sensitivity of the receiver circuitry (Jorgensen *et al.,* 1973). The acoustic burst is a three-dimensional region of sound intensity and any flow particles passing this region produce Doppler signals which are detected by the receiver. Since multiple scatterers flowing at different velocities are present in the practical environment the received signal is a spectrum of frequencies containing the Doppler shifts of all moving particles. The result of this spectral broadening is that in small tubes where the velocity gradients are high the velocity profiles are considerably distorted. This distortion is caused by the averaging which takes place over the sample volume. It is assumed that the measured velocity is proportional to the average of the velocities within the sample volume weighted by the associated intensity distribution of the measuring volume. Mathematically, the measured velocity profile v_m can be expressed as a three-dimensional convolution of the real velocity profile v_t with the sample volume intensity function i (Jorgensen & Garbini, 1973):

$$v_m(r) = \frac{\int_0^r \int_{z_1}^{z_2} \int_{y_1}^{y_2} v_t(x,y,z) i(r-x,y,z) dxdydz}{\int_{z_1}^{z_2} \int_{y_1}^{y_2} \int_{x_1}^{x_2} i(x,y,z) dxdydz}, \tag{2.15}$$

where r is the range variable (distance along path of ultrasonic propagation).

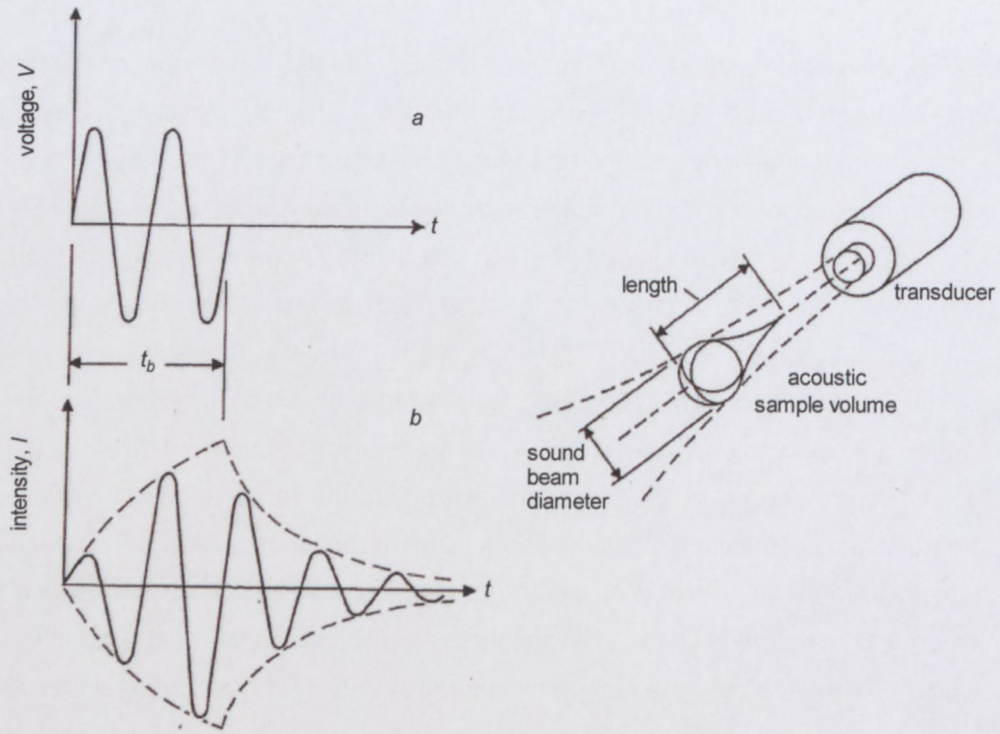

Figure 2.8: Transducer response and sample volume geometry (Jorgensen *et al.*, 1973)

The convolution procedure can be dramatically simplified by assuming that the sample volume has only one dimension, its length and that it is characterised by the acoustic intensity along the ultrasonic beam axis. Since the measured length of the sample volume is both its largest dimension and is coincident with the direction of convolution and since the intensity is the highest at the beam centre, these assumptions prove to be reasonable (Jorgensen & Garbini, 1974). Equation 2.15 then reduces to a one-dimensional convolution:

$$v_m(r) = \int_0^r v_t(x)\, i(r-x)dx\,. \tag{2.16}$$

Another way of calculating the measured profile is by applying the time convolution theorem, which states that the Fourier transform of the convolution ($*$) of two functions is equal to the product of the two Fourier transforms ($\mathcal{F}(f_1(t) * f_2(t) = F_1(w)F_2(w)$ where $\mathcal{F}$ is the Fourier transform operator and $F_1(w)$ and $F_2(w)$ are the Fourier transforms of $f_1(t)$ and $f_2(t)$ respectively (Floyd, 2003)). After a few more transformations the real or 'true' velocity profile can be calculated using a deconvolution process:

$$v_t(r) = \mathcal{F}^{-1}\left(\frac{V_m(k)}{I(k)}\right), \tag{2.17}$$

where k has the inverse dimension of the spatial coordinate r (Flaud *et al.,* 1997). Figure 2.9 shows a velocity profile measured (circles) in laminar blood flow. The accompanying solid line curve is the theoretical profile derived from the bulk flow rate. Also shown is the corrected profile (blocks), as determined from the measured profile and sample volume characteristics, deconvolved using the simplified algorithm. It can be observed that the measured profile overshoots the diameter (7 mm) and that the maximum magnitude is slightly less than the corrected or theoretical profile. The one-dimensional deconvolution procedure was also successfully implemented on velocity profiles measured in blood flow by Black and How (1989). Hughes and How (1994) applied a slightly modified version of the deconvolution algorithm for estimation of wall shear rates in pulsating flow. In all cases deconvolution significantly improved the accuracy of the wall shear rate determination.

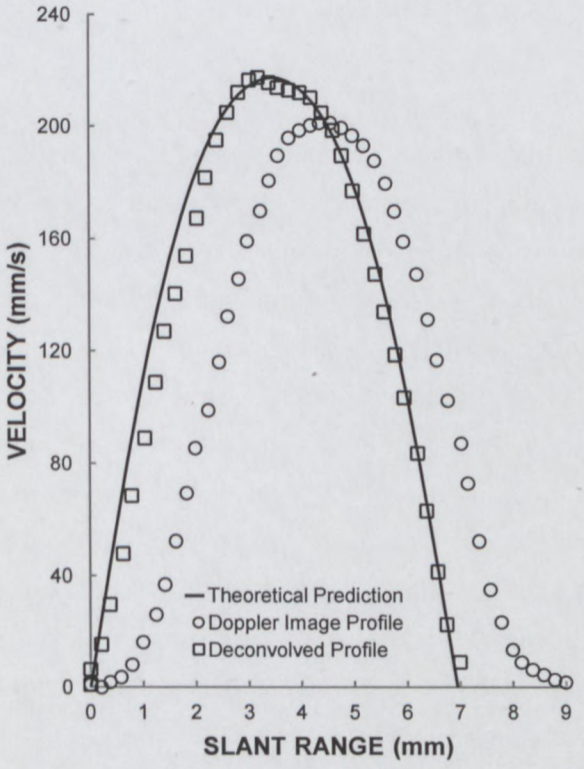

Figure 2.9: Deconvolution of fully developed laminar flow using the one-dimensional algorithm (Jorgensen and Garbini, 1974)

Flaud *et al.* (1997) significantly improved distortion of velocity profiles induced by the finite size of the sample volume by using a uni-dimensional and normalised sample volume in a new deconvolution process. The deconvolution procedure was based on an iterative process where the sample volume length was varied until a profile with the least variance or noise was obtained. A similar approach was used for correction of distorted velocity profiles in this research. More information on deconvolution procedures and test setups for characterising sample volumes as well as UVP systems can be found in Jorgensen *et al.* (1973), Walker *et al.* (1982) and Birkhofer (2007).

2.3 FLOW MEASUREMENT AND MODELLING IN COMPLEX GEOMETRIES

This section presents previous work done in flow modelling/simulation as well as flow behaviour measurements using different techniques in complex geometries such as contractions, expansions, open channels and valves. Empirical work done on loss coefficients and flow behaviour of non-Newtonian fluids in complex geometries is also discussed.

2.3.1 Introduction

Significant environmental benefits primarily related to reduce water consumption can be obtained by using high density slurry and paste tailing transport systems. By increasing the solid concentration of mining slurries substantial water savings can be achieved (Paterson, 2004). One of the fundamental criteria upon which conventional settling slurry transport systems are designed, is minimum transport velocity. The selection of a suitable operating velocity presents the design engineer with a considerable challenge. The slurry transport systems are in many cases designed to operate in laminar flow (Paterson, 2004). However, laminar settling of high volume thickened tailings that require large diameter pipelines can be a problem, as has been reported in several pipelines that operate in laminar flow (Cooke, 2002). Also, in the absence of reliable energy loss estimates the design engineer is forced to make conservative estimates that lead to the selection of inefficient, oversized pumps (Fester *et al.*, 2007).

Flow through complex geometries such as abrupt contractions and enlargements, as well as valves are important problems in fluid dynamics, because they are integral

components and frequently occur in pipeline systems. Understanding the energy loss mechanisms in complex geometries is therefore a prerequisite to good engineering design of pipeline systems (McNeil & Morris, 1995). Thus far energy losses in complex geometries have been analysed using theoretical simulations such as Computational Fluid Dynamics (CFD) or similar software. Experimental work based on empirical methodologies has also been used for improving energy loss predictions in pipeline design. More recently, velocity field measurement techniques have been used for more detailed flow behaviour measurements in different complex geometries.

2.3.2 Flow modelling using Computational Fluid Dynamics (CFD)

Flow simulations or modelling are often useful in design of industrial processes involving flows of complex non-Newtonian fluid suspensions. These theoretical predictions are based on mass and momentum conservation principles and constitutive equations are needed to describe the flow behaviour of the flowing material (Thompson *et al.,* 1999). In the complex flow simulation field, scientists are continuously trying to improve the accuracy of theoretical predictions by producing new designs of computational meshes as well as code or solvers for governing flow problems (Stickel & Powell, 2005; Stickel *et al.,* 2006).

2.3.2.1 Contractions

The flow from a large cross-section via an abrupt smaller cross-section entry (see Figure 2.10), which is commonly called contraction flow, has been one of the most visited subjects in the numerical simulation studies (and experimental work) for more than two decades (Xue *et al.,* 1998). Alves *et al.* (2004) studied the effect of contraction ratios in viscoelastic flow through abrupt contractions using a finite volume method. Results obtained from the simulations, in terms of stream line patterns, were in good agreement with previous visualisation photographs. Later, Alves and Poole (2007) numerically investigated divergent flow for different hyperbolic contraction ratios. It was found that both inertia and/or shear-thinning are not required for divergent flow to be observed. Oliveria *et al.* (2007) carried out a comprehensive numerical study of the effects of the contraction ratio upon viscoelastic flow through axisymmetric contractions. Recently, Lubansky *et al.* (2007) provided an analytical solution to predict the flow, vortex and pressure drop behaviour in abrupt axisymmetric contractions for fluids which exhibit large Trouton ratios.

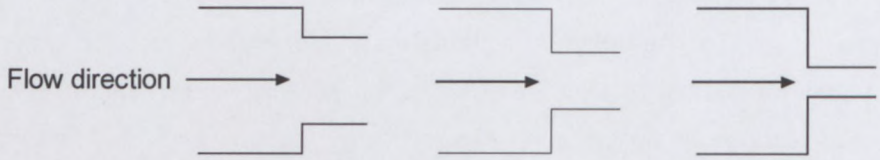

Figure 2.10: Example of different abrupt contractions

2.3.2.2 Expansions

Flow of non-Newtonian fluids through a sudden expansion of various ratios (same as in Figure 2.10, but with opposite flow direction) is a classical problem, which has been studied extensively. Alexandrou *et al.* (2001) studied steady flow of Herschel-Bulkley fluids in a canonical three-dimensional expansion. The effect of the geometry ratios on the flow was significant, where the 4:1 expansion was more pronounced than when compared to the 2:1 expansion. Mitsoulis and Huilgol (2004) investigated entry flows through abrupt expansions for Bingham plastics exhibiting a yield stress and provided corrections for easy to use quick engineering calculations. Three different viscoelastic models were compared in a numerical investigation of sudden expansion flows by Poole *et al.* (2007). All models performed similarly, however, at lower Deborah numbers, different results than previous studies had suggested, were obtained for the length and intensity of the downstream recirculation region. Manica and Bortoli (2004) developed a numerical technique to simulate non-Newtonian laminar flow passing through a sudden expansion. The differences between Newtonian and power-law fluids for a 3:1 ratio were investigated.

2.3.2.3 Valves

Valves are commonly found in piping systems in the mining and process industries, to shut off or regulate the flow. Reliable loss estimates are needed in order to design pipeline systems efficiently and thus engineers are always improving the design of various types of flow regulators such as diaphragm, butterfly and ball valves. CFD simulations are used to investigate the flow through valves in order to estimate the energy losses. Adair and Fisher (1999) improved and compared three different simulation programs for two-phase flow though safety relief valves (and pipes). Morris (1996) proposed a new safety valve model in which the flow characteristics are

described by a discharge coefficient (for valve nozzle) and a loss coefficient (for valve body). The model provided a more detailed and useful description of the flow through the safety valve. Impact erosion in valve geometries is also important in industry. Wallace *et al.* (2004) investigated techniques to predict the rate of wear in industrially relevant valve geometries using CFD. Results were compared to empirical models and it was found that previous average erosion rates were under predicted by up to 60%. In another study Park and Chung (2006) investigated the hydrodynamic torque of a butterfly valve using theoretical flow models. Improvements were made to previous available models using a newly devised iterative scheme for problem solving and the present results can be used in further research on butterfly valve designs.

2.3.2.4 Open channel

Open channels are very prevalent in water systems (irrigation and water transportation), waste water treatment as well as transportation of highly concentrated mining slurries to tailing dams. The presence of a free surface adds an extra dimension to the complexity of open channel flow than compared to normal pipe flow and researchers are continuously striving for more accurate non-Newtonian flow models (Chow, 1959). Several computational schemes for viscoelastic flows with free surfaces have been developed in the last decade (Keunings, 1990; Sato & Richardson, 1994; Mao & Khayat, 1995; Mei & Yuhi, 2001, Wang & Yu, 2007). Cheng (2007) analytically investigated the power-law index for velocity profiles in open channel flows. It was concluded that the proposed approach for evaluating the shear velocity or bed shear stress may serve as a good alternative to the use of the log law, but that there limited quantitative experimental data available to properly evaluate the power-law index method. Kra and Merkley (2004) developed a computational model for improving the accuracy of the 'float' method for estimating open channel discharge. Although improvement was made on the accuracy of flow rate measurements, there are still some significant improvements to be made. The numerical model do not compensate for all involved parameters (wall roughness, slope, channel shape) which influence the surface velocity and consequently mathematical models need to be experimentally and numerically tested to determine flow conditions under which they can be reasonably applied.

2.3.3 Experimental data and empirical models

2.3.3.1 Valves and other pipe fittings

There are very few experimental results available for viscous fluids in pipe fittings such as contractions, elbows, orifices and valves. Often experimental studies do not agree with one another or with analytical and numerical studies. Thus more data is needed which can be used for validation and design purposes (Fester *et al.,* 2008). Significant contributions have been made to a sadly neglected topic in literature, determining loss coefficient data for non-Newtonian fluids flowing in complex geometries, by Fester *et al. (*2007), Mbiya *et al.* (2007) and Fester *et al. (*2008). A large database of loss coefficients for different ratios of sudden contractions as well as different diaphragm valve openings were provided for a wide range of Newtonian and non-Newtonian fluids, which is now available for those who are investigating energy losses through complex geometries. Turian *et al.* (1998) investigated flow of concentrated non-Newtonian slurries and provided useful friction loss data in various geometries such as pipe bends, fittings, valves and venturi meters. Nigen and Walters (2002) also provided experimental data (at various flow rates and contractions ratios) for polymer solutions in both axisymmetric and planar contractions. Results provided scope for a new computational model on contracting flow problems for constant viscosity and elastic fluids. Fu and Ger (1999) used a combination of experimental data and models to develop a novel method for accurate determination of characteristics of compressible gas flow through valves.

2.3.3.2 Open channel

Significant contributions to highly viscous non-Newtonian open channel flow have been made by Haldenwang (2003). A substantial database as well as experimental procedures for non-Newtonian rectangular open channel flow was provided by Haldenwang and Slatter (2006), which can be used for efficient design of open channels in the mining industry. Haldenwang *et al.* (2002) and Haldenwang (2003) developed empirical models for laminar and turbulent flow of non-Newtonian fluids exhibiting a wide range of rheological properties. A detailed review of Newtonian and non-Newtonian rectangular open channel flow was given by Alderman and Haldenwang (2007). It was concluded that further research is required to eliminate discrepancies between predicted and actual velocities.

The nature of the free surface flow in this research work was delineated by evaluating the Reynolds number proposed by Haldenwang *et al.* (2002) and Haldenwang and Slatter (2006) for the flow of Herschel-Bulkley model fluids:

$$Re_H = \frac{8\,\rho\,V^2}{\tau_y + K\left(\frac{2V}{R_h}\right)^n}. \tag{2.18}$$

Note that Equation 2.18 includes the limiting cases of power-law fluid ($\tau_y = 0$), Bingham plastic fluid ($n = 1$) and Newtonian fluids ($n = 1$ and $\tau_y = 0$).

De Kee *et al.* (1990) developed new theoretical equations which describe the flow behaviour of viscoplastic fluids exhibiting a yield stress in open channel (free surface) laminar sheet flow. The point velocity distribution across the flow depth is given by (see Figure 2.11):

$$V_z^{>} = \frac{nK}{(n+1)\rho g \sin\alpha}\left(\frac{\tau_0}{K}\right)^{\left(\frac{n+1}{n}\right)}\left(1-\frac{\tau_y}{\tau_0}\right)^{\left(\frac{n+1}{n}\right)}\left(1-\left(\frac{\tau_y}{\tau_0}\,\frac{n-\frac{\tau_y}{\tau}}{n-\frac{\tau_y}{\tau_0}}\right)^{\left(\frac{n+1}{n}\right)}\right) \tag{2.19}$$

for $x_0 \leq x \leq h$ and

$$V_z^{<} = \frac{nK}{(n+1)\rho g \sin\alpha}\left(\frac{\tau_0}{K}\right)^{\left(\frac{n+1}{n}\right)}\left(1-\frac{\tau_y}{\tau_0}\right)^{\left(\frac{n+1}{n}\right)} \tag{2.20}$$

for $0 \leq x \leq x_0$.

The formulae proved to be mathematically and physically rigorous within the assumed conditions (laminar sheet flow, steady state, fully developed flow, no wall-slip). Good agreement was found between experimental data, but more fundamental work involving model suspensions is needed for validation of theoretical predictions.

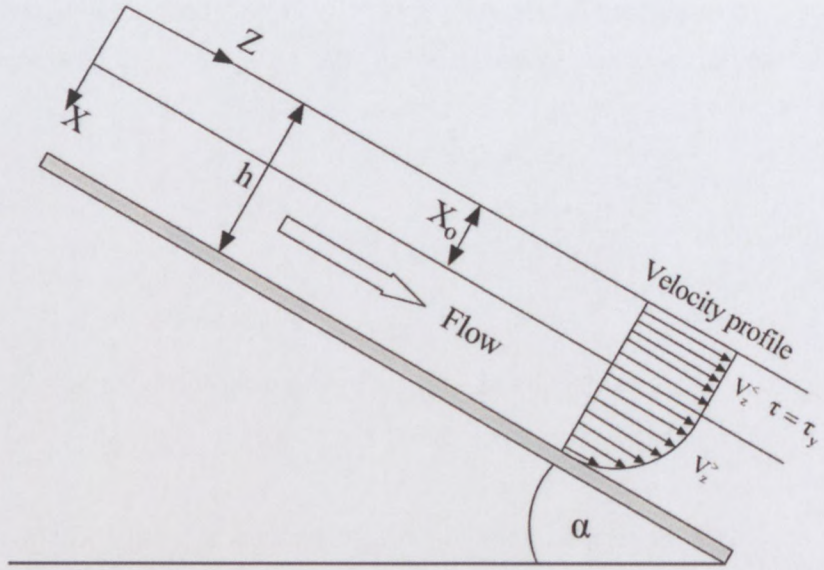

Figure 2.11: Schematic of flow configuration (De Kee *et al.*, 1990)

2.3.4 Techniques for flow measurements in complex geometries

In spite of a considerable effort in recent years to resolve difficulties with the simulation of complex flow problems, some outstanding issues remain. The reason for this is that more detailed observations of velocity and pressure fields are experimentally not possible (Binding *et al.*, 2006). Also, equations used for theoretical analysis of complex flows are sometimes dramatically simplified and the implications of these simplifying assumptions need to be quantified. Even assuming that the simplifications are plausible, local data of different complex flows is needed before representative forms of flow equations can be constructed (Thompson *et al.*, 1999). Numerical results are also often compared to experimental visualisation techniques such as digital or analog (film-based) photography (Baloch *et al.*, 1996; Nigen and Walters, 2002; Ganvir *et al.*, 2007) or empirical models (Edwards *et al.*, 1985; Turian *et al.*, 1998; Fu & Ger, 1999; Pal & Hwang, 1999; Podolsak *et al.*, 1997; Fester *et al.*, 2007; Lubansky *et al.*, 2007; Fester *et al.*, 2008). However, it does not provide detailed quantitative information of the complex flow behaviour that can be used for developing more accurate constitutive models. A new generation of experiments that map velocity and/or concentration fields in more complex flows would prove useful e.g. flow in contraction, expansion, open channel, valve (contraction-expansion) and other complex geometries (Stickel & Powell, 2005).

2.3.4.1 LDA and other techniques

According to literature there are many different techniques for studying flows of multiphase and complex fluids. Laser Doppler Anemometry (LDA) is a very well established technique (Bopp *et al.,* 1989) that possesses a high time and spatial resolution (Frank *et al.,* 1996). This technique has previously been used to verify pulsed ultrasound velocity measurements (Shandas *et al.,* 1995; Shekarriz & Sheen, 1998) for medical and industrial applications. In some cases good comparisons can be made between UVP and LDA, such as flow measurements in concentrated pulp suspensions in pipe flow (Wiklund *et al.,* 2004). However, LDA cannot be used in opaque fluids as well as highly concentrated suspensions without considerable effort to match refractive indices of the suspended phase and the liquid (Teufel *et al.,* 1992; Powell, 2008). Particle Image Velocimetry (PIV) is also a powerful technique which can give two-dimensional velocity vector field of complex flow patterns (Rothstein and McKinley, 2001). However, in another study it was concluded that the accuracy is much lower than that of a velocity profile sensor such as LDA or UVP (Shirai *et al.,* 2007). Although PIV has made drastic progress recently, it still cannot be applied to opaque fluid systems and has the requirements for transparent and thin measuring cells (Obayashi *et al.,* 2008). Other velocity profile measurement techniques such as Electrical Impedance Tomography (EIT) (Etuke & Bonnecaze, 1998), x-ray radiography and neutron radiography (Mondy *et al.*, 1986) are also available, but experimental and cost limitations forces one to consider an alternative approach. Another technique which is highly accurate and versatile is Magnetic Resonance Imaging (MRI), but the experimental apparatus are too expensive and requires that the apparatus used to be designed around the particular application, thus making it difficult to implement (Powell *et al.,* 1994; Powell, 2008). Also, the requirements for transparent and thin measuring cells, for example made from glass, makes MRI an impractical solution for industrial applications.

2.3.4.2 Ultrasonic Velocity Profiling

UVP is an ideal method for studying non-Newtonian flow in pipelines and complex geometries, as it is inexpensive, portable, works with opaque systems and easy to implement relative to other available techniques (Takeda, 1999; Powell, 2008). Some studies have been conducted on complex flow measurements in complex geometries using UVP.

Bouillard *et al.* (2001) conducted velocity measurements in stirred tanks of Newtonian and non-Newtonian fluids for laminar and turbulent regimes. Although LDA was used for reference measurements, it was not possible to measure in opaque fluid mixtures, and as a result UVP was found to have adequate accuracy (+/- 30%) for complex velocity measurements in the industrial environment. Ein-Mozaffari and Upreti (2009) used CFD as well as UVP to optimise a mixing system for yield pseudoplastic fluids. It was found that the numerical results were in good agreement with that obtained from UVP. Obayashi *et al.* (2007) constructed a system for two-dimensional velocity vector measurements using a normal ultrasonic transducer as a receiver and a focusing transducer as both an emitter and receiver. Two directional velocity components of a periodic velocity fluctuation in a wake of a rotating cylinder were measured. According to results obtained the applicability of this measurement system has been confirmed. UVP has also been used to measure velocity profiles in opaque pulp fibre suspensions in a cylindrical hydrocyclone by Bergström and Vomhoff (2004). They concluded that UVP provided new information that was not previously available and that it may potentially be useful for verification of multiphase separation models using CFD simulations. Another interesting study was done by Takeda and Kikura (2002) where they investigated mercury flow contained in a stainless steel wall in the configuration of a liquid metal target of a spallation neutron source called SINQ. One and two-dimensional flow maps were successfully produced using UVP and results were found to be feasible.

Ouriev and Windhab (2003) performed two-dimensional time averaged flow mapping for shear-thinning and dilatant suspensions through a cylindrical contraction. The authors summarised the main disadvantages or limitations as follows: flow must be stationary and developed, no velocity information close to wall interfaces, attenuation and absorption problems and the area of the vortexes could not be measured due to transducer installation setup. Another interesting application is the hyperbolic contraction flow method for determining extensional rheological properties of different fluids. Since the geometry of the human throat and hyperbolic contraction is essentially the same, this method can also be used to determine the mouthfeel of semi-solid foods (elongational viscosity). It is also a useful tool for testing the applicability of constitutive equations (Stading, 2008). Zatti *et al.* (2009) measured velocity profiles inside a hyperbolic contraction at multiple positions using UVP to obtain more detailed flow behaviour of non-Newtonian fluids. During this research this measurement method will be improved by using a high precision robotic arm and custom written software.

UVP performs poorly in clear water with low acoustic scattering levels. Artificial seeding of the flow can be used to increase the acoustic scattering level. The effect of the concentration of hydrogen bubble reflectors on the quality of velocity profiles during turbulent flow of water was investigated by Birkhofer (2007). The tests were conducted in a 0.5 m wide and 40 m long open channel setup at EPFL (École Polytechnique Fédérale, Lausanne). This was further optimised by Meile *et al.* (2008) for open channel surge flow measurements. Lemmin and Rolland (1997) evaluated UVP in two different open channel flows at EPFL as well in the field (rivers and lakes). It was concluded that UVP is a good research tool for hydraulic research and for field studies, especially in opaque fluids, and can lead to further understanding of the turbulent water flows. Larrarte (2006) measured velocity fields within sewers using UVP method. The main objective was to collect measurement data for validation of numerical simulations. Good experimental data was obtained for initial approximations in the numerical part of the project. Recently, Peters *et al.* (2010) investigated the pressure-driven flow of a suspension of spinning particles in a rectangular channel. The particles were dispersed in a slightly conducting oil and were subjected to an electrical field in order to polarize the particles for rotation (Quincke rotation). Good agreement between results obtained from UVP and theoretical velocity distributions was obtained for all test conditions.

2.4 RHEOLOGY

Rheology is defined as the science of deformation and flow of matter. "The term 'rheology' originates from the Greek: 'rheos' meaning 'the river', 'flowing', 'streaming'. Thus, rheology is literally 'flow science'" (Mezger, 2002). Fluids can be classified into two types namely: Newtonian and non-Newtonian fluids. A fluid is characterised as a non-Newtonian fluid when the relationship between the shear stress and shear rate is non-linear. Figure 2.12 depicts different non-Newtonian fluids as a function of shear rate vs. shear stress, also known as a rheogram. A flow curve for a Newtonian fluid is also shown. Note the linear relationship between shear rate and shear stress, which also passes through the origin. More information on different flow regimes, fluid behaviour, non-Newtonian models, rheometry for non-Newtonian models and pipe flow can be found in Steffe (1996), Kotzé (2008) and Norton (2011).

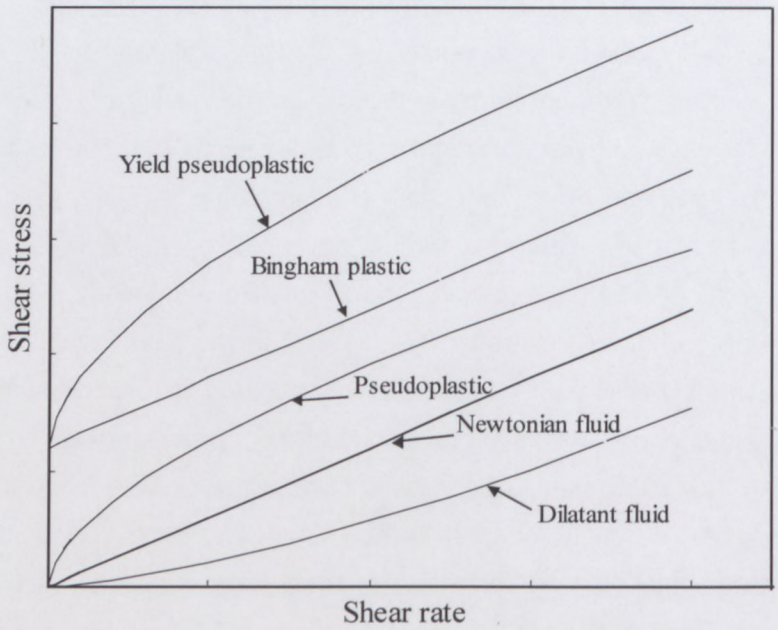

Figure 2.12: Flow curves for Newtonian and non-Newtonian fluids (Chhabra & Richardson, 1999)

2.4.1 Non-Newtonian pipe flow

There are three different flow regimes, namely laminar, turbulent and transitional flow. Osborne Reynolds was the first to investigate these flow regions and developed the Reynolds number, which is proportional to the ratio between inertial and viscous forces (Chhabra & Richardson, 1999). Slatter and Lazarus (1993) formulated a new Reynolds number, Re_2, for non-Newtonian fluids:

$$Re_2 = \frac{8\rho V^2}{\tau_y + K\left(\frac{8V}{D}\right)^n}. \tag{2.21}$$

The use of Re_2 proved to be a reliable predictor of the laminar / turbulent transition and is recommended for design purposes (Slatter & Lazarus, 1993). During this research work Equation 2.21 was used to determine the flow regime for non-Newtonian fluid flow.

For fully developed flow, the relationship between the wall shear stress τ_w, the volumetric flow rate Q and the shear stress τ, are as follows:

$$\frac{Q}{\pi R^3} = \frac{1}{\tau_w^3}\int_0^{\tau_w} \tau^2 f(\tau) d\tau \,, \tag{2.22}$$

where $\tau_w = \frac{R}{2}\left(\frac{-\Delta P}{L}\right)$ and $\left(\frac{-\Delta P}{L}\right)$ are equal to the pressure drop per unit length of the pipe. The shear stress τ at any radius r in the pipe is:

$$\tau = \frac{r}{2}\left(\frac{-\Delta P}{L}\right). \tag{2.23}$$

For a given material, a graph of $\frac{Q}{\pi R^3}$ vs. τ_w gives a unique line for all values of R and $\frac{-\Delta P}{L}$ (Chhabra & Richardson, 1999).

The shear rate at the pipe wall is given as $\frac{4Q}{\pi R^3}$ or $\left(\frac{8V}{D}\right)$. The problem with tube viscometry is that the $\left(\frac{8V}{D}\right)$ values obtained are not the true shear rate values but the wall shear rate values for a non-Newtonian fluid. Thus, this pseudo shear rate has to be transformed to the true shear rate, $(\dot{\gamma})$.

According to Chhabra & Richardson (1999), for flow curves of unknown form, Equation 2.22 (after some manipulation) yields:

$$f(\tau_w) = \left(\frac{8V}{D}\right)\left\{\left(\frac{3}{4}\right) + \frac{d(\log 8V/D)}{4d(\log \tau_w)}\right\}. \tag{2.24}$$

Various forms of this equation are used, a common form being:

$$\dot{\gamma}_w = \dot{\gamma}_{wN}\left(\frac{3n'+1}{4n'}\right), \tag{2.25}$$

where $\dot{\gamma}_{wN} = \left(\frac{8V}{D}\right)$.

The expression for n' is:

$$n' = \frac{d(\log \tau_w)}{d(\log \dot{\gamma}_{wN})}. \tag{2.26}$$

From Equation 2.26 it can be seen that n' is obtained by plotting a log-log pseudo shear diagram with τ_w versus $\dot{\gamma}_{wN}$ for the laminar flow region, and then obtaining the slope of the tangent of the graph. The slope of this pseudo shear diagram will only be approximately constant if the fluid is a power-law fluid (Chhabra & Richardson, 1999). A detailed Rabinowitch-Mooney transformation procedure for pipe viscometer data can be found in Haldenwang (2003). Non-Newtonian fluids can be described by different rheological models and is discussed in the next sections.

2.4.2 Rheological models

2.4.2.1 Power-law model

This is the most common rheological model used to characterise a pseudoplastic or shear-thinning fluid, where viscosity decreases with increasing shear rate. The mathematical model for this kind of behaviour is:

$$\tau = K(\dot{\gamma})^n, \tag{2.27}$$

where τ is the shear stress and $\dot{\gamma}$ the shear rate. In this equation, K and n are two empirical curve-fitting parameters and are known as the fluid consistency coefficient and the flow behaviour index respectively (Chhabra & Richardson, 1999).

Rheological properties have a strong influence on the shape of velocity profiles in pipe flow. Thus it is important to understand these profiles for calculating rheological parameters of a particular fluid. Equation 2.27 can be integrated (assuming zero velocity at the pipe wall) to give the radial velocity distribution:

$$v = \left(\frac{nR}{(1+n)}\right)\left(\frac{R\Delta P}{2LK}\right)^{\frac{1}{n}}\left(1-\left(\frac{r}{R}\right)^{1+\frac{1}{n}}\right), \tag{2.28}$$

where r is the radial position along the pipe radius R and ΔP the pressure drop across the length L.

2.4.2.2 Bingham plastic and Herschel-Bulkley model

Some non-Newtonian fluids do not flow until a critical yield stress τ_y is exceeded. The application of a stress greater than the yield stress results in the formation of a moving plug in the centre of the pipe. A Bingham plastic model is the simplest model which describes the flow behaviour of a non-Newtonian fluid with a yield stress.
The flow curve of a yield-pseudoplastic fluid (see Figure 2.12) can be described using the Herschel-Bulkley model:

$$\tau = \tau_y + K(\dot{\gamma})^n. \tag{2.29}$$

The radial velocity profile can be determined by integration of Equation 2.29:

$$v = \left(\frac{n}{(1+n)}\right)\left(\frac{\Delta P}{2LK}\right)^{\frac{1}{n}}\left(\left(R-R_{plug}\right)^{1+\frac{1}{n}} - \left(r-R_{plug}\right)^{1+\frac{1}{n}}\right), \tag{2.30}$$

where $R_{plug} = \dfrac{2L\tau_y}{\Delta P}$ is the plug radius.

It will be noted that the Herschel-Bulkley model can easily be modified to describe Newtonian, Bingham, pseudoplastic and yield-pseudoplastic behaviour (Steffe, 1996).

2.5 THE UVP-PD RHEOMETRIC METHODOLOGY

Understanding the flow behaviour and flow dynamics of a complex multiphase fluid system at any point in the production or pipeline where the fluid is in motion is essential. In all processing plants, fluids need to be transported in pipes between different processing units (Wiklund, 2007). Predicting the flow behaviour using theoretical models can lead to more cost effective and efficient pipeline designs. The rheological characterisation of the fluids has a direct effect on the effectiveness of flow predictions in pipes or pipe fittings (Haldenwang, 2003). Commercial process rheometers are sometimes unreliable due to the direct influence on the microstructure of measuring geometries and the invasive methods on which they are based (Ouriev & Windhab, 2002). Certain authors believe that capillary or tube viscometers are best suited for determining rheological parameters in-line as the geometries are similar to a pipeline (Lazarus & Slatter, 1988). However, tube viscometry is a procedure which is very time consuming, even under conditions with no random errors, and design engineers simply do not have the luxury of unlimited time to entertain the diversities of experimental research (Haldenwang *et al.* 2006).

The UVP-PD methodology allows the determination of rheological parameters by combining Ultrasonic Velocity Profiling (UVP) with Pressure Difference (PD) measurements. It is an alternative method for in-line, non-invasive rheological characterisation of opaque complex fluid systems and is a promising candidate in the search for new in-line rheometers.

The UVP-PD methodology consists of several components, starting with an instrument designed to measure profiles using a pulsed ultrasonic technique. Accurate ultrasonic transducers, flow adapters for transducer installation, pressure sensors, data acquisition schemes as well as software development and data processing are required for this in-line rheometric method. Regardless of the actual set-up (experimental flow loops and ultrasound equipment), the UVP-PD methodology requires several processing steps. A flowchart of the data acquisition and processing steps involved in an in-line rheometer based on the UVP-PD methodology is given in Figure 2.13. More information on the UVP-PD methodology and experimental setup can be found in Steger (1994), Muller *et al.* (1997 & 1998), Ouriev (2000), Birkhofer (2007), Wiklund (2007) and Norton (2011).

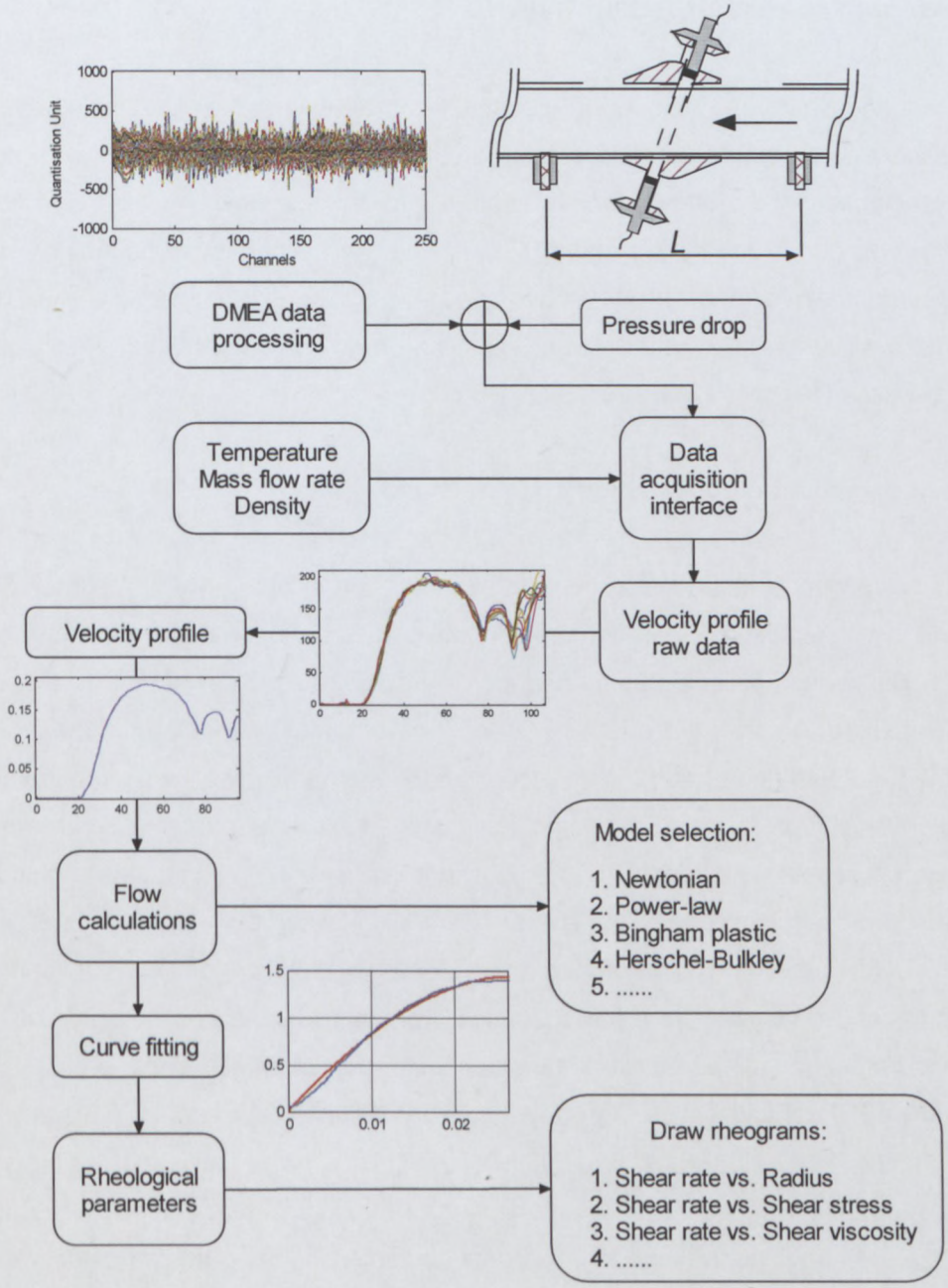

Figure 2.13: General flowchart of the UVP-PD methodology (adapted from Wiklund, 2007)

The processing steps may, of course, vary from one application to another, depending on what kind of information the operator wants in each particular situation.

2.5.1 Research studies based on UVP-PD

The non-invasive technique of measurement of velocity profiles using UVP and pressure drop has been investigated by many authors for in-line rheological characterisation of non-Newtonian fluids in laminar pipe flow. An extensive literature study was conducted by Wiklund (2003). An overview of the investigations on UVP-PD measurements carried out by various research groups is also discussed in Birkhofer (2007), Wiklund (2007) and Kotzé (2008). Therefore, only recent work (2007 – present) is discussed in the following sections.

2.5.1.1 Development and optimisation

Extensive work in the development and optimisation of the UVP-PD methodology was done in a scientific collaboration project between SIK - The Swedish Institute for Food and Biotechnology, Göteborg, Sweden and ETH - Swiss Federal Institute of Technology, Zurich, Switzerland. The work was made by Birkhofer (2007), Wiklund (2007) and Wiklund *et al.* (2007). The extended methodology allows measurements of radial velocity profiles and rheological properties in-line, in real-time. The method has been successfully tested with a wide range of model and industrial fluids, under realistic processing conditions. The software developed, based on Matlab® and the UVP-DUO Active X libraries driver, provides a complete tool with a GUI for data acquisition from all hardware devices (pressure sensors, velocity of sound measurements, temperature). An extended and complete commercial UVP-PD software, RheoFlow™ was then developed by Wiklund (Wiklund and Stading, 2008; Wiklund *et al.*, 2010) which is capable of rapid data processing and can serve as a basis for in-line real-time process monitoring of rheological properties. Direct access to DMEA data enables the user to implement custom velocity estimation algorithms, such as FFT based algorithms. Depending on the application and flow structure, time and frequency domain algorithms can be selected for velocity estimation. Spectral analysis proved to be valuable as it provided quality information such as signal amplitude and signal-to-noise ratio, but also simplified identification of signal artifacts and causes of velocity errors. The method developed for measuring velocity of sound as well as attenuation of test fluids provides accurate measurement of rheological properties under real process conditions. Furthermore, the method provides a tool for measuring solids concentration of fluids in-line. Finally, Birkhofer (2007) and Wiklund (2007) concludes that the accuracy of profile measurement could be further improved by either

introducing new transducer technology and/or by investigating the sample volume and deconvolution of profiles, which would be relevant for the rheological calculations especially in the vicinity of the near pipe wall interface. This research work attempts to further increase the accuracy of experimental velocity profiles and the UVP-PD methodology by introducing new transducers as well as advanced signal processing techniques.

2.5.1.2 Food suspensions

Young *et al.* (2008) successfully measured rheological properties in-line of complex, opaque fat blends using the UVP-PD method. Model systems of 25% Akomic, 75% rapeseed oil; and 25% Akomic, 74% rapeseed oil and 1% Grindsted® Crystalliser 110 were compared under real process conditions with UVP-PD. Results indicated that the sample containing the crystalliser had twice the viscosity of the control. In-line results are in good agreement with off-line results and it is now possible to investigate the physics of fat blends under real, dynamic conditions.

Birkhofer *et al.* (2008a) investigated the dynamic response of the cocoa butter shear crystallisation process to a step reduction in temperature using the UVP-PD method. In addition, the velocity of sound, attenuated amplitude and temperature was continuously recorded by using newly developed software. It was possible to monitor the crystallisation process by measuring the speed of sound as well as the flow behaviour (shear-thinning) using the new software. Birkhofer *et al.* (2008b) performed in-line tests on highly concentrated model suspensions which consisted of PA 12 particles in rapeseed oil. Good comparison was found between shear viscosities measured off-line and in-line using the UVP-PD method.

Wiklund and Stading (2008) successfully tested the in-line rheometric method (UVP-PD) for a range of industrial and model suspensions. Model suspensions included glass beads suspended in glycerol, starch particles suspended in an aqueous syrup solution and polyamide particles in rapeseed oil. Industrial suspensions included cellulose pulp and several kinds of foods. The agreement was good between apparent viscosities measured in-line and off-line using conventional rheometers. However, off-line rheometers failed for particle sizes greater than the shear gap limitation and thus this in-line technique served as a valuable tool for processing monitoring of industrial suspensions with large particle sizes.

High speed rheological measurements including data processing in real time was performed for the first time by Wiklund *et al.* (2010) for a wide range of concentrated industrial and model suspensions. Very good agreement between off-line and in-line viscometric measurements was found for each system in a comparison over a shear rate range and temperature that matched the conditions in the experimental flow loop.

2.5.1.3 Mineral suspensions

Kotzé *et al.* (2008) investigated the capabilities of the UVP-PD technique for the rheological characterisation of different concentrations of non-Newtonian slurries. The experimental investigation covered a wide range of solids concentrations (5% to 12%), slurry relative densities (1.03 to 1.198), flow rates (0.07 to 0.50 l/s) and yield stresses (0 to 50 Pa). The measurement technique was evaluated and tested with highly concentrated non–Newtonian CMC solutions as well as bentonite and kaolin mineral suspensions. The agreement between the UVP-PD method, tube viscometry and conventional rheometry was found to be good (within 15%) for all of the highly concentrated mineral suspensions investigated over a given range of shear rates.

2.5.2 Current limitations with the UVP-PD methodology

The UVP-PD methodology has been successfully applied to a wide range of fluid systems, however, there are still a few problems remaining. Even today, UVP measurements are almost exclusively being made with simple transducer setups where the transducer is placed in flush with the liquid or through a thin transparent Plexiglas pipe. The main problem is the distance between the ultrasonic transducer's surface and focal point, the near-field, where the pressure field is highly irregular and thus measurements are prevented in this region. This has lead to simple flow adapter designs for transducer housing that enable the transducer surface with direct contact to the test fluid, thus ensuring maximum ultrasonic energy transfer into the fluid system as well as eliminating any beam refraction. However, this setup leaves a cavity before the wall interface which causes measurement uncertainty due to fluid flow and increased velocities beyond the actual pipe wall.

It is possible to measure through material layers, thus eliminating the cavity problem, but ultrasonic beam refraction and absorption causes errors in parameters such as the Doppler angle and sound speed, and reduces penetration depth in attenuating fluids. Several methods for correcting the measured velocities in the near wall region have been proposed, but with limited success (Wunderlich & Brunn, 2000; Xu & Aidun, 2005). Also, it has been shown by Messer and Aidun (2009) that the physical ultrasonic beam shape changes when measuring through material layers. If the acoustic properties of the transducer change, more errors due to increased sample volume dimensions (widening of ultrasonic beam) are introduced into the velocity measurement.

Determining the actual wall interface (when measuring through material layers) or liquid-wall interface (when measuring with direct contact to test fluid) can become extremely complicated, especially when measuring velocity profiles with limited spatial resolution or when attenuation distorts the quality of near wall velocity data. It has been shown that by changing the wall position by less than 0.37 mm (or one channel) the rheological parameters determined using the UVP-PD method vary significantly (Kotzé, 2008; Wiklund *et al.,* 2007). The problem of uncertain wall positions has forced users to obtain rheological data of the test fluid using other methods such as off-line rotational rheometry in order to adjust wall interface positions that yield the correct fluid properties. This defies the purpose of the UVP-PD methodology, as one would like to develop an instrument which can measure rheological properties without any *a priori* knowledge of the fluid characteristics.

This problem could be reduced by the introduction of new ultrasonic transducers incorporating a delay line, which is discussed in more detail in Chapter 3. The delay line is a material optimised for beam forming that contains the near field distance. This delay line should be fixed ahead of the transducer and in flush with the pipe wall, thus making it possible to have the focal point of the ultrasound beam at the wall interface. This technology will minimise the divergence angle and the precision of velocity profile and wall shear rate measurements would be increased. In addition, the experimental problem of sedimentation and clogging of the cavities ahead of the transducers, as found by Birkhofer *et al.* (2008) and Wiklund (2007), would be solved. The UVP-PD method has recently been optimised to include simultaneous real-time measurements of rheological properties and Solid Fat Content (SFC) of complex fat blends under true dynamic processing conditions (Wassell *et al.*, 2010). The complete system developed

by SIK includes the latest delay line transducer technology. A transducer of this kind has been evaluated and tested for complex flow as well as in-line rheometric measurements during this research.

2.6 CONCLUSION

The UVP system has important advantages over alternative point-velocity measurement techniques. It has been shown how erroneous velocity data close to wall interfaces due to the finite size of the sample volume and measurement through material wall layers can be removed using a deconvolution procedure. Despite the improved accuracy deconvolution has not been widely used in the medical field. Also, to the author's knowledge, it is believed that this algorithm has never been applied for measurements in the fluid engineering industry. This may be a result of its complexity and because it has not been evaluated for different materials and under a full range of flow conditions.

UVP has already been used for flow mapping in complex geometries such as stirred tanks, open channel, contractions, liquid metal target of neutron spallation source configuration and cylindrical hydrocyclone. However, it has not been used for complex flow measurements of opaque non-Newtonian fluid suspensions in a diaphragm valve and open channel before. According to literature, there is a lack of experimental data for validation of theoretical estimations in different complex geometries. Energy losses are usually calculated using design equations based on assumptions such as the shape of the velocity profile inside pipe fittings, which is critical in determining the quantity of kinetic energy and momentum that the fluid has. More detailed quantitative experimental data would assist in developing accurate constitutive flow equations as well as efficient pipeline designs. The UVP system should be considered as an important tool for assisting in complex flow problems by validating theoretical predictions with experimental results. Therefore, this system needs to be evaluated and if necessary, optimised in order to increase measurement accuracy as much as possible. With detailed and accurate experimental flow data available, it should be possible to develop more accurate flow models using CFD in combination with measured results.

In-line rheological characterisation can be achieved by using UVP in combination with Pressure Difference (PD) measurements to obtain the complete flow curve from a single measurement. This method has been evaluated and tested over a wide range of model and industrial fluid suspensions. However, there are still some outstanding problems that remain regarding this methodology. These problems could be reduced by the introduction of a special delay line transducer.

From the literature it can be concluded that the UVP technique has not yet been thoroughly studied nor optimised for accurate measurement of rheological properties as well as non-Newtonian flow behaviour in complex geometries and thus this proposed research should be considered as an important contribution to both the adaptation and improvement of this technique as well as its application in the fluid engineering industry.

CHAPTER THREE

METHODS OF INVESTIGATION AND APPARATUS

CHAPTER THREE

METHODS OF INVESTIGATION AND APPARATUS

3.1 INTRODUCTION

In this chapter, the apparatus used for data acquisition in the evaluation, optimisation and validation of the UVP system and UVP-PD rheometric method are described.

Some of the experimental tests were conducted at the Swedish Institute for Food and Biotechnology (SIK), Gothenburg, during November 2009 and April 2010. The experimental flow loop fitted with a hyperbolic contraction and other equipment used for acoustic characterisation of ultrasonic transducers are described.

All of the apparatus and instruments were used specifically for this project in order to establish the following:

- Non-Newtonian flow behaviour measurements in three complex geometries (hyperbolic contraction, open channel and 50% open diaphragm valve) using different transducers and advanced signal processing techniques.
- High resolution acoustic mapping of various ultrasonic transducers, including a new delay line transducer.
- Velocity profile measurements using new transducers, different parameter settings and custom velocity estimation algorithms.
- Accurate in-line rheological characterisation of all the slurries, using the tube viscometer (three pipes).
- Conventional off-line rheological characterisation of the slurries, using a rotary rheometer.
- In-line rheological characterisation using the UVP-PD rheometric method in three different pipe diameters (comparison between optimised system and methodology using conventional transducers).

Materials that were tested were water for calibration purposes, kaolin clay in water mineral suspensions, bentonite in water suspensions and carboxymethyl cellulose (CMC) in water solutions, all at various concentrations.

3.2 APPARATUS

The different apparatus used for gathering the experimental data for the work presented in this thesis were three different flow loops (tube viscometry and UVP-PD), off-line rheometer and the ultrasonic instrumentation. A specially designed diaphragm valve was constructed and is also described.

3.2.1 Rheometers

Two different rheometer models were used for off-line rheological characterisation of the fluids during the research. All the experiments were performed using the Couette (cup and roughened bob, measuring gap = 1.13 mm) geometry. Viscosity was measured over different shear rate ranges, depending on the type of material.

The Swedish Institute for Food and Biotechnology (SIK), Gothenburg

A controlled stress rheometer (Rheologica StressTech, Rheologica Instruments, Lund, Sweden) was used to obtain flow curves for the CMC 2.63% w/w solutions during the hyperbolic contraction study at SIK. The rheological parameters were used to calculate Reynolds numbers for non-Newtonian pipe flow as well as theoretical velocity profiles for comparison with results obtained using UVP.

Material Science and Technology (MST), Cape Town

The conventional rheometer used at the Material Science and Technology (MST) group was a Paar Physica MCR300 (Anton Paar, Randburg, South Africa, www.advancedlab.co.za) instrument which was equipped with an air bearing. Flow curves were created for CMC, bentonite and kaolin suspensions and the results were compared with in-line tube viscometry as well as with that obtained using the UVP-PD method.

3.2.2 Experimental flow loops

Various experimental flow loops were used during this research. The flow loops at the FPRC were equipped with specially designed flow adapters, which enabled in-line rheometric measurements in three pipe diameters using the UVP-PD methodology.

3.2.2.1 Contraction flow loop (SIK)

The flow loop at SIK was fitted with a hyperbolic contraction and consisted of a stainless pipe of internal diameter 48.5 and 22.5 mm which was connected to a 100 l tank. A pump (Alfa Laval, ALC1-D/150, 2 kW) was installed along with a flow meter (Endress & Hausser Discomag DMI 6531, accuracy 0.017 l/s between flow rate range of 0.25 l/s and 4.42 l/s for aqueous suspensions). The upstream straight pipe section was 50 D in length to ensure fully developed flow before the contraction section. The hyperbolic contraction is discussed in more detail in Section 3.3.5.

3.2.2.2 Flume flow loop (MST)

The flume is 10 m long with a width of 300 mm and depth of 300 mm with a partitioning section that can be fitted to the centre of the flume to form a 150 mm wide flume. The slope of the flume can also be changed using an electrically powered hydraulic ram fitted to the flume, which can tilt the flume from 0 to 5 degrees. The inlet tank has a capacity of 600 l and is fitted with baffles to streamline the flow. The mixing tank has a capacity of 200 l and is fitted with an electrically driven mixer which runs continuously during the experiments. Two digital vernier type depth gauges are mounted perpendicular to the flow surface on the flume. The depth gauges are linked electronically to the same personal computer (PC), as used throughout the research, with an RS232 interface. The layout of the flume is schematically depicted in Figure 3.1.

There are two pumps installed in the flume flow loop at the MST, namely the progressive cavity positive displacement pump and the centrifugal pump. The progressive cavity positive displacement pump is driven by a 17 kW motor which is regulated by a variable speed drive. This pump is able to deliver 25 l/s of water through the pipe rig (Haldenwang, 2003). The centrifugal pump is used for high flow rates, as

the progressive cavity positive displacement pump could not obtain turbulence with the denser slurries due to low flow rates. The centrifugal pump is driven by a 37 kW motor and is also regulated by a variable speed drive.

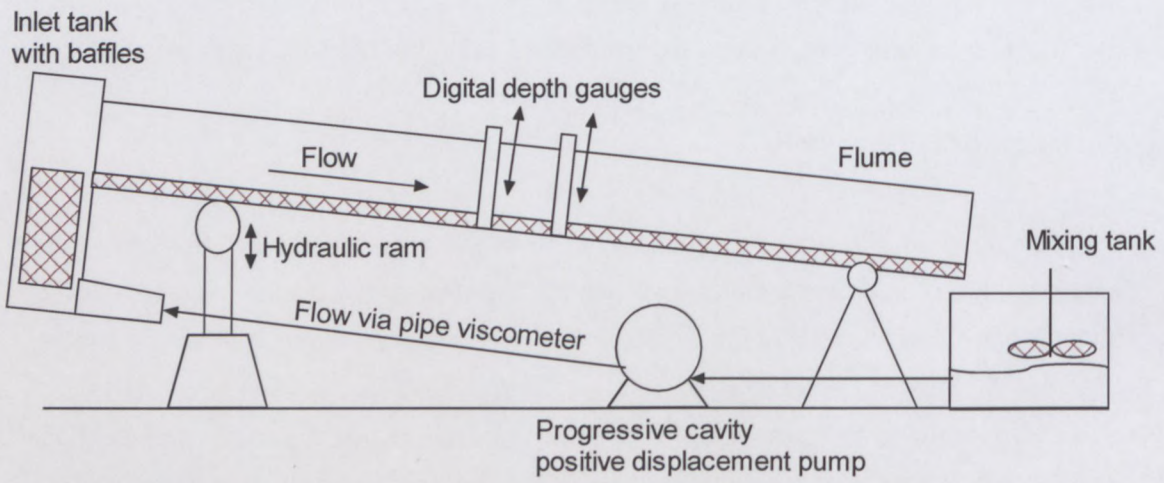

Figure 3.1: Layout of the 10 m tilting flume

The flume rig is also linked to an in-line tube viscometer with three different diameter tubes, namely, 13 mm, 28 mm and 80 mm. Each line is also fitted with an electromagnetic flow meter to measure the flow rate. Pressure tappings that provided static absolute pressure points, so that differential pressure could be measured, were included on each pipeline. The holes drilled into the pipe walls were 3 mm in diameter and the inside of the pipe was cleaned carefully so that no roughness was left at the tapping entry. Pressure adapters made from PVC, were specially designed and fitted to the pressure tappings. Each adapter contained a 3 mm hole at the side, which was fitted with a valve. This was used to flush any air or dirt out of the pressure configuration before measurements were taken, see Kotzé (2008).

In addition, the relative density and temperature of the slurries are measured with a mass-flow meter. The flow depth in the flume is measured at two positions with digital depth gauges which are operated manually. All the data are sent electronically to a data acquisition system which is linked to a PC for further digital processing and storage. A detailed description of the complete flume rig can be found in Haldenwang (2003) and Haldenwang and Slatter (2006). During this research an extra 16 mm stainless steel pipe equipped with pressure tappings and flow adapters for in-line rheometric measurements using the UVP-PD method was linked to the tube viscometer of the flume rig.

3.2.2.3 Valve flow loop (MST)

The valve flow loop consisted of a 100 mm progressive cavity positive displacement pump with variable speed drive (maximum volumetric flow of 11 l/s) to enable tests at different flow rates. Three Polyvinyl chloride (PVC) pipes with inner diameters of 52.8 mm, 43 mm and 23 mm were used for tube viscometry tests. The diaphragm valve is installed in the 52.8 mm pipe which was fitted with a temperature probe and 50 mm flow meter (Krohne IFC 010D – DN40) with an accuracy (for water) of 0.5% of the measured value for $V \leq 0.4$ m/s and 0.002 m/s for $V > 0.4$ m/s. The mixing tank had a capacity of 1700 l and was fitted with an electrically driven mixer that ran continuously during the tests. The rig was also equipped with a weigh tank which is used for flow meter calibration of non-Newtonian fluids. Pressure measurements were conducted using differential pressure transducers (Fuji Electric) with maximum range of 130 kPa and an accuracy of 0.25%. A similar setup can be found in Fester *et al.* (2007). Flow adapters were installed in-line in the 52.8 and 23 mm pipes for rheological characterisation of the test fluids using the UVP-PD methodology. The flow adapter and transducer installation techniques are discussed in more detail in Section 3.2.3.3. Figure 3.2 shows a schematic diagram of the valve rig and Figure 3.3 shows the two flow adapters installed in the UVP-PD flow loops of the valve rig.

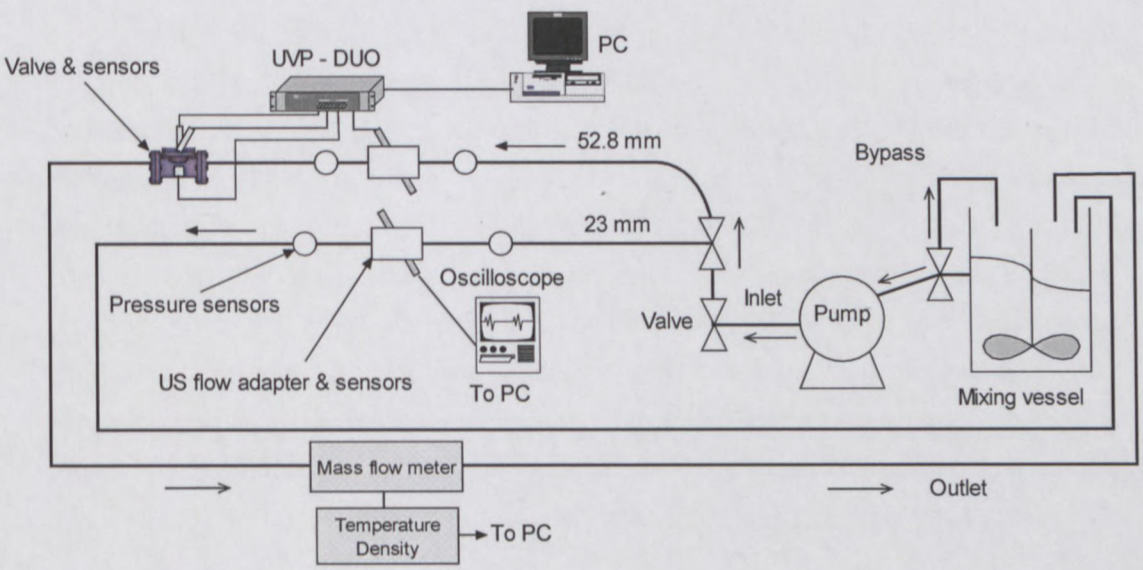

Figure 3.2: Schematic illustration of the valve rig

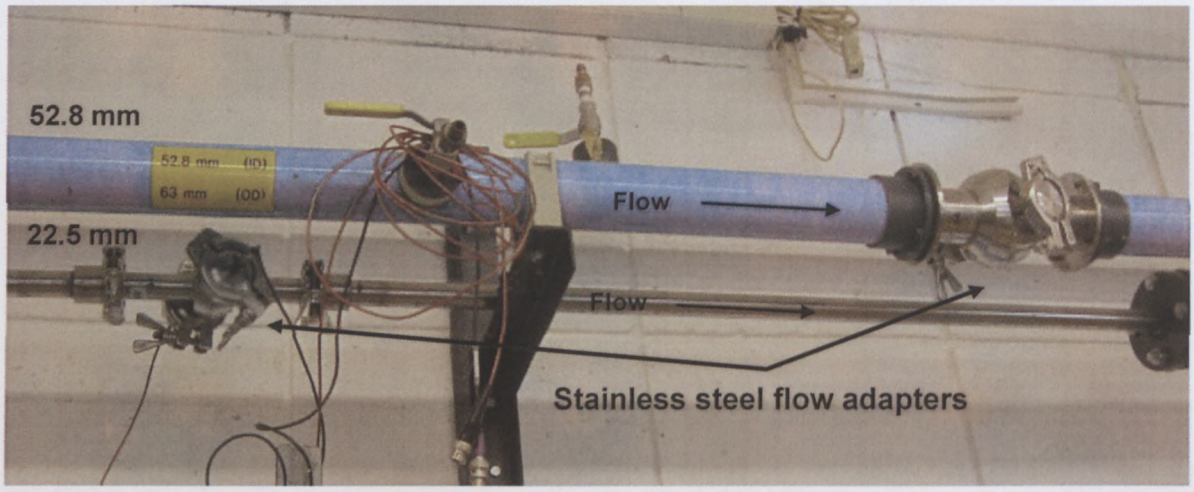

Figure 3.3: Flow adapters installed in UVP-PD flow loop (valve rig)

3.2.3 Ultrasound instrumentation

3.2.3.1 UVP monitor and parameters

A commercial UVP monitor (UVP-DUO) from Met-Flow SA, Switzerland was used during this research. The UVP-DUO is a pulsed wave system, which uses quadrature phase demodulation as directional detection method to obtain the Doppler shift frequency (see Section 2.2.5). The instrument uses a time domain algorithm for the frequency estimation. This algorithm uses an autocorrelation technique described by Barber *et al.* (1985). Detailed description of the specifications, limitations and parameters of this particular UVP monitor can be found in Met-Flow SA (2002), Wiklund (2007) and Birkhofer (2007). The quality of the acoustic velocity profile measurements depends on correct interpretation and optimisation of the fundamental acoustic parameters of the UVP monitor and since extensive tests were conducted with different parameter settings using two ultrasonic transducers (conventional and delay line), a detailed description of these parameters is necessary. The following acoustic parameters can be adjusted for the optimisation of a pulsed ultrasonic velocity profile measurement (refer to Figure 2.6, Section 2.2.4 for more information):

- *Channel width:* This is the length of the measuring or sample volume. The channel width directly influences the spatial resolution of velocity determination.
- *Number of cycles:* Number of wavelengths in the emitted burst. More cycles in a single ultrasonic burst will increase the signal-to-noise ratio, but will also increase the channel width, which decreases the spatial resolution.
- *Channel distance:* This is the distance between the centres of two adjacent channels or measuring volumes in the measuring window. The channel distance must be carefully selected, otherwise channel overlapping will occur.
- *Measurement window:* This is the distance between the first channel and the last one. When more channels are selected, the measurement window increases.
- *Maximum depth:* This parameter is the maximum measurable depth of the ultrasonic beam.
- *Maximum velocity:* This is the maximum measurable velocity and must be optimised in order to prevent aliasing.
- *Number of repetitions:* This is the number of pulses emitted for a single valid velocity profile measurement. More emitted pulses per profile measurement will increase the signal-to-noise ratio, but will also increase the time needed to measure one profile. Thus the time resolution between velocity profile measurements will decrease.
- *US voltage:* The peak-to-peak voltage applied to the transducer is controlled by this parameter setting. The voltage setting depends on the strength of the ultrasound attenuation and the concentration of particle reflectors in the fluid.
- *RF Gain (start, end):* Compensation during amplification of the received echo according to an exponential law. Gain start is the gain setting at the beginning of the reception period and gain end is the gain setting at the end of the reception period.
- *Starting depth:* Distance between the first channel and the surface of the transducer.

There are quite a few parameters which have an influence on each other when a particular parameter setting is modified. This makes the optimisation of the UVP system for ultrasonic velocity profile measurements into quite a difficult challenge. For each unique application, time must be given for selecting the optimum UVP parameters to ensure accurate velocity profile measurements. A detailed description of the important parameters and limitations of the UVP system can be found in Met-Flow SA (2002) and Kotzé (2008). These parameters include aliasing and the sampling frequency, maximum velocity vs. maximum depth, Doppler angle, spatial resolution, size of measuring volumes as well as channel overlapping.

3.2.3.2 Ultrasonic transducers

In this research, plain-wave type conventional ultrasonic transducers supplied by Imasonic, France, which operate in transmitting and receiving mode, were used. A more detailed description, as well as technical information about these ultrasonic transducers, can be found in Met-Flow SA (2002). A new transducer, which incorporate a delay line was designed and manufactured by Signal Processing SA (SPSA), Switzerland. The delay line is a material optimised for beam forming that contains the near-field distance. This delay line is fixed ahead of the transducer and is in flush with the pipe wall, thus making it possible to have the focal point of the ultrasonic beam at the wall interface. In Table 3.1, the geometric dimensions and major acoustic parameters are given for both transducers (conventional), as given by the manufacturers. The sensor housing diameter is 8 mm and the length of the transducer is 60 mm. Transducers with a central basic frequency (f_o) of 4 MHz were chosen in order to obtain good compromise between spatial resolution, which is due to their short wavelength, and penetration depth (less attenuation). The 4 MHz sensors have a fixed active beam diameter of 5 mm and were used for velocity profile as well as sound velocity measurements.

Table 3.1: Imasonic and SPSA ultrasonic transducer specifications

Manufacturer	Centre frequency (MHz)	Active diameter (mm)	Housing diameter (mm)	Overall length (mm)	Near-field distance (mm)	Divergence half-angle (deg)
Imasonic	4	5	8	60	16.9	2.2
SPSA	4	5	8	90	16.9	2.3

The new delay line transducer has similar physical characteristics (length, frequency), except for the fixed material at the transducer's surface. The ultrasonic beam characteristics such as beam angle, beam intensity as well as near-field distance, was evaluated using a hydrophone and high precision robotic setup, and is discussed in Chapter 5. Figure 3.4 shows a schematic diagram of the delay line transducer. Since the transducers are installed at an angle of 20 degrees with respect to the lateral (Figure 3.5), the delay line material is cut at the same angle in order to ensure that the transducer surface is in flush with the pipe wall interface. The surface of the delay line material also has a slight curvature, which is optimised to the internal pipe curvature

(diameter 52.8 mm). Stainless steel discs are fitted to the transducers for ease of installation. The flow adapters have similar discs and the transducers can be installed or removed by simply fitting a tri-clamp around the flow adapter and transducer discs (see Section 3.2.3.3, Figure 3.5).

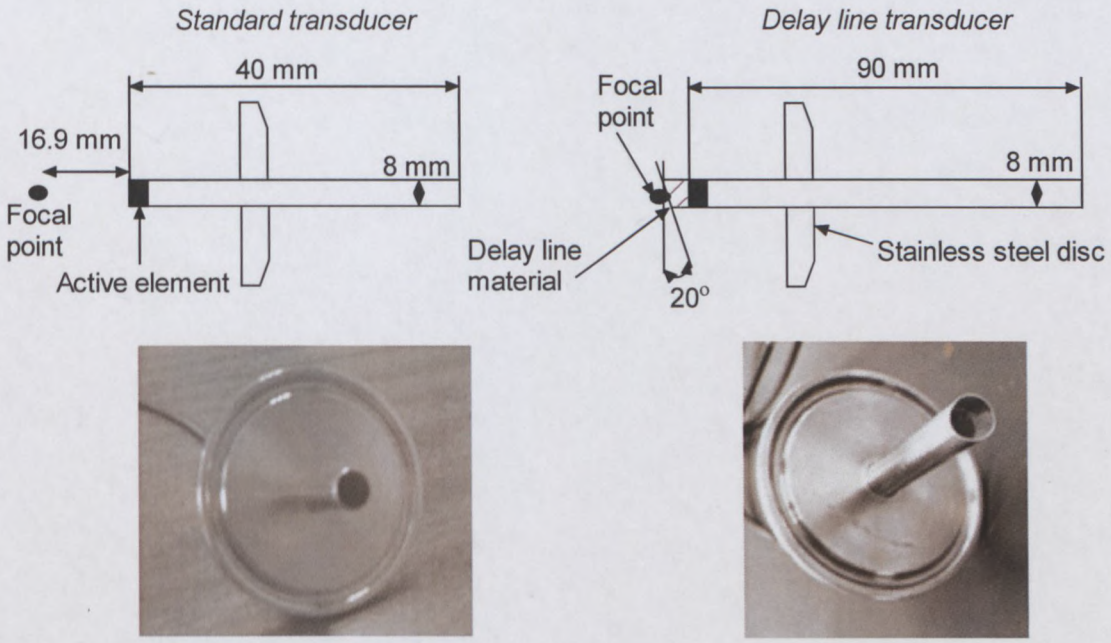

Figure 3.4: Schematic diagram of new ultrasonic delay line and standard transducers

3.2.3.3 Flow adapters and transducer installation

Good and stable positioning of the ultrasound transducer is essential for the successful measurement of velocity profiles. This especially concerns the angle at which the transducer is fixed. In this research, special flow adapters (22.5 and 52.8 mm) made from stainless steel was designed at the Swedish Institute for Food and Biotechnology (SIK) for stable and repeatable positioning of the transducers. The MST at Cape Town is also equipped with two 16 mm flow adapter cells, one designed for delay line transducers and one for conventional transducers. More information on these flow adaptors can be found in Kotzé (2008) and Kotzé *et al.*, (2008). All the flow adapter cells were designed for simultaneous measurements of velocity profiles and acoustic properties in-line. Conventional transducers were mounted in flush with the pipe through cavities with diameters equal to the housing diameter of the transducer, but installed at a distance equal to the near-field length (~17 mm) from the actual pipe wall

interface. This was done to avoid measurements in the near-field zone where the ultrasound field is highly irregular and not fully developed (Wiklund, 2007). However, the new delay transducers were installed in flush with the pipe wall, thus leaving no cavity between the transducer surface and wall interface. This also solved the experimental problem of sedimentation and clogging of the cavities ahead of the transducers, as found by Birkhofer *et al.* (2008) and Wiklund (2007). The schematic layout of the 52 mm flow adapter cell is shown in Figure 3.5.

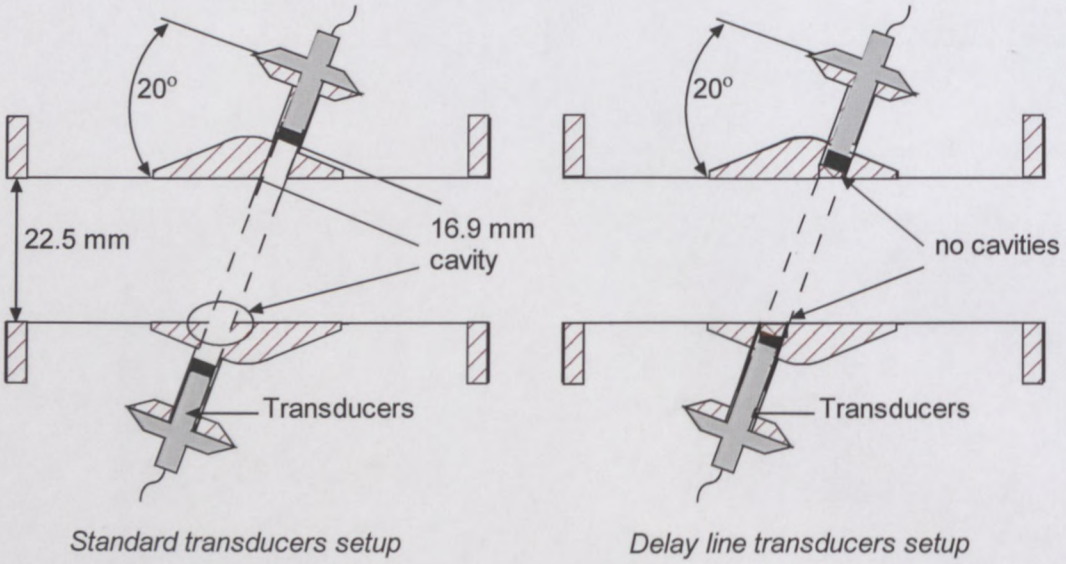

Standard transducers setup *Delay line transducers setup*

Figure 3.5: Schematic illustration of the flow adapter fitted with different transducers

Wiklund and Stading (2008) and Wiklund (2007) showed that this setup is generally the most favourable for simultaneous measurements of velocity profiles and acoustic properties such as in-line velocity of sound. The transducers were mounted in such a way so that the sensors could be removed by simply loosening tri-clamps in order to flush the flow adapter before measurements were taken (in the case of using conventional transducers). This was done in order to remove initial air and to avoid problems with sedimentation and clogging of the cavities in front of the transducers. The setup also makes it possible to re-install transducers in exactly the same position and distance from the liquid-wall interface. Figure 3.6 shows a 22.5 mm stainless steel flow adapter installed in the UVP-PD flow loop at the MST.

Figure 3.6: Flow adapter (22.5 mm) fitted with two transducers

More information on this particular design of flow adapter and transducer setup can be found in Shekarriz and Sheen (1998), Birkhofer (2007), Wiklund (2007), Wiklund *et al.* (2007) and Birkhofer *et al.* (2008a).

3.2.3.4 Needle hydrophones

In order to improve the transducer design it is essential to have detailed knowledge about the acoustic sound field generated by a transducer. A high performance hydrophone (Precision Acoustics Ltd, http://www.acoustics.co.uk) measurement system was used for ultrasonic transducer characterisation. The system is equipped with different diameter (0.075, 0.2, 0.5 and 1 mm) interchangeable probes, DC coupler and a submersible preamplifier. Figure 3.7 shows the setup for measuring acoustic properties using a needle hydrophone: PVdF hydrophones plug into a submersible preamplifier with a nominal voltage gain of 8 dB. The preamplifier also has a 50 Ω output impedance to reduce susceptibility to electromagnetic noise interference. The measured signal gets fed to a 28 V DC coupler, which is connected to the user's measurement system. An Agilent 100 MHz Digital Oscilloscope (Model 54622A) oscilloscope with RS232 connectivity to a PC was used to record data at different points along a two-dimensional grid. In this research a 1 mm needle hydrophone was used in order to measure low pressures 40 mm away from the ultrasonic transducers' surface.

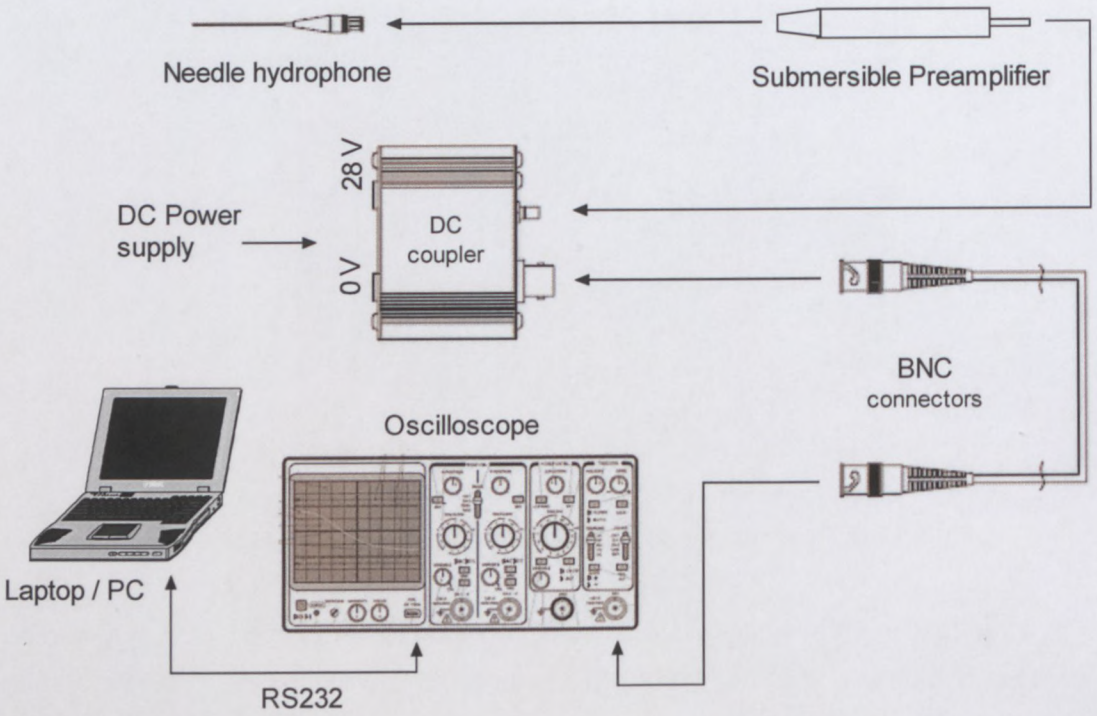

Figure 3.7: Schematic layout of the needle hydrophone setup

3.2.4 Diaphragm valve design and construction

A commercial diaphragm valve (Dynamic Fluid Control Pty Ltd, Johannesburg, South Africa, www.dfc.co.za) was reverse engineered and re-manufactured using a rapid prototyping (3DP™) technique of multilayer printing (Sachs *et al.*, 1993; Jacobs, 1996; Hong *et al.*, 2001). Firstly, a rubber lined valve was cut in half using a 0.35 mm precision blade. The rubber of one half of the valve was burned off in order to expose the cast iron. It was then prepared for 3D imaging by applying white powder to the bare steel surface together with small white paper rings. A special camera was used to determine spatial co-ordinates from the its surface and the image was relayed to a CAD drawing package, Solidworks 2009 (Dassault Systèmes SolidWorks Corp., Concord, MA, USA, www.solidworks.com), thus recreating a 3D image of half of the valve geometry. A mirror image of the same half enabled a full valve and with the valve geometry known, it was then possible to design and create ports in which to install ultrasonic transducers in the valve, especially with regard to, and as close as possible to the valve center. The reason for choosing the centre position is because most of the energy loss occurs at this region. Information from the CAD drawing was relayed to a

3D printer (Z-Corp., Burlington, MA, USA, www.zcorp.com), which was used to grow the three-dimensional object. Figure 3.8 shows the design of the valve fitted with three ports for velocity profile measurements.

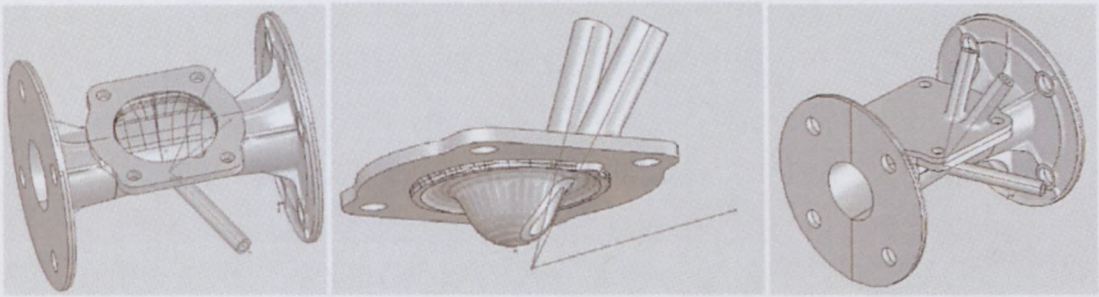

Figure 3.8: Isometric view of three port diaphragm valve design

After the initial evaluation of the three port valve, two more valves were designed by the Adaptronics Advanced Manufacturing Technology Laboratory (AMTL) at the Cape Peninsula University of Technology (CPUT). In this case the valve design was kept the same, except that an extra port for transducer housing was manufactured at the bottom centre of the valve, thus obtaining a total of four measurement lines. The reasons for installing an extra port at the centre line of the valve as well as the positions of the measurement lines are discussed in Section 3.3.7. As mentioned before, two valves were manufactured; one was designed for housing the delay line transducers and the other for conventional ultrasonic transducers. Figure 3.9 shows the valve and ultrasonic transducers installed in the valve flow loop at the MST in Cape Town.

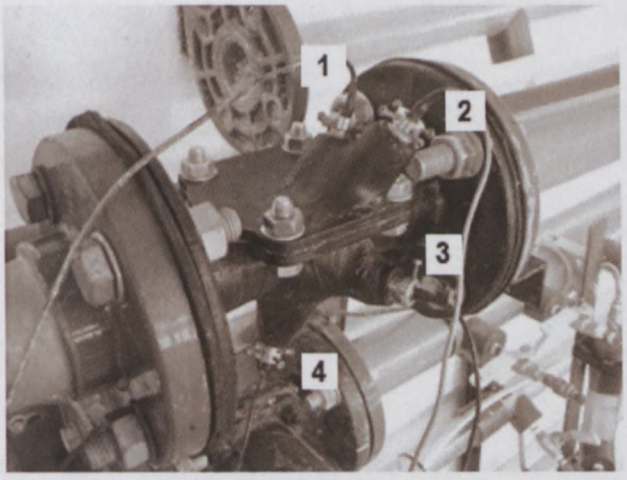

Figure 3.9: Isometric view of four port diaphragm valve installed in the pipe rig

More information on the design and manufacturing procedure of a similar diaphragm valve, but equipped with six ports, can be found in Humphreys *et al.* (2011). The methodology followed by the authors was the same for the valves used during this research.

3.3 EXPERIMENTAL PROCEDURES AND INVESTIGATION

3.3.1 Tube viscometer tests

Extensive tube viscometry tests were conducted throughout this research as the rheological parameters were important for determining Reynolds numbers for non-Newtonian flow. Results from tube viscometry were also used for comparison with other rheological techniques as well as calculating theoretical profiles for validation of measured profiles using the UVP system. The following procedure is followed in order to establish a range of differential pressure and velocity values. The procedure is the same for all pipe diameters (Haldenwang, 2003).

- Before any mineral suspension is tested, the point pressure transducers and mass-flow meter are calibrated.
- The tube viscometer rig is calibrated by conducting water tests in all three tubes and the results are compared with the Colebrook-White equation.
- About 200 litres of slurry are mixed in the main mixing tank until the mineral suspension is properly hydrated and well mixed.
- An off-line relative density test is done for a representative sample. This is also compared with the in-line density value obtained from the mass-flow meter. If the required concentration is not achieved, more solids or water are added and mixed, depending on whether a higher or lower concentration is required.
- During the mixing process, the mineral suspension is circulated through all three pipes so that initial water in the system is mixed in the slurry. All the valves from the pressure adapters are also opened to flush out water in the system. The in-line density is monitored until it has stabilised, showing that the slurry concentration will be constant throughout the tests.
- The flow rate is regulated by controlling a valve which diverts excess flow through a by-pass line back into the mixing tank. This also helps to ensure that the slurry is well mixed during pipe tests.

- The specially written visual basic programme for the tube viscometer test on the PC is opened and the data is exported to an Excel spreadsheet.
- When the desired flow rate is set and constant, the data acquisition device is triggered and the program samples flow rates and point pressures over a preset time interval.
- The average flow rate and pressure is calculated and exported to the Excel spreadsheet. These values are visually displayed on a graph plotting wall shear stress against pseudo shear rate. By visually looking at results obtained during tests, one can quickly spot errors related to flow rate or differential pressure.
- This process is repeated with a range of flow rates until sufficient data points are recorded over the desired pseudo shear rate range.
- All sets of data points are plotted on the same graph, which enables one to see whether any errors, such as wall slip, are present. The overlapping of laminar flow data of all three tubes indicates that no obvious errors are present and that the plotted curve is the flow curve of the material on a pseudo shear diagram.

Tube viscometer tests took about an hour to complete, provided that no errors occur during the test. A detailed procedure for establishing a range of differential pressure and velocity values can be found in Chhabra and Richardson (1999), Haldenwang (2003) and Kotzé (2008).

3.3.2 Acoustic characterisation of ultrasonic transducers

For acoustic characterisation tests a stainless steel needle setup was used in combination with a high precision (+/- 0.03 mm) robotic arm (KUKA Roboter GmbH, http://www.kuka-robotics.com). Four ultrasonic transducers (4 MHz, 5 mm active element) were tested: one Signal Processing SA (SPSA) delay line transducers, one Imasonic delay line transducer (1st generation), one Signal Processing SA and one Imasonic standard transducers. The ultrasonic transducer was moved in a 2-dimensional field from the centre of the needle using the robotic arm. This enabled measurement of a range of acoustic intensities in increments of 0.1 mm (in the Y direction) and 1 mm (in the X direction), which gave a complete acoustic map of the ultrasonic transducer (see Figure 3.8). Tap water was used throughout all the tests and the temperature was continuously monitored using a temperature sensor submerged in the tank. A complete Graphical User Interface (GUI) was written in Matlab® to control the robot arm using a RS232 interface between the robot controller box and PC. It is also possible to automate the measurement procedure as it can take up to 6-8 hours

for one complete acoustic map, depending if no errors occurred (robot failure or temperature changes).

In these tests the transducers were used to transmit and receive the acoustic wave that is reflected from the needle. However, it was found that due to transducer ringing, measurements were not possible close to the needle, which was especially important for determining the position of focal points of the newly designed delay line transducers. Qualitative results were, however, still obtained using this technique and it was possible to compare acoustic characteristics of different transducers.

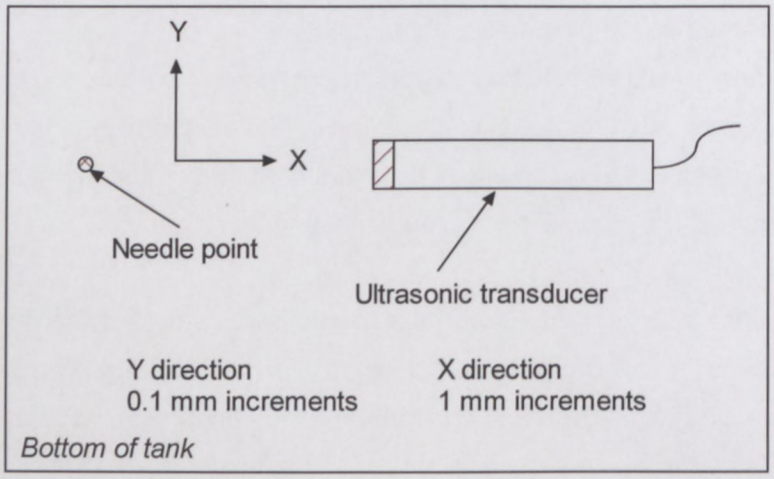

Figure 3.10: Measurement procedure for acoustic characterisation

In order to obtain accurate acoustic data close to the transducer's surface the stainless steel needle was replaced with a high performance needle hydrophone measurement system (described in Section 3.2.3.4). The same measurement procedure shown in Figure 3.10 was used for the needle hydrophone measurements. A one mm needle hydrophone was used for all tests as it was a good compromise between spatial resolution and detection of small ultrasonic intensities far from the transducer surface. Figure 3.11 shows the robot arm and needle hydrophone setup together with a delay line transducer submerged in the water tank at SIK.

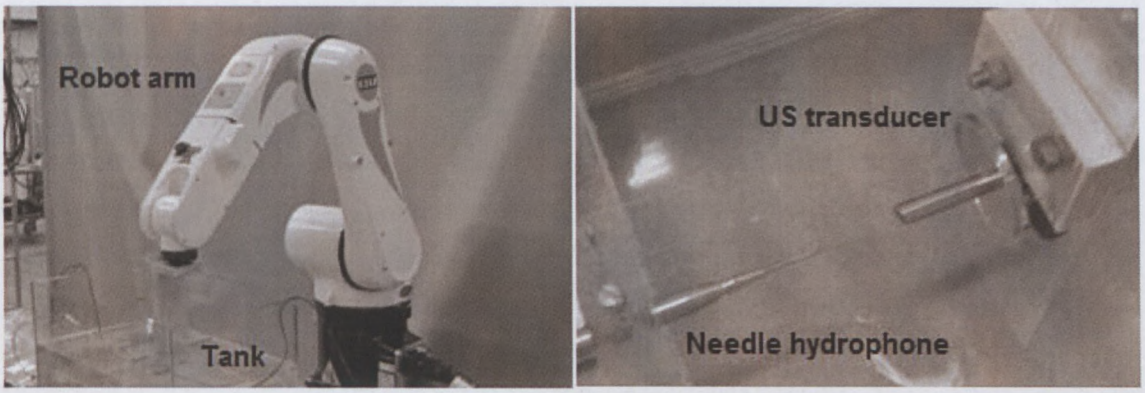

Figure 3.11: Transducer characterisation using needle hydrophone and robot setup

Results obtained using both techniques (stainless steel needle and needle hydrophone) are shown in Chapter 5.

3.3.3 Velocity estimation using DMEA data

The communication with the UVP instrument works via a TCP/IP protocol over an ethernet connection. There are two options to interact with the instrument. One is the software included from the manufacturer which provides a GUI to set the UVP parameters and record the velocity profiles. Statistical analysis tools are also available in the software and data can be exported in text files for further processing. An alternative way is the ActiveX library from Met-Flow which allows a 3rd party software application to communicate with the UVP-DUO. This ActiveX library ('UVPAX') was improved considerably by Wiklund (2007) and Birkhofer (2007). The UVPAX library allows access to all the features of the UVP instrument, including Demodulated Echo Amplitude (DMEA) data for each pulse emission, which is not available in the commercial software. This made it possible to use a Matlab® based application to set parameters, record profiles calculated on the instrument's Digital Signal Processor (DSP) and implement alternative velocity estimation algorithms using DMEA data. Furthermore, direct access to DMEA data or 'raw data' allows increased control of signal quality and gain amplification levels, detection of signal artifacts as well as correction of aliasing phenomena, as shown by Wiklund (2007).

Velocities can either be estimated in the time or frequency domain, see Chapter 2, Section 2.2.5. In this research both time and frequency domain algorithms were written and estimated profiles were compared under different test conditions. The complex Doppler signal is given by:

$$f(t) = I(t) + iQ(t), \tag{3.1}$$

where *I(t)* and *Q(t)* are the in-phase and co-phase signal components, respectively. The Fourier transform of the Doppler Signal is calculated as follows:

$$\hat{f}(\omega) = \int_{-\infty}^{\infty} f(t)e^{-i\omega t}dt, \tag{3.2}$$

and the power spectrum *S(ω)* is given by:

$$S(\omega) = \widehat{f^*}(\omega)\hat{f}(\omega). \tag{3.3}$$

The frequency domain velocity estimator implements the Burg algorithm, a parametric spectral estimation method, which returns an estimate of the power spectrum of the complex echo signal constructed from the in-phase (*I*) and co-phase (*Q*) echo data (DMEA data). The Doppler frequency corresponding to the maximum power point or peak is selected for velocity estimation using Equation 2.11.

The time domain algorithm determines the Doppler frequency shift in terms of the measured *I* and *Q* components of the complex experimental Doppler signal (Barber *et al.*, 1985):

$$f_d = \frac{1}{2\pi PRF} tan^{-1}\left(\frac{\sum_{i=1}^{M}(Q_i * I_{i-1} - Q_{i-1} * I_i)}{\sum_{i=1}^{M}(I_{i-1} * I_i + Q_{i-1} * Q_i)}\right). \tag{3.4}$$

This approach is based on the expression for the instantaneous rate of change of phase which separates rapidly varying from slowly varying terms. This technique solely relies on signal processing in the time domain, which makes it significantly simpler to implement relative to the classic FFT approach. Equation 3.4 was directly implemented using recorded DMEA data for estimation of velocity profiles. Results obtained using both algorithms are concluded in Chapter 5.

3.3.4 Deconvolution procedure

The deconvolution procedure used for correction of distorted velocity profiles is based on a similar methodology described by Flaud *et al.* (1997) in Section 2.2.6 (Chapter 2). Firstly the sampling window is discussed, followed by the deconvolution algorithm used to determine the correct or true velocity profile.

3.3.4.1 Sampling windows

The flow adapter design described in Section 3.2.3.3 allows simultaneous measurement of velocity profiles and the speed of sound in the liquid medium. This installation method also made it possible to record the waveform from the transmitting transducer by using the opposite transducer as a receiver. Software was developed in Matlab® to record the waveform measured by a digital oscilloscope (Agilent 100 MHz) over a maximum of 2000 points. The waveform or sampling window is normalised before deconvolving it with the measured velocity profile. It was found that the shape and length of the sampling window significantly controls the outcome of the deconvolution procedure, i.e. any errors will result in a deconvolved profile which contains large amount of noise and distortion. The magnitude of the deconvolved profile is also particularly sensitive to the overall shape and area of the sampling window. Therefore the described technique of continuously monitoring the sampling window is especially important as the shape and length of the window varies according to the velocity of sound in the medium, temperature, density as well as attenuating properties of a particular test fluid. Figure 3.12 shows a sampling window constructed from a measured waveform (sampling volume) used in the deconvolution procedure. The window (striped line) is described by the envelope of the exponential rise and decay of the intensities which lie on the sample volume axis (see Figure 2.8, Chapter 2).

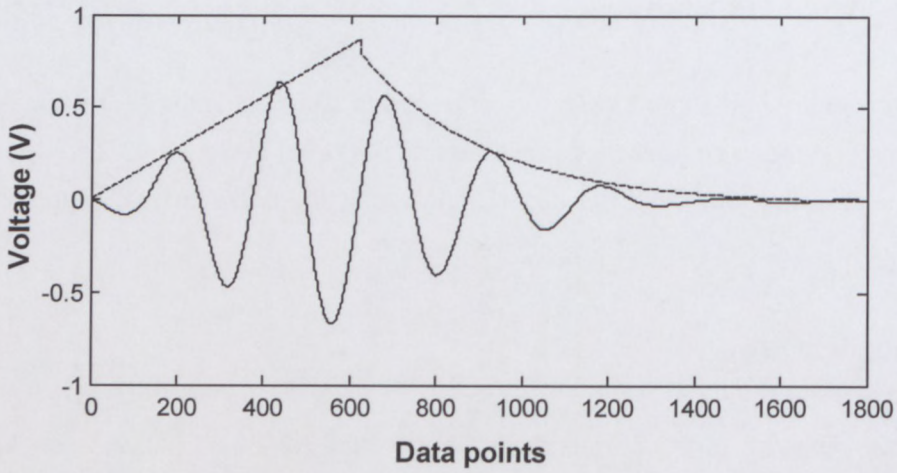

Figure 3.12: Sampling window construction

3.3.4.2 Methodology for deconvolution of measured velocity profiles

Figure 3.13 describes the algorithm used in the deconvolution procedure for correcting erroneous velocity data due to finite size of the sampling volume. Firstly, a velocity profile is recorded, followed by the velocity of sound parameter and waveform shape. It is also necessary to multiply the measured velocity profile by the integral of the sampling window within the flow field to account for the normalising function in the primary model assumption, Equation 2.15. It is not a constant value, because upon entry and exit only part of the sampling window is contained within the flow field. Discrete Fourier transforms are used to carry out the deconvolution in the rest of the algorithm. Unwanted noise is removed with a digital low pass filter before the final deconvolved profile is used for detailed flow analysis.

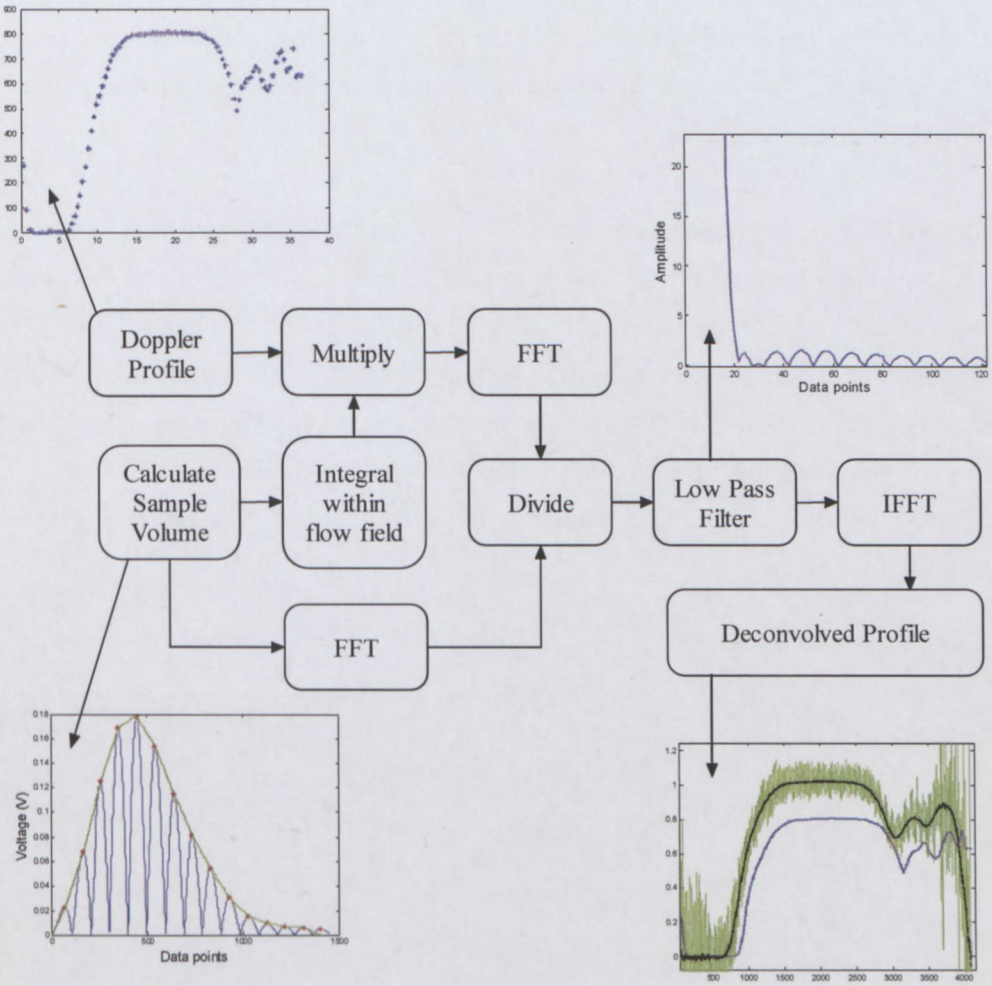

Figure 3.13: Deconvolution methodology

The most important feature of this algorithm is that it requires only information of the measured profile and sampling window length and shape. No prior knowledge of the nature of the true velocity profile is required.

3.3.5 Flow measurement and analysis in hyperbolic contraction

The hyperbolic contraction used in the research work at SIK was made of Polymethyl Methacrylate (PMMA), which has good mechanical properties for minimal ultrasonic energy absorption. The contraction was installed in a 20 l tank and was filled with the same CMC used for testing in the flow loop to ensure that the same fluid medium is between the ultrasonic transducer and contraction wall layer. The carboxymethyl

cellulose (CMC) was thus used as coupling fluid to minimise ultrasonic wave refraction and reflection. The wall thickness of the contraction was also optimised to integers of half wavelengths for maximum ultrasonic transfer between the coupling fluid and contraction material wall layers.

In this study velocity profiles were measured through the contraction wall interface and not by installing transducers in direct contact with the test fluid, i.e. a non-invasive measurement method was used. The valve geometry as well as physical properties of the material was too complex for measurements through wall interfaces and thus two measurement techniques for velocity profile measurements using UVP are presented. Figure 3.14 shows the experimental setup for the hyperbolic contraction tests. The transducer was moved along the contraction length in the X-direction using a high precision robotic arm.

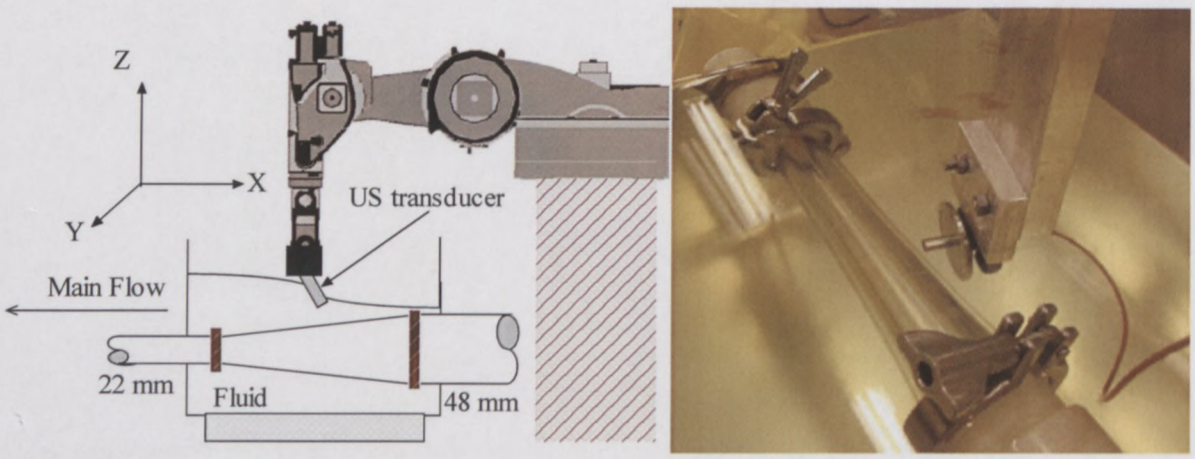

Figure 3.14: Hyperbolic contraction setup with robotic arm

This enabled measurements from developed to contracting flow and from the results a complete flow map of the velocity field inside the contraction was constructed using the range of measured velocity distributions (91 profiles). In order to determine an accurate flow map it was important to calculate the wall interfaces at each particular position along the contraction length. The hyperbolic contraction radius is described by the following equation:

$$R = R_1 \Big/ \left[d \cdot \left(R_1^2 / R_2^2 - 1 \right) + 1 \right]^{0.5} \quad (3.5)$$

The position of the first wall layer was calculated using the maximum velocity of the first measured velocity profile and subtracting the relevant radius. The rest of the wall positions were determined by recording the distance travelled along the hyperbolic contraction length (*d*) and using Equation 3.5.

3.3.6 Flow measurement and analysis in open channel

This section describes the measurement technique used to obtain complete flow maps of non-Newtonian flow using UVP in an open channel. Velocity profiles were also validated by calculating the bulk flow rate and comparing it to a reference electromagnetic flow meter.

3.3.6.1 Transducer positioning and installation

In this project six velocity profiles were measured at different positions around an artificial open channel or flume. Velocity profiles were measured using 4 MHz, 5 mm active element ultrasonic transducers (conventional and delay line transducers), which were installed at 20° with respect to the lateral and in direct contact with the fluid in order to minimise attenuation of the ultrasonic energy wave. This installation method (similar approach to flow adapter design discussed in Section 3.2.3.3) leaves a cavity between the transducer surface and flume surface interface, as shown in Figure 3.15. The reason for the cavity is due to the near field distance in front of the ultrasonic transducer, which varies with different transducers. In this region the pressure (ultrasonic) wave is irregular and thus this region is avoided for point velocity measurements. The same transducer housing ports were used for the delay line transducers. However, the delay line transducers are installed in flush with the flume surface or side wall, thus eliminating problems caused by the cavity.

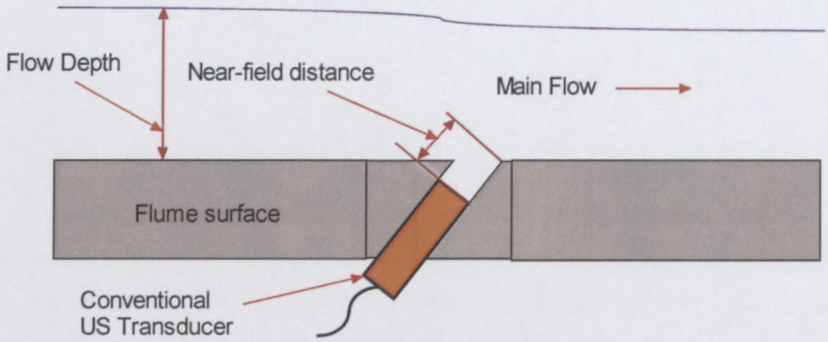

Figure 3.15: Housing of ultrasonic transducers in open channel

Figures 3.16 and 3.17 show the positions where the ultrasonic transducers were installed. Four transducers were installed at the bottom (surface) of the flume and two transducers at one of the side walls (see Figure 3.17). Profiles were only measured over one half of the flume as the flow was assumed to by symmetrical across the flume cross-section.

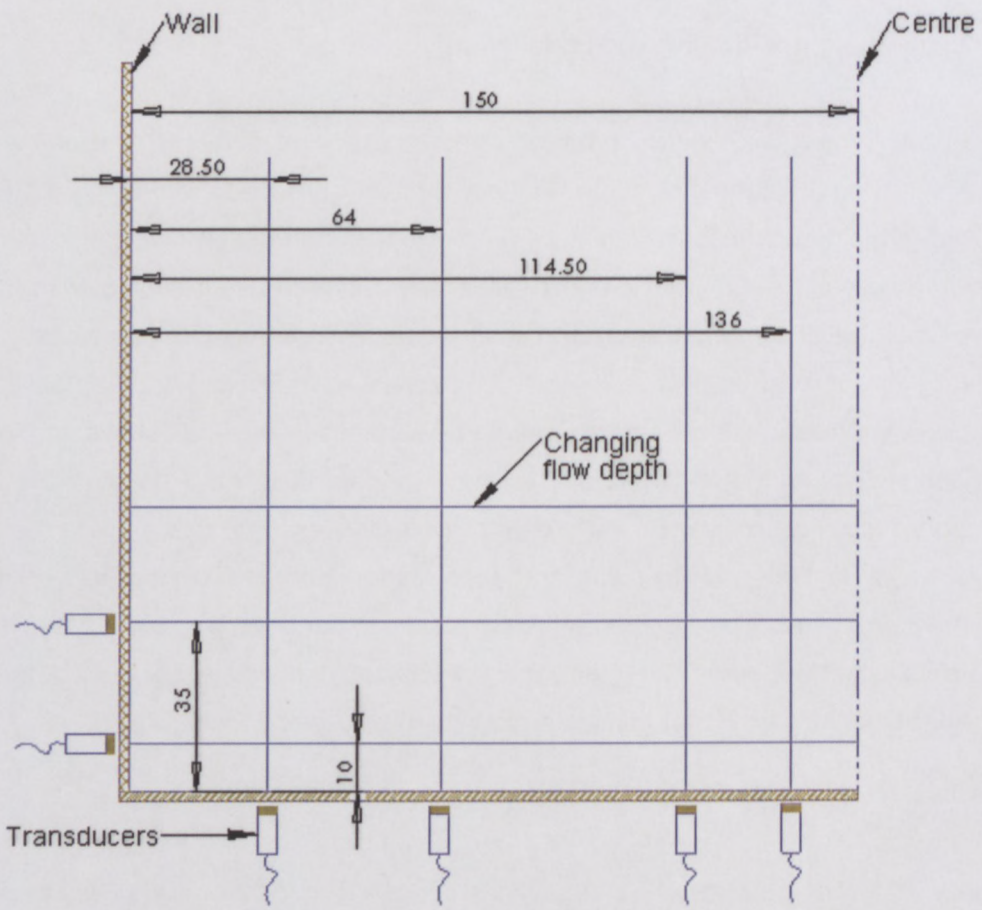

Figure 3.16: Schematic illustration of transducer installation layout for flume

Flume side wall *Flume bottom surface*

Figure 3.17: Ultrasonic transducer installation for 300 mm flume

3.3.6.2 Wall interface calculation using DMEA data

Since conventional transducers were installed with direct contact to the test fluid (cavity setup), it was important to determine the wall interface at the flume surface. During ultrasonic pulse emissions high amplitude echoes were recorded at the fluid and free surface (air) interface. This is due to the high acoustic impedance mismatch between a liquid and air medium. The echoes could be monitored on an oscilloscope, but it was also possible to simultaneously record the DMEA data and measure velocity profiles, making it possible to compare the echo and velocity data and subsequently calculate the position of the flume bottom surface. Figure 3.18 shows the average of ten velocity profile measurements at the centre position of the flume for bentonite 6% w/w. Figure 3.19 shows the DMEA data for all the pulse emissions.

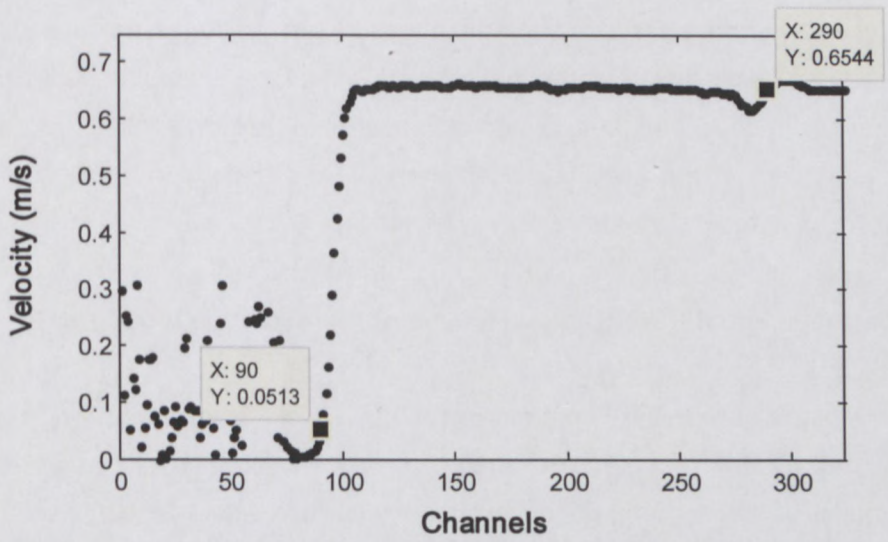

Figure 3.18: Velocity profile measurent at centre position of flume

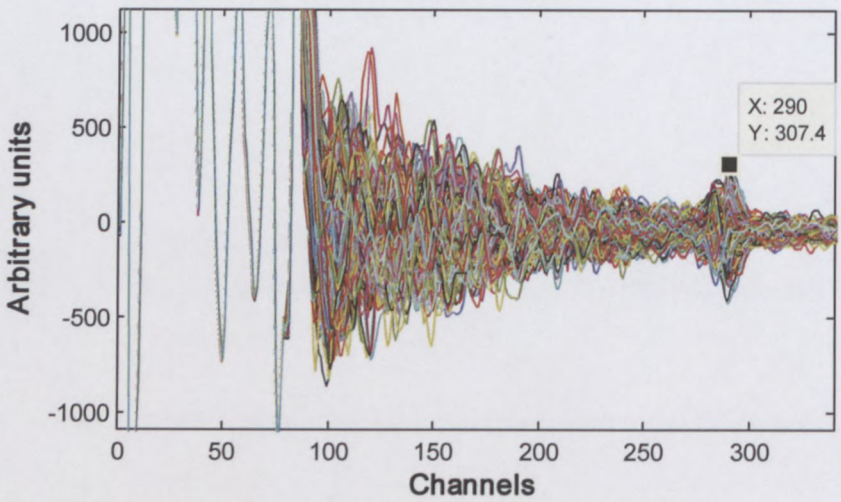

Figure 3.19: DMEA data for successive pulse emissions

Note that between 1 and +- 90 channels the cavity containing the transducer's near-field length is present, which causes inaccurate velocity estimation, as shown by the scattered velocity points in Figure 3.18. Figure 3.19 shows that further away from the transducer surface the echo amplitude decreases as the energy get absorbed in the system until a relatively large echo amplitude occurs, which maximum position is shown by the marker (channel 290). This position is the fluid/air interface and the measured flow depth (using digital verniers – Mitutoyo, accuracy 0.02 mm) was simply subtracted to obtain the flume's bottom surface or wall interface. In this case the measured flow depth was 69.53 mm and at a spatial resolution of 0.37 mm the calculated wall position was channel 90 (see Figure 3.18). This technique was used for all the velocity measurements in the lateral direction. Unfortunately it was not possible to use echo data for measurements conducted in the radial direction (see two transducer positions in Figures 3.16 and 3.17), as the penetration depth was too large (flume width of 300 mm). In this case the wall interfaces were determined by physical measurement of the cavity between the wall and transducer surface and by visual inspection of the measured velocity profiles.

3.3.6.3 Flow maps and flow rate calculation using triangulation algorithm

The complex geometry co-ordinates and velocity magnitudes were analysed in Matlab® R2007b. Figure 3.20 shows six velocity profiles after post data analysis (removal of erroneous data due to reflected wave effect) and mirrored around the centre of the flume. A linear interpolation method was used to construct complete two-

dimensional flow maps over the flume cross-section from the six experimental velocity profiles using a fine mesh grid. The spatial resolution of the mesh used was 0.25 mm over the hydraulic (flow) area of the flume. This was then integrated to obtain the average flow rate and was compared to the bulk flow rate measured using an electromagnetic flow meter (Krohne IFC 010D – DN40, accuracy 0.5% of measured value).

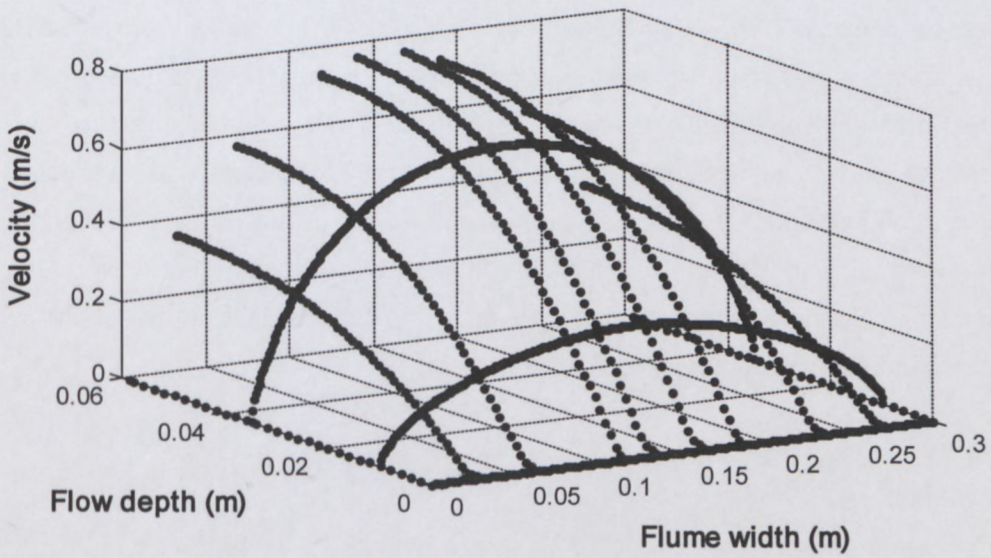

Figure 3.20: Experimental profiles used for 2D flow map and bulk flow rate calculation

This combined post data analysis was used to verify results obtained from velocity profiles measured using UVP.

3.3.7 Flow measurement and analysis in diaphragm valve

In this project velocity profiles were measured at different positions at the centre (contraction) of a fully open diaphragm valve. A diaphragm valve was reverse engineered and re-manufactured using a rapid prototyping technique of multilayer printing (see Section 3.2.4). The diaphragm valve project proved to be very complicated due to the unique geometry at the centre position. The centre position was chosen for flow analysis because most of the energy losses occur in this region. This project continues work done by Humphreys *et al.* (2011). The valve project is divided into two phases, the 1st part consisted of measurements in a three port valve followed by post data-analysis (evaluation phase) and the 2nd part included an extra port for added detailed flow information to increase the accuracy of flow maps and validation of velocity profiles. Figure 3.21 shows the internal model of the 50% open diaphragm valve when viewed at the center plane. It can be observed that this model is symmetrical around the vertical axis and thus the same velocity distributions were assumed at both sides of the axis.

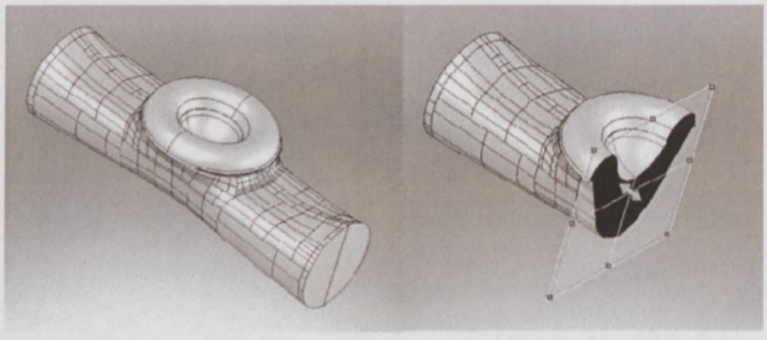

Figure 3.21: 3D representation of the diaphragm valve's internal structure

Initially a triangulation method was approached, but not enough data was available during the preliminary tests. Three assumed velocity distributions were arbitrarily drawn using Solidworks 2009 (Dassault Systèmes SolidWorks Corp., Concord, MA, USA, www.solidworks.com) and all geometry coordinates were exported to Matlab® (The Math-Works Inc., Natick, MA, USA) for flow calculations. This is illustrated in Figure 3.22 (dimensions shown in mm). The three measurement lines (TDX Lines 1-3) are the directions of the wave propagation of each ultrasonic transducer respectively. The challenge was to assume a realistic pattern of the velocity distribution at the center of the valve geometry.

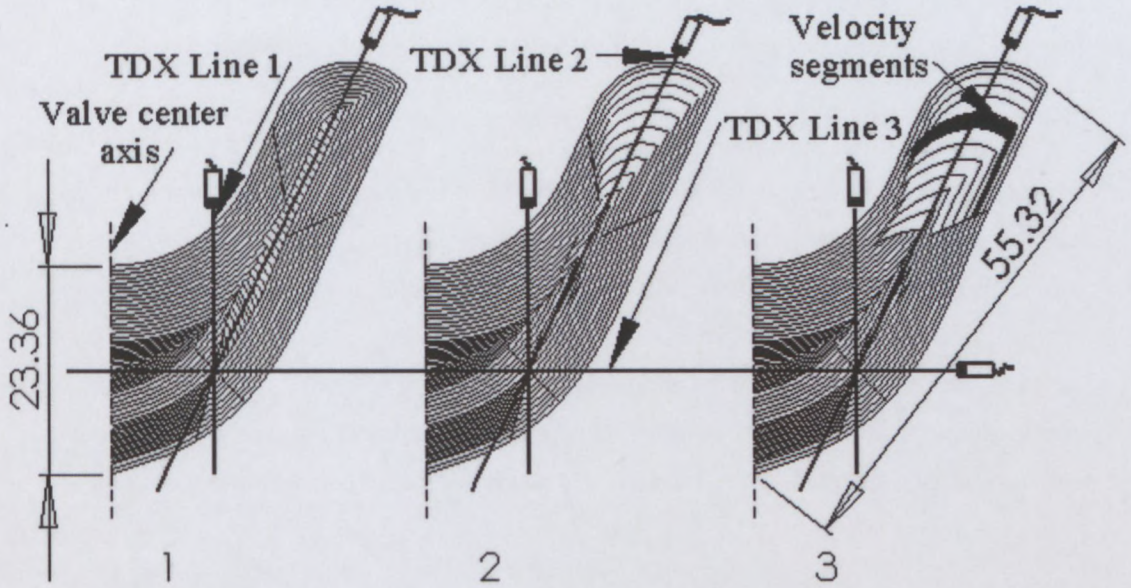

Figure 3.22: Three different velocity distribution drawings showing transducer positions and measurement lines

An average of the point velocities measured across a particular segment was determined and this value was assumed to be the same across the entire segment (see highlighted segment, Figure 3.22). These assumptions also lead to additional errors, as *a priori* knowledge of the flow field of this complex geometry is not available. Near wall positions could be calculated using the maximum velocity as the centre position and subtracting the physical penetration depth for experimental profiles across a symmetrical axis (TDX Line 3). Since all the transducers were physically installed at the same distance (near-field length, 16.9 mm), the same channel was used for the asymmetrical measurements (TDX Lines 1-2) as the near wall position. The opposite walls were determined by visual inspection and using the sound velocity, physical geometry of the valve as well as angle of inclination.

Separate flow rates were calculated for each area/flow segment and added together to yield a total volume flow rate:

$$Q_T = \sum_{n=1}^{N} \left(V_n \cdot A_n \right), \tag{3.6}$$

where V_n is the measured velocity across a particular flow/area segment, A_n, which is calculated by Solidworks 2009 and N is the total number of segments. This calculated

flow rate was then compared to the flow rate measured using an electromagnetic flow meter and an error difference percentage was determined for comparison.

For more accurate validation of velocity profiles measured in the complex valve geometry and comparison between two different transducers (conventional vs. delay line transducer), a triangulation technique for calculating the flow rate must be used. It was found that an extra measurement line (velocity profile measurement) at the centre of the valve geometry is sufficient for determining a flow map and subsequently the bulk flow rate for comparison to a reference flow meter. Figure 3.23 shows the same valve geometry at the centre position as well as measurement lines used for validation and comparison of profiles measured using two different ultrasonic transducers.

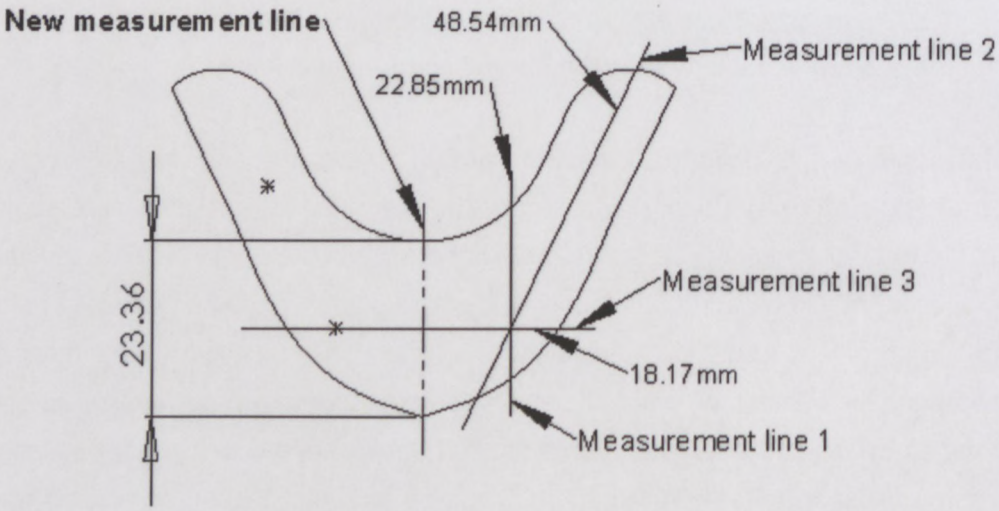

Figure 3.23: New valve with added measurement line for triangulation

A similar approach described in the previous section for determining a two-dimensional flow map as well as bulk flow rate by triangulation and integration was used for the four port valve tests.

3.4 CALIBRATION PROCEDURES

The calibration procedure for the electronic measuring systems is explained in the following section. Signal outputs from the instruments are standard 4-20 mA current output and are connected to a data acquisition unit with a 100 ohm resistance. Analog-to-digital converters (Hewlett Packard 34970A) were used to read the output voltages from the measuring instruments and to convert it to digital format for signal processing.

3.4.1 Pressure transducers

High and low range differential pressure transducers were used during the tests. High-range pressure sensors ranged from 0 – 130 kPa and low range pressure sensors ranged from 0 – 6 kPa. The pressure sensors were calibrated with an air pump while pressure readings were taken with a digital manometer. Detailed calibration procedures can be found in Haldenwang (2003) and Kotzé (2008). A typical test result for the calibration of a high-range (0 – 130 kPa) differential pressure transducer is shown in Figure 3.24 below.

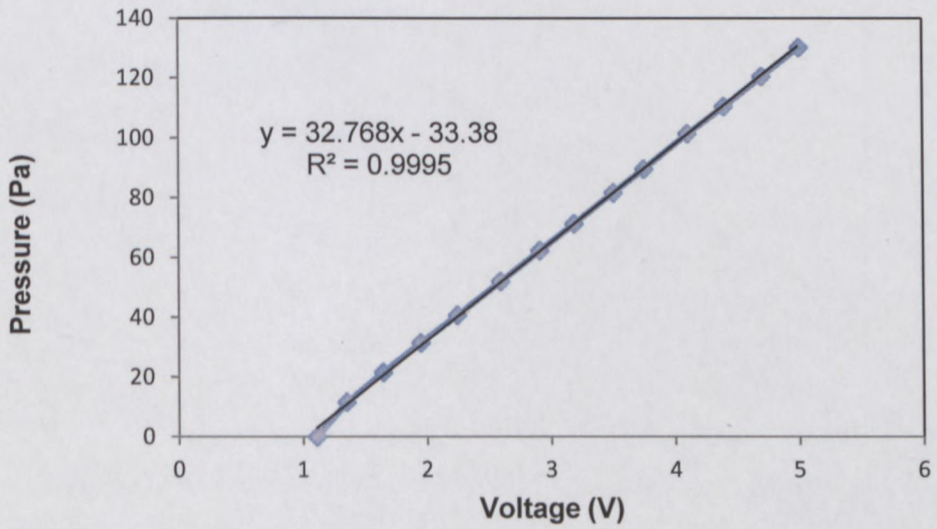

Figure 3.24: High-range differential pressure transducer calibration constants

According to the manufacturers, the accuracy of the pressure transducers is within 0.25 % of full scale. This means that, for the high-range (0-130 kPa) pressure transducer the pressure error is +/- 325 Pa and for the low-range (0-6 kPa) pressure sensor the pressure error is +/- 15 Pa.

3.4.2 Flow meter

Electromagnetic flow meters were used as a reference for comparison with the UVP analysis. Thus it was important to determine errors and uncertainty associated with the flow meters, especially for non-Newtonian fluids. This was determined experimentally. A weigh tank equipped with load cells was calibrated against reference weights, which was weighed using a high precision electronic scale. Following the calibration, the weighing procedure was evaluated by filling the tank with water and recording the reading output from the load cell. A correlation coefficient of $R^2 = 0.9997$ was obtained from the water measurements. Flow rates for water and a non-Newtonian fluid were measured using the weigh tank ('bucket and stopwatch method') and the electromagnetic reference flow meter. Figure 3.25 shows that a correlation coefficient of $R^2 = 0.98$ was obtained between the two measuring methods for a non-Newtonian fluid over a range of 0.12 to 4.5 l/s. In this case the weigh tank was used as the reference (B & S).

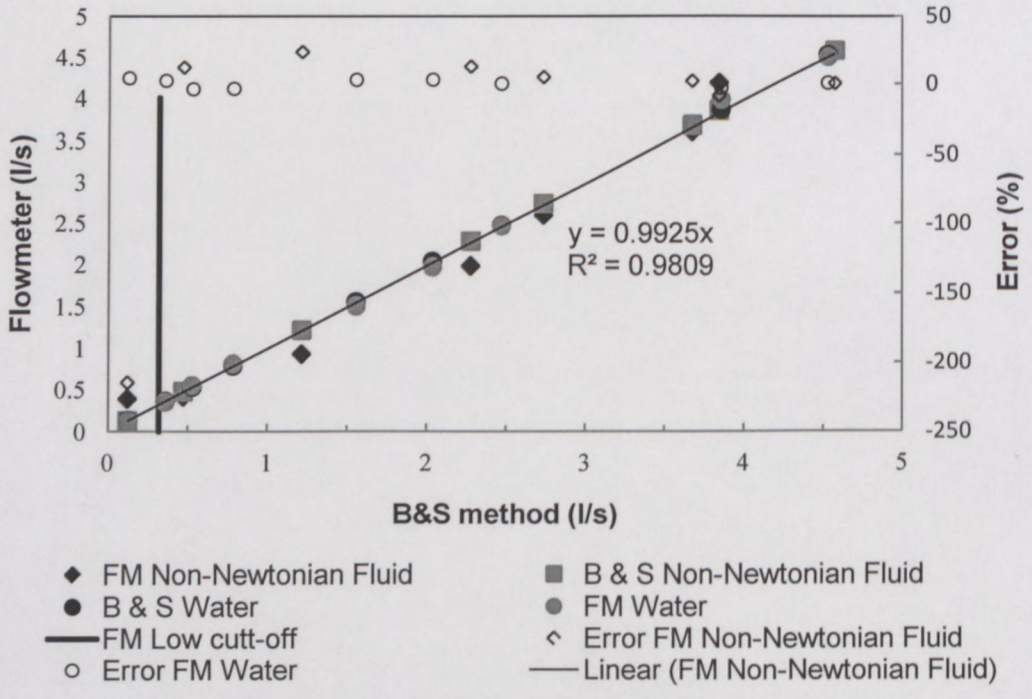

Figure 3.25: Flow meter error comparison between water and a non-Newtonian fluid (Kotzé *et al.*, 2011)

It can be seen in Figure 3.25 that the errors increase significantly for the non-Newtonian fluid in the low flow rate range (less than 0.5 l/s). The relative standard error was 1.2% for the non-Newtonian fluid compared to the manufacturer's value of 0.5% for water. Based on the manufacturer's specification of 0.4 m/s where the errors increase significantly, the flow rate limitation equates to 0.32 l/s, and thus this range with large uncertainty was avoided. The test work was therefore conducted at a minimum flow rate of 0.5 l/s. More information on reference measurements using an electromagnetic flow meter can be found in Kotzé *et al.* (2011).

3.4.3 Clear water test in tube viscometer

After calibration of the mass-flow meter and pressure sensors, water tests were conducted in all three pipes of the tube viscometer.

The Colebrook-White equation for turbulent flow in pipes is given by:

$$\frac{1}{\sqrt{4f}} = -2\log\left(\frac{k}{3.7D} + \frac{2.51}{Re\sqrt{4f}}\right). \tag{3.7}$$

This is used to calculate the friction factor f. The Darcy expression for friction head is as follows:

$$h_f = \frac{4fLV^2}{2gD}. \tag{3.8}$$

By substituting Equation 3.7 into $\tau_w = \frac{D\Delta P}{4L} = \frac{D\rho g h_f}{4L}$, one can deduce that:

$$\tau_w = \frac{f\rho V^2}{2}. \tag{3.9}$$

Figure 3.26 shows theoretical and experimental data plotted on linear axes for the 28 mm pipe installed in the flume rig.

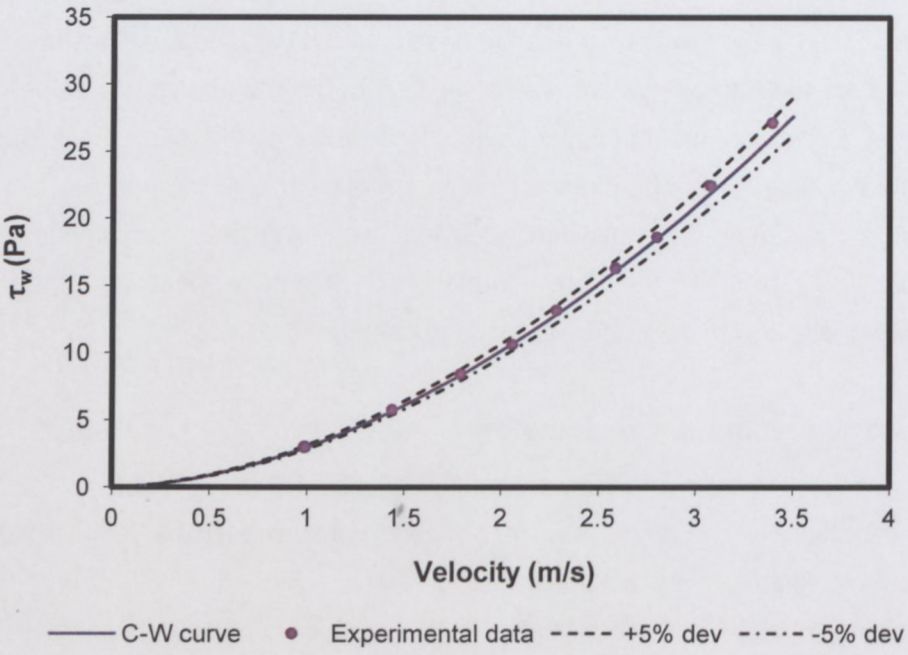

Figure 3.26: Clear water test data against Colebrook-White equation in 28 mm pipe

If the pipe is not smooth, the value for k can be optimised to find the actual pipe roughness (Slatter, 1994). It was found that all the pipes were smooth, i.e. $k = 0$. Since the pressure transducers and flow meter are tested together during the clear water test, the test result indicate that the combined error is less than 5% over the velocity range tested, as shown in Figure 3.26. Similar results were found for the other pipes (flume rig and valve rig) used during this research project.

3.4.4 UVP-DUO monitor

The Doppler shift frequency is directly related to the velocity value and therefore the UVP monitor does not require a calibration procedure. However, the UVP monitor needs calibration of the internal clock to present accurate data. This is done by the manufacturer, Met-Flow SA in Switzerland (Met-Flow SA, 2002).

3.5 COMBINED ERRORS

Certain derived quantities such as shear stress and shear rate are dependent on more than one measurement. The same measurement is taken a number of times and the average value is extracted. This is done in order to overcome random errors due to electrical noise, for instance (Morris, 2001). Pressure and flow rate measurements were averaged over ten readings and velocity profile measurements were averaged over 100 or ten recordings, depending on the type of algorithm used. In this section the possible errors in tube viscometry and velocity profile measurements are discussed.

3.5.1 Tube viscometry

Haldenwang (2003) and Slatter (1994) refer to Brinkworth (1968) for a procedure that quantifies the combined error using a root mean square approach.

The highest expected error ΔX, if X is a function of N quantities is:

$$\left(\frac{\Delta X}{X}\right)^2 = \sum\left(\frac{\partial X}{\partial N}\right)^2\left(\frac{N}{X}\right)^2\left(\frac{\Delta N}{N}\right)^2. \tag{3.10}$$

The wall shear stress and pseudo shear rate is calculated from the pipe diameter, pressure drop and flow rate measurements. Equation 3.10 was used to calculate the combined errors for the following calculations.

3.5.1.1 Wall shear stress

The highest expected error calculating the wall shear stress using Equation 3.11 was:

$$\left(\frac{\Delta\tau_w}{\tau_w}\right)^2 = \left(\frac{\Delta P}{4L}\frac{D}{\tau_w}\frac{\Delta D}{D}\right)^2 + \left(\frac{D}{4L}\frac{\Delta P}{\tau_w}\frac{\Delta(\Delta P)}{\Delta P}\right)^2 + \left(-\frac{D\Delta P}{4L^2}\frac{L}{\tau_w}\frac{\Delta L}{L}\right)^2. \tag{3.11}$$

The results for all the pipe diameters as well as low and high range differential pressure transducers (DPT) are graphically depicted in Figure 3.27 and Figure 3.28.

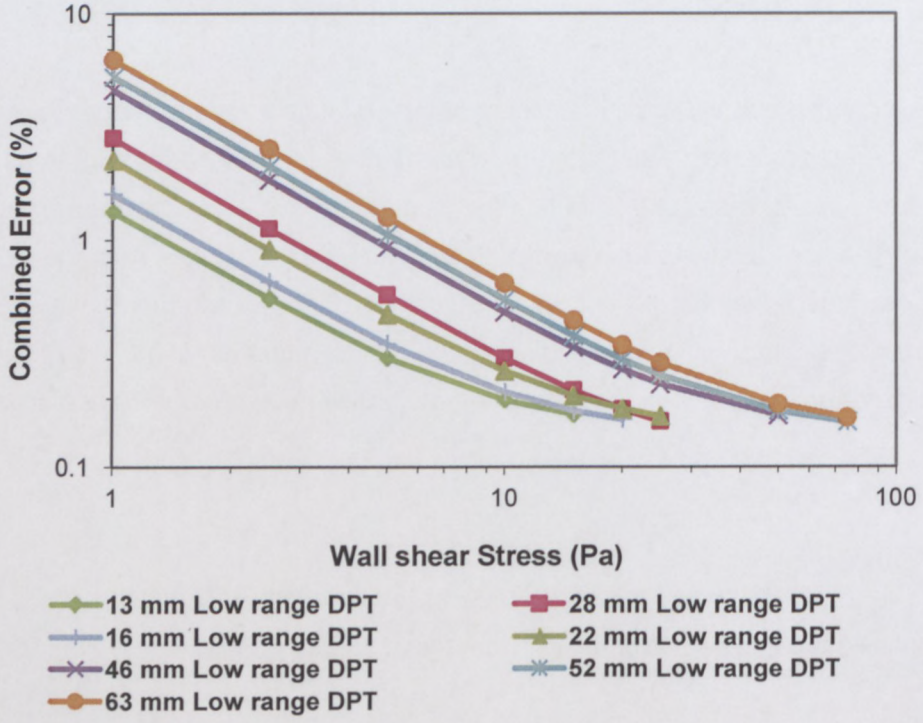

Figure 3.27: Pipe wall shear stress combined errors for low range DPT

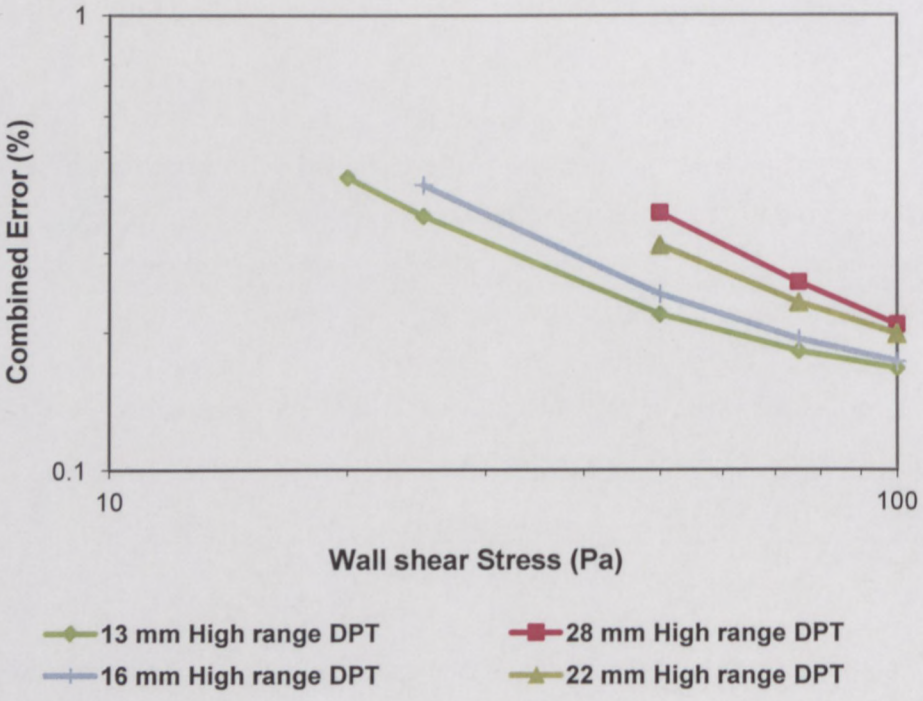

Figure 3.28: Pipe wall shear stress combined errors for high range DPT

There is a steep increase in error percentage at the very low range, which was expected due to very low differential pressures at this range. The low-range (0-6 kPa) pressure sensors yielded a lower error when compared to the high-range (0-130 kPa) pressure transducers over the range 10 – 100 Pa, which was also expected. The differential pressures across the 52, 46 and 63 mm pipes were generally low for the same shear stress compared to the smaller diameter pipes (13 – 28 mm) and thus the low range pressure sensors were sufficient for all measurements on the larger pipes during this work. The high-range pressure transducers can be replaced with a lower range (e.g. 0 – 30 kPa) in order to reduce the combined error percentage at the high wall shear stress range. This is discussed in Chapter 5.

3.5.1.2 Pseudo shear rate

The highest expected error calculating the pseudo shear rate using Equation 3.10 was expressed as:

$$\left(\frac{\Delta 8V/D}{8V/D}\right)^2 = \left(\frac{\Delta G}{G}\right)^2 = \left(-\frac{32Q}{\pi D^3}\frac{Q}{G}\frac{\Delta Q}{Q}\right)^2 + \left(-\frac{96Q}{\pi D^4}\frac{D}{G}\frac{\Delta D}{D}\right)^2. \tag{3.12}$$

The results are graphically displayed in Figure 3.29.

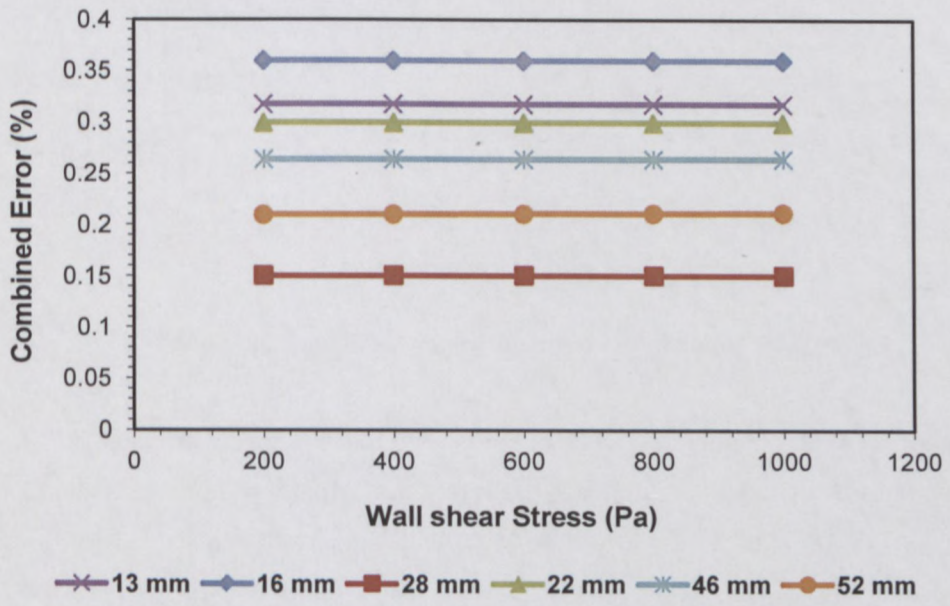

Figure 3.29: Highest combined errors for calculating pseudo shear rate

The combined errors for pseudo shear rate are low when compared to the wall shear stress because shear rate was only related to the volumetric flow measurement and the inner diameter of the pipes.

3.5.2 Velocity profiles

The estimated velocities are directly related to the velocity of sound measurement as well as the Doppler angle, see Equation 2.11. Therefore, errors may arise if these parameter inputs are incorrect. The relationship between velocity of sound error and the consequent error in the estimated point velocity is shown in Figure 3.30. It is important to be aware of the temperature dependence of the velocity of sound in suspensions. Since the velocity of sound in water varies by approximately 3 m/s per °C at 20 °C, an error in temperature of 5 °C will produce an error of ±15 m/s in the velocity of sound measurement, and subsequently contribute 1% error in all of the velocity points in the recorded velocity distribution.

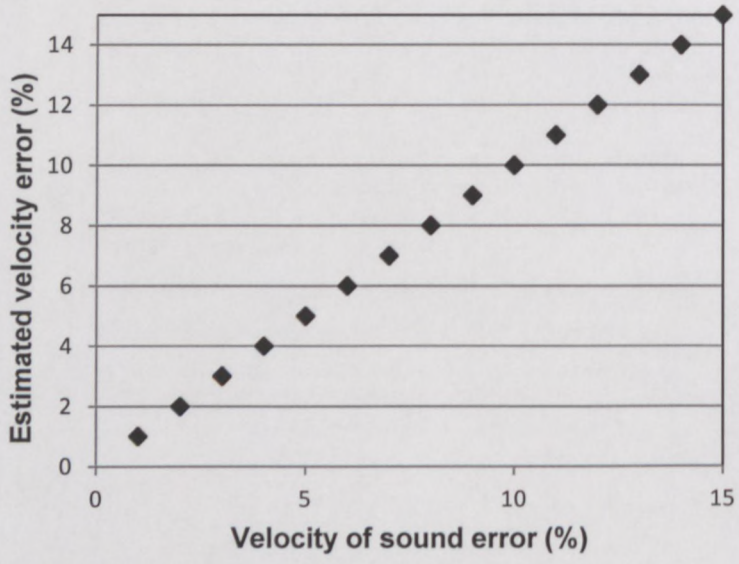

Figure 3.30: Velocity of sound vs. estimated flow velocity error

Another important limitation of UVP is the crucial role played by the Doppler angle (θ). This angle is defined as the angle between the ultrasonic beam direction and the direction of the flow inside the pipe or pipe fitting. According to Equation 2.11 the Doppler angle is a variable which influences the magnitude of velocity estimation significantly. If UVP is to be used to map unknown velocity fields, the problem of not

knowing the Doppler angle *a priori* must be mitigated (Powell, 2008). Figure 3.31 illustrates the error in point velocity estimation for a given Doppler angle error. Note that 20 degrees +/- 2 degrees constitutes a Doppler angle error of +/- 10%.

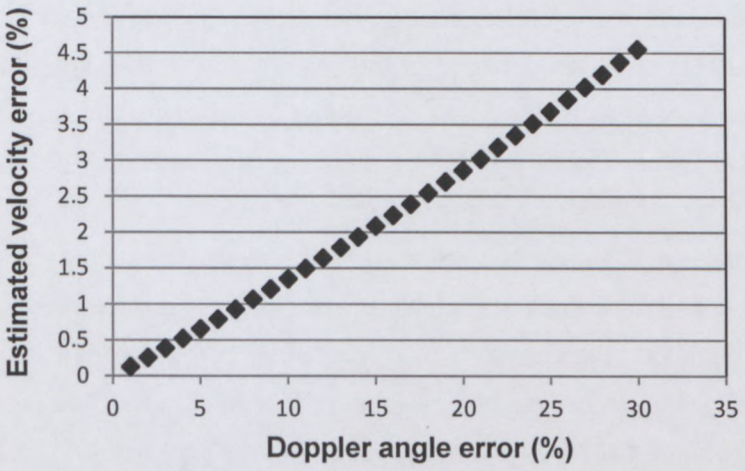

Figure 3.31: Velocity of sound vs. estimated flow velocity error

Apart from the Doppler angle and velocity of sound parameters, UVP system settings as well as the actual ultrasonic beam shape also influences the accuracy of velocity profile measurements. For example, using four cycles per pulse in a small diameter pipe will result in a profile measurement with limited spatial resolution and as a consequence contain insufficient information close to the pipe wall, where the velocity gradient is high. Higher number of cycles per pulse introduce more energy in the system (and thus further measurement depths), but also result in larger and wider sample volumes, which decreases the accuracy of velocity measurements due to averaging effects across the pulse geometry. Furthermore, measurement through wall material layers changes the shape of the acoustic beam, the propagation of the ultrasonic burst and the intensity distribution of the returning echo and as a consequence decreases the overall accuracy of the UVP method (Messer and Aidun, 2009). Identifying errors or artefacts in velocity profiles measured using UVP depend on the experience of the user. Although UVP is still easy to implement relative to other velocity profiling methods (see Section 2.3.4.1), it is not a technique that someone could use with no prior knowledge or skills in a relevant field. This research work attempts to simplify the implementation of UVP even further by introducing a new delay line transducer and advanced signal processing techniques, which could correct errors associated with UVP.

3.6 MEASURED VARIABLES

3.6.1 Temperature

The temperature was monitored in order to try to stay within an acceptable temperature range during tests. The temperature of the mineral suspensions is measured using thermocouples as well as by the mass-flow meter in-line, which is connected to a data acquisition unit that reads the temperature in degrees Celsius into an Excel spreadsheet. Temperature monitoring is especially important for velocity profile, sound speed and rheological measurements as temperature has an influence on ultrasound propagation as well as apparent viscosity of certain non-Newtonian fluids. Preliminary tests were conducted off-line in a rheometer in order to investigate the flow behaviour at different temperatures of the non-Newtonian fluids used in this research. Figure 3.32 shows a rheogram of CMC 7% w/w at two different temperatures, 20 and 25 °C.

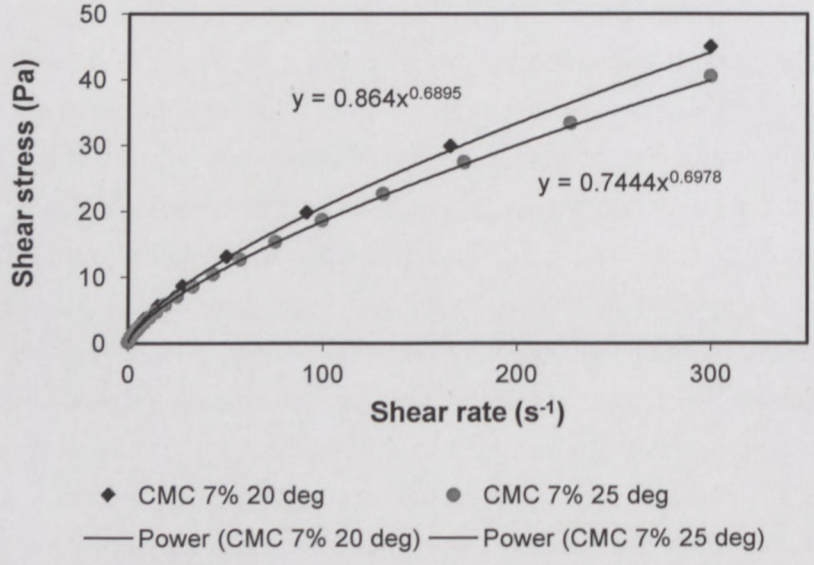

Figure 3.32: Clear water test data against Colebrook-White equation in 28 mm pipe

It was determined that the viscosity of the CMC fluid decreased with ±14% for an increase of 5°C. Kaolin and bentonite suspensions proved to be less sensitive to temperature changes. During any test the temperature did not vary by more than 2 degrees Celsius. The temperature variation of 2 °C was mainly present during tube viscometer tests, as these tests were considerably longer.

During the ultrasound tests the temperature did not vary as the time of measurement is significantly faster than the previous method (process conditions were kept constant, i.e. flow rate and pressure). Therefore the effect of temperature on tube viscometer and ultrasound tests was deemed negligible. Also, during off-line tests the temperature was kept constant at the same value measured during in-line tests by the rotational rheometer, thus ruling out any errors due to temperature variation. Based on previous results obtained from tube viscometry and history of the model suspensions used at the MST, the effect of temperature variation on fluid viscosity was deemed negligible (Haldenwang, 2003).

3.6.2 Velocity of sound

Velocity of sound was measured in-line using the flow adapter discussed in Section 3.2.3.3. The sound velocity was determined by "Acoustic Time of Flight Measurement" (AToM) and a known fixed transducer distance. As mentioned before, the flow adapter construction allows the installation of two ultrasound transducers opposite each other. The transmitting transducer was connected to the UVP monitor and the receiving transducer was connected to the digital oscilloscope. In order to ensure accurate in-line velocity of sound measurements, the distance between the two transducers has to be accurate. The sound speed in water was measured off-line and also used to fill the flow adapter completely with both transducers installed (delay line and conventional transducers). Using the digital oscilloscope (Agilent 100 MHz Model 54622A), the acoustic time of flight was measured and the distance was calculated using Equation 3.13:

$$H = t_d \cdot c\,, \tag{3.13}$$

where H is the distance between the two opposite transducers. Such a calibration procedure was applied to all of the in-line flow adapters before velocity of sound of mineral suspensions were measured. Similar setups for measuring the sound speed of fluids in-line are described in Wiklund (2007), Birkhofer (2007) and Kotzé *et al.* (2008).

The velocity of sound measurement was particularly important for correct implementation of the deconvolution procedure (discussed in Section 3.3.4). The length of the sampling window is dependent on the speed of sound in the medium and any

errors may result in deconvolved velocity profiles which are shifted incorrectly (discussed in Chapter 5) or that are completely distorted.

It must be mentioned that particle sedimentation of fluids inside cavities when using the flow adapter and standard transducer installation setup (described in Section 3.2.3.3) may cause temperature as well as density changes, which could result in significant errors in velocity of sound measurements. This problem was not found during this work as only model fluids were used and not industrial suspensions such as concrete, which could settle inside cavities. Model fluids and suspensions were mainly used in order to achieve a good comparison between results obtained using standard and delay line transducers.

3.7 FLUIDS TESTED

The materials used in this research were selected to represent a wide range of rheological properties. Carboxymethyl cellulose (CMC) was selected for the power-law fluid and is generally regarded as an ideal solution for experimental work (Haldenwang, 2003). Bentonite was selected as the Bingham plastic mineral suspension. The yield pseudoplastic or shear-thinning mineral suspension selected was kaolin clay. This material has been used at the Material Science and Technology (MST) group over a very long period of time and is reasonably stable (Haldenwang, 2003). Water was selected for calibration purposes.

3.7.1 Water

Municipal tap water was used as a basis or reference for the other slurries as water is a chemically reasonably stable fluid. As large volumes of water were used for testing and mixing the mineral suspensions, municipal tap water was the only option. Tap water was also used at SIK for acoustic characterisation of ultrasonic transducers.

3.7.2 Carboxymethyl cellulose (CMC)

CMC is a polymer solution and is used in the industry as a thickening agent. The polymer was mixed with water in order to produce a pseudoplastic solution. CMC is generally regarded as an ideal non-Newtonian power-law fluid for experimental work,

especially when ultrasonic tests are concerned as CMC offers excellent wave scattering/reflection and minimal attenuation. At SIK CMC sodium salt (Alfa Aesar GmbH & Co KG, Karlsruhe, Germany, www.alfa.com) 2.63% w/w was used for the hyperbolic contraction tests. Concentrations (Protea Chemicals, Bryanston, South Africa, http://www.proteachemicals.co.za) tested at the MST in complex geometries and in-line rheometer (UVP-PD method) varied from 3.5 - 6.5% per weight. The same concentrations were tested in a rheometer to obtain off-line rheological parameters which were then compared with the in-line results obtained from the pipe viscometers and ultrasound method.

3.7.3 Bentonite

Bentonite powder (Protea Chemicals, Bryanston, South Africa, http://www.proteachemicals.co.za) was mixed with water to obtain different concentrations of bentonite:water suspensions. The concentrations varied from 5 - 8.5% per weight and were used for tests in the open channel and in-line rheometer (for different pipe diameters). All of the concentrations were rheologically tested in-line by using the pipe viscometer as well as off-line by using a conventional rheometer. Particle size distribution measurements were conducted at the MST. The Mastersizer2000 from Malvern Instruments was used to conduct the test. Figure 3.33 and Figure 3.34 show the particle size distribution for kaolin and bentonite, respectively.

3.7.4 Kaolin

Dry kaolin powder (Protea Chemicals, Bryanston, South Africa, http://www.proteachemicals.co.za) was used to prepare the kaolin:water suspensions. The kaolin was obtained from one source and supplied by the MST group. Different concentrations were prepared ranging from 13 to 17% per volume. The kaolin suspensions were mixed in a mixing tank and left overnight for mixing to ensure that the suspensions were properly mixed. Kaolin clay was mainly used for in-line rheometric tests using different transducers and further comparison was made to rheological results obtained from conventional off-line rheometer and in-line pipe viscometer. Kaolin suspensions attenuate the ultrasonic energy significantly (Kotzé *et al.*, 2008) and thus this model fluid was not used for tests in complex geometries, where large penetration depths were required.

The fluids tested in this work were treated as time independent to a certain degree. This assumption is valid provided that the fluid under test is presheared to its rheologically stable state. This was pragmatically not a problem in the tube apparatus, where the fluid is continuously sheared in the tank, pump and tube sections. All fluid samples were pre-sheared in the off-line rotational rheometer at the highest shear rate (1000 s^{-1}) for one minute before a flow curve was measured and used for comparison with tube viscometry and ultrasonic rheometry (UVP-PD methodology). The samples were pre-sheared in order to break down time dependent structures and to closely simulate the conditions of the in-line tests (Kotzé *et al.*, 2008).

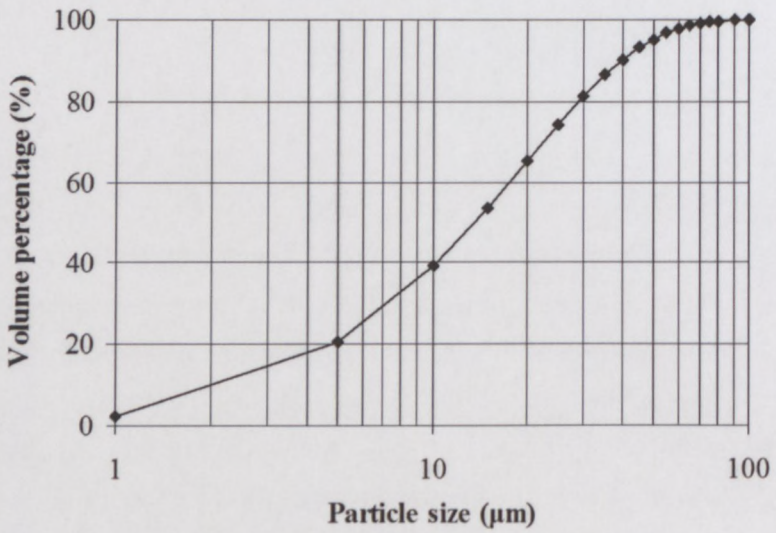

Figure 3.33: Particle size distribution of kaolin

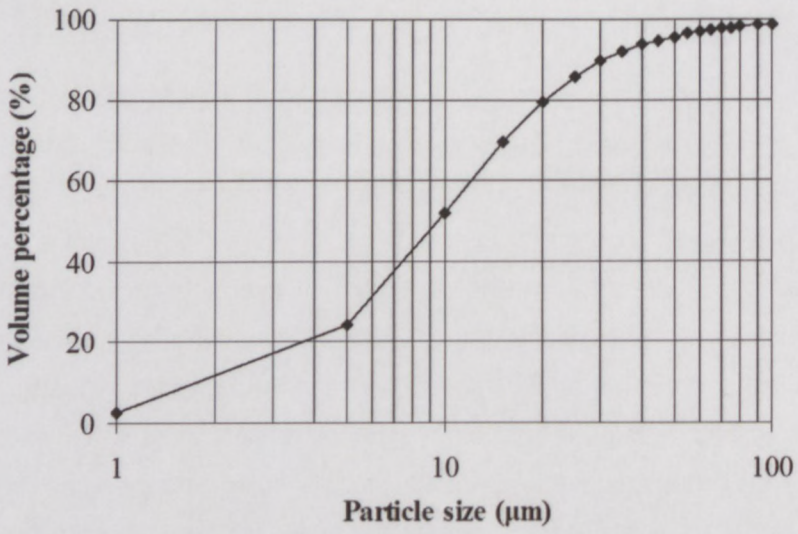

Figure 3.34: Particle size distribution of bentonite

3.8 CONCLUSIONS

3.8.1 Empirical behaviour

The present UVP system with a method for measuring sound velocity in-line using specially designed flow adapters has a significant advantage as erroneous velocity of sound values due to temperature changes may result in inaccurate velocity profiles. Furthermore, the waveform measured by the oscilloscope is recorded using custom software, which enables continuous monitoring of the sample volume as the properties may change with different parameters such as attenuation, temperature and speed of sound.

The effect of time frame aliasing was very noticeable throughout tests. Time frame aliasing was removed by adjusting the PRF. However, this effect can only be spotted by monitoring the received echo from ultrasound emissions.

Reflected wave effect was recognised in almost all of the measured velocity profiles. This was predominant in the flume tests as the air/liquid interface at the free surface provided a high acoustic impedance mismatch. However, this was easily corrected for by interpolating the velocity profile to the free surface interface. This effect did not influence the calculation of rheological parameters using the UVP-PD methodology as only the first half (radius of the pipe) was used for post data analysis.

Sedimentation problems were much more noticeable during the flume tests than when compared to the pipe tests using conventional transducers with the cavity setup. The main reason for this is due to the installation positions of the transducers at the bottom of the flume surface. During pipe tests the transducers are mounted across the radial axis of the pipe, thus minimising particles or trapped air inside the cavities.

3.8.2 Experimental equipment and procedures

The equipment was equipped with all the necessary instrumentation to measure flow rates, point pressures, temperature, velocity profiles and speed of sound in the investigated fluid.

Software was developed (not by the author) for the tube viscometers to sample the data and log it in spreadsheets where the results were displayed in graphical format for a user-friendly interface between operator and test rig.

Post data analysis was an important part of the UVP measurements. Software was developed to determine the bulk flow rate in a complex geometry using a triangulation technique. Software was also developed for velocity profile curve fitting in order to obtain the desired rheological parameters of the investigated mineral suspensions.

As part of the optimisation of the UVP system custom software was written for automatic control of a high precision robotic arm used for acoustic characterisation of ultrasonic transducers. An algorithm was developed and extensively tested for deconvolution of erroneous velocity data due to finite size of the sampling volume as well as sampling process through material wall layers.

The equipment was commissioned with clear water tests.

Calibration and test procedures were developed to accurately produce pipe flow data in order to establish relevant rheological parameters of all the mineral suspensions tested. Furthermore, care was taken with the calibration of a reference flow meter used for validation of experimental profiles in complex geometries by testing the accuracy and performance with non-Newtonian fluids.

The experimental errors pertaining to the pipe viscometers and UVP system have been analysed and discussed and are deemed to be within acceptable limits.

Several concentrations of bentonite and kaolin suspensions, as well as CMC solutions, were used for the tests. This yielded a wide range of fluids with varying rheological properties.

Initial results obtained were used to evaluate the UVP system for measurement of non-Newtonian fluids in complex geometries. After improvements were made to the UVP system, results obtained using a conventional transducer as well as special delay line transducer in combination with signal processing techniques were analysed and compared. The UVP-PD methodology was also tested using new transducers and rheological results were compared to that obtained from in-line tube viscometry and conventional off-line rotary rheometry.

CHAPTER FOUR

EXPERIMENTAL EVALUATION OF UVP FOR COMPLEX FLOW MEASUREMENTS

CHAPTER FOUR

EXPERIMENTAL EVALUATION OF UVP FOR COMPLEX FLOW MEASUREMENTS

4.1 INTRODUCTION

The objectives and motivation for the tests were to evaluate the accuracy of the UVP system for detailed non-Newtonian flow behaviour measurements in complex geometries. The following geometries were used:

- ***Hyperbolic contraction***

  The hyperbolic contraction can be used to determine extensional rheological properties of different fluids, which is directly linked to the mouthfeel of semi-solid foods (elongational viscosity) in the food industry. This study also continuous work done by Zatti *et al.* (2009), who measured velocity profiles inside a hyperbolic contraction at multiple positions using UVP.

- ***Rectangular open channel (width 300 mm).***

  Visualisation of non-Newtonian flow inside open channels could provide new information that can be used to improve current open channel designs for more efficient transportation of thickened mineral slurries.

- ***Diaphragm valve (50% open).***

  More detailed observations of velocity fields in pipe fittings such as contractions, elbows, orifices and valves can be used for validation of theoretical simulations using CFD. Design engineers would then be able to predict energy losses more accurately and therefore develop more efficient pipelines for industrial applications.

During this study only conventional ultrasonic transducers and UVP monitor (Met-Flow SA, Switzerland) were used as test fluids for velocity profile measurements. CMC solutions were used for the hyperbolic contraction and diaphragm valve tests. CMC solutions and bentonite suspensions were tested in the open channel. Tube viscometer (pipe) data and off-line rotational rheometric data were used to rheologically characterise the test fluids. The rheological parameters obtained using tube viscometry were used to calculate Reynolds numbers for non-Newtonian pipe flow. The flow behaviour in the hyperbolic contraction was measured through the material wall layers using an ultrasonic transducer submerged in a tank filled with the same test fluid, thus using CMC as acoustic coupling fluid (see Section 3.3.5 for the experimental setup). In contrast, the valve geometry as well as physical properties (material) of the open channel boundaries was too complex for velocity profile measurements through the wall interface and thus two different ultrasonic measurement techniques are presented. Tube viscometer (pipe) as well as rotary viscometer data can be found in Appendix A.

4.2 FLOW MEASUREMENTS IN HYPERBOLIC CONTRACTION

The theoretical and experimental velocity distribution inside the hyperbolic contraction, obtained using Equation 2.28 and UVP for CMC 2.63% w/w (K = 0.68, n = 0.82; obtained using off-line rheometry), is shown in Figure 4.1. In order to ensure accurate flow rate readings and constant test conditions, measurements were conducted in the optimum range of the electromagnetic flow meter at 0.6 l/s. The system settings used for the velocity profile measurements are displayed in Table 4.1. The flow velocity resolution (Met-Flow SA, 2002) did not exceed 20 mm/s and an average of 128 profiles was used. Transducers were mounted at an angle of 15 degrees with respect to the lateral, i.e. the Doppler angle was 75 degrees. All other tests (pipe, flume and diaphragm valve) were done with a Doppler angle set at 20 degrees. It was found experimentally that a Doppler angle of 75 degrees yielded better results when velocity profiles were measured through the contraction wall material layers. The calculated Reynolds number (Re_2) using Equation 2.21 was 1700, thus tests were done laminar flow. Also, the theoretical velocity distribution does not seem constant (Figure 4.1) as sudden 'jumps' in velocity magnitudes can be observed. The reason for this is due to viscosity and temperature changes in the fluid, which caused the flow rate to change. This was monitored and included in the theoretical calculations to enable accurate comparison between the UVP measurements and theoretical estimations.

Table 4.1: UVP parameter settings for CMC 2.63% w/w contraction tests

Gain	US Voltage (V)	Number of cycles/pulse	Number of US pulse reps.	Sound speed (m/s)
7-9	150	2	1024/2048	1548

Theoretical (calculated using Equation 2.30) and experimental velocity profiles along the contraction length were integrated in order to obtain the flow rate. The integration was made from the wall to the contraction centre, thus only 50% of the profile was needed. The average error difference percentage between the theoretical and experimental integration was 10.37%. This error was mainly due to the temperature dependant properties of the CMC sodium salt, which showed a decrease in viscosity with increasing temperature from fluid pumping effects. Figure 4.2 shows a measured and theoretical velocity profile 7 mm from the contraction limit position (as shown by the black line in Figure 4.1). The gradient of the experimental profile shows a slight increase between the radius and wall positions. These errors may have occurred due to changes in sound velocity as a result of measuring though material layers with different acoustic impedances. However, velocity profiles can still be used to derive elongational viscosity for fluid characterisation in the food industry (see Section 2.3.4.2).

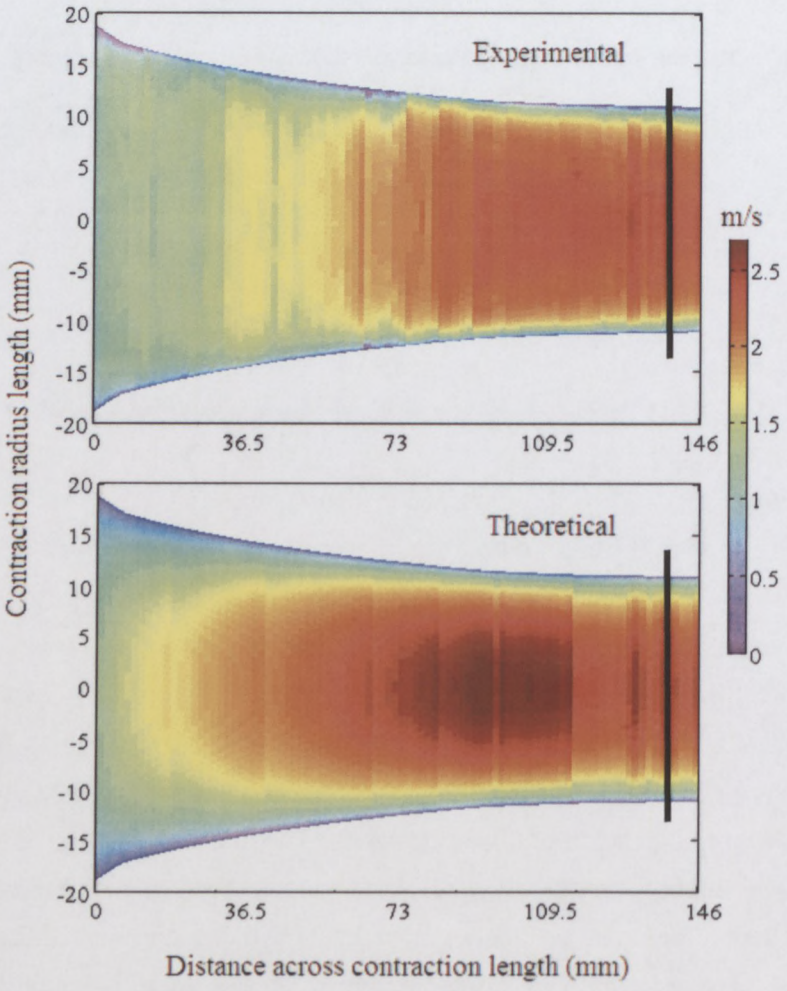

Figure 4.1: Experimental and theoretical velocity distribution across contraction length for CMC 2.63% w/w

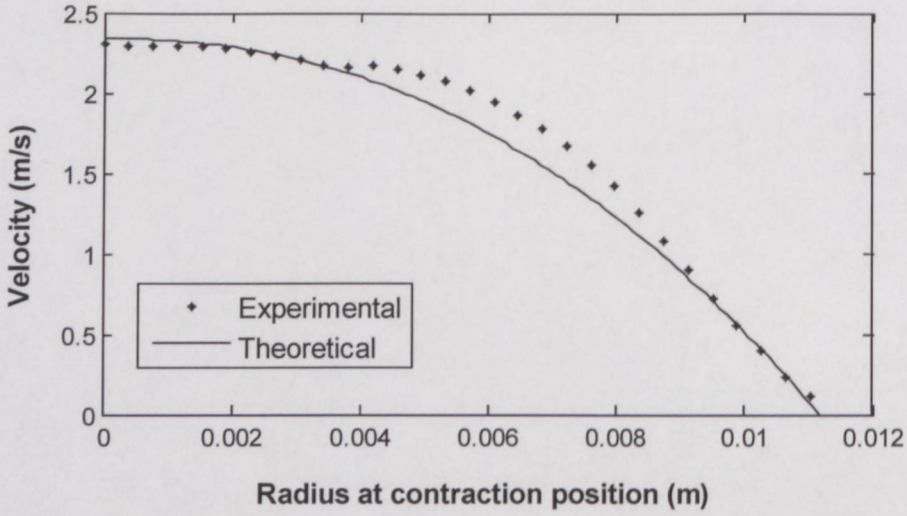

Figure 4.2: Experimental vs. theoretical velocity profile inside hyperbolic contraction

Even when using a material with good acoustical properties as well as optimised wall thickness a significant amount of energy is still required to overcome ultrasonic absorption and penetration depths when measuring through material layers. This loss of energy can also cause problems when measurements inside attenuating fluids are of interest, which is the case with most industrial suspensions. A transducer with lower emitting frequency can be used, but at a cost of decreased spatial resolution. This will complicate estimation of wall positions even further, where measurement channels overlap or are present beyond the wall layer / interface (Kotzé *et al.*, 2011). Estimation of the wall positions is essential for flow or fluid property calculations. Wiklund *et al.* (2007) showed a significant variation in rheological parameters when wall positions were changed by only one channel distance (less than 0.5 mm). A method of determining the maximum velocity as the centre position could be used, but his technique fails for even moderate shear-thinning fluids due to the limited velocity resolution at the centre. This approach also fails for velocity profiles measured across an asymmetrical axis e.g. in a valve geometry. Wiklund *et al.* (2007) introduced several techniques for wall detection, but concluded the accuracy to be within one channel, unless access to RF-data can be obtained.

Furthermore, Messer and Aidun (2009) showed that measurement through wall material layers influence the accuracy of UVP by investigating the effects caused when measuring through rigid impermeable walls. It was concluded that wall boundary layers changes the shape of the acoustic beam, the propagation of the ultrasonic burst and the intensity distribution of the returning echo and as a consequence decreases the overall accuracy of the UVP method.

4.3 FLOW MEASUREMENTS IN OPEN CHANNEL

CMC 5.26% w/w and bentonite 5.29% w/w were tested in the open channel at the MST laboratory. All tests were conducted at a slope of 1 degree. Velocity profiles measured at different positions are compared to theoretical predictions. Two-dimensional flow maps were constructed from all six experimental profiles and integrated to obtain the volume flow rate. The calculated flow rate was compared to a reference flow meter in order to verify the accuracy of the combined measurements. Rheological parameters were obtained using tube viscometry.

4.3.1 Profiles measured in CMC solution

4.3.1.1 Velocity profiles and sheet flow comparison

Tables 4.2 and 4.3 summarise the range of experimental conditions and UVP parameter settings for the CMC 5.26% w/w (K = 0.92, n = 0.69) tests. Note that based on these parameter settings the energy input to the contraction system was substantially higher than when compared to the velocity profile measurements inside the flume. This was due to installation of ultrasonic transducers with direct contact with the test fluid, thus minimising energy losses due to energy absorption and reflection. It was possible to use an average of 500 profiles due to the low number of US pulse emissions (256) required for velocity measurements.

Table 4.2: CMC 5.26% w/w flume flow conditions

Q (l/s)	H (mm)	Re_H	Regime
6.79	58.7	164	Laminar
13.13	71.7	327	Laminar

Table 4.3: UVP parameter settings for CMC 5.26% w/w flume tests

Gain	US Voltage (V)	Number of cycles/pulse	Number of US pulse repetitions	Sound speed (m/s)
3-5	90	2	256	1520

An example of a centreline plot for CMC 5.26% w/w at a flow rate of 2.72 l/s is shown in Figure 4.3. Also included here are the predictions of Equations 2.19 and 2.20. It can be observed that there is a good correlation of the theoretical prediction with the experimental data. Figure 4.4 shows how the theoretical profile deviates from the experimental profile less than 100 mm away from the centre. Similar results were found for the other laminar flow results (13.13 l/s).

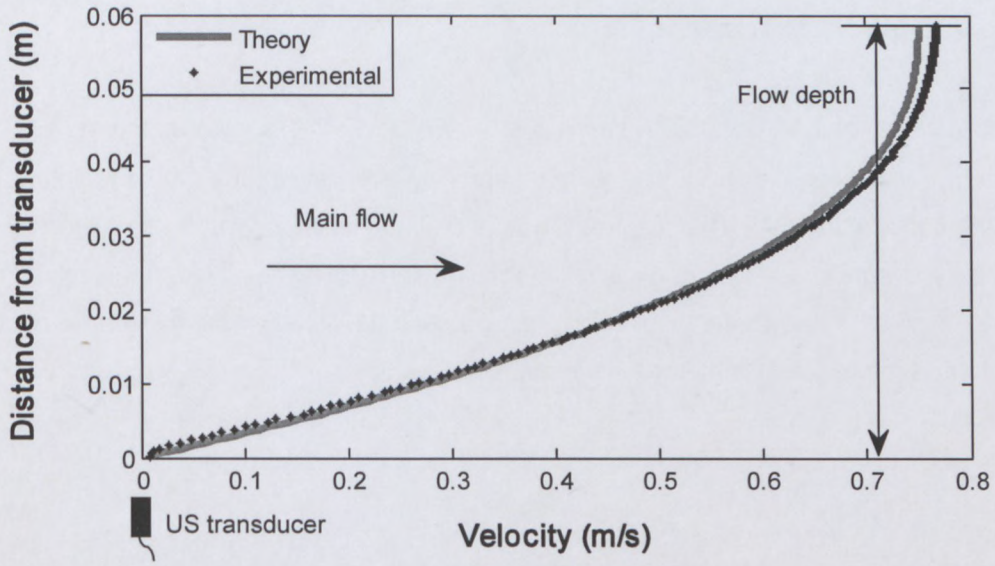

Figure 4.3: Experimental profile vs. Equations 2.19-2.20 for CMC 5.26% (Re_H = 164, Q = 6.79 l/s)

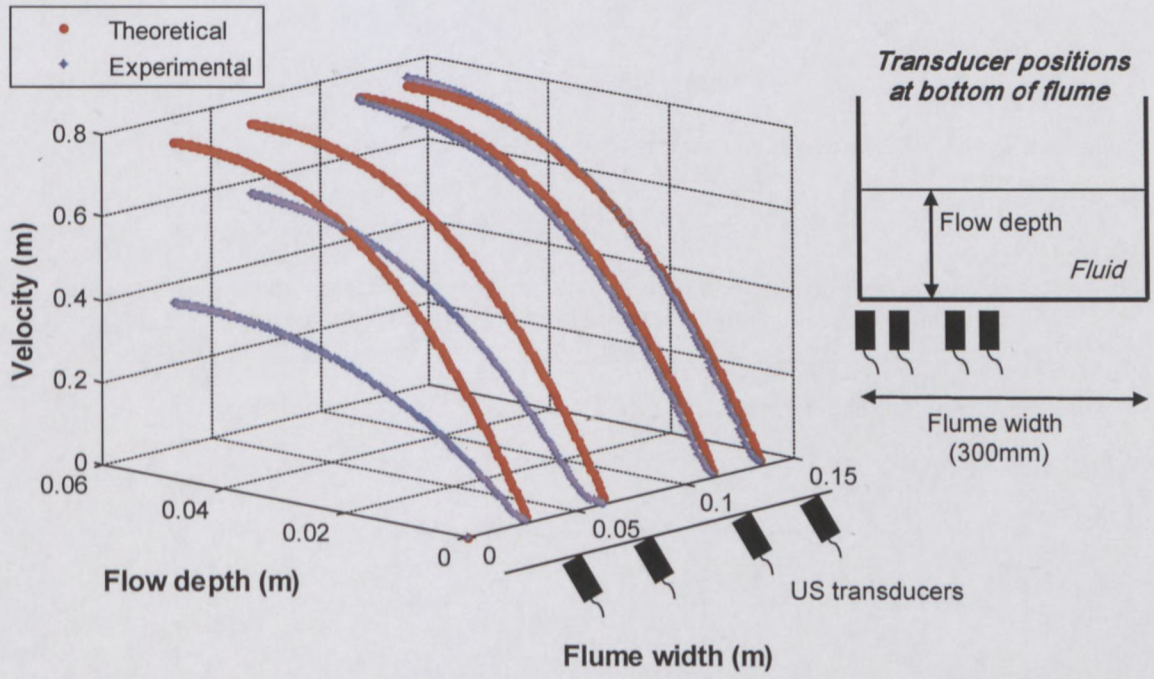

Figure 4.4: CMC 5.26% w/w flume center to wall experimental profile vs. Equations 2.19-2.20 (Re_H = 164, Q = 6.79 l/s)

4.3.1.2 Flow maps for CMC solution

The contour plot of the 5.26% w/w CMC at Re_H = 164 is shown in Figure 4.5. The difference between the flow rates measured by the flow meter and the integrated contour plot was 6.3%. This inspires confidence in the reliability of the detailed velocity measurements presented here. Similar results were found for the other laminar flow data. Table 4.4 shows the error difference percentage between the integrated contour plots and reference flow meter for two different flow rates.

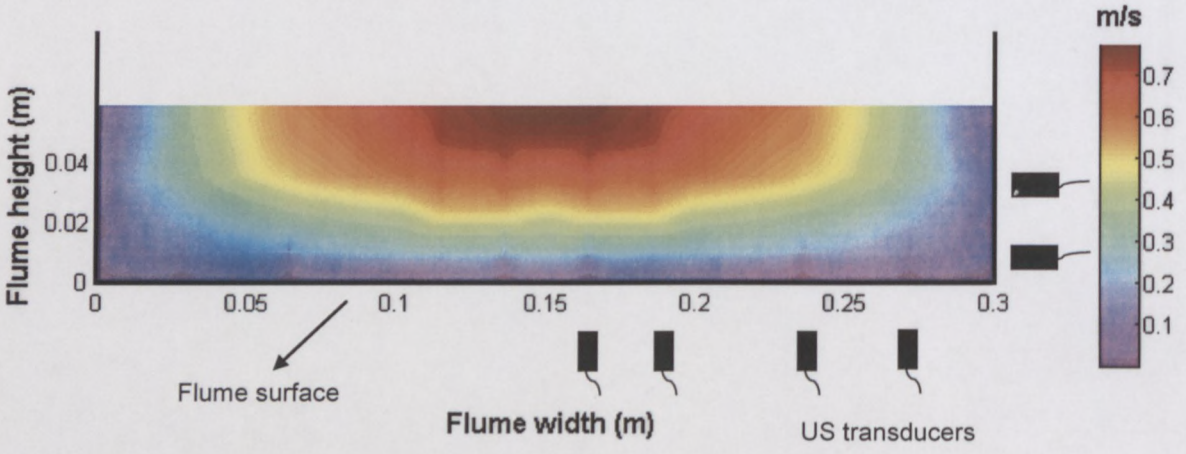

Figure 4.5: CMC 5.26% w/w experimental laminar flow map (Q = 6.79 l/s, Re_H = 164)

Table 4.4: Percentage difference between volume flow rates obtained from integration of flume experimental profiles and reference electromagnetic flow meter

Flow meter (l/s)	Integration (l/s)	Flume vs.flow meter (%)
6.79	6.36	6.3
13.1	12.8	2.53

4.3.2 Profiles measured in bentonite suspension

4.3.2.1 Velocity profiles and sheet flow comparison

The centreline velocity profile showing the model predictions and the experimental data for the 5.29% w/w bentonite suspension (K = 0.008, n = 1, τ_y = 2.6) is shown in Figure 4.6. Experimental conditions and UVP parameter settings are displayed in Tables 4.5 and 4.6.

Table 4.5: CMC 5.26% w/w flume flow conditions

Q (l/s)	H (mm)	Re_H	Regime
3.12	22.6	438	Laminar
4.36	24.3	723	Laminar

Table 4.6: UVP parameter settings for CMC 5.26% w/w flume tests

Gain	US Voltage (V)	Number of cycles/pulse	Number of US repetitions	Sound speed (m/s)
3-5	90	2	256	1560

The agreement between the theoretical prediction and measured profile seem to be good. However, the velocity gradients close to the flume surface (0 – 0.01 m) do not agree very well. This is due to the combination of the transducer installation method (see Section 3.3.6.1) and high velocity gradient of the Bingham profile. There is an increase in velocity at the surface interface due to influence of the cavity, which distorts the measured velocity profile. Note that this distortion did not occur during the CMC tests, which suggests that the cavities have a more significant influence on plug flows where the velocity gradients are high.

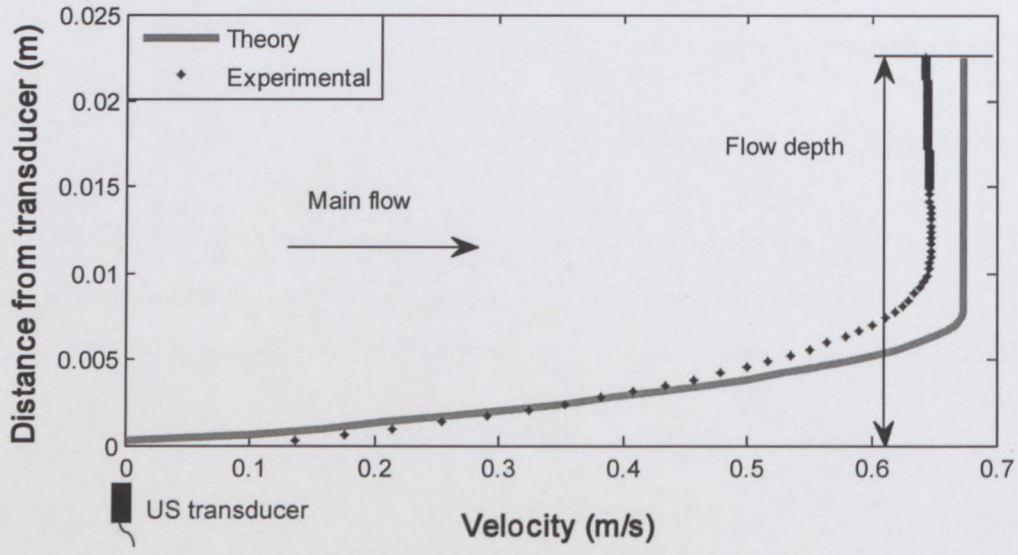

Figure 4.6: Experimental profile vs. Equations 2.19-2.20 for bentonite 5.29%
(Re_H = 438, Q = 3.12 l/s)

It is interesting to note that for the 5.29% v/v bentonite suspension the deviation of the predicted from the measured profile with distance from the centreline (see Figure 4.7) is not so sudden as for CMC (see Figure 4.4). This could be ascribed to the formation of the plug which extends towards the side wall. The sheet flow model still holds to about 50 mm from the side wall.

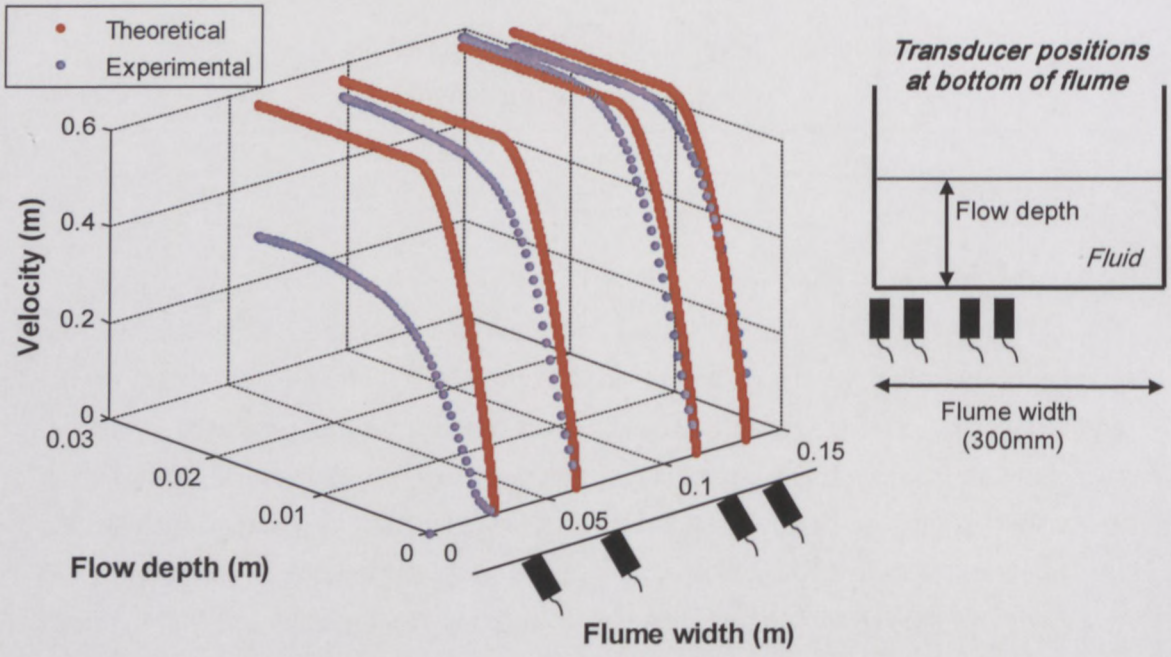

Figure 4.7: Bentonite 5.29% w/w flume centre to wall experimental profile vs. Equations 2.19-2.20
(Re_H = 438, Q = 3.12 l/s)

4.3.2.2 Flow maps for bentonite suspension

Figure 4.8 shows the contour plot for bentonite 5.29% w/w at a flow rate of 3.12 l/s (laminar flow). The error difference between the measured flow rate and calculated flow rate was 6.46%. It can be observed that there are velocity 'spikes' present close to the bottom surface of the flume (marked with crosses in Figure 4.8), which is due to the high velocity gradient of the plug flow (notice that this was not observed for CMC results, Figure 4.5). Similar results were found for other laminar velocity data. The 'spikes' can be removed by either adding or shifting the radial measurement line (Measurement line 1, see Section 3.3.6.1) closer to the surface so that the triangulation algorithm can interpolate between the 'spikes', thus improving the overall quality of the contour plot. However, this was not possible due to the physical beam shape of the ultrasonic transducers. Moving the transducer too close to the bottom surface may cause the ultrasonic beam to overlap with the flume surface material and consequently result in severe distortion of the measured velocity profiles. Table 4.7 shows the error difference percentages between the calculated and measured bulk flow rate for two different flow rates.

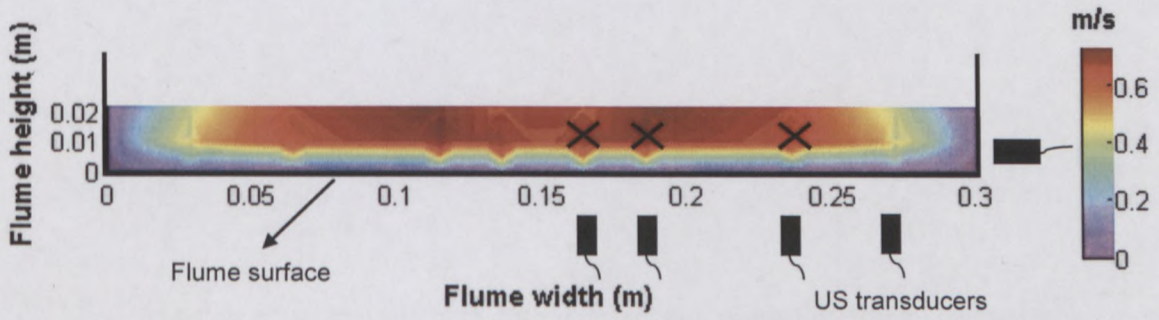

Figure 4.8: Bentonite 5.29% experimental laminar flow map (Q = 3.12 l/s, Re_H = 438)

Table 4.7: Percentage difference between volume flow rates obtained from integration of flume experimental profiles and reference electromagnetic flow meter

Flow meter (l/s)	Integration (l/s)	Flume vs.flow meter (%)
3.12	2.92	6.46
4.36	4.27	2.07

The error difference percentages (Table 4.7) validate the accuracy of the velocity profiles measured using standard ultrasonic transducers. The cavities between the transducer front and flume surface did not seem to influence the measured velocity profiles significantly. This could be due to the combination of the large flow area and free air surface present in open channel flow. The large boundaries provide velocity gradients which are not as high as that found in smaller diameter pipes for example, which lead to less distortion in the experimental profiles (increase in velocities beyond wall interfaces). However, during tests the cavities were filled with bentonite particles as well as pump residue and transducers needed to be removed and flushed frequently to ensure accurate measurements (see Figure 4.9). This setup may not be suitable for industrial applications where transducers need to be fixed in order to monitor transient flows, e.g. laminar to turbulent transition.

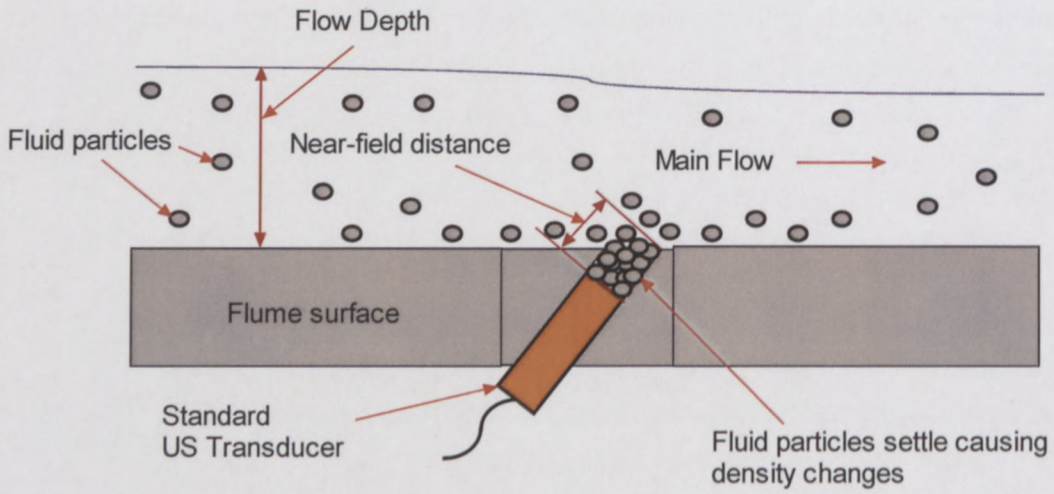

Figure 4.9: Fluid particles settling inside cavities (standard transducer installation)

4.4 FLOW MEASUREMENTS IN DIAPHRAGM VALVE

CMC 6.15% w/w (K = 0.074, n = 0.85) was tested in a 50% open diaphragm valve (described in detail in Section 3.2.4, Chapter 3) at the MST laboratory. A triangulation technique to construct a two-dimensional flow map and calculate the bulk flow rate could not be used during these preliminary tests due to insufficient experimental data. Instead area distributions in combination with velocity data (as described in Section 3.3.7) were used and results were compared to a reference flow meter.

4.4.1 Velocity profiles

Velocity profiles measured at three different flow rates (0.5 l/s, 0.99 l/s, 1.7 l/s) in a straight pipe (D = 52.8 mm) is shown in Figure 4.10. Figures 4.11 - 4.13 show velocity profiles measured at the same flow rates inside the valve across TDX Lines 1-3.

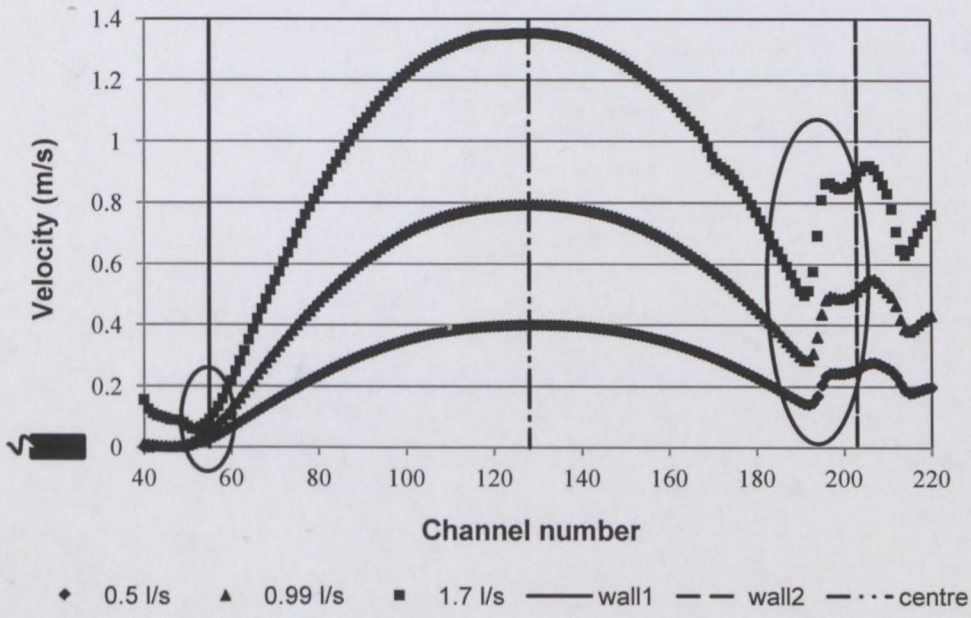

Figure 4.10: Radial profiles measured in a 52.8 mm pipe using UVP for CMC 6.15% w/w

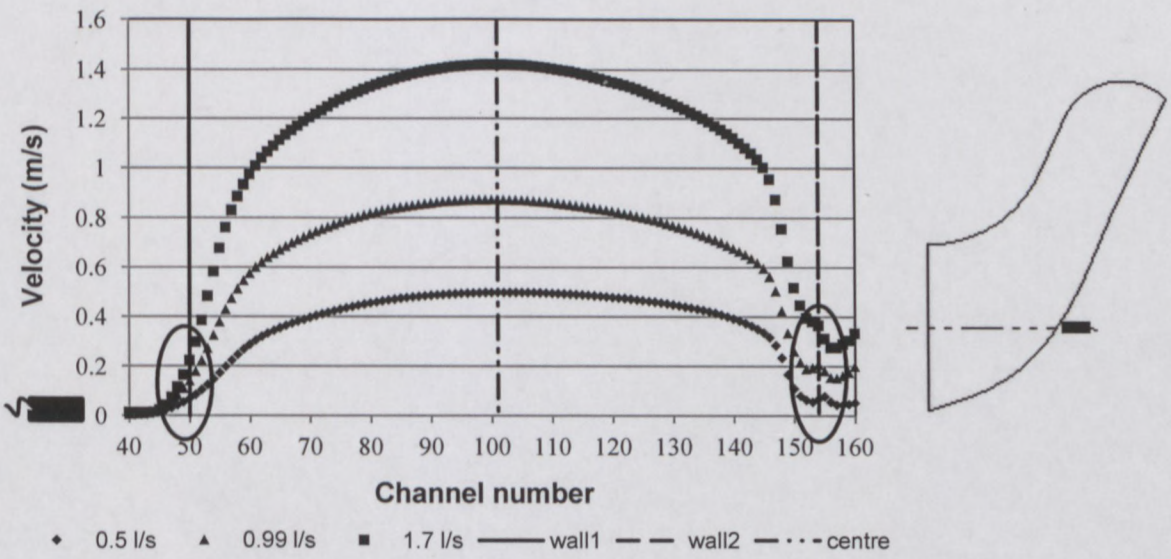

Figure 4.11: Radial profiles measured in valve across TDX Line 3 for CMC 6.15% w/w

The experimental profiles obtained from the straight pipe in laminar flow shows a typical power-law point velocity distribution. Results obtained from measurements across TDX Line 3 are symmetrical around the centre position (dotted lines) and was expected due to measuring across a symmetrical axis in the valve. It can also be observed that the magnitudes of velocity measured in the valve are slightly higher than compared to that obtained in pipe flow.

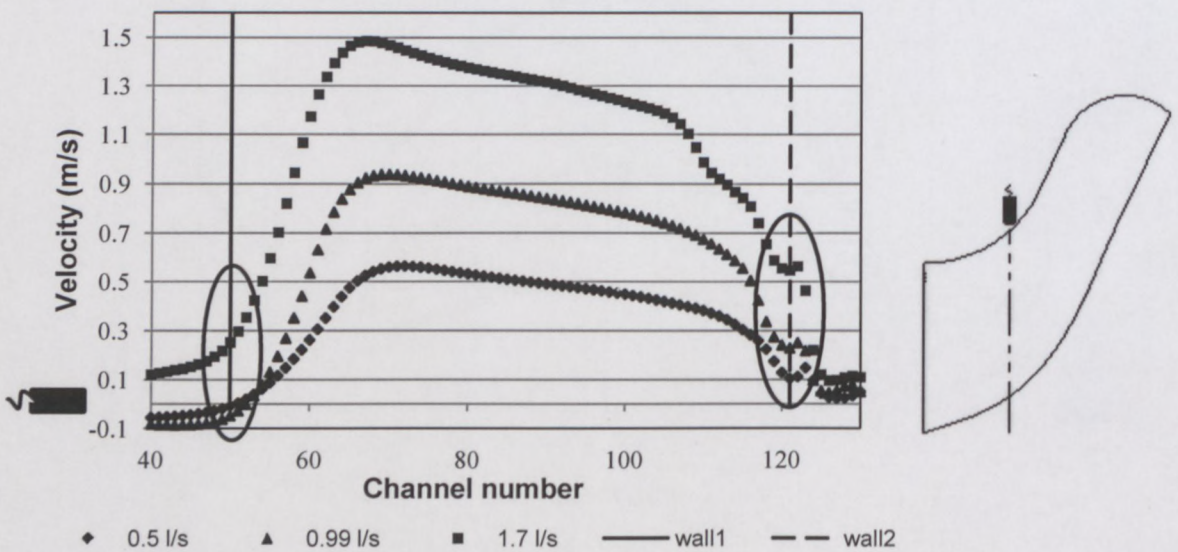

Figure 4.12: Lateral profiles measured in valve across TDX Line 1 for CMC 6.15% w/w

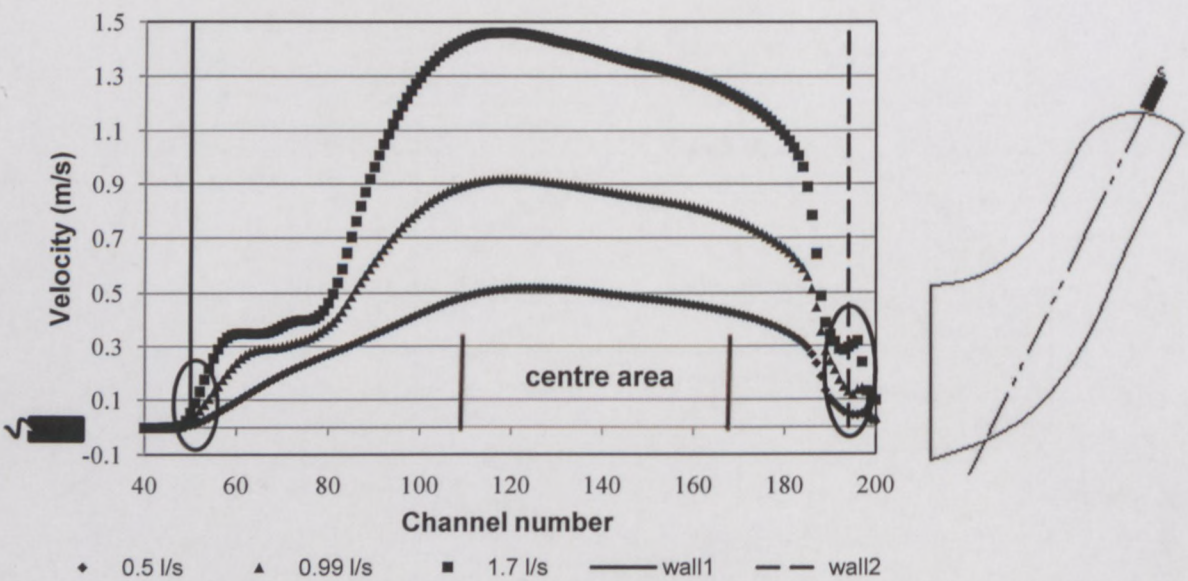

Figure 4.13: Diagonal profiles measured in valve across TDX Line 2 for CMC 6.15% w/w

Figure 4.12 shows a sharp increase in velocity close to the near wall for all of the lateral measurements. This could be due to the fluid pushing against and under the diaphragm creating higher speeds than compared with velocities measured at a different position in the valve. Velocity profiles measured across the diagonal position (TDX Line 2) shows an increase of velocity from the near wall and steady decrease from the centre area of the valve. At higher flow rates the linear increase of velocity from the near wall to the maximum velocity (as in the 0.5 l/s case) seems to stay constant for some distance, which suggest that most of the fluid flow occurs beyond the valve's upper regions or centre area (see Figure 4.13).

It can be observed that every experimental velocity profile has non-zero velocities (marked with circles) at the wall interfaces (marked with solid and broken lines, wall1-wall2). Firstly, the increase in velocity at the first wall interface (wall1) is due to the cavities situated in front of the transducer surfaces, where flow occurs before the actual wall position. The increase in velocity at the opposite wall interface (wall2), is due to multiple ultrasonic reflections from the wall, which is inherent in UVP. This reflected energy is scattered back by the moving particles inside the fluid to produce detected Doppler shifts and consequently the UVP instrument starts to plot an image profile (Jorgensen *et al.,* 1973). When measuring in simple or symmetrical geometries, only half of the measured profile is needed, as in the case of pipe flow or across a symmetrical axis (Figures 4.10 – 4.11). Here the effect of multiple ultrasonic reflections is not important as the first half of the experimental profile is assumed to be similar at both sides from the centre position or maximum velocity for a power-law fluid (dotted lines). However, if velocity profiles in complex or asymmetrical geometries are measured, it is essential to acquire accurate velocity data at both wall interfaces, where the velocity gradients are high. One method to compensate for multiple wall reflections is to install another transducer at the opposite wall, thus measuring from both sides. This method is also useful for reducing the effects of ultrasonic attenuation, but will introduce another cavity to the system, unless a different type of transducer is used.

4.4.2 Velocity distributions

Three velocity distributions drawn in Solidworks 2009 (see Section 3.3.7) are presented in Figures 4.14 – 4.16 for 0.5 l/s. The first design shows an unrealistic velocity distribution along the top regions where zero velocities occupy most of the area. A 20.6% difference between the calculated (0.4 l/s) and measured (0.5 l/s) volume flow

rate was determined using this design. Given the unrealistic velocity distribution at the top regions (abrupt changes in velocity magnitudes) it was decided to test an alternative distribution of segments with the same experimental velocity profiles.

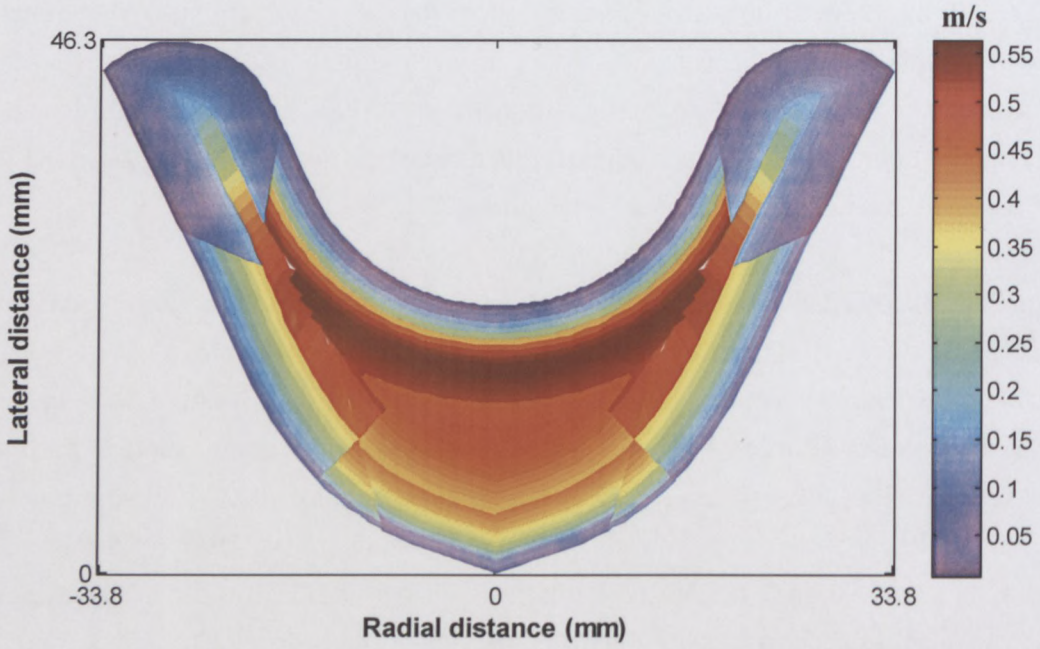

Figure 4.14: Velocity distribution 1 colourmap

Figure 4.15 shows the 2nd distribution drawn with Solidworks 2010/11 and based on the previous design (Figure 4.14) it can be seen that it is quite different. This distribution yielded a 17% difference between the calculated (0.42 l/s) and measured flow rate, which is a 3% improvement when compared to the previous design. The upper regions also look more realistic in Figure 4.15, but there are still areas that assume the highest measured velocities (white colour) next to regions where much lower magnitude of velocities are hypothesised (marked with circle). Therefore that particular area was changed to produce the result shown in Figure 4.16. The 3rd distribution yielded the most accurate flow rate (0.43 l/s) and the error difference percentage dropped to 14.86%, which is an improvement when comparing results obtained using previous velocity distributions.

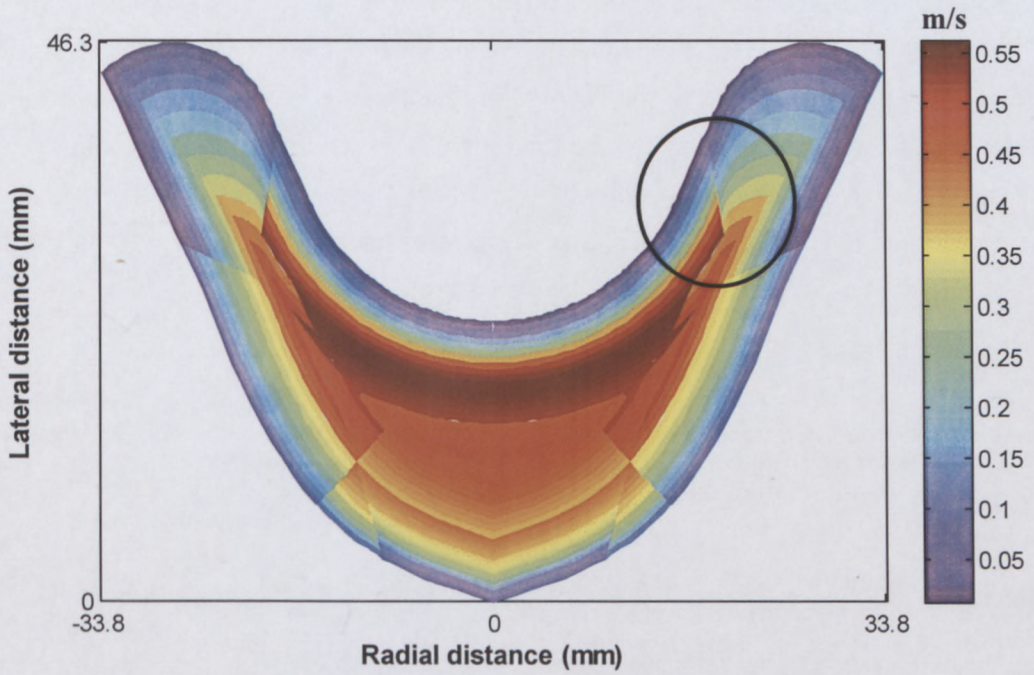

Figure 4.15: Velocity distribution 2 colourmap

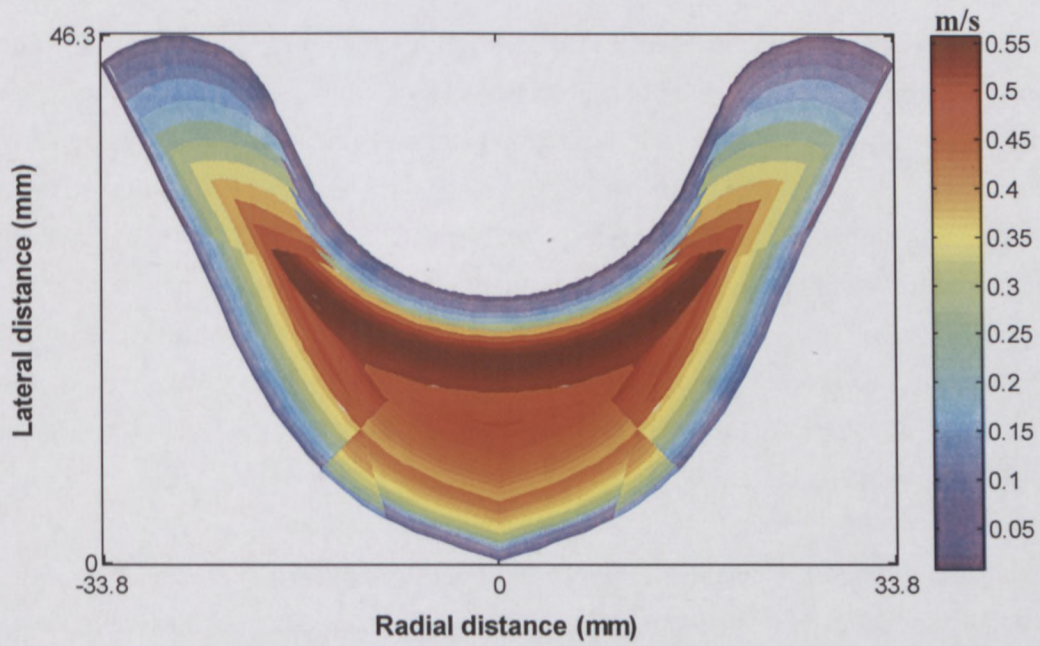

Figure 4.16: Velocity distribution 3 colourmap

A comparison of different flow rates obtained by integration of velocity profiles measured in the pipe as well as determined using the manually drawn flow field (Figure 4.16) with the measured (electromagnetic) volume flow rate is shown in Table 4.8. For these tests it was assumed that the flow meter results were correct as it as calibrated with a weigh tank (see Section 3.4.2). With increasing flow rate the error difference percentage between the valve (using UVP) and flow meter results increase. This was due to more significant distortion of velocity profiles at the wall interfaces as much higher velocities were present with increasing flow rates.

Table 4.8: Percentage difference between volume flow rates obtained from flow meter, integration of velocity profile in a pipe and calculation using the velocity distribution of the diaphragm valve and Equation 3.6

Flow meter (l/s)	Velocity Profile Integration (l/s)	Integration vs. Flow meter (%)	Valve flow rate calculation (l/s)	Valve vs. Flow meter (%)
0.50	0.490	2.00	0.426	14.86
0.72	0.723	0.42	0.581	19.36
0.99	0.973	1.77	0.770	22.18
1.30	1.376	5.82	0.970	25.35
1.70	1.660	2.34	1.269	25.38

Some important observations can be made from the colourmap in Figure 4.16. The majority of the flow seems to be at the centre area of the valve and not at the upper regions (see Figure 4.13). Also, the highest measured magnitudes of velocity appear to be just below the valve diaphragm (see Figure 4.12). The next step was to add an extra measurement line at the centre position (see Figure 3.23, Section 3.3.7) of the valve in order to observe the flow behaviour across the lowest area (highest contraction) of the diaphragm valve. The new information made available using another transducer made it possible to use a triangulation algorithm in order to eliminate errors caused by the assumption of velocity magnitudes where no experimental data was available. These results are presented in Chapter 6.

It is also very important to have information about the physical characteristics of the ultrasonic transducer's beam when measuring in complex geometries such as a valve. If measuring in narrow regions (TDX Line 2 for example) the user must make sure that the beam does not overlap with wall interfaces, which will distort velocity profiles significantly.

4.5 CONCLUSION

Based on the experimental results it was possible to do continuous high - resolution flow mapping of the complete velocity field along a hyperbolic contraction using a high precision robotic arm. Experimental results showed good agreement with theoretical predictions and the maximum error was 10%. Initial results obtained in the flume proved to be very encouraging for future research in non-Newtonian open channel flow. The error difference between the integrated contour plots ranged from 2% to 6.5%. It was also possible to measure quantitative velocity data at various flow rates for non-Newtonian flow inside a highly complex geometry, such as a diaphragm valve, for the first time. The difference between calculated and measured flow rates varied from 15 to 25%.

Profiles measured in the diaphragm valve showed a significant increase in velocity at the wall interfaces, which should theoretically be zero. This increase in velocity also distorts the overall flow profile, especially close to the walls where the velocity gradients are high. The cavity setup thus makes it difficult or near impossible to obtain the true velocity profile across a particular axis in a highly complex geometry. One could measure through material layers to avoid the influence of cavities inside the flow area. However, this is sometimes not even possible due to physical material properties (attenuation of ultrasonic energy). Even when the material of the geometry is optimised for maximum ultrasonic energy transfer (hyperbolic contraction study, Section 4.2), significant energy loss still occurs, which makes this method not suitable for industrial applications. Furthermore, measuring through material layers complicates estimation of wall positions and Doppler angles vary due to ultrasonic beam refraction, which influences the accuracy of velocity profiles.

This problem could be reduced by the introduction of new ultrasonic transducers that allows measurements directly at the transducer front. A transducer of this kind, where the focal point of the ultrasonic beam is located at the transducer front/wall interface, was evaluated and results are discussed in Chapter 5. Based on initial findings and future improvements, UVP will prove to be a useful tool for validating CFD simulations in highly complex geometries.

CHAPTER FIVE

OPTIMISATION OF PULSED ULTRASOUND MEASUREMENTS

CHAPTER FIVE

OPTIMISATION OF PULSED ULTRASOUND MEASUREMENTS

5.1 INTRODUCTION

This chapter summarises all the test data obtained during the evaluation and optimisation of pulsed ultrasound measurements using different ultrasonic transducers. The main objectives were to increase the overall accuracy of velocity measurements using a new delay line transducer in combination with advanced signal processing techniques. Transducers were acoustically characterised using two techniques (echo and receiving mode, described below) and velocity profiles were measured with various combinations of UVP system parameter settings. Velocity profiles obtained using standard and delay line transducers were deconvolved (as described in Section 3.3.4, Chapter 3) in order to improve data close to wall interfaces. Profiles were measured in three different pipe diameters (16, 22.5 and 52.8 mm) for three different non-Newtonian fluids (CMC, bentonite and kaolin suspensions) and results before and after the deconvolution procedure are compared. Furthermore, profiles were obtained under a range of test conditions for two different transducers using custom velocity estimation algorithms and DMEA data (see Section 3.33). CMC solutions and bentonite suspensions were tested in two pipe diameters (22.5 and 52.8 mm) in order to obtain different shapes of profiles (e.g. plug flow) with different velocity gradients. Tube viscometer (pipe) data were used to rheologically characterise the test fluids in order to calculate Reynolds numbers for non-Newtonian pipe flow. Tube viscometer (pipe) data as well as rheograms (after Rabinowitch-Mooney transformation) of the different fluids used are shown in Appendix A, for reference.

5.2 ACOUSTIC CHARACTERISATION

The shape or lateral dispersion of the ultrasonic beam is the determinant of the lateral resolution of the UVP system. It is possible to design the size of the sample volume by defining the desired ultrasonic beam shape using different ultrasonic transducers (focal characteristics) and UVP system parameter settings (e.g. voltage, number of cycles per ultrasonic pulse). As described in Section 2.2.8 (Chapter 2), the ultrasonic beam shape

or more specifically, the sample intensity volume, mainly determines the sensitivity and accuracy of the UVP technique. Therefore, ultrasonic beam measurements were performed to gain detailed information about the actual beam shape of the given transducers as well as the actual echo intensities received by the transducers.

Four ultrasonic transducers (4 MHz, 5 mm active element) were tested in tap water using a stainless steel needle and high precision needle hydrophone. Two standard and two delay line transducers from Imasonic and Signal Processing SA (SPSA) were tested. Results obtained using the delay line transducer (1st generation) from Imasonic, France, is only included here for comparison with the delay line transducer (2nd generation) from Signal Processing SA, Switzerland. Acoustic data obtained during this work is divided into two sub-sections: results obtained using a standard stainless steel needle and that obtained using a needle hydrophone setup.

5.2.1 Stainless steel needle

When using this measurement method for acoustic characterisation of ultrasonic transducers (described in Section 3.3.2, Chapter 3), the transducer is used for transmitting and receiving acoustic intensities. Since the ECHO out connection of the UVP monitor is after the digital amplifier (Met-Flow SA, 2002), it is important to keep the gain settings in the UVP system parameters constant, e.g. an amplification gain setting of 1-1. Using a time ramp (gain setting of 1-3 or 3-5) will result in amplification of acoustic intensities further away from the transducer surface and consequently cause significant measurement errors. Figure 5.1 and 5.2 shows a 2D acoustic map for the SPSA and Imasonic standard transducers. The system parameter settings are displayed in Table 5.1. Note that when working in this mode (transmitting and receiving) the PRF should ideally be as low as possible. Since the maximum distance between the needle and transducer surface was 40 mm, a PRF (7.4 kHz) was selected to ensure a maximum distance of +/- 100 mm.

Table 5.1: UVP parameter settings for acoustic characterisation using stainless steel needle

Gain	US Voltage (V)	Number of cycles/pulse	Number of US pulse reps.	Sound speed (m/s)	PRF (kHz)
1-1	150	2	256	1480	7.4

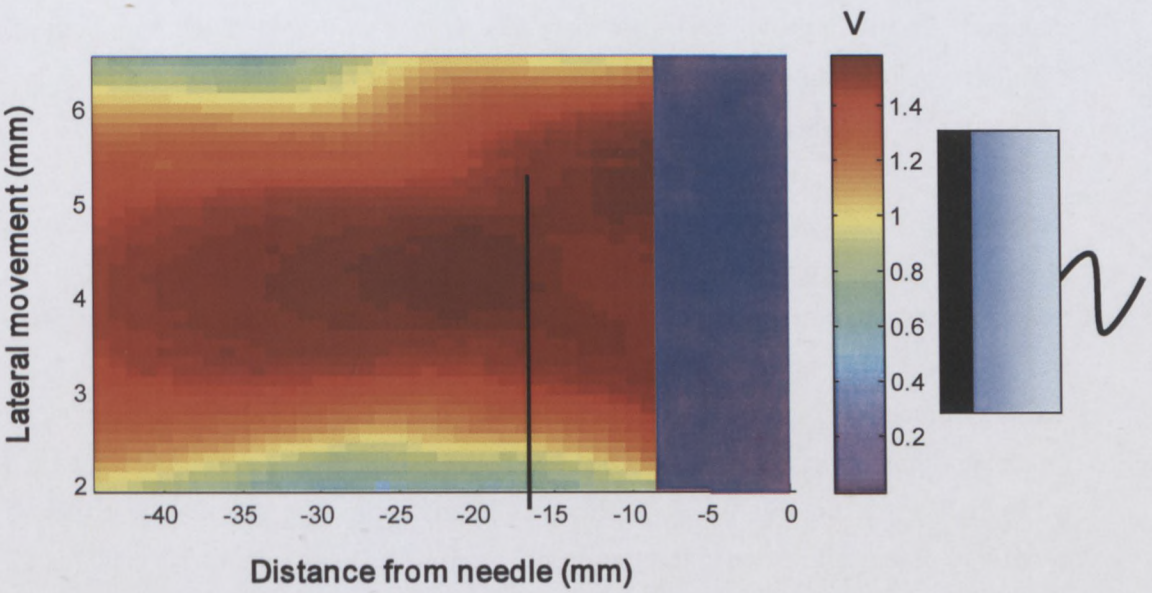

Figure 5.1: Acoustic map of Imasonic standard transducer using echo mode

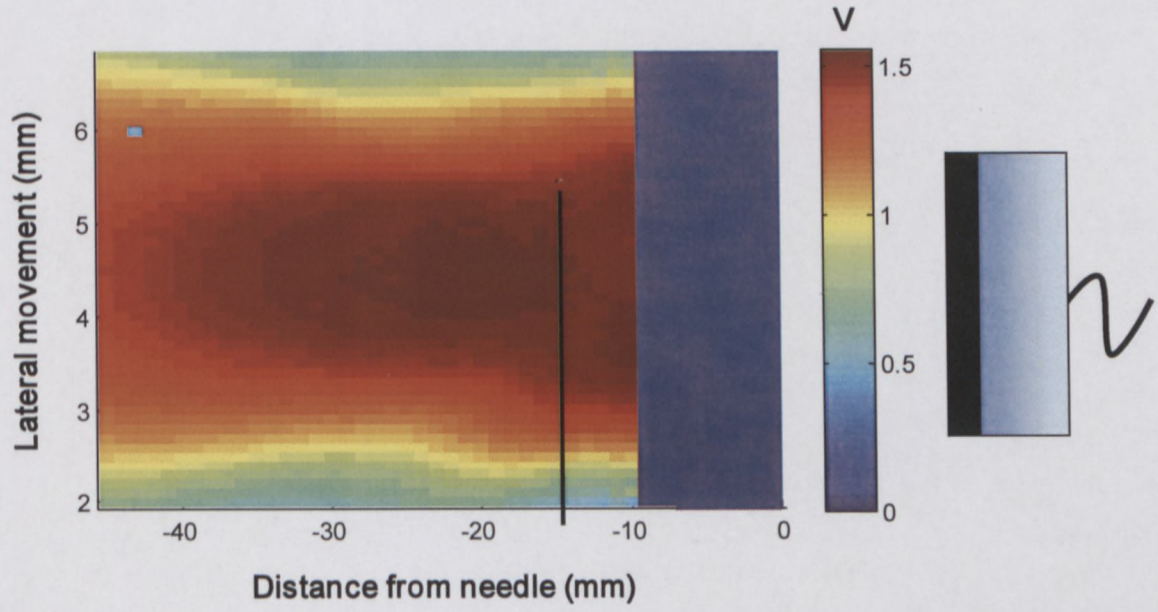

Figure 5.2: Acoustic map of SPSA standard (high temperature) transducer using echo mode

Note that between 0 – 9 mm from the transducer surface (blue area, 0 V) it was not possible to measure acoustic intensities due to the received waveforms interfering with the emitted pulse due to multiple ultrasonic reflections. The focal point seems to be around 16.5 mm for the Imasonic standard transducer and 15 mm for the SPSA transducer (shown by the black line). This means that when using a flow adapter design where transducers are installed in direct contact with the test fluid, the cavity between the wall interface and transducer surface can be reduced to the focal point distance 15 mm (for the SPSA transducer). However, a cavity with a shorter length will still distort velocity data close to the wall, but will increase the energy input to the fluid system as the transducer is closer to the wall interface.

From the results it can be seen that it was still possible to measure qualitative acoustic beam shapes for both transducers. Figure 5.3 shows an acoustic map obtained using the SPSA delay line transducer. It is clear that there is an angle offset after the delay line material. The result, however, does not exactly show where the focal point is, which is important since the focal point needs to be at the wall interface (i.e. beyond the delay line material surface), ensuring that no velocity measurements are conducted within the transducer near-field. Therefore, a different measuring technique was utilised in order to obtain data close to the transducer front, which is presented in Section 5.2.2 below.

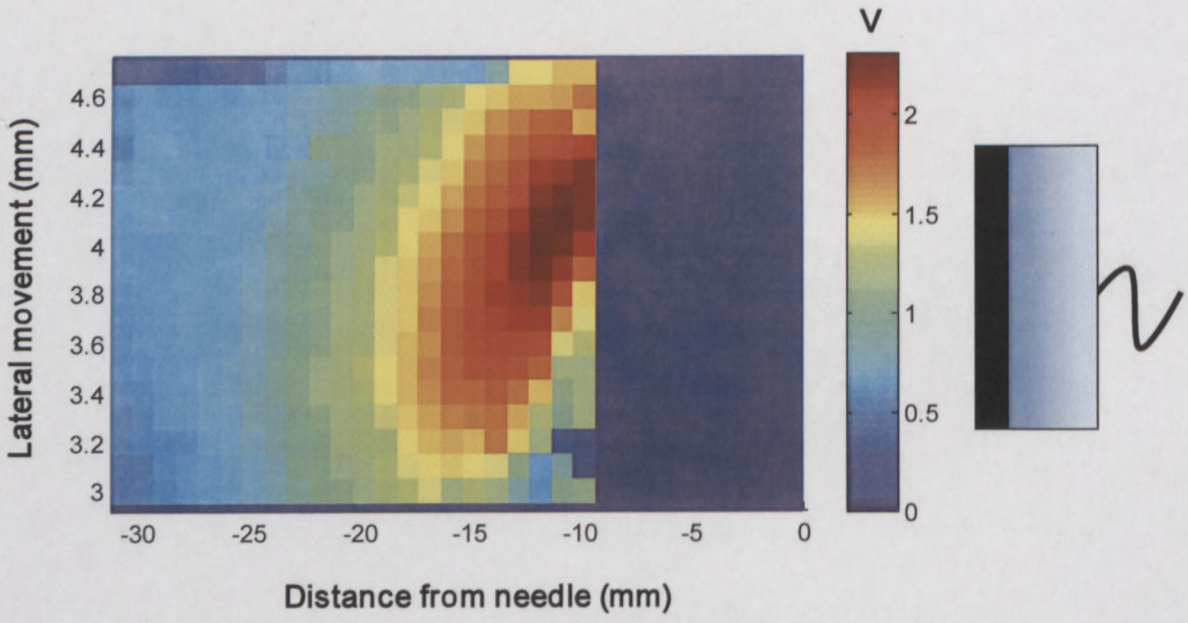

Figure 5.3: Acoustic map of SPSA delay line transducer using echo mode

5.2.2 Needle hydrophone

Figure 5.4 shows the complete acoustic map for the SPSA delay line transducer using the needle hydrophone setup (described in Section 3.2.3.4), Chapter 3). The results were interpolated in order to produce a more detailed representation of the acoustic field. The colour bar positioned at the right shows the intensity values in voltage (V). The same UVP system parameters were selected for these tests (see Table 5.1). Firstly it can be observed that the acoustic field of the transducer is fixed at an angle (with respect to the transducer).

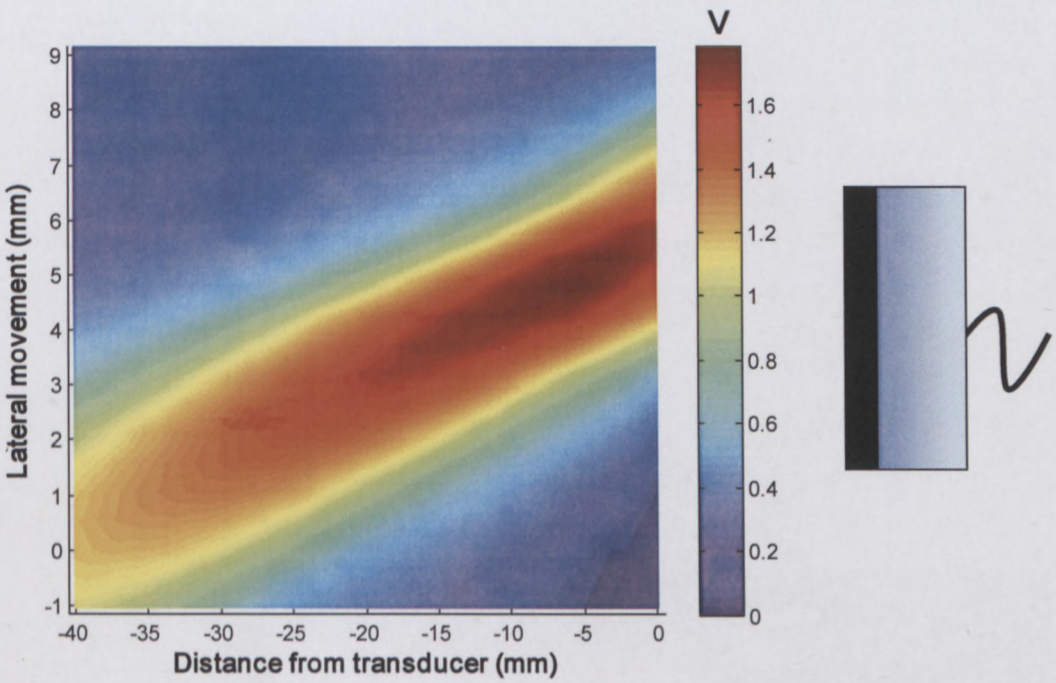

Figure 5.4: Acoustic map of SPSA delay line transducer

Figure 5.5 shows the angle offset determined using a CAD drawing package, Solidworks 2010/11. The angle with respect to the transducer was determined at 7.4 degrees. Also, notice that the focal point of the delay line transducers are situated just beyond the delay line material (curvature), which means no velocity measurements are taken within the near-field, where the acoustic pressure field is irregular.

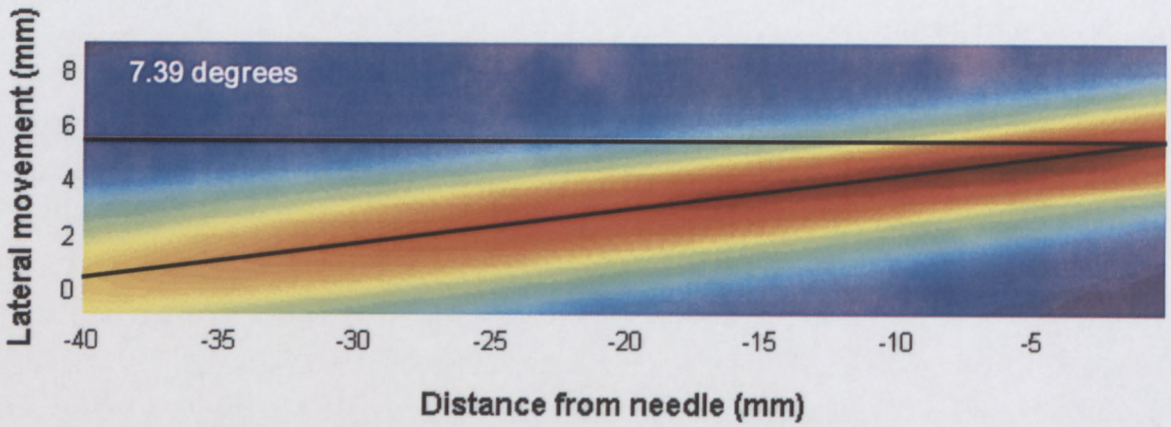

Figure 5.5: Acoustic angle offset for SPSA delay line transducer

Figure 5.6 shows the acoustic map obtained using the same experimental setup and a different delay line transducer, manufactured by Imasonic, France. Since the curvature of the delay line is longer than compared to SPSA delay line transducers, it was possible to measure close and round the edge of the delay line curvature. Based on the results it can also be seen that the acoustic beam path is at an angle offset with respect to the transducer.

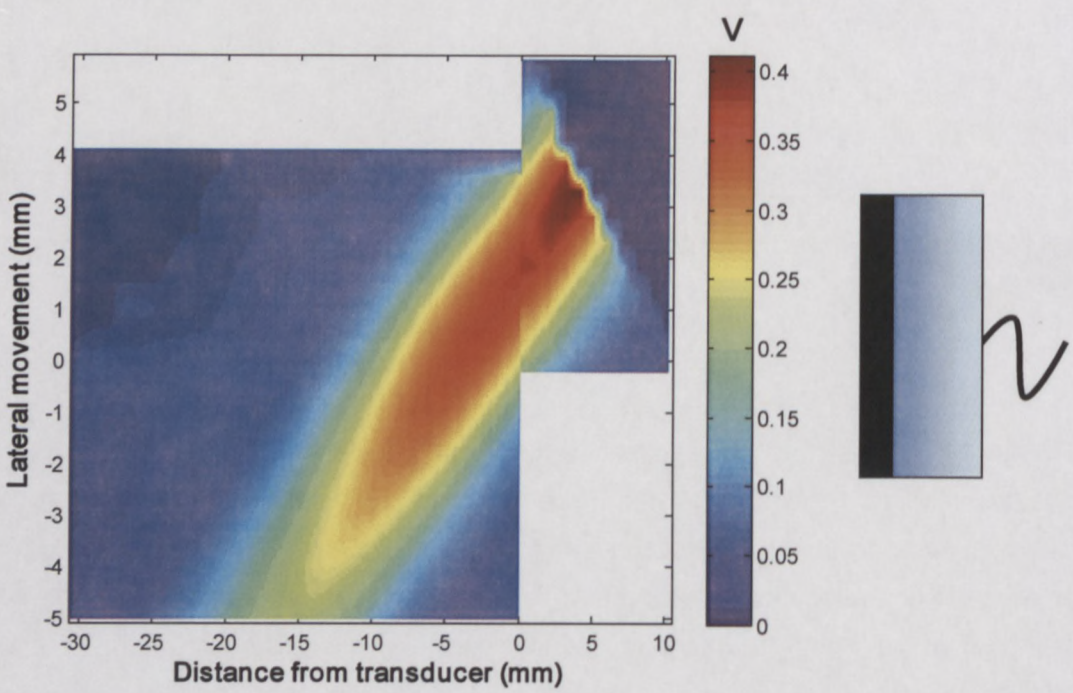

Figure 5.6: Acoustic map of Imasonic delay line transducer

Notice (Figure 5.6) that the angle offset is significantly larger than the Signal Processing delay line transducers (observe the maximum distance from the transducer was -30 mm). Also, the maximum voltage obtained from the Imasonic transducer was significantly lower than the Signal Processing SA transducers (1.6 V versus 0.4 V). In this case the focal point is also positioned close to the curvature, but due to the considerable loss of energy as well as the large acoustic beam angle deviation, it was decided to disregard this type of transducer design / modification.

For comparison two standard (4 MHz, 5 mm active element) transducers, Signal Processing SA (high temperature) and Imasonic, were acoustically characterised. Figures 5.7 – 5.8 display the acoustic maps of the two transducers, respectively. More or less the same acoustic intensities were measured for the two transducers (+- 2.5 V). However, when compared to the Signal Processing delay line transducers the Imasonic transducer signal intensities are 1.5 times higher, showing that there is a loss of energy, possibly caused by the delay line material. In this case the acoustic beam directions are parallel with respect to both transducers. The focal point of the SPSA transducer seems to be at around 15 mm from the surface, whereas for the Imasonic transducer it seems to be at around 17 mm (similar to the results obtained using the stainless steel needle setup).

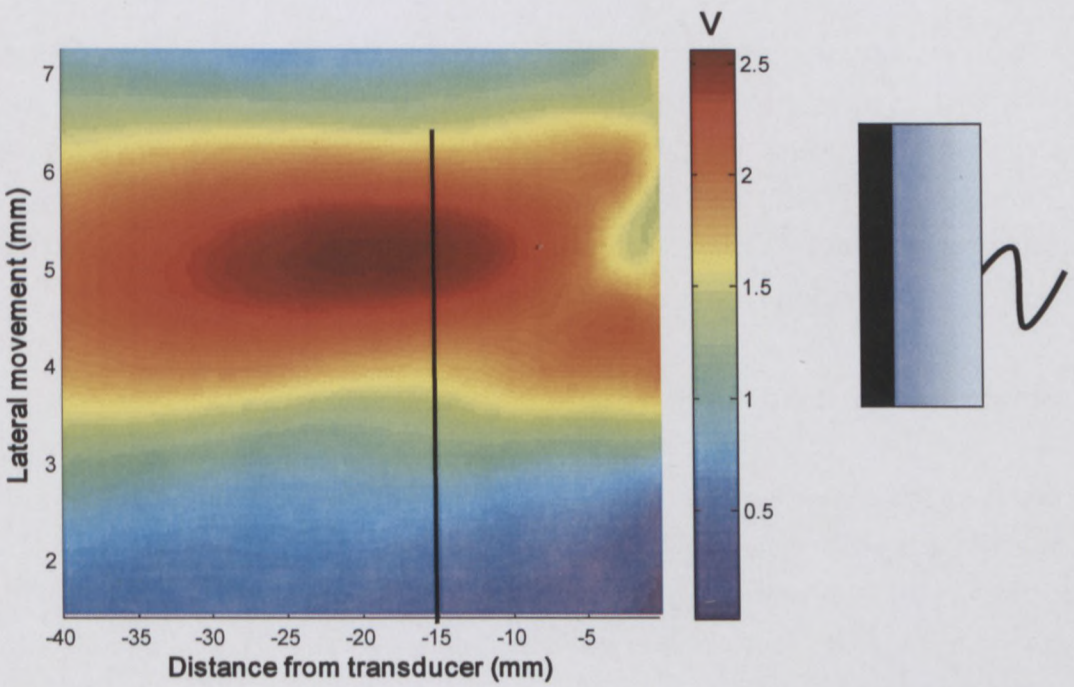

Figure 5.7: Acoustic map of Signal Processing SA High Temp transducer

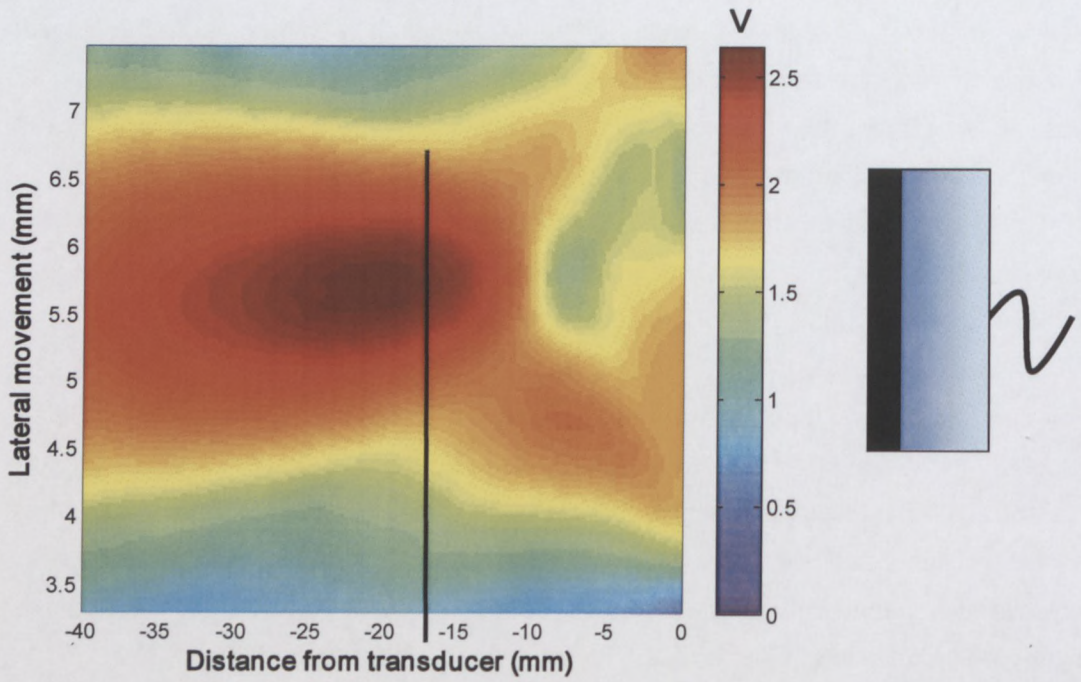

Figure 5.8: Acoustic map of Imasonic standard transducer

5.3 PROFILES MEASURED WITH DIFFERENT PARAMETER SETTINGS

Velocity profiles were measured in CMC 6.15% w/w (K = 0.074, n = 0.85) with different UVP system parameter settings (Emission Voltage, PRF, Amplification Gain and Cycles/Pulse) in a 52.8 mm diameter pipe. The results obtained from two delay line transducers (DL1, DL2) and two Imasonic standard transducers (MF1, MF2) were compared. Transducer description and specifications can be found in Section 3.2.3.2 in Chapter 3. All tests were conducted in laminar flow (Q = 0.82 l/s, Re_2 = 526).

5.3.1 Forward and reverse flow direction

In this analysis 'negative' flow is referred to as velocity profile measurements made against the direction of fluid flow and 'positive' flow with the direction of fluid flow. Table 5.2 shows the UVP settings used for velocity profile measurements. Figure 5.9 shows the comparison for 'negative' flow between one delay line (DL1) and one standard (MF1) transducer.

Table 5.2: UVP parameter settings for CMC 6.15% w/w straight pipe tests

Gain	US Voltage (V)	Number of cycles/pulse	Number of US pulse reps.	Sound speed (m/s)	Doppler angle (°)
3-5	30	2	256	1521	70

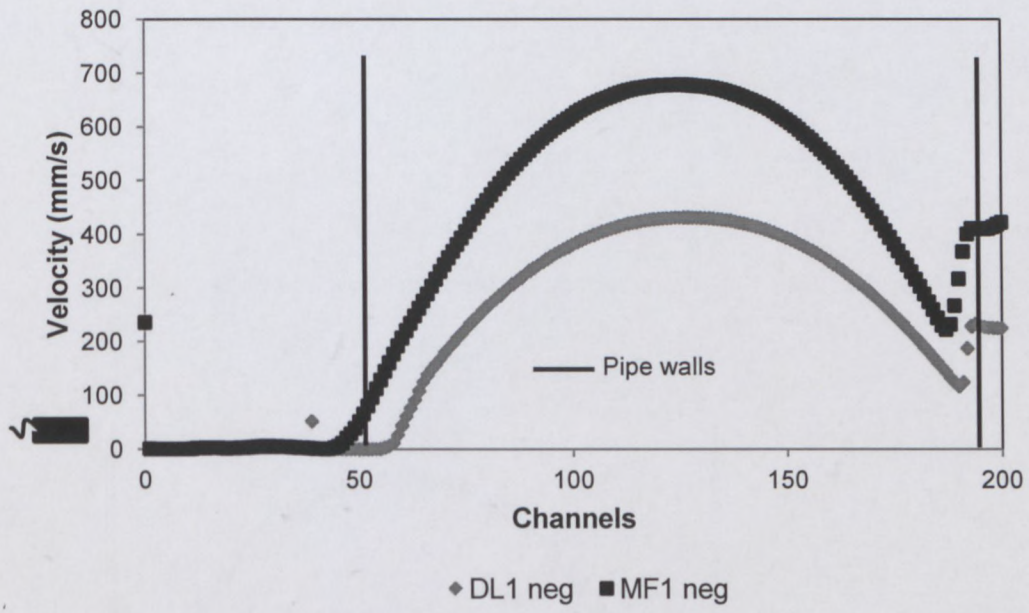

Figure 5.9: DL1-MF1 comparison for 'negative' flow at 0.82 l/s

Figure 5.10 shows results obtained using MF1 and DL1, but for 'positive' flow. Similar results were obtained for both directions of flow. Figure 5.11 shows a comparison between two other transducers (MF2 and DL2) for positive flow. Similar results were found when MF1 and DL2 were compared and vice versa. Based on these results it can be seen that the delay line transducers yielded a skewed or 'S' shape profile close to the wall interface or delay line material. Also, a +/- 40% difference between the maximum velocity obtained by both transducers for all measured profiles were observed. For repeatability profiles obtained by one transducer for both directions of flow were compared. Figure 5.12 shows a velocity profile comparison for transducer DL1 for both directions of flow. Similar results were found for the other transducers.

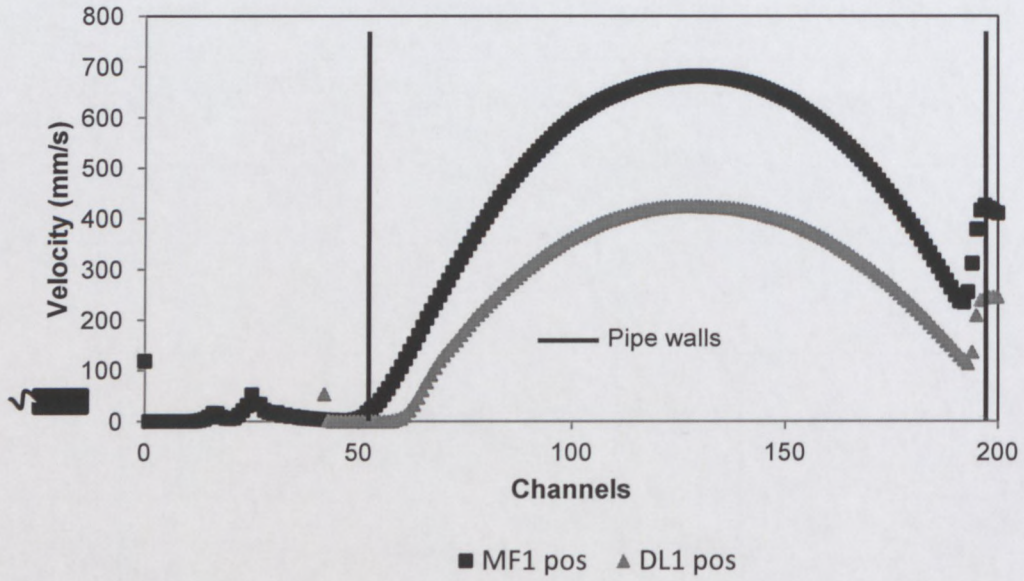

Figure 5.10: DL1-MF1 comparison for 'positive' flow at 0.82 l/s

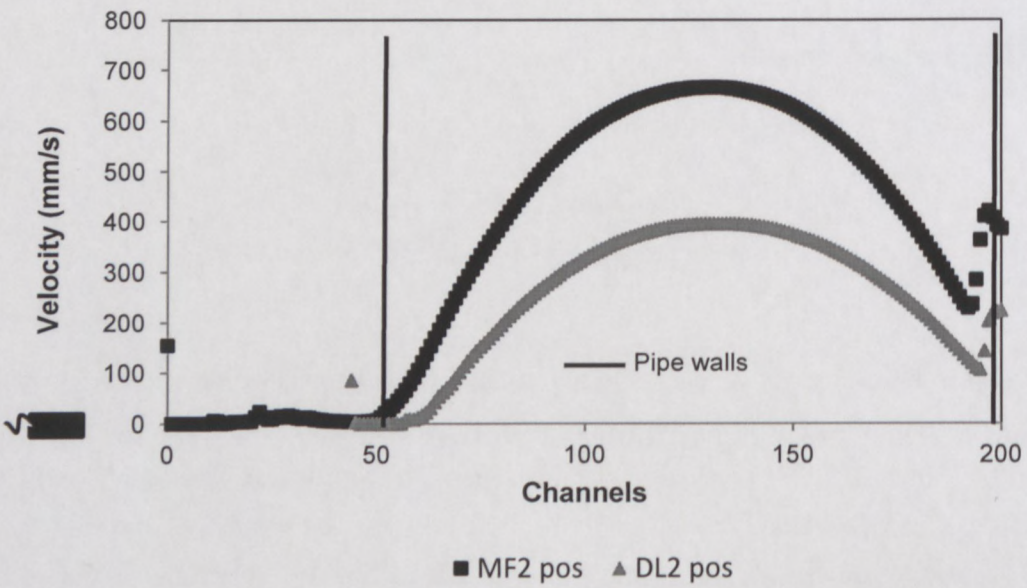

Figure 5.11: DL2-MF2 comparison for 'positive' flow at 0.82 l/s

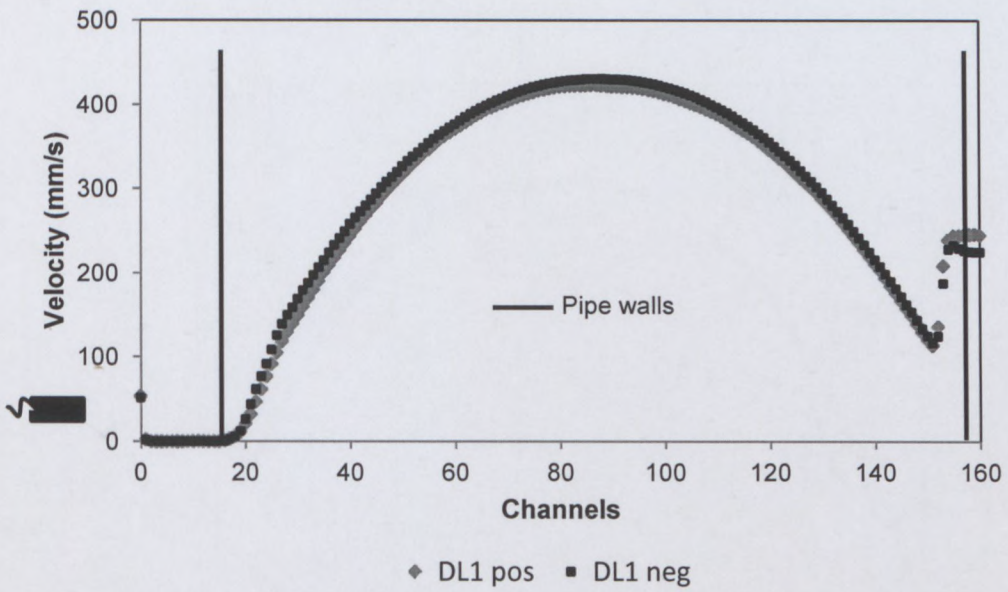

Figure 5.12: DL1 comparison for 'positive' and 'negative' flow at 0.82 l/s

5.3.2 Gain amplification

Table 5.3 shows the UVP parameter settings for profiles measured with different gain settings. Results from transducers DL2 and MF2 are shown in Figures 5.13 – 5.14. It can be seen that at higher gain settings (G7-9) the delay line transducer produces a more distorted profile than when compared to that obtained using transducer MF2. Similar results obtained from varied gain settings were found with the input voltage set at 60V and number of cycles per pulse at two for both transducers. Based on these results the delay line material seems to influence measurements close to the wall interface when too much amplification is employed (e.g. G7-9 setting). This means that the user should be very careful when adjusting gain settings in order to avoid significant errors during a measurement. More information on the gain amplification settings and time ramps can be found in Met-Flow SA (2002).

Table 5.3: UVP parameter settings for varied gain amplification settings

Gain	Voltage (V)	Number of cycles/pulse	Number of US pulse reps.	Sound speed (m/s)	Doppler angle (°)
Varied	150	4	256	1521	70

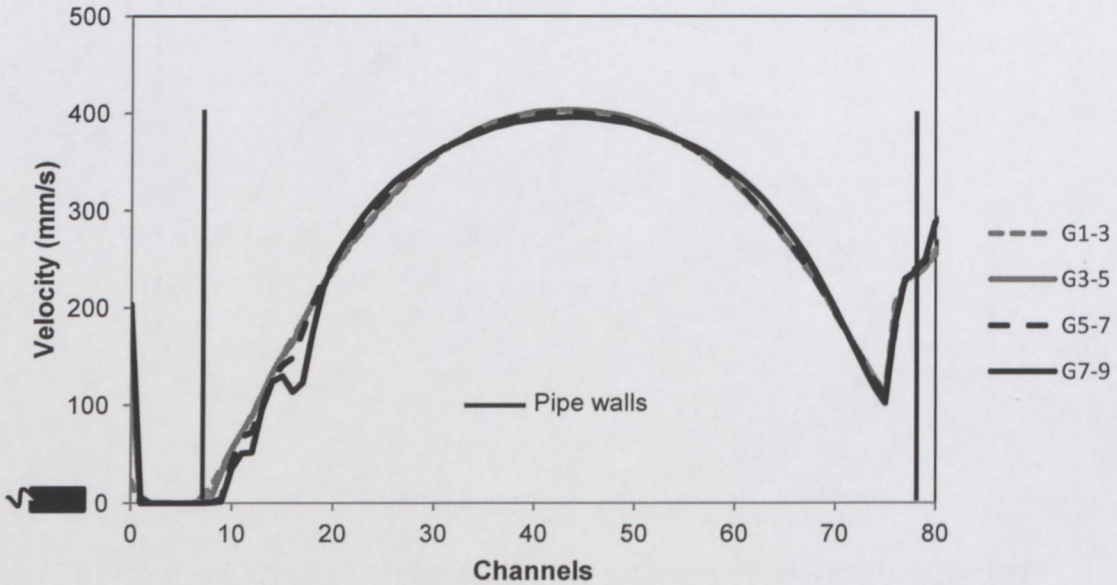

Figure 5.13: DL2 velocity profile measurements at different gain settings

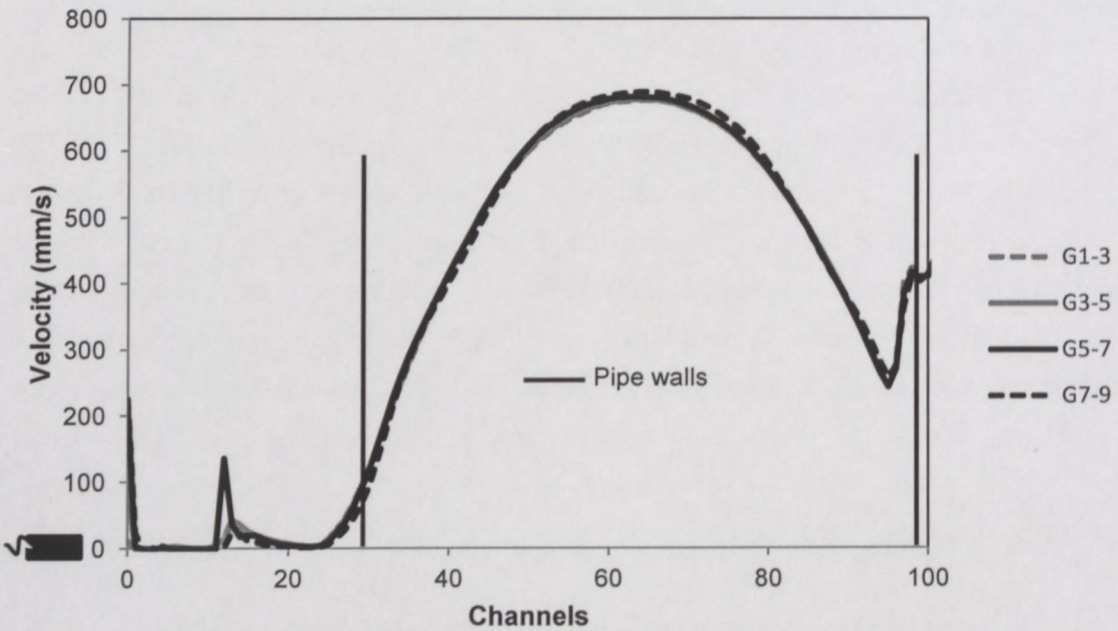

Figure 5.14: MF2 velocity profile measurements at different gain settings

5.3.3 Voltage

Velocity profiles were also measured with different voltage settings while the other system parameters were kept constant. Table 5.4 shows the UVP parameter settings for these tests. Figure 5.15 and 5.16 shows the velocity profiles measured with transducers DL2 and MF2 respectively. No significant discrepancies were observed between profiles measured at different voltage settings when compared with both transducers. The same results were observed for the other transducers (DL1 and MF1).

Table 5.4: UVP parameter settings for varied voltage settings

Gain	Voltage (V)	Number of cycles/pulse	Number of US pulse reps.	Sound speed (m/s)	Doppler angle (°)
3-5	Varied	2	256	1521	70

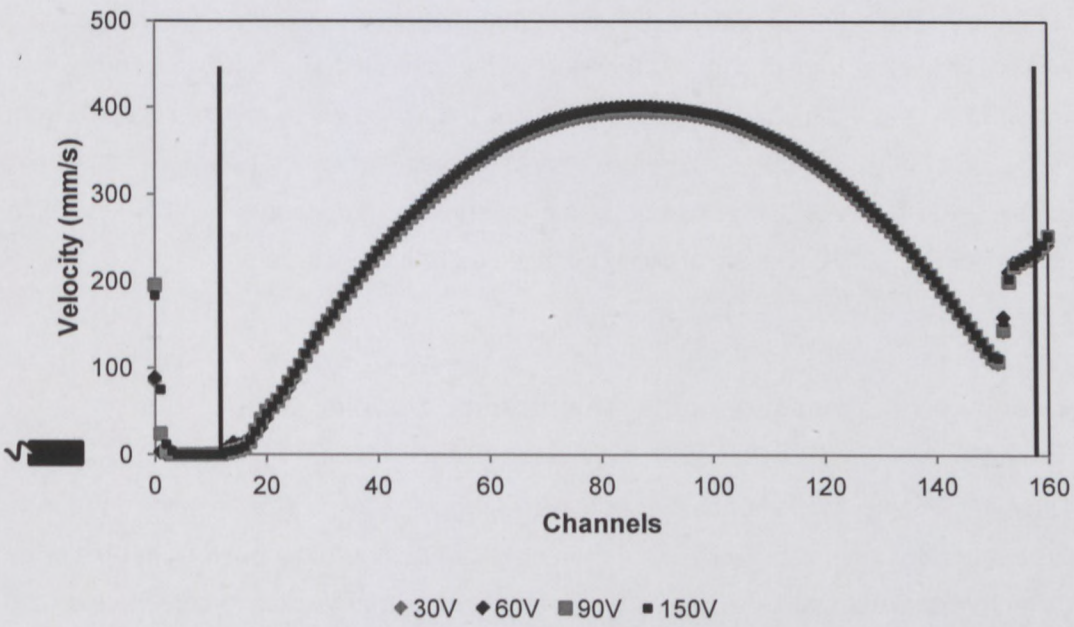

Figure 5.15: DL2 velocity profile measurements at different voltage settings

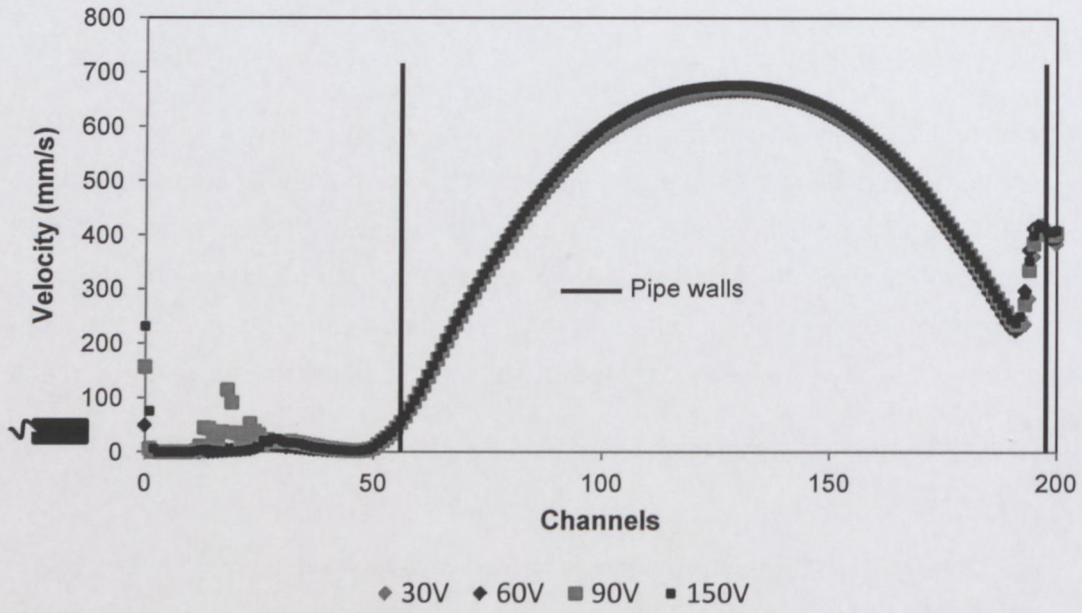

Figure 5.16: MF2 velocity profile measurements at different voltage settings

Tests were conducted where the PRF value was varied and remaining UVP settings were kept constant. Exactly the same velocity profiles were measured with the delay line transducers (DL1, DL2) and Imasonic (MF1, MF2) transducers when compared separately. The same skewness of profiles and magnitude difference were measured with the delay line transducers. Furthermore, when the number of cycles per pulse was varied from 2 to 4 similar velocity profiles were measured when results obtained from DL1-2 and MF1-2 are compared separately. The main difference between the profiles measured with 2/4 cycles per pulse is the increase or decrease in spatial resolution (Met-Flow SA, 2002). Results of these tests are therefore not included.

5.3.4 Velocity profile measurement with corrected Doppler angle

Since the Doppler angle is not the same as the angle of transducer installation (due to US beam refraction, see Figure 5.5), the angle can be corrected in order to obtain the correct velocity magnitudes. Figure 5.17 shows measured velocity profiles across the ultrasonic beam direction for Imasonic and SPSA delay line transducers. Here the Doppler angle for the delay line transducer changed from 70° to 70 + 7.4 = 77.4°. The magnitudes of the maximum velocities at the centre of the pipe seem to correlate. However, the velocity profile measured by the delay line transducer shows a skewness

close to the pipe wall interface (see Figure 5.17). This distortion is due to the finite sample volume passing through the delay line material and the pipe diameter or measuring distance. The measured velocity profile can thus be described by the convolution of the finite sample volume with the theoretical or 'true' velocity profile (see Section 2.2.8, Chapter 2). A deconvolution process (see Section 3.3.4, Chapter 3) can be implemented in order to correct distorted velocity profiles, which is discussed in Section 5.4.

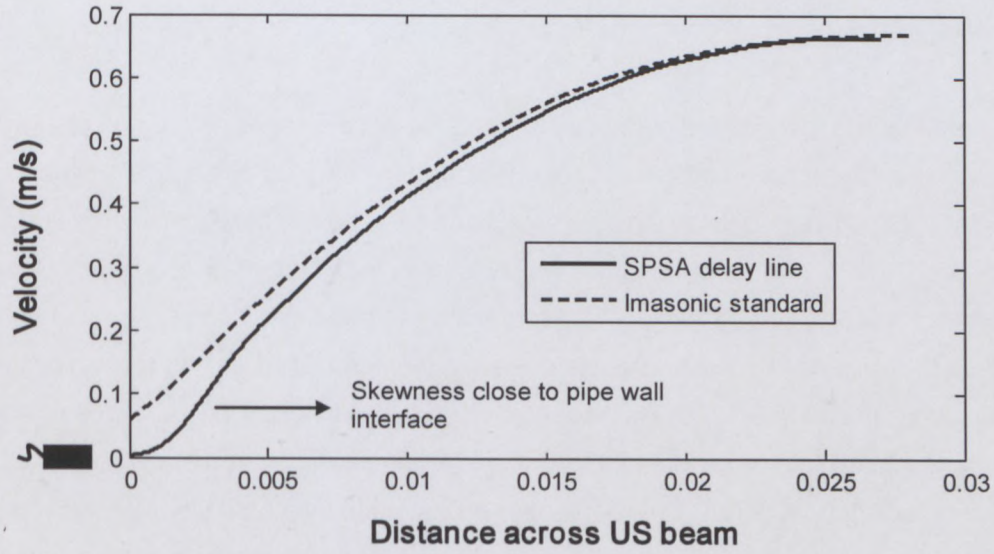

Figure 5.17: SPSA delay line transducer result after Doppler angle correction

5.4 DECONVOLUTION OF VELOCITY PROFILES

5.4.1 Sample volume lengths and profile shifting

According to Jorgensen *et al.* (1973) and Jorgensen and Garbini (1974) the measured profile will overshoot the actual distance of a geometry by exactly the length of the sample volume (see Figure 2.9, Chapter 2). This is due to the sampling process or convolution of the finite sample volume (impulse response) with the true velocity distribution within the flow field. Figure 5.19 shows a velocity profile measured in CMC 7% w/w using a standard transducer from Imasonic, installed at 18.56 mm from the pipe (diameter 16 mm) wall in order to avoid measurements in the near-field zone.

Figure 5.18 shows the waveform measured used to determine the window shape and length for deconvolving the measured profile (illustrated by a solid line in Figure 5.19). The UVP system parameters used for the profile measurement are shown in Table 5.5. A method of calculating the wall interface position is to find the maximum velocity (in the case of power-law profiles) and to subtract the pipe radius. This means that when the maximum point on the profile is used and the radius of the pipe (8 / cos 20° = 8.513 mm across US beam) is subtracted, then the position of the wall interface should be 18.56 mm, which is the actual distance. However, it can be observed that the maximum point of the measured profile is shifted with a distance equal to +/- half of the sample volume (1.7 / 2 ≈ 0.85 mm) due to the convolution effect.

Also, note that the magnitudes of the velocity profiles are the same before and after the deconvolution procedure. The reason for this is due to the Size of Sample Volume to Diameter (SSV/D) ratio. The sample volume sizes (or lengths) during this work varied between 1.7 to 2.2 mm, depending on which transducer, number of cycles per pulse and type of fluid was used (velocity of sound in the medium). Taking the maximum length (2.2 mm) and the smallest pipe diameter (16 mm) used in this research, the SSV/D ratio equates to 0.1375. The convolution effect for different SSV/D ratios is well described in literature (Jorgensen & Garbini, 1974; Black and How, 1989; Flaud *et al.*, 1997) for blood flow. A SSV/D ratio of 0.3 to 0.5 was found by the previously mentioned authors to have a more significant effect on the shape and magnitude of the measured profile. Since the maximum SSV/D ratio was 0.1375 in this work the measured profiles were not severely distorted (change in magnitude and significant shift in distance) for all experimental tests conducted.

Table 5.5: UVP parameter settings for CMC 7% w/w pipe tests using standard transducer

Gain	US Voltage (V)	Number of cycles/pulse	Number of US pulse reps.	Sound speed (m/s)	Doppler angle (°)
3-5	90	2	256	1538	70

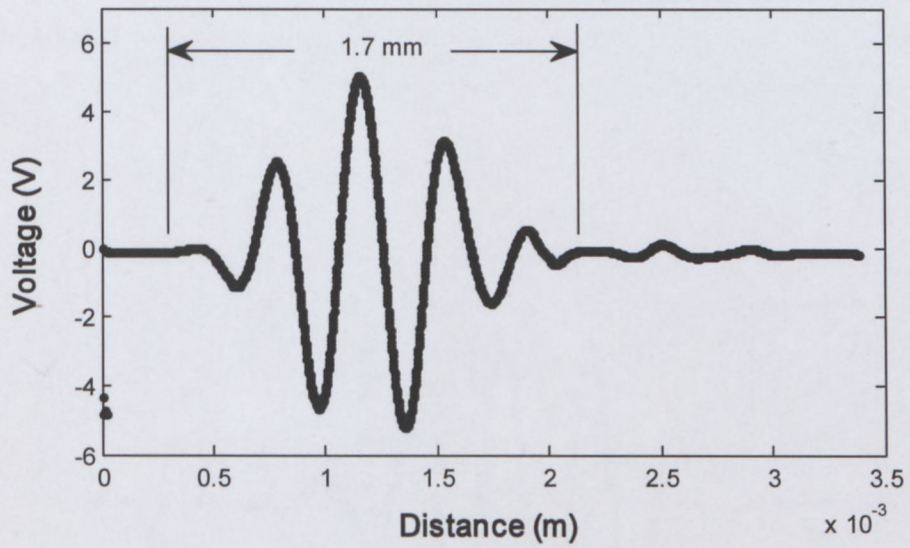

Figure 5.18: Waveform measured in CMC 7% w/w using standard transducer

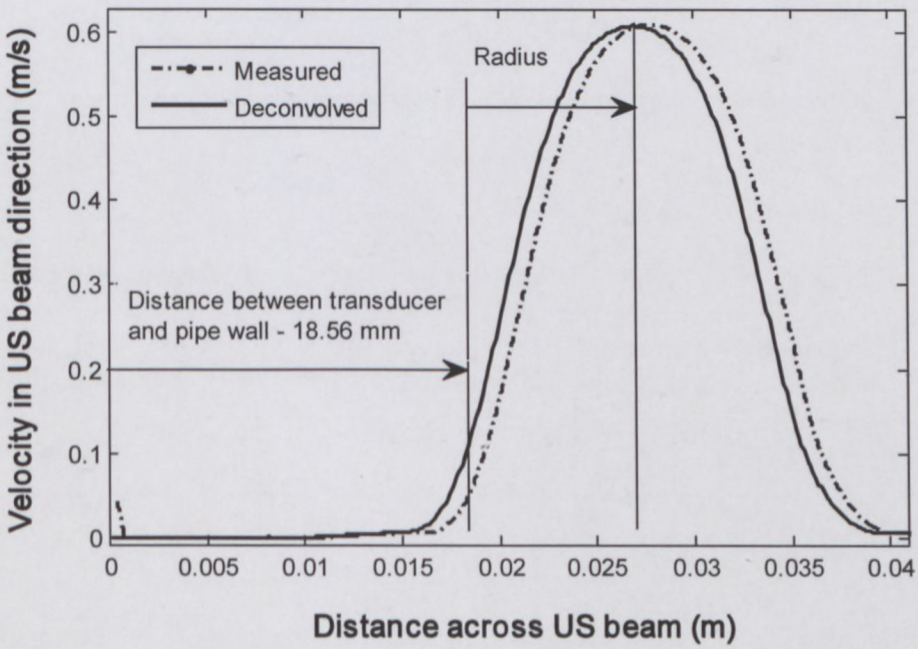

Figure 5.19: Velocity profile shift after deconvolution (standard transducer)

The same profile shifting was observed with profiles measured using the delay line transducers. Figure 5.20 shows a waveform measured in CMC 7% w/w using a delay line transducer. Note that the sample volume length is longer (22%) than the length of the standard transducer's sample volume, which is due to more ringing of the

piezoelectric crystal in the delay line transducer. Figure 5.21 shows the velocity profile measured in a 16 mm pipe with system parameter settings (shown in Table 5.6) before and after implementing the deconvolution procedure.

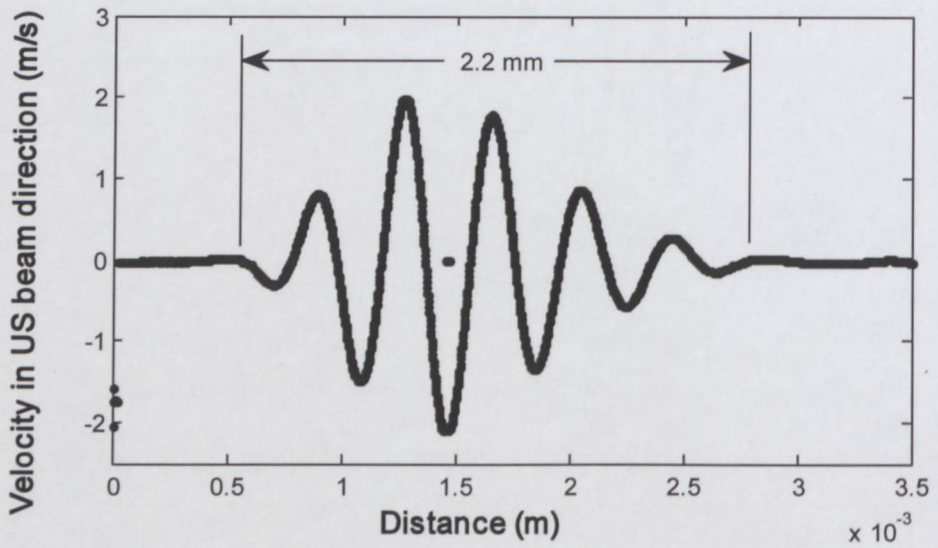

Figure 5.20: Waveform measured in CMC 7% w/w using delay line transducer

Table 5.6: UVP parameter settings for CMC 7% w/w pipe tests using delay line transducer

Gain	US Voltage (V)	Number of cycles/pulse	Number of US pulse reps.	Sound speed (m/s)	Doppler angle (°)
5-7	90	2	256	1489	77.4

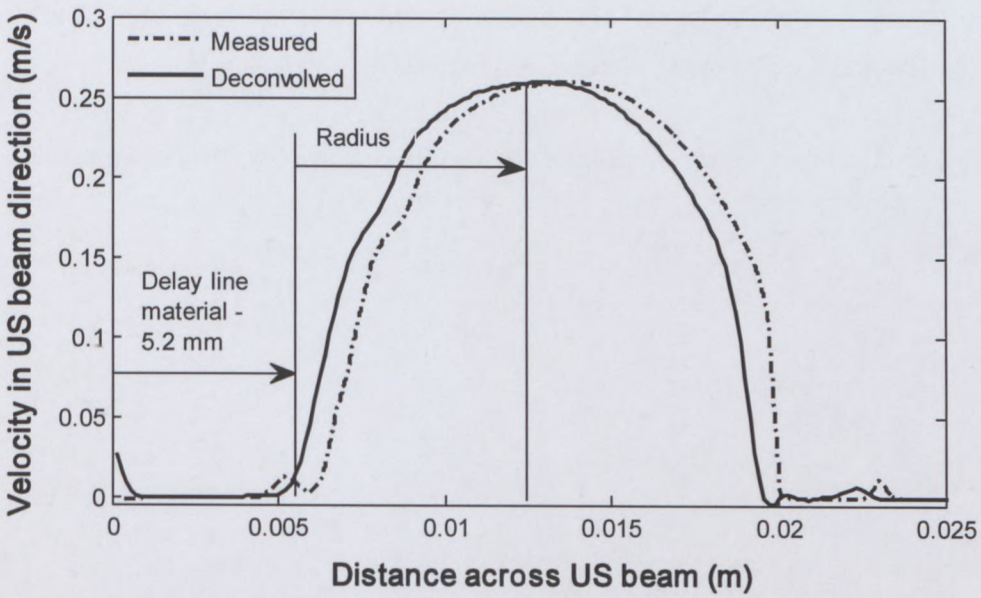

Figure 5.21: Velocity profile shift after deconvolution (delay line transducer)

The distance of the delay line material across the ultrasonic beam is 5.2 mm and it can be seen that after deconvolution the profile is shifted towards the surface of the delay line material. It can also be observed that the profile is skewed just before the radius. This is not due to the convolution effect, but rather the ultrasonic transducer surface (diameter 8 mm) at the pipe (diameter 16 mm) wall. The ratio of the transducer to pipe diameter in this case is 0.5, which means that a large part of the curvature of the pipe is still left open after the transducer is installed, i.e. the transducer is not installed entirely flush with the pipe geometry. This causes irregular flow close to the curvature and thus affects the measured velocity profile. The same observation regarding the magnitudes of the profiles after deconvolution can be made for both standard and delay line transducers.

The profile shifting due to the convolution effect provides the user with a constant wall interface parameter, i.e. the distance between the transducer surface and pipe wall. It is then unnecessary to work backwards by using the maximum velocity point for power-law profiles and subtracting the pipe radius. This method also fails for plug flow profiles as there is no reference point to work with and thus a constant and more importantly correct wall interface parameter would prove to be invaluable. This can be illustrated by the deconvolution of a plug flow profile obtained using a delay line transducer and using the known wall interface parameter of 5.2 mm (length of delay line material). Figure 5.23 shows a velocity profile measured in bentonite 6.9% w/w in a 16 mm pipe

before and after deconvolution. The system parameters and measured waveform (sample volume) are shown in Table 5.7 and Figure 5.22, respectively.

Table 5.7: UVP parameter settings for bentonite 6.9% w/w pipe tests using delay line transducer

Gain	US Voltage (V)	Number of cycles/pulse	Number of US pulse reps.	Sound speed (m/s)	Doppler angle (°)
3-5	90	2	256	1495	77.4

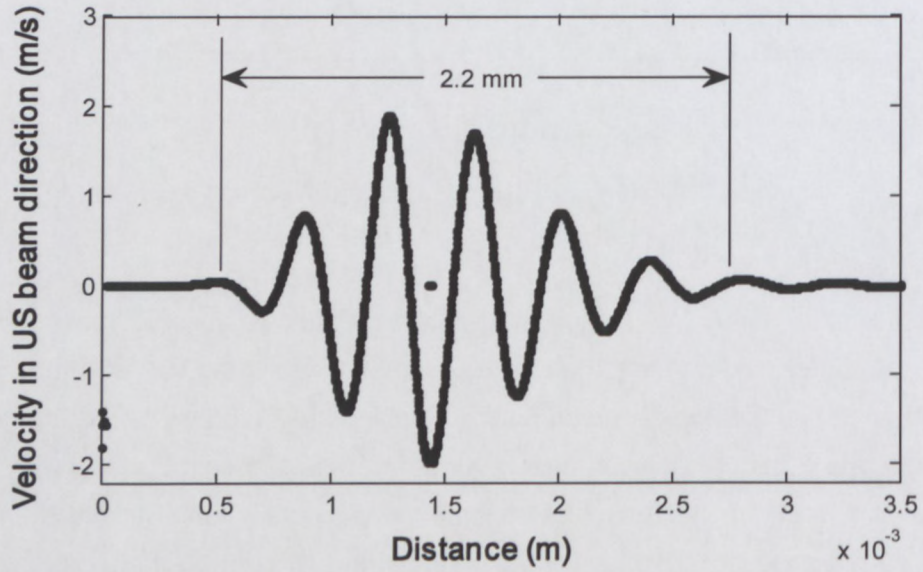

Figure 5.22: Waveform measured in bentonite 6.9% w/w using delay line transducer

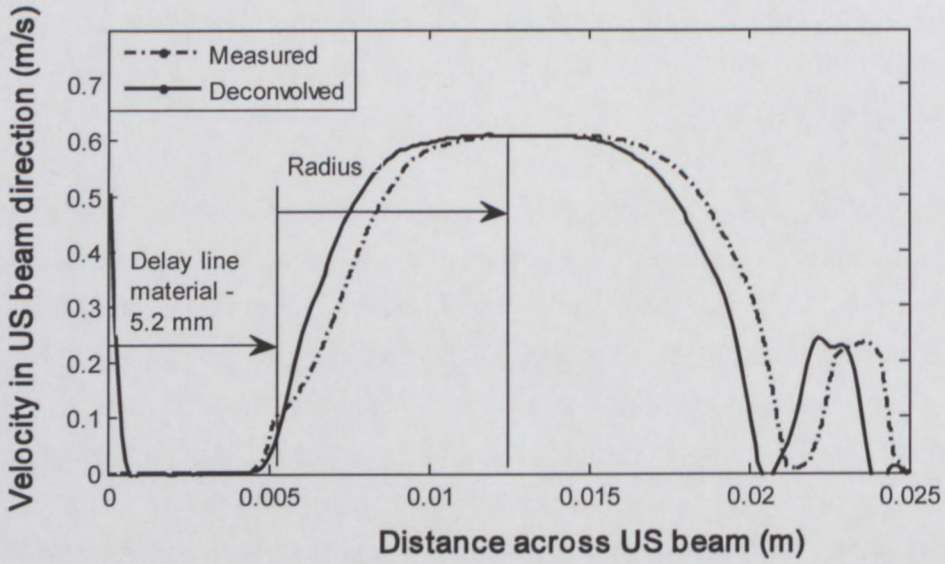

Figure 5.23: Velocity profile shift after deconvolution (bentonite 6.9% w/w, delay line transducer)

Note that after deconvolution the profile shifts back to the surface of the delay line material. Although the velocities are not exactly zero at the delay line surface (or pipe wall) after deconvolution, the data points can still be forced to zero for practical purposes. This is, however, still a major improvement as it was found that when testing standard transducers in fluids which inhibit particle settling with time (such as bentonite and kaolin suspensions), the profile shifting was more pronounced. This means that even after deconvolving a profile measured by a standard transducer installed in the cavity setup, the profile will not shift to the correct wall interface position. Since this did not occur during CMC tests, the reason for this is due particle build-up inside the cavities, which alters the velocity of sound (density changes) and consequently alters the profile distance across the pipe or geometry.

To illustrate the effect of profile shifting for different sample volume lengths, velocity profiles were measured at 2 and 4 cycles per pulse while the rest of the system parameters were kept constant. Figure 5.24 shows the profiles measured using the delay line transducer for kaolin 17% v/v in a 16 mm pipe.

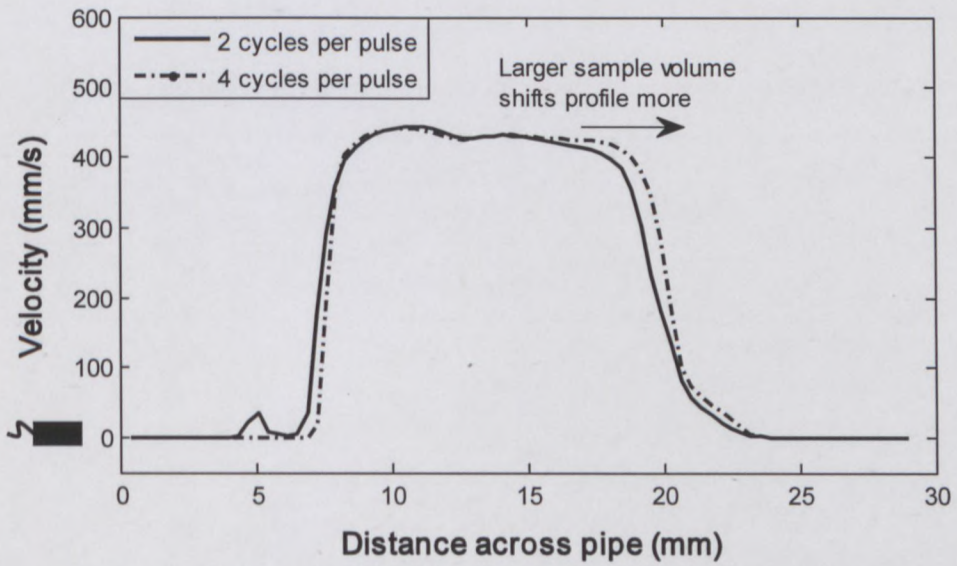

Figure 5.24: Profile shifting for 2/4 cycles per pulse setting

It can be seen that with increasing sample volume size (2 cycles – 2.3 mm and 4 cycles – 3.15 mm) the experimental profile shifts further away from the transducer surface. It is thus very important to measure the waveform shape and length accurately in order to correct the velocity data close to the wall interface.

5.4.2 Overlapping of measuring volumes

From Figure 5.18 it can be seen that the length of the sample volume was 1.7 mm for a standard transducer (Imasonic, France). Based on the UVP system parameters (Table 5.2) the channel distance (see Section 3.2.3) was 0.38 mm (Met-Flow SA, 2002), which means that overlapping of the sample volumes occurred during the velocity profile measurement (Figure 5.19). To test the overlapping effect profiles were measured in a larger pipe (diameter 52.8 mm) in order to use a wide range of channel distance settings. Figure 5.25 shows velocity profiles measured with different channel distance settings of 0.38 to 3.02 mm while maintaining the rest of the system parameters constant, shown in Table 5.8. It can be observed that all four profiles agree with one another, the only difference being the spatial resolution (0.38 – 3.02 mm) of the different measurements. This illustrates that accurate measurements can still be obtained with sample volumes overlapping one another. This sampling process (overlapping of finite sampling volumes) is well described by Jorgensen *et al.* (1973). Similar results were found for the delay line transducers for all channel distance settings and are therefore not included here.

Table 5.8: UVP parameter settings for channel distance variation tests

Gain	US Voltage (V)	Number of cycles/pulse	Number of US pulse reps.	Sound speed (m/s)	Doppler angle (°)
3-5	90	2	256	1520	70

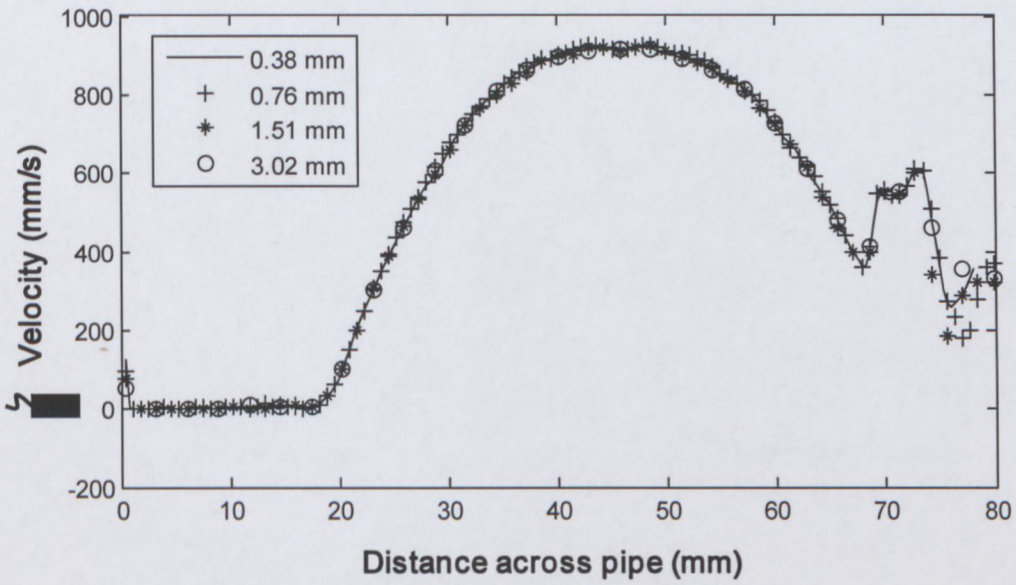

Figure 5.25: Velocity profile measurements with channel distance variation (standard transducer)

To further test the overlapping of sample volumes, velocity profiles were measured in CMC 3.5% w/w in a 16 mm diameter pipe using a standard ultrasonic transducer. Two and four cycles per pulse as well as four cycles with 50% overlapping were selected while other system parameters were kept constant (see Table 5.9). Overlapping of 50% was achieved by setting the channel distance to half of the sample volume length in the UVP software (version 3), which means that double the spatial resolution is obtained. Figure 5.26 shows the results obtained for the different channel distance and cycles per pulse settings. Note that the 50% overlap profile (circles) has double the spatial resolution than the 4 cycles per pulse profile (stars). It can be seen that even when forcing channel overlapping accurate results are still obtained, considering that the actual sample volume length is +/- 1.7 mm. Similar results were found for delay line transducer in all pipe diameters and fluids, including bentonite and kaolin suspensions.

Table 5.9: UVP parameter settings for channel overlapping tests

Gain	US Voltage (V)	Number of cycles/pulse	Number of US pulse reps.	Sound speed (m/s)	Doppler angle (°)
3-5	90	2-4	256	1485	70

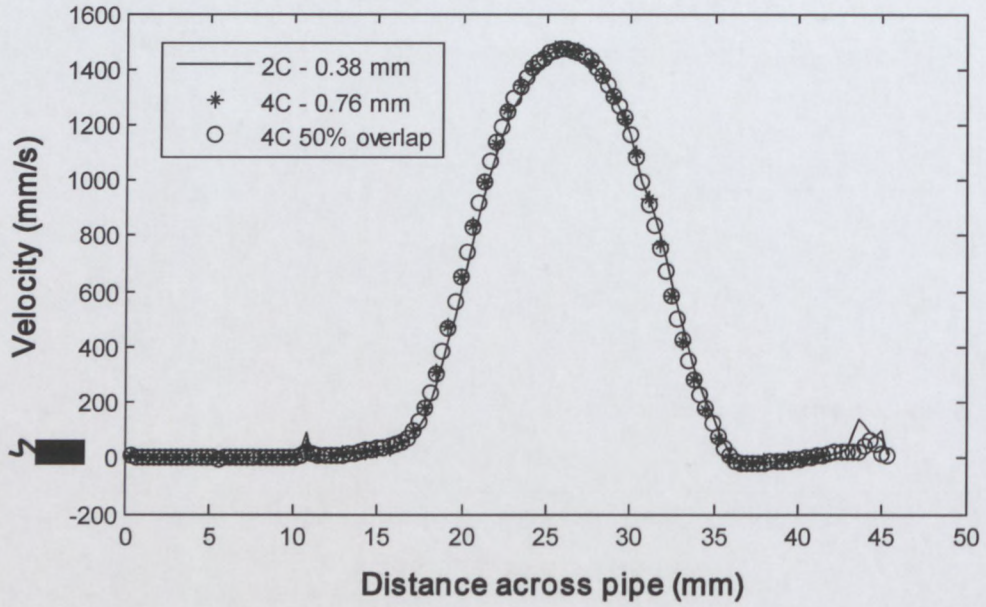

Figure 5.26: Velocity profile measurements with channel overlapping (standard transducer)

Forcing system parameter settings so that measuring volumes overlap can prove to extremely useful when measuring in attenuating fluids. Figure 5.27 shows two measurements taken in kaolin 17% v/v in a 16 mm pipe. In this case it can be seen that when 2 cycles per pulse was selected there was a loss of information after about 30 mm due to attenuation of the ultrasonic energy, even at highest voltage and gain amplification settings. However, when 4 cycles per pulse were selected with 50% overlapping the energy input was increased and as a result the penetration depth was increased and the entire profile could be measured while maintaining the same spatial resolution as when using 2 cycles per pulse.

Table 5.10: UVP parameter settings for forced channel overlapping tests

Gain	US Voltage (V)	Number of cycles/pulse	Number of US pulse reps.	Sound speed (m/s)	Doppler angle (°)
7-9	150	2/4	1024	1490	70

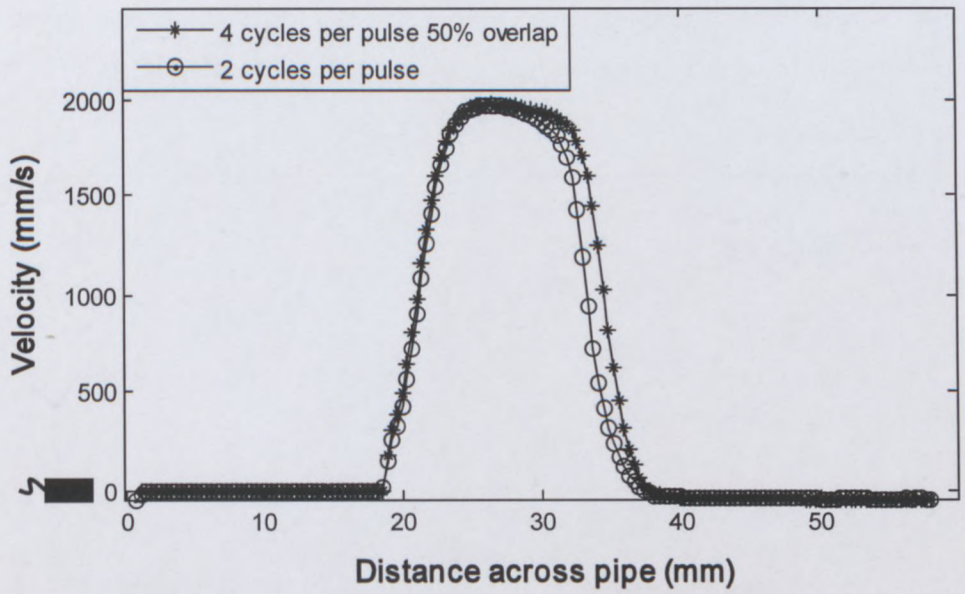

Figure 5.27: Increase of penetration depth using channel overlapping

5.4.3 Comparison between velocity profiles before and after deconvolution

Since the setup with standard transducers distorts the measured velocity profile physically due to the large cavities present at the wall interfaces, the deconvolution procedure will not be useful for correction of erroneous data at the pipe walls. Therefore all the results obtained using the standard transducer were not deconvolved. Velocity profiles obtained using the delay line transducers are presented before and after implementing the deconvolution procedure.

5.4.3.1 Velocity profiles measured in 16 mm pipe

Figure 5.28 shows profiles measured in a 16 mm diameter pipe using a standard and delay line transducer for CMC 7% w/w (K = 1.43, n = 0.67) at a bulk flow rate of 0.141 l/s (Re_2 = 988). A major improvement between the results obtained using the delay line transducer after deconvolution can be observed. A theoretical velocity profile (Equation 2.28, Section 2.4.2) was also plotted for comparison (using the pipe viscometer data). The difference in magnitude between the profiles measured using the standard and delay line transducer was due to slight variations in flow during the measurements. The most important observation here is the increase in velocity at the pipe wall for the profile measured using the standard transducer (shown by diamonds). Here the effect

of the cavity is more pronounced even for a power-law fluid with no yield stress as the diameter of the transducer (8 mm) is half of the pipe diameter (16 mm).

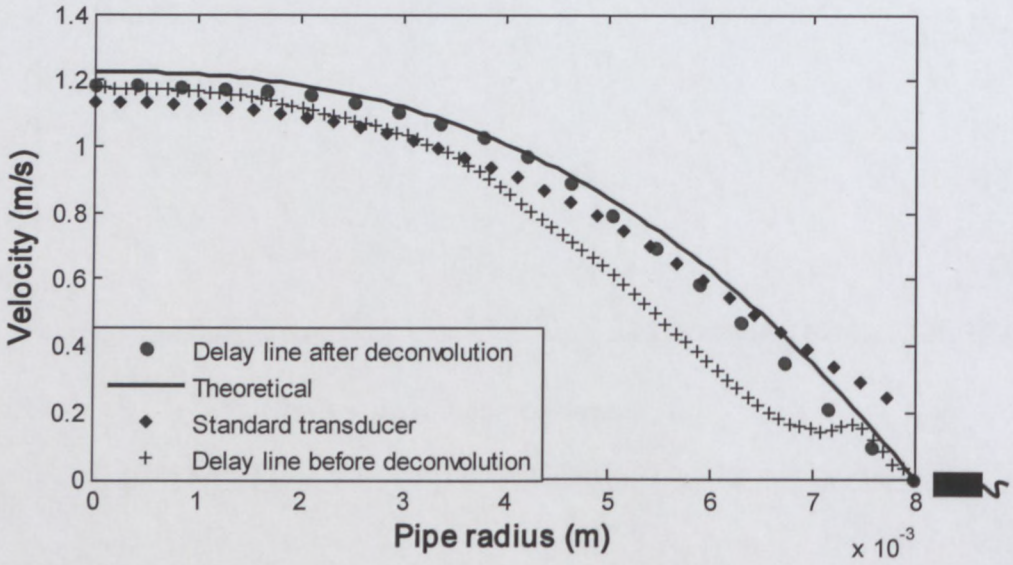

Figure 5.28: Comparison of profiles after deconvolution (CMC 7% w/w, 16 mm pipe)

Figure 5.29 shows a comparison of velocity profiles measured in bentonite 6.9% w/w (K = 0.006, n = 1, τ_y = 9) at a flow rate of 0.4 l/s (Re_2 = 1900). Velocity profiles measured in kaolin 17% v/v (K = 0.54, n = 0.47, τ_y = 16.77) at a flow rate of 0.2 l/s (Re_2 = 330) are shown in Figure 5.30. The same observations can be made between the results obtained using the standard and delay line transducers. In the case of measuring in fluids with a yield stress the cavity distorts profiles (diamonds) more significantly due to the high velocity gradients present close to the pipe walls. When comparing the profiles before and after deconvolution (crosses and circles), it can be seen that the deconvolution procedure improved the velocity data close to the wall significantly (in both bentonite and kaolin suspensions). The velocity profiles shown after implementing the deconvolution procedure also show better agreement with the theoretical profile, calculated using rheology obtained from in-line tube viscometry.

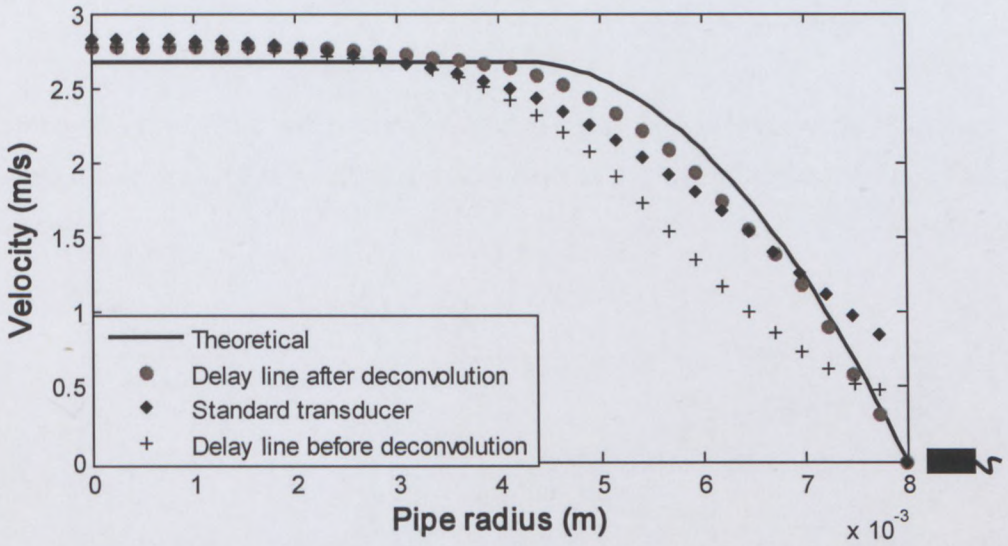

Figure 5.29: Comparison of profiles after deconvolution (bentonite 6.9% w/w, 16 mm pipe)

Due to the attenuating properties of the kaolin suspensions, it was not possible to measure velocity profiles using a standard transducer. According to the acoustic measurements of the different transducers (Section 5.2), the standard transducers generated more acoustic energy than when compared to the delay line transducer. However, due to the cavity between the transducer surface and pipe wall, which was filled with the test fluid, most of the energy was absorbed before the ultrasonic pulse can propagate across the pipe diameter. In this case the delay line transducer could measure profiles in this particular fluid as the only material (which also absorbs energy, see Section 5.2) between the wall interface and transducer surface is the actual delay line material and not the attenuating test fluid.

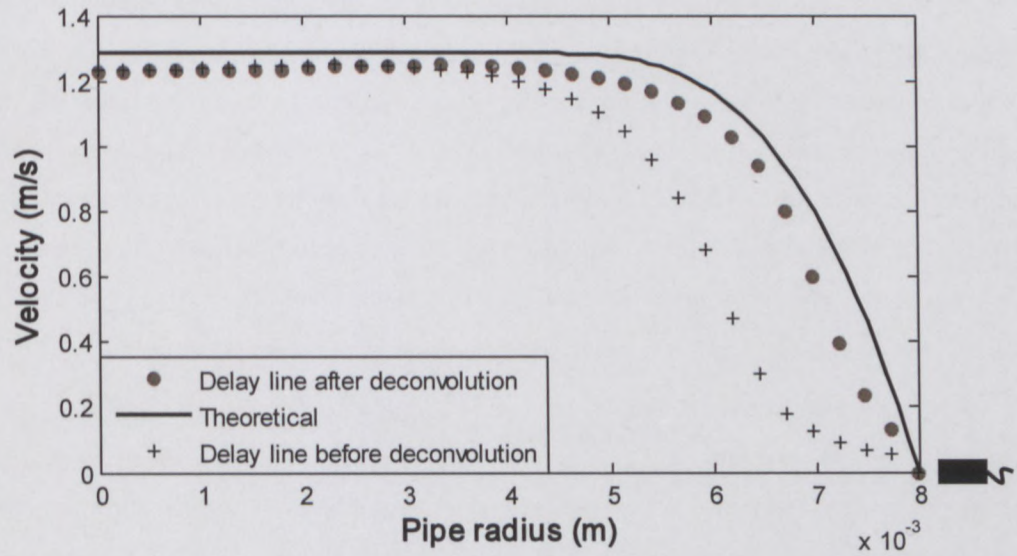

Figure 5.30: Comparison of profiles after deconvolution (kaolin 17% w/w, 16 mm pipe)

5.4.3.2 Velocity profiles measured in 22.5 mm pipe

Figure 5.31 shows profiles measured in a 22.5 mm diameter pipe using a standard and delay line transducer for CMC 3.25% w/w (K = 0.217, n = 0.81) at a bulk flow rate of 0.32 l/s (Re_2 = 275).

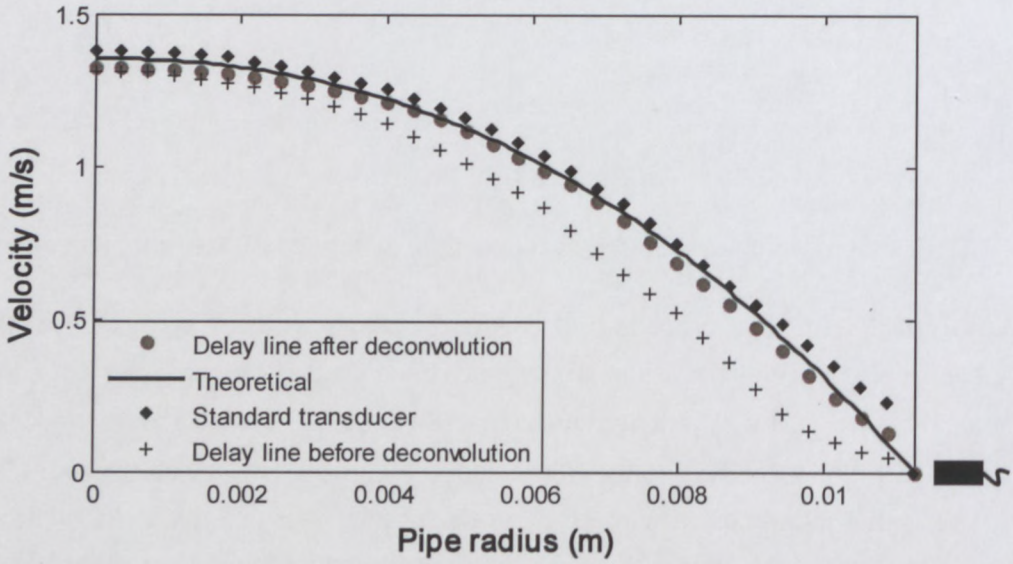

Figure 5.31: Comparison of profiles after deconvolution (CMC 3.25% w/w, 22.5 mm pipe)

Both profiles measured using the delay line (after deconvolution) and standard transducers show good agreement with the theoretical velocity profile (Equation 2.28). However, the velocity data from the standard transducer (diamonds) show that there is still an increase in velocity at the pipe wall due to the cavity between the wall interface and transducer surface. When comparing results obtained in a 16 mm pipe the errors close to the pipe wall seem less pronounced. The reason for this is simply the increase in pipe diameter (from 16 to 22.5 mm), which ensure that the maximum velocity point at the centre of the pipe is further away from the cavity, i.e. the high velocity gradients are not as significant then when compared to smaller diameter pipes. This was also observed for velocity profiles measured in bentonite 6.7% w/w (K = 0.0084, n = 1, τ_y = 8.74). Figure 5.32 show profiles measured at a flow rate of 1.2 l/s (Re_2 = 324) as well as a theoretical prediction for comparison. Good agreement was found between the profile measured using the delay line (after deconvolution) and standard transducers as well as theory.

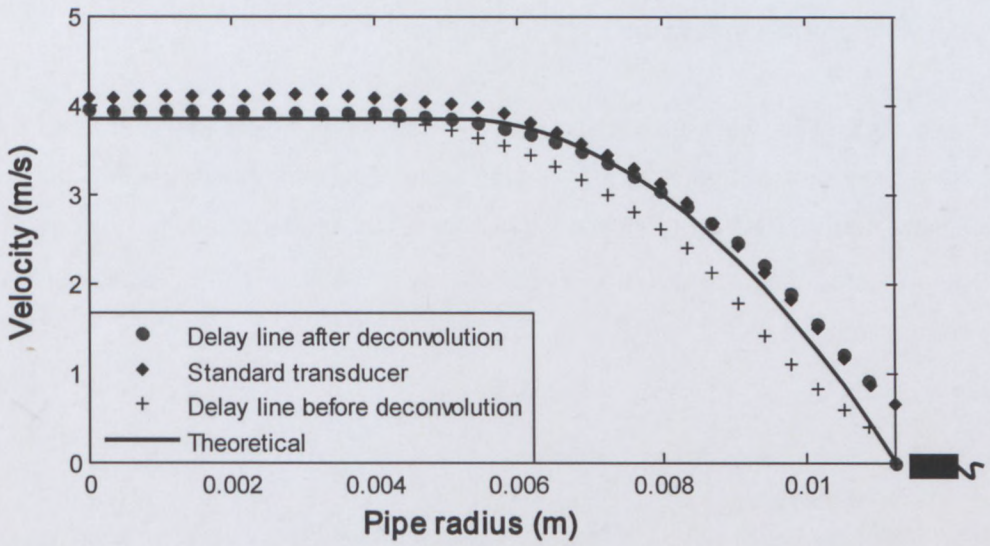

Figure 5.32: Comparison of profiles after deconvolution (bentonite 6.7% w/w, 22.5 mm pipe)

Figure 5.33 shows a profile measured in a 22.5 mm diameter pipe using a delay line transducer for kaolin 13% v/v (K = 1.022, n = 0.34, τ_y = 2.5) at a bulk flow rate of 0.51 l/s (Re_2 = 1360). It was not possible to measure velocity profiles using the standard transducer as the energy was attenuated and absorbed inside the cavity (described in previous sub-section). The velocity profile measured using the delay line transducer shows considerable distortion between the pipe wall and plug flow region. Here the deconvolution procedure seems to improve the velocity data, especially close to the pipe wall where the velocity gradient is high.

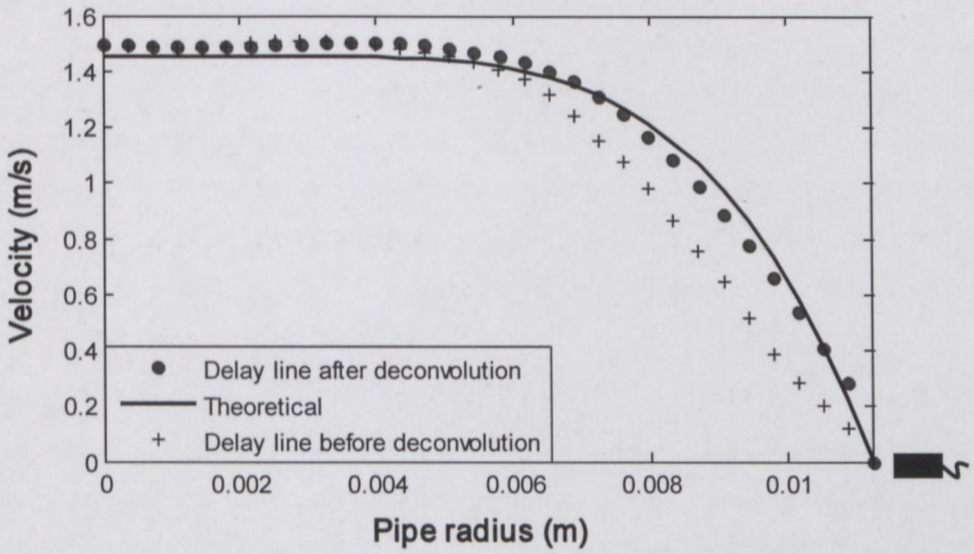

Figure 5.33: Comparison of profiles after deconvolution (kaolin 13% v/v, 22.5 mm pipe)

5.4.3.3 Velocity profiles measured in 52.8 mm pipe

Velocity profiles were also measured in a large pipe (52.8 mm diameter) using two transducers for comparison. Figure 5.34 show results obtained for CMC 6.15% w/w at a flow rate of 0.82 l/s (Re_2 = 481). A theoretical profile calculated using rheological parameters obtained from tube viscometry (K = 0.094, n = 0.81) is also presented for comparison.

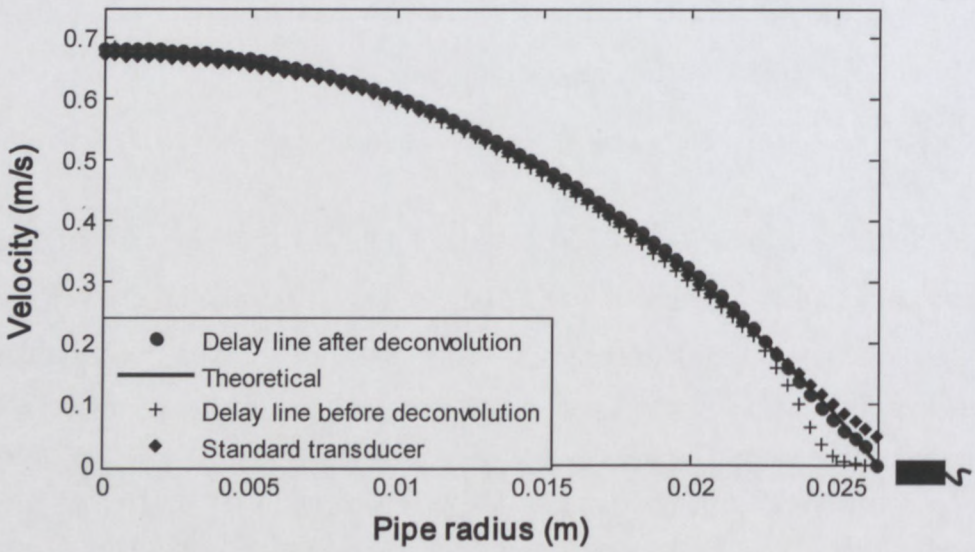

Figure 5.34: Comparison of profiles after deconvolution (CMC 6.15% w/w, 52.8 mm pipe)

Good agreement was found between the theoretical prediction and delay line transducer after implementing the deconvolution procedure, especially close to the pipe wall. The velocity profile measured by the standard transducer also show good agreement towards the centre of the pipe, but closer to the wall the velocity is higher due to the cavity present at the pipe wall interface. However, when comparing the entire profile across the pipe radius the result seems accurate even with the errors caused by the cavity setup.

Velocity profiles measured in bentonite 8% w/w (K = 0.0128, n = 1, τ_y = 18.7) at a flow rate of 2 l/s (Re_2 = 298) are shown in Figure 5.35. Similar observations can be made for the results obtained in the bentonite suspension. Both transducers measured accurate velocity profiles when compared to the theoretical estimation. The velocity data close to the pipe wall show good agreement with theory, even with the cavity

setup for standard transducer installation. Unfortunately it was not possible to measure velocity profiles in kaolin suspensions using both transducers, as the large pipe radius (R = 26.4 mm) was too large to penetrate in the attenuating fluid suspension. Next generation transducers where the delay line material absorbs less energy thus ensuring larger penetration depths might reduce problems with velocity measurements in attenuating fluids, which occur frequently in industry. This is currently under development.

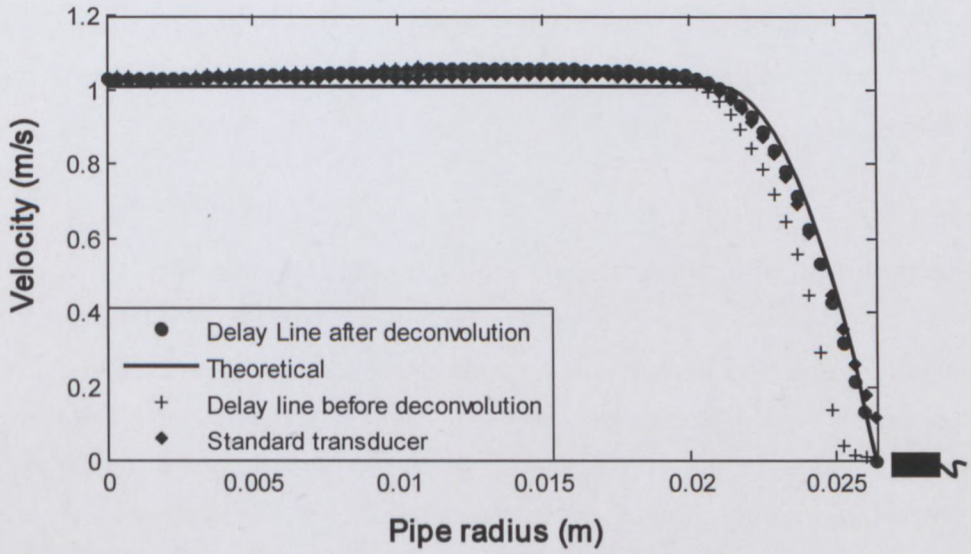

Figure 5.35: Comparison of profiles after deconvolution (bentonite 8% w/w, 52.8 mm pipe)

From the results it can be noted that as the pipe diameter increases the distortion caused by the cavity seems less significant. An Ultrasonic Transducer Diameter to Pipe Diameter (UTD/PD) ratio can thus be introduced to serve as a guideline for UVP applications. Table 5.11 shows the different UTD/PD ratios for the three pipe diameters used during this work. The ultrasonic transducer diameter (8 mm) was the same throughout this research work.

Table 5.11: UTD/PD ratios for three different pipes

Pipe diameter (mm)	Transducer diameter (mm)	UTD/PD ratio
16	8	0.50
22.5	8	0.36
52.8	8	0.15

It was found that a high UTD/PD ratio significantly distorts the measured velocity profile, unless a delay line transducer is used. Experimental profiles showed significant improvement for a UTD/PD ratio of 0.36 and lower (52.8 mm pipe). However, even when accurate and qualitative profiles can be obtained using standard transducers installed in larger pipes, the problem of ultrasonic energy absorption and attenuation is still present due to the cavities between the wall interface and transducer surface. Furthermore, when measuring in more complex, industrial fluids, problems of particle sedimentation inside the cavities cause velocity of sound and Doppler angle variations, which can distort the measured profile significantly (Wiklund, 2007). During this work only model mineral suspensions were used and thus these problems were not encountered for velocity profile measurements using standard transducer installation setups.

5.4.4 Deconvolution of profiles measured in complex geometries

Results obtained after implementing the deconvolution procedure on velocity profiles measured in three different pipe diameters for three different non-Newtonian fluids covering a wide range of rheological properties showed good agreement with theoretical estimations. Based on previous results, profiles measured in complex geometries were deconvolved with confidence and assumed correct, since there were no theoretical prediction available in a highly complex geometry such as a diaphragm valve. Velocity profiles were measured in a 300 mm rectangular flume and 50% open diaphragm valve. Figure 5.36 shows a profile measured using the delay line transducer before and after deconvolution at the centre of the flume bottom surface (see Figure 3.16) in bentonite 6% w/w (K = 0.0067, n = 1, τ_y = 11) at a flow rate of 10.67 l/s (Re_H = 315).

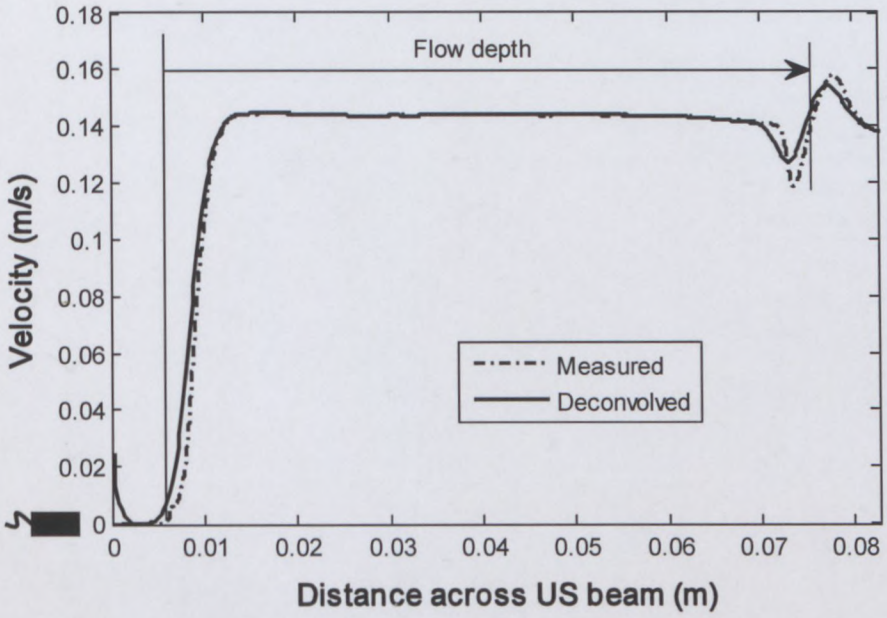

Figure 5.36: Deconvolution of profile measured using delay line transducer in rectangular flume

The magnitude of the velocity profile was similar before and after deconvolution due to the large flow depth present in open channel flow (H = 69 mm). Due to this large measurement depth the profiles obtained using standard transducers were also similar to that obtained after implementing the deconvolution procedure. The main difference between the profiles before and after deconvolution was the shifting (according to sample volume length) of the deconvolved profile (see Figure 5.19), as found during the straight pipe tests (see previous sub-sections). Velocity profiles measured in CMC fluids using delay line (after deconvolution) and standard transducers were also similar, since the velocity gradient for a power-law fluid is lower than fluids which have a yield stress (e.g. Bingham and yield-pseudoplastic fluids) and therefore the influence of the cavities were not as significant (including combination of high flow depths).

The same results were obtained when profiles measured in the diaphragm valve geometry were deconvolved. Figure 5.37 shows a profile measured using the delay line transducer across the centre measurement line (see Section 3.3.7, Figure 3.23) for CMC 6% w/w (K = 3.39, n = 0.61). All measurements were conducted in laminar flow; the profile in Figure 5.37 was measured at a bulk flow rate of 0.54 l/s (Re_2 = 15). The position of the deconvolved profile shifted towards the delay line material surface while the magnitude of the profile stayed the same. Similar results were found for velocity

profiles measured at different positions (see Figure 3.23) at the centre area of the valve.

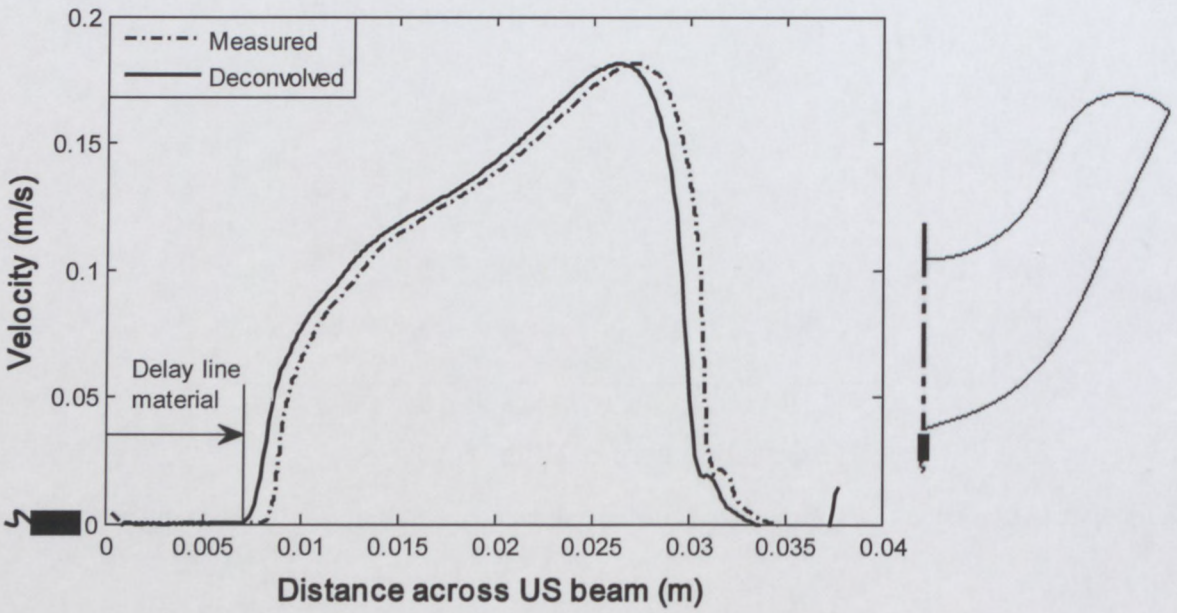

Figure 5.37: Deconvolution of profile measured using delay line transducer in diaphragm valve

The velocity profiles measured using standard transducers did not show good comparison to that obtained using the delay line transducer and combination of the deconvolution procedure. Here the cavities seemed to distort the profiles more significantly due to high velocities present at the contraction part of the valve. Furthermore, the measurement lines were not exactly the same for both transducers due to the angle variation (beam refraction) of the delay line transducers (see Figure 5.5). When measuring in a highly complex geometry such as a diaphragm valve the flow directions are not as constant as found in a rectangular flume which means that a change in beam angles could result in different Doppler angles which consequently cause a variation in velocity magnitudes. This is explained in detail in the next chapter.

5.5 VELOCITY ESTIMATION USING DMEA DATA

The aim of this study was to compare the quality and quantity of velocity profiles obtained using different velocity estimation algorithms. Measurements were conducted using two transducers (delay line and standard) in two different pipes (diameters 22.5 and 52.8 mm) and in two non-Newtonian fluids (CMC and bentonite suspension). The algorithms used (Time and Frequency Domain (TD / FD) techniques) were both compared with the commercial software algorithm (also time domain) which is integrated in the DSP of the UVP monitor. A wide range of UVP system parameter settings were tested during velocity profile measurements in order to completely evaluate the custom velocity estimation algorithms (similar to the tests in Section 5.3, but using different velocity estimators). This work was part of a collaborative project with SIK, Gothenburg, Sweden and therefore only the significant findings will be presented here. Detailed results from this research work can be found in Holmbom (2011).

5.5.1 Comparison of algorithms at different system settings

Figure 5.38 shows velocity profiles measured using a delay line transducer at different voltage settings (30 - 150 V) while the other system parameters were kept constant, shown in Table 5.12. The profiles (Figure 5.38) were measured in CMC 3.25% w/w (K = 0.217, n = 0.81) in a 22.5 mm pipe at a flow rate of 0.32 l/s (Re_2 = 275). Since a profile could be obtained at the lowest voltage setting (30 V) using DMEA data and a custom Time Domain (TD) algorithm, only the results obtained at different voltage settings from the commercial software (Met-Flow) are presented.

Table 5.12: UVP parameter settings for varied voltage settings (custom algorithms)

Gain	US Voltage (V)	Number of cycles/pulse	Number of US pulse reps.	Sound speed (m/s)	Doppler angle (°)
1-3	30-150	2	64	1476	77.4

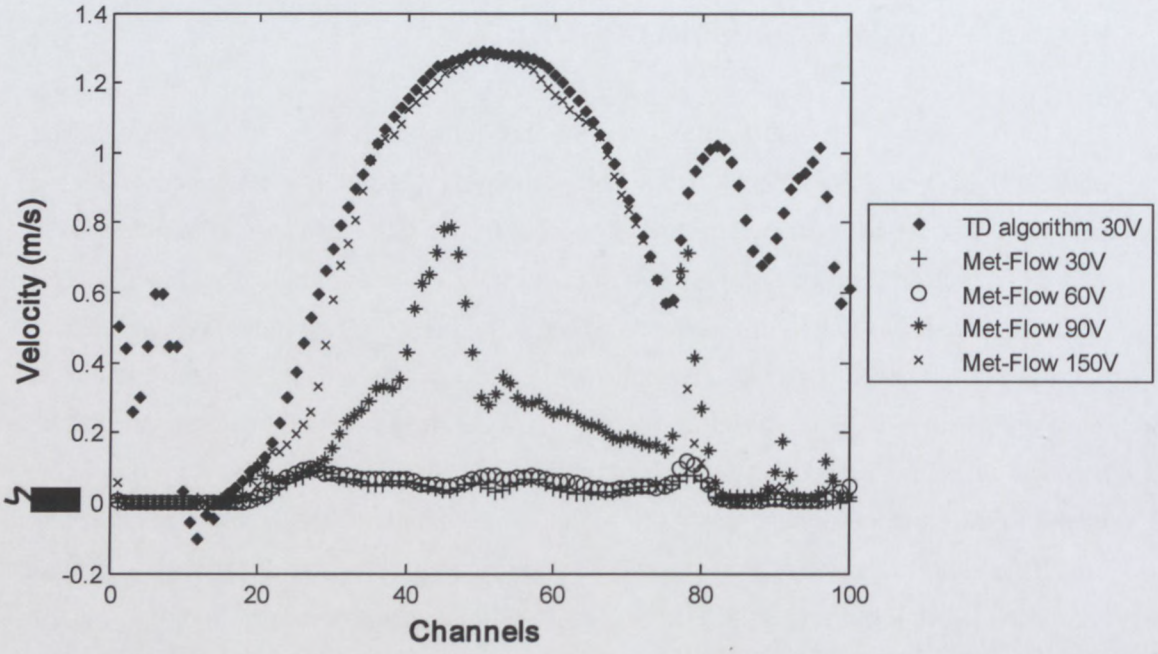

Figure 5.38: Comparison of profiles obtained using two different algorithms and four voltage settings

It can be observed that a good qualitative profile (shown with diamonds) was obtained at the lowest voltage setting using DMEA data and the time domain (TD) velocity estimator. Velocity profiles estimated using the built in algorithm of the UVP monitor seemed to correlate better with the TD algorithm as the voltage was increased (see Met-Flow 150 V result). Similar results were found using the standard transducer, except that the profiles measured at 90 V already showed good agreement with the custom algorithm, due to the higher energy output of the standard transducer in the CMC fluid. Also, when the time domain algorithm was replaced with the frequency domain algorithm similar profiles were obtained for both transducers at different voltage settings. However, some discrepancies were found between the time and frequency domain algorithms when compared separately. This is explained in Section 5.5.2.

Figure 5.39 shows profiles measured using the delay line transducer in bentonite 8% w/w (K = 0.0128, n = 1, τ_y = 18.7) at a flow rate of 0.5 l/s (Re_2 = 156). The UVP system parameters (shown in Table 5.13) were kept constant while the number of ultrasonic pulse repetitions (32 - 512) per profile was varied.

Table 5.13: UVP parameter settings for varied pulse repetition settings (custom algorithms)

Gain	US Voltage (V)	Number of cycles/pulse	Number of US pulse reps.	Sound speed (m/s)	Doppler angle (°)
1-3	30	2	32-512	1512	77.4

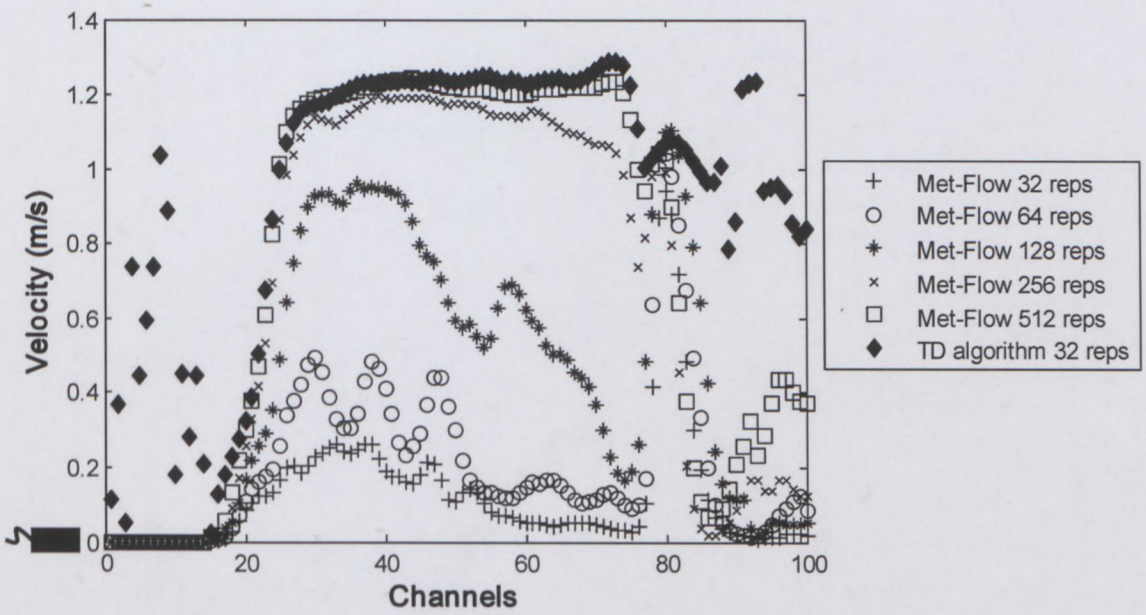

Figure 5.39: Comparison of profiles obtained using two different algorithms and five pulse repetition settings

The algorithm used by the commercial software (Met-Flow) could only produce a velocity profile with a pulse repetition setting of 512, where the profile calculated using the custom algorithm (TD) was obtained using a pulse repetition setting of 32. Similar results were found in the larger pipe (diameter 52.8 mm) and for profiles measured in CMC fluids. Since a profile can be obtained at very low pulse repetition settings the time resolution (time taken for one profile) of the UVP technique has significantly improved. This improvement was also found when using an alternative velocity estimation algorithm in the frequency domain.

5.5.2 Comparison between custom and commercial algorithms

Three velocity estimators (one commercial and two custom algorithms) were compared under the same system parameters and test conditions. Figure 5.40 and 5.41 show

velocity profiles measured in CMC 3.25% w/w and bentonite 8% w/w, respectively. Delay line transducers were used and measurements were conducted in a 52.8 mm pipe in laminar flow. The UVP system parameter settings for measurements in CMC and bentonite suspensions are shown in Table 5.14 and 5.15.

Table 5.14: UVP parameter settings for CMC 3.25% w/w measurements in 52.8 mm pipe

Gain	US Voltage (V)	Number of cycles/pulse	Number of US pulse reps.	Sound speed (m/s)	Doppler angle (°)
1-3	150	2	128	1476	77.4

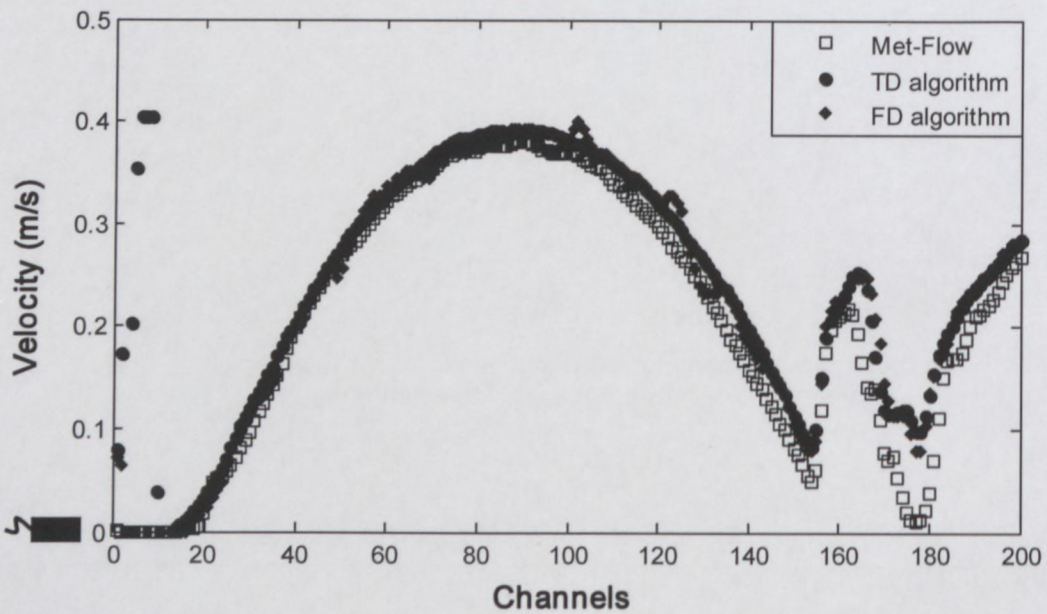

Figure 5.40: Comparison of profiles obtained using three different velocity estimators (CMC 3.25% w/w, 52.8 mm pipe)

Table 5.15: UVP parameter settings for bentonite 8% w/w measurements in 52.8 mm pipe

Gain	US Voltage (V)	Number of cycles/pulse	Number of US pulse reps.	Sound speed (m/s)	Doppler angle (°)
3-5	60	2	256	1512	77.4

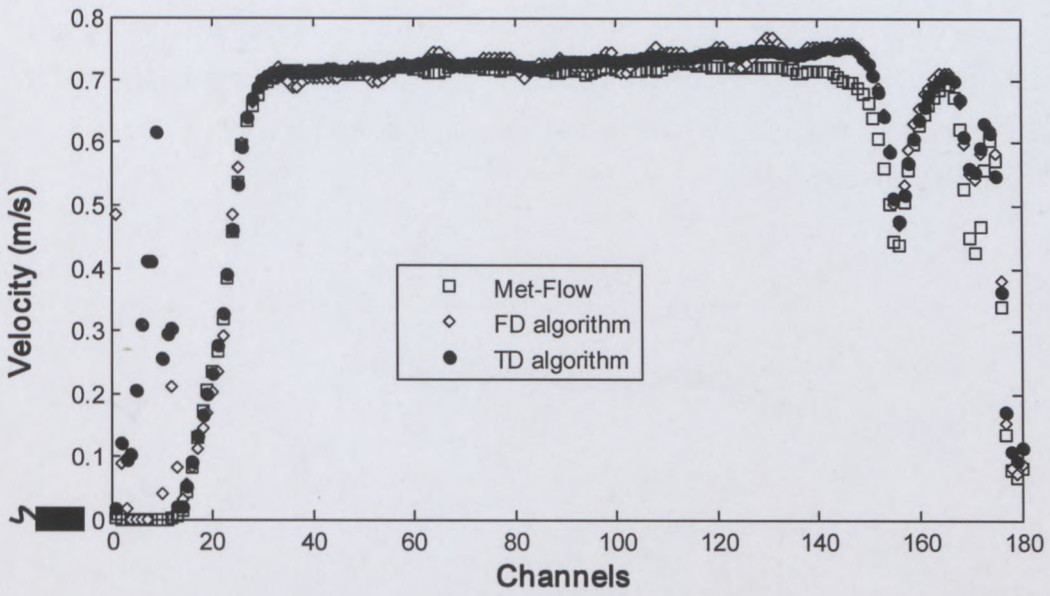

Figure 5.41: Comparison of profiles obtained using three different velocity estimators (bentonite 8% w/w, 52.8 mm pipe)

Based on the results seen in Figures 5.40 – 5.41 the frequency domain (FD) algorithm produced profiles (diamonds) where the magnitudes of the estimated velocities seem to vary around the profile calculated using the time domain algorithm (TD). This effect was more pronounced further away from the pipe wall, where the signal-to-noise ratio was lower due to attenuation of ultrasonic energy. The time domain algorithm (circles) showed better performance where the signal-to-noise ratio was low throughout all the flow measurements. Increasing the energy output of the transducers by adjusting system parameters such as number of cycles per pulse or voltage did not seem to improve the results obtained using the frequency domain algorithm. Both algorithms produced scattered velocity data (see Figures 5.38 – 5.41) between the transducer surface and wall interface, where no flow was present, i.e. inside the delay line material. The same was observed when using standard transducers with the cavity setup; however, this can be removed by implementing a digital filter in the velocity estimation algorithm. Note that the Met-Flow algorithm produced good quality profiles (blocks) with high voltage and pulse repetition rates (see Tables 5.14 and 5.15). There were some velocity magnitude differences close to the opposite pipe wall, which could be due to small changes in flow conditions during tests or attenuation of ultrasonic energy. Very good agreement (within 5%) was found between all calculated velocity profiles close to the transducer, where the signal-to-noise ratio was highest. When comparing the frequency domain algorithm (Figure 5.42) for measurements conducted in a 22.5 mm pipe under the same test conditions (see Table 5.15) for the same

bentonite fluid suspension, it can be observed that the FD algorithm yielded good results (diamonds) across the entire diameter of the pipe. Good agreement (R^2 = 0.96) was found across the pipe diameter between the time domain and Met-Flow (also time domain) algorithms (blocks and circles).

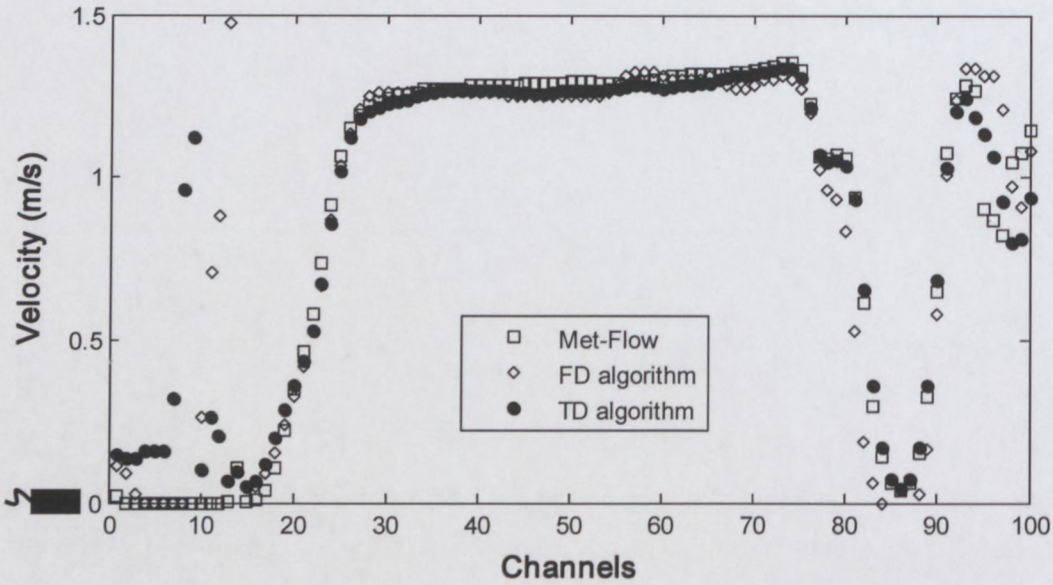

Figure 5.42: Comparison of profiles obtained using three different velocity estimators (bentonite 8% w/w, 22.5 mm pipe)

It is clear that the frequency domain algorithm's performance suffers from low signal – to-noise ratios, whereas the algorithm based in the time domain was superior for all comparative tests conducted during the research work. The time domain algorithm also calculated velocity profiles +/- 30% faster (depending on the data block sizes, number of profiles and pulse repetitions) than the frequency domain velocity estimator. However, it is beneficiary for the user to have access to both algorithms as the frequency domain algorithm gives extra information on the signal quality of each measurement channel across the experimental velocity profile. This enables simplified identification of signal artefacts and causes of velocity errors (Wiklund, 2007).

5.6 CONCLUSION

Acoustic characterisation of ultrasonic transducers was an important part of the development of a new delay line transducer. Since one of the main objectives of this research work was to enable accurate UVP measurements in complex geometries, knowledge of the actual beam shape was essential. When measuring in narrow regions in a complex geometry, the user must ensure that the ultrasonic beam does not overlap with the physical material as this could distort velocity profiles significantly. Also, after correcting the beam angle variation found with the delay line transducer, the profiles agreed well with that measured using standard transducers with no angle refraction. Another important aspect is that by acoustically characterising the transducers the energy output is obtained which is essential for measurements in attenuating fluids as found in almost all industrial application. These measurements provide good indication of the ultrasonic transducer performance, which can be used for future improvements of next generation transducers.

UVP system parameter settings showed that the delay line transducer operate well over the entire range of system settings, except for the amplification gain settings. This could be due to multiple ultrasonic reflections inside the delay line material, which if amplified, could cause distortion close to the material surface (pipe wall interface). However, the distortion is very noticeable at the wall region and can easily be corrected for by adjusting the amplification gain settings.

Results obtained after implementing a deconvolution procedure on velocity profiles measured using delay line transducers showed significant improvement, especially close to the pipe walls, where the velocity gradients are high. It was found that for larger pipe diameters the standard transducer setup can provide good quality velocity profiles, but the problem with particle sedimentation inside the cavity is still present. Also, when measuring in an attenuating fluid the cavity fills up with the test fluid, which prevents flow behaviour measurements even when using a transducer with higher acoustic energy output. The delay line transducer reduces both these problems at the same time by eliminating the cavity and providing the focal point of the ultrasonic beam at the delay line material surface, which is installed at the pipe wall interface.

The algorithms for both time and frequency domain could produce profiles at much lower energy input (voltage settings) as well as low ultrasonic pulse repetition settings, where the commercial algorithm was unable. By acquiring DMEA data and using an alternative velocity estimation algorithm the UVP technique is able to measure flow profiles in more attenuating fluids and achieve high time resolution (profiles can be measured with repetition rate as low as 32). This improvement will enable detailed flow behaviour measurements for industrial applications where attenuating fluids are encountered frequently as well as where fast transient flows are of interest.

Based on the presented results, the UVP technique was optimised by using a specially designed (2^{nd} generation) delay line transducer, advanced signal processing techniques and custom velocity estimation algorithms. In Chapter 6 velocity profile measurements in complex geometries using the optimised methodology are compared to that obtained using a standard transducer and commercial velocity estimation technique.

CHAPTER SIX

APPLICATION AND VALIDATION OF OPTIMISED UVP SYSTEM

CHAPTER SIX

APPLICATION AND VALIDATION OF OPTIMISED UVP SYSTEM

6.1 INTRODUCTION

The objectives for these particular tests were to verify the optimised UVP system by comparing velocity profiles measured in two complex geometries using both standard and delay line transducers. This chapter summarises results obtained in a 50% open diaphragm valve and 300 mm rectangular flume for CMC solutions and bentonite suspensions. The accuracy of results was verified and compared by calculating the bulk flow rates and comparing to a reference electromagnetic flow meter.

Furthermore, the UVP technique was used in combination with a pressure difference method (PD) to establish rheological parameters of the non-Newtonian fluids using optimised methodology (delay line transducer, deconvolution procedure) and standard methods. Conventional methods such as off-line rotary viscometry and tube viscometry were used to validate results determined by the UVP-PD method. A new in-line technique - Ultrasonic Velocity Profiling (UVP) with combined Flow Depth (FD) measurement (UVP-FD) for obtaining rheological parameters of fluids in open channel flow applications is also presented. This method was evaluated using standard transducers for two different non-Newtonian fluids. The fluids that were investigated yielded a wide range of rheological properties. Results of carboxymethyl cellulose (CMC) solutions, as well as bentonite and kaolin clay mineral suspensions of various concentrations are presented.

All the velocity profiles measured using the delay line transducer in this work have already been corrected for by implementing the deconvolution procedure discussed previously (Section 3.3.4, Chapter 3; Section 5.4, Chapter 5), and thus only the final deconvolved profiles are presented throughout Chapter 6.

6.2 FLOW MEASUREMENTS IN OPEN CHANNEL

CMC 4.5% w/w and bentonite 6.5% w/w were tested using two transducers (delay line and standard) in the open channel at the FPRC laboratory. All tests were conducted at a slope of 1 degree (similar test conditions as in Chapter 4). Velocity profiles measured at different positions are compared to theoretical predictions. Two-dimensional flow maps were constructed from all six experimental profiles and integrated to obtain the volumetric flow rates, which were compared to that measured using an electromagnetic flow meter. Rheological parameters were obtained using tube viscometry.

6.2.1 Profiles measured in CMC solution

6.2.1.1 Velocity profiles and sheet flow comparison

Tables 6.1 and 6.2 summarise the range of experimental conditions and UVP parameter settings for the CMC 4.5% w/w (K = 0.75, n = 0.59) tests. It was possible to use an average of 300 profiles due to the low number of US pulse emissions of 256 (sampling time 112 ms) required for qualitative velocity measurements.

Table 6.1: CMC 4.5% w/w flume flow conditions

Q (l/s)	H (mm)	Re_H	Regime
10.5	49.75	639	Laminar
14.5	56.88	884	Laminar

Table 6.2: UVP parameter settings for CMC 4.5% w/w flume tests

Gain	Voltage (V)	Number of cycles/pulse	Number of US pulse reps.	Sound speed (m/s)	Doppler angle (°)
5-7	90	2	256	1490	70 / 77.4

Profiles measured at the centre of the flume bottom surface using both transducers (delay line and standard) for CMC 4.5% w/w at a flow rate of 10.5 l/s is shown in Figure 6.1. Also included here are the predictions of Equations 2.19 - 2.20 using the rheology obtained from tube viscometry. It can be observed that there is a good correlation of the theoretical prediction (solid line) with the experimental data (both transducers – diamonds and circles). The effect of the cavity did not distort the profiles measured using the standard transducers due to the large flow height (H = 49.75 mm) present.

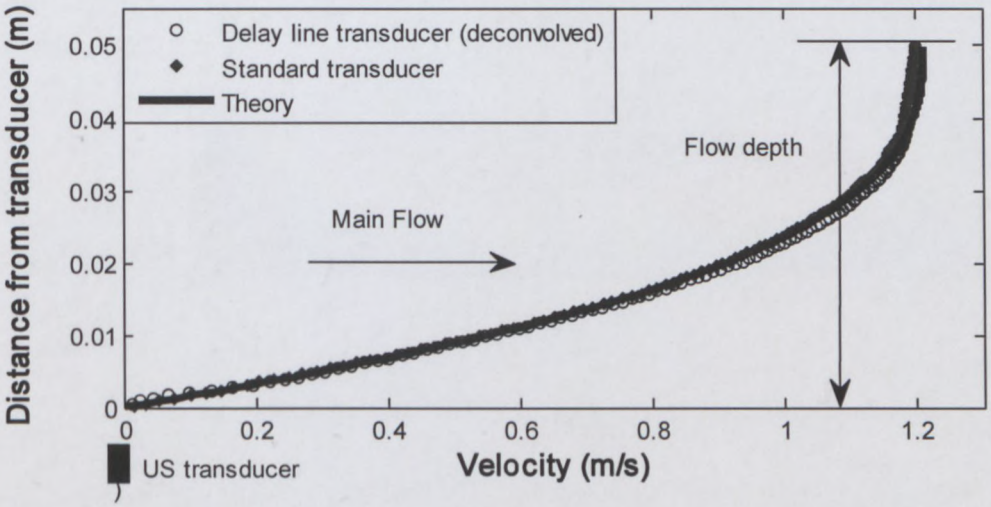

Figure 6.1: Experimental profiles measured using delay line and standard transducers vs. Equations 2.19-2.20 for CMC 4.5% w/w

The theoretical profile deviated from the experimental profile less than 100 mm away from the centre, as found during the preliminary tests in Chapter 4 (see Figure 4.4). Since good correlation between results obtained using both transducers was found the same deviation was assumed and therefore not presented here. Similar results were found for profiles measured at a higher flow rate (Q = 14.5 l/s).

6.2.1.2 Flow maps for CMC solution

The contour plot of the CMC 4.5% w/w at Re_H = 639 obtained using both transducers are shown in Figure 6.2 and 6.3. The difference between the flow rates measured by the flow meter and the integrated contour plot was 4.87% and 5.81% for the standard and delay line transducers, respectively. The agreement between the two results was very good (error difference of +/- 1%), which inspires confidence in the reliability of the detailed velocity measurements using delay line transducers presented here.

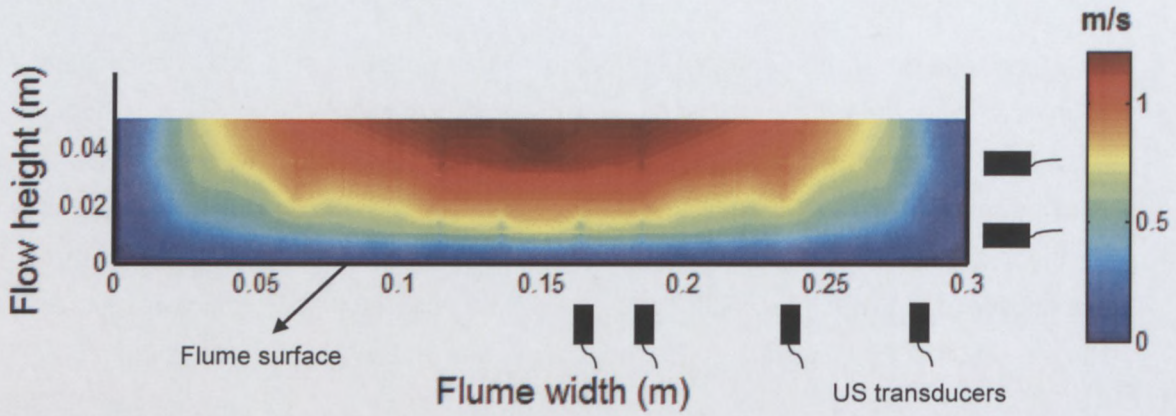

Figure 6.2: CMC 4.5% w/w experimental laminar flow map (standard transducers)

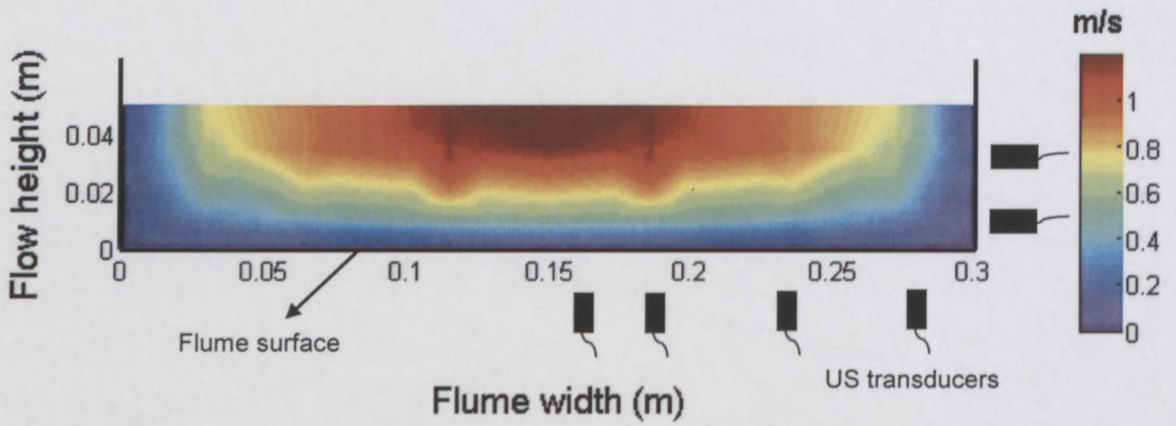

Figure 6.3: CMC 4.5% w/w experimental laminar flow map (delay line transducers)

Similar results were found for the other laminar flow data (for both transducers) and are therefore not presented here. Table 6.3 shows the error difference percentage between the integrated contour plots (obtained using standard and delay line transducers) and reference electromagnetic flow meter, for two different flow rates. The small difference between the error difference percentages were due to variations in flow rate during measurements (see Table 6.3 and 6.6).

Table 6.3: Percentage difference between volume flow rates obtained from integration of flume experimental profiles and reference electromagnetic flow meter

Elec. mag. flow meter (l/s)	Integration (standard) (l/s)	Integration (delay line) (l/s)	Flume (standard) vs. flow meter (%)	Flume (delay line) vs. flow meter (%)
10.5	9.99	9.89	4.87	5.81
14.05	13.52	12.99	3.75	7.54

6.2.2 Profiles measured in bentonite suspension

6.2.2.1 Velocity profiles and sheet flow comparison

The centreline velocity profiles showing the model predictions and the experimental data for both delay line and standard transducers in bentonite 6.5% w/w (K = 0.0068, n = 1, τ_y = 11) is shown in Figure 6.4. Experimental conditions and UVP parameter settings are displayed in Tables 6.4 and 6.5.

Table 6.4: Bentonite 6.5% w/w flume flow conditions

Q (l/s)	H (mm)	Re_H	Regime
10.67	68.95	315	Laminar
20.83	73.57	907	Laminar

Table 6.5: UVP parameter settings for bentonite 6.5% w/w flume tests

Gain	Voltage (V)	Number of cycles/pulse	Number of US pulse reps.	Sound speed (m/s)	Doppler angle (°)
3-5	150	2	256	1522	70 / 77.4

The agreement between the theoretical prediction and measured profiles were good (delay line R^2 = 0.93; standard R^2 = 0.92), except for some magnitude differences at the plug-flow region, which could be due to small changes in flow conditions. The velocity data measured by the standard transducers close to the wall agrees well with the theory, which was not the case during preliminary tests in the flume (see Figure 4.6, Chapter 4).

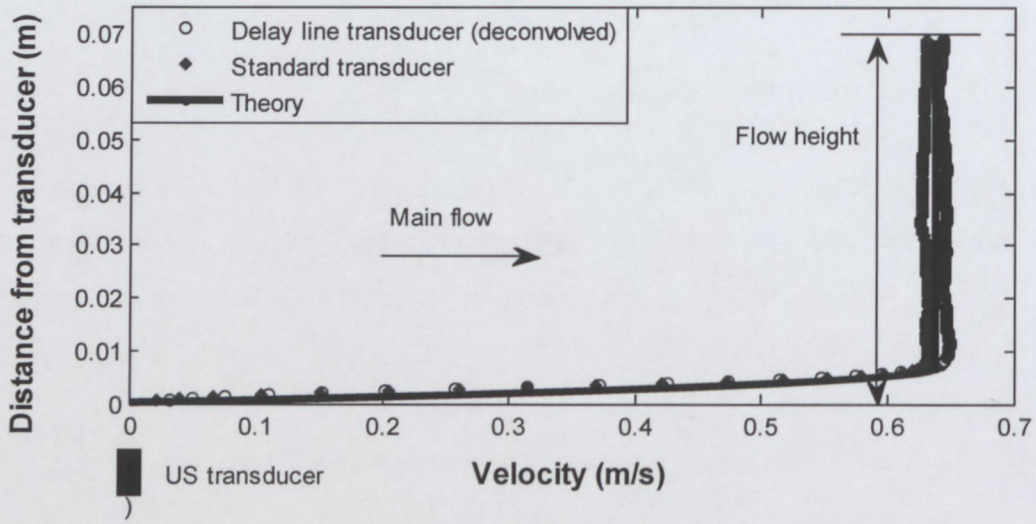

Figure 6.4: Experimental profiles measured using delay line and standard transducers vs. Equations 2.19-2.20 for bentonite 6.5% w/w

It has been suggested (Chapter 4, Section 4.3.2) that the cavities between the surface of the standard transducers and wall interfaces have a more significant influence on plug flows where the velocity gradients are high. However, a higher concentration bentonite (6.5% vs. 5.29% w/w) was used which caused the fluid suspension to settle around the flume walls during tests (illustrated in the next section). Even after removing air and dirt when flushing the transducers, the bentonite particles seemed to fill the cavities and settle before tests could be started. As a result the bentonite particles created a plug where no fluid beyond the wall interface could flow. This effect was beneficiary during these tests when using standard transducers and consequently profiles with accurate gradients and velocity data close to the wall could be measured. It seems that based on these results in the flume geometry where large flow depths / heights occur (here H = 69 mm) the delay line transducers are not necessary. However, it must be stressed again that this model suspension offers little attenuation to ultrasonic energy and thus it was possible to measure accurate velocity profiles using both standard and delay line transducers. Since the cavities fill up with the fluid that is used, an attenuating fluid will prove to be impossible to penetrate if the ultrasonic energy needs to overcome the entire length (near-field distance - usually around 16 mm) of the cavity. Furthermore, as discussed in Section 4.3.2 (Chapter 4),

density changes inside the cavities could introduce more errors, especially when more complex fluids are introduced (Wiklund, 2007).

The delay line transducers could also measure accurate velocity profiles across the flume geometry, but previously mentioned problems are reduced due to the cavity being eliminated. The sheet flow model (Equations 2.19-2.20) still holds to about 50 mm from the side wall due to the formation of the plug extending towards the side walls (similar to the results found in Chapter 4, see Figure 4.7), and is therefore not included in here.

6.2.2.2 Flow maps for bentonite suspension

Figures 6.5 and 6.6 shows the contour plots for bentonite 6.5% w/w at a flow rate of 20.83 l/s (laminar flow). The error difference between the measured flow rate and calculated flow rate was +/- 7.5% for results obtained using both standard and delay line transducers. It can be observed that for both flow contour plots no flow was measured around both corners of the flume surface (marked with circles in Figures 6.5 – 6.6). This was due to the high yield stress / viscosity of the bentonite suspension which caused the particles to settle around the corner walls with time. This example also shows how UVP can be used to monitor changing flows in open channels for highly viscous non-Newtonian fluids. This is particularly important when transporting highly viscous fluids to tailing dams (e.g. in the mining industry) as blockages could cause the processing plant to shut down and consequently impact economic and environmental aspects.

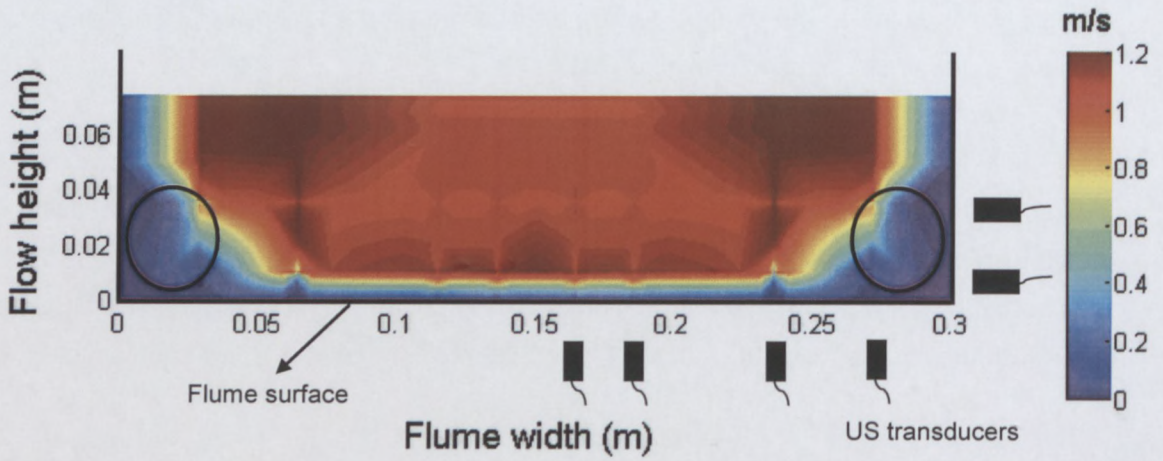

Figure 6.5: Bentonite 6.5% w/w experimental laminar flow map (standard transducers)

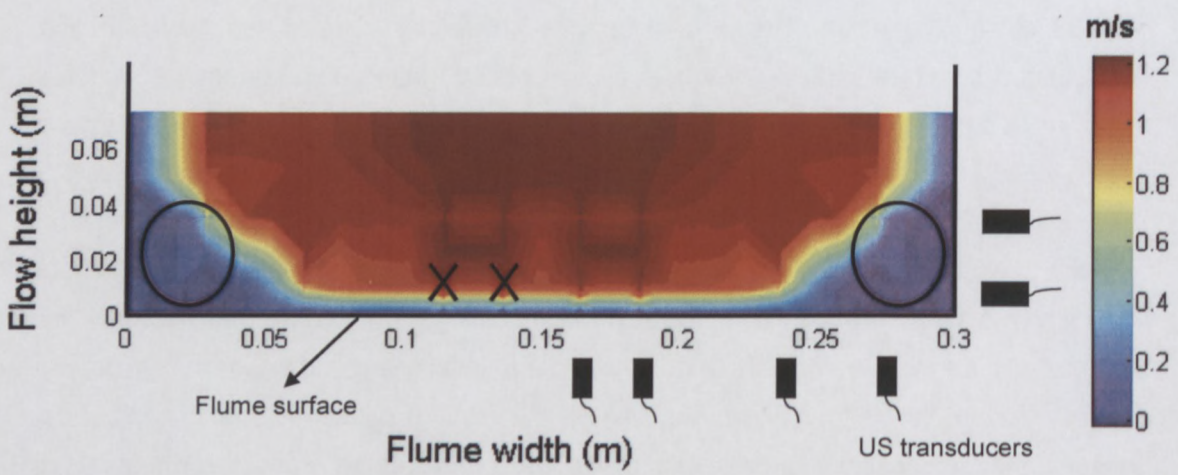

Figure 6.6: Bentonite 6.5% w/w experimental laminar flow map (delay line transducers)

The velocity 'spikes' (shown by crosses in Figure 6.6) were less significant due to the combination of the large flow height (69 mm) and bentonite particles settling inside the cavities during tests, as discussed previously. Table 6.6 shows the error difference percentages between the calculated and measured bulk flow rate for two different flow rates. Since an error of +/- 5 – 10% is obtained when integrating an experimental velocity profile in a straight pipe (Kotzé, 2008), the difference percentages (Table 6.6) validate the accuracy (less than 10%) of the velocity profiles measured in the rectangular open channel.

Table 6.6: Percentage difference between volume flow rates obtained from integration of flume experimental profiles and reference electromagnetic flow meter

Elec. mag. flow meter (l/s)	Integration (standard) (l/s)	Integration (delay line) (l/s)	Flume (standard) vs. flow meter (%)	Flume (delay line) vs. flow meter (%)
10.67	9.77	10.1	8.44	5.34
20.83	19.26	19.22	7.55	7.73

Based on the results it is clear that UVP is able to measure and monitor detailed non-Newtonian flow behaviour in open channels. However, further tests are required in different geometries (e.g. triangular and trapezoidal shapes) to evaluate the limitations of the UVP technique. The most important conclusion with regard to measurements in open channels for industrial purposes where complex fluids with attenuating properties are encountered frequently, is that according to previous results obtained (Section 5.5, Chapter 5 – kaolin suspensions), it will only be possible to monitor flow behaviour properties using the delay line transducer. The combination of the delay line material, where the focal point is situated at the wall interface, and implementation of the deconvolution procedure makes this measurement method the most suitable for industrial applications in open channel flow.

6.3 FLOW MEASUREMENTS IN DIAPHRAGM VALVE

The objectives and motivation for these tests were to compare results obtained using delay line and standard transducers in a newly designed diaphragm valve with four installation ports (see Section 3.25, Chapter 3). CMC 6% w/w (K = 3.54, n = 0.6) was tested in a 50% open diaphragm valve at the FPRC laboratory. The bulk flow rate was calculated and results were compared to a reference flow meter.

6.3.1 Velocity profiles

A new measurement line (TDX Line 1) has been introduced across the centre line of a newly designed diaphragm valve in order to calculate the bulk flow rate using the added velocity information (see Figure 3.23, Section 3.3.7). Figure 6.7 shows the region of the valve that was investigated (centre area) along with all the positions and measurement lines of the transducers used (delay line and standard).

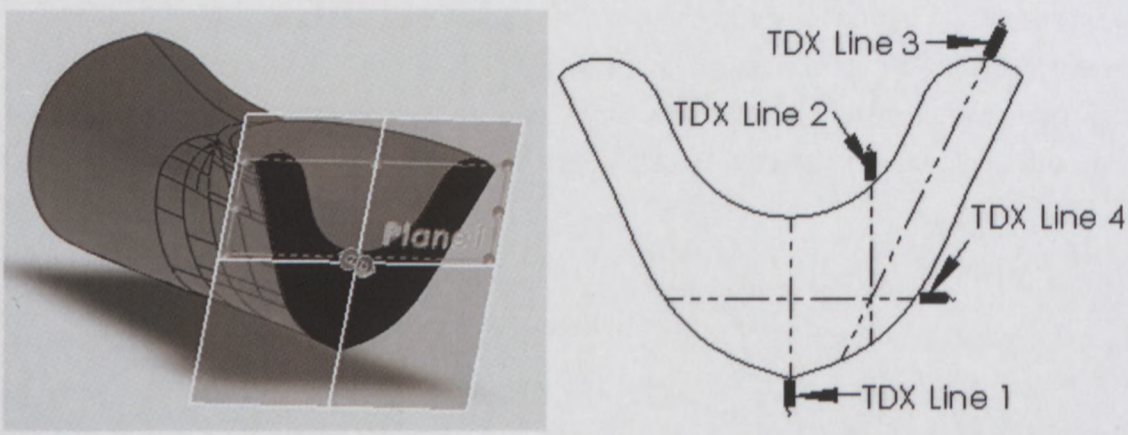

Figure 6.7: Position of ultrasonic transducers around centre area of diaphragm valve

Figures 6.8 – 6.9 show velocity profiles measured using two different transducers (delay line and standard) at the same flow rates (Q = 0.54 - 1.6 l/s) inside the valve across TDX Line 1 (centre line), which is shown by the striped line on the valve schematic (only half of valve is shown due to symmetry around centreline, see Figure 6.7).

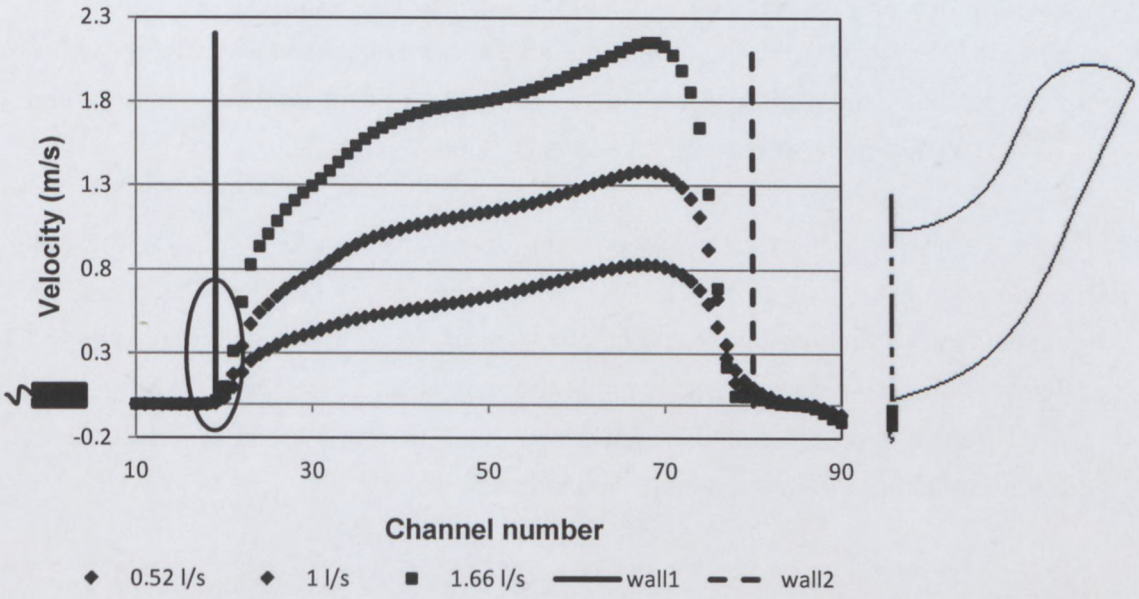

Figure 6.8: Centre profiles measured using delay line transducers in valve for CMC 6% w/w

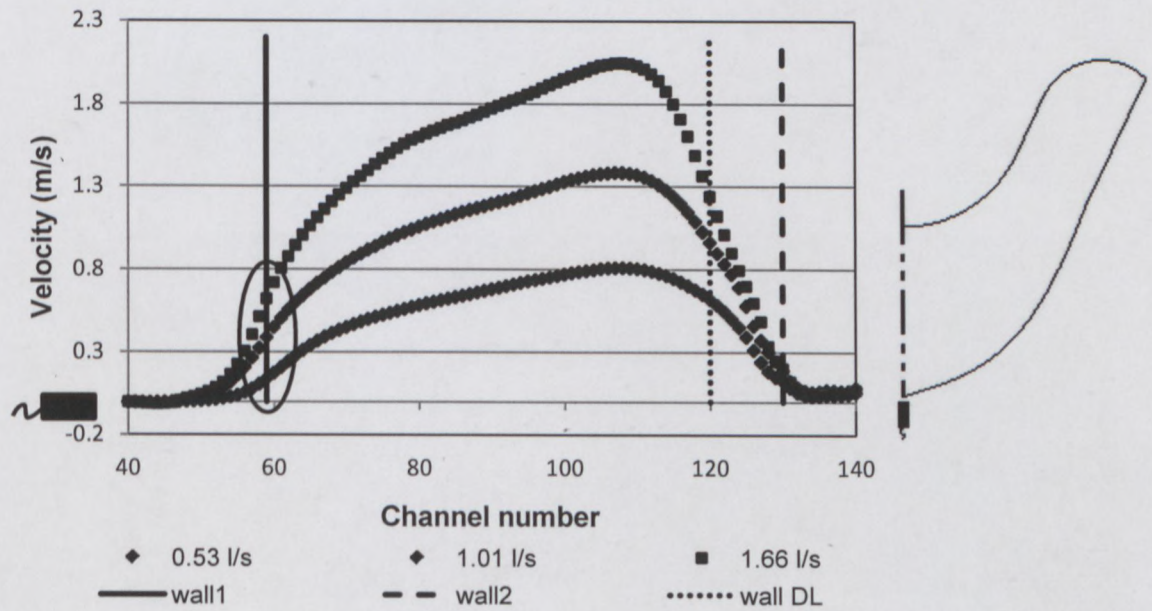

Figure 6.9: Centre profiles measured using standard transducers in valve for CMC 6% w/w

Both results show an abrupt increase in velocity, where the highest velocities seem to be at the region close to the diaphragm, which was expected. An important observation that can be made from Figures 6.8 – 6.9 is the velocities measured at the wall interfaces, shown by the circle, for both transducers. The standard transducer

measured velocities as high as 0.8 m/s at the wall interface (wall1, Figure 6.9) for the 1.66 l/s test due to the cavities between the transducer surface and wall. The delay line transducer measured realistic velocity data close to the wall region for all the measured flow rates by eliminating the cavity, as shown in Figure 6.8 (wall1).

Figure 6.9 also shows an extra wall position (dotted line, wall DL), which is the wall position when measuring velocity profiles with a delay line transducers. The difference in penetration depths are due to the combination of the complex valve geometry and difference in ultrasonic beam angles of the two transducers. Figure 6.10 illustrates the two different beam angles and measurement lines of the delay line and standard transducers across the centre area of the diaphragm valve.

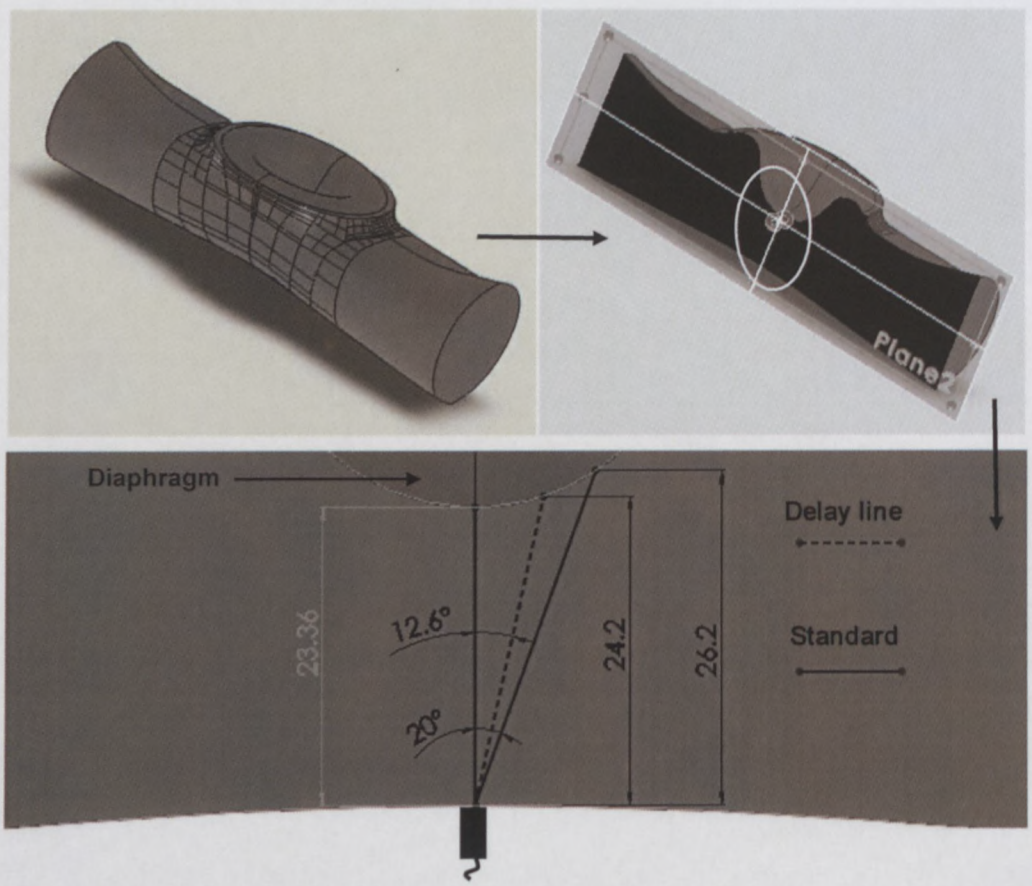

Figure 6.10: Measurement lines of delay line and standard transducers across TDX Line 1

It can be observed that due to the beam refraction of the delay line transducer (see Figure 5.5, Section 5.2.2), the penetration depth (valve surface to opposite wall interface) of the standard transducer is 2 mm longer. The implication of this is very

significant, especially when transforming the velocity data across the centre (shown by grey line, Figure 6.10) by using the Doppler angle (Met-Flow SA, 2002). Since the distance across the centre line is shorter than the actual measured distance using the UVP method, velocity data will overlap with the wall and consequently result in erroneous flow rate calculation or validation of CFD models. Ideally the beam propagation should be as close to the perpendicular as possible, but for UVP to work an angle is needed in order to measure the relative movement of suspended particles after successive pulses. When measuring inside simple geometries such as straight pipes, the penetration depths will stay constant for all variations of ultrasonic beam propagation. It is therefore necessary that the user needs to accurately know the position of measurement lines inside highly complex geometries, such as a diaphragm valve. Unfortunately the difference in beam angles between the two transducers made it not possible to compare results for example on the same axis. Also, two separate diaphragm valves were constructed, which was optimised for delay line and standard transducer installation, and were not installed at the same time during tests due to constraints in the flow loop. This meant that although the same flow rates were more or less achieved for all tests, not exactly the same flow could be obtained inside both valves. The most important objectives in this particular study were to investigated and compare the velocity data close to wall interfaces as well as the accuracy and magnitude of measured velocities obtained using two different transducers.

Figures 6.11-12 shows a sharp increase in velocity close to the near wall for all of the lateral measurements (TDX Line 2) using both standard and delay line transducers (similar results were found in Section 4.4, Chapter 4 for standard transducers). In this case significantly higher velocities were measured at the wall interface using standard transducers (shown by circle, Figure 6.11). This was due to the cavity situated at a region of the valve where high velocities relative to the rest of the valve were present (i.e. under the diaphragm) and thus this measurement setup caused even more distortion of experimental velocity profiles. The profiles measured using the delay line transducers shows a very high gradient from the transducer surface, but no unrealistic velocities were measured beyond the wall interface.

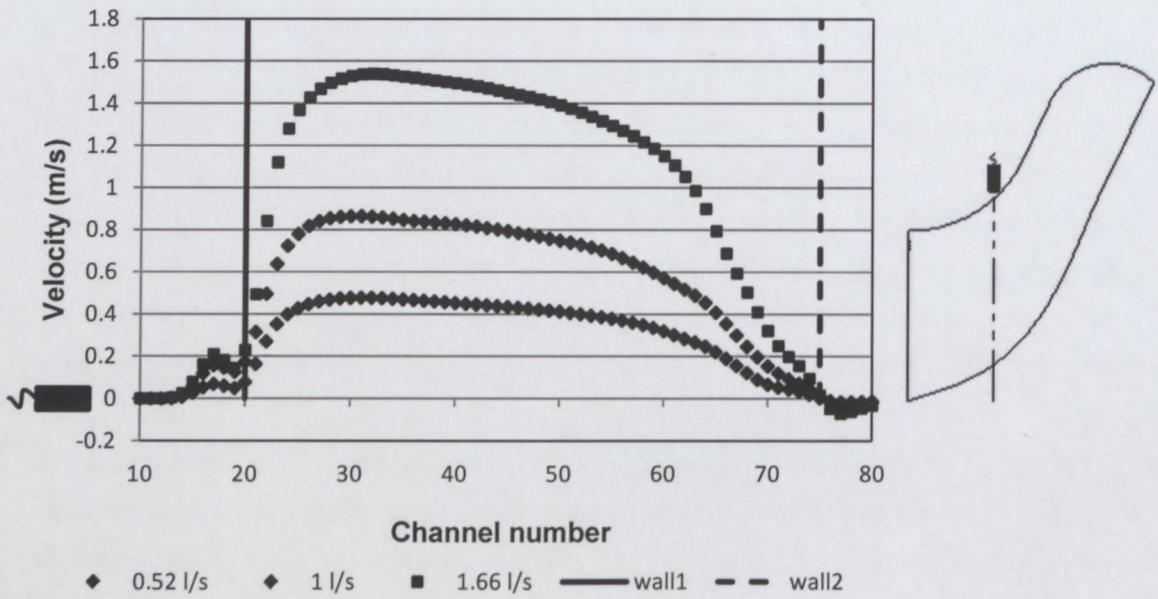

Figure 6.11: Lateral profiles measured using delay line transducers in valve for CMC 6% w/w

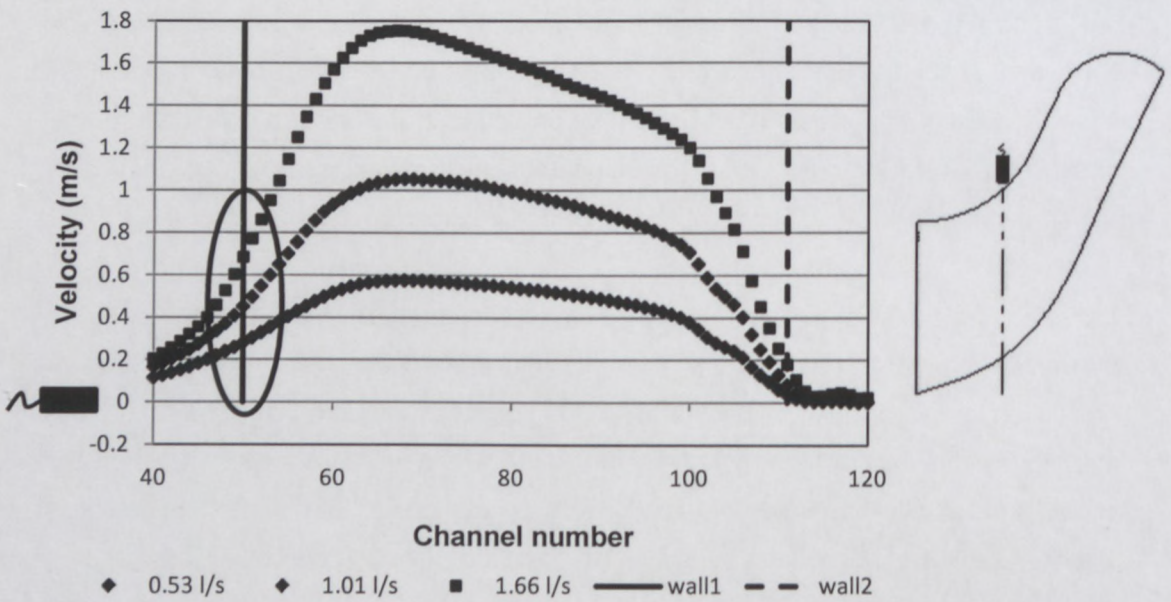

Figure 6.12: Lateral profiles measured using standard transducers in valve for CMC 6% w/w

Velocity profiles measured (shown in Figures 6.13 – 6.14) across the diagonal position (TDX Line 3) show an increase of velocity from the near wall and steady decrease from the centre area of the valve for both transducers (see Figures 6.13 - 6.14). Although not exactly the same flow conditions were obtained for both transducer installation setups, the shape and magnitude of velocity profiles measured using the delay line transducer (Figure 6.13) was significantly different than that obtained using the

standard transducer (Figure 6.14). For this particular measurement line (TDX Line 3) and more or less the same flow rate, the delay line transducer measured higher magnitude of velocities than when compared to that measured using the standard transducer. This could be due to the difference in Doppler angles (angle between fluid flow and ultrasonic beam), which can result in large variations of velocity magnitudes (see Figure 6.10).

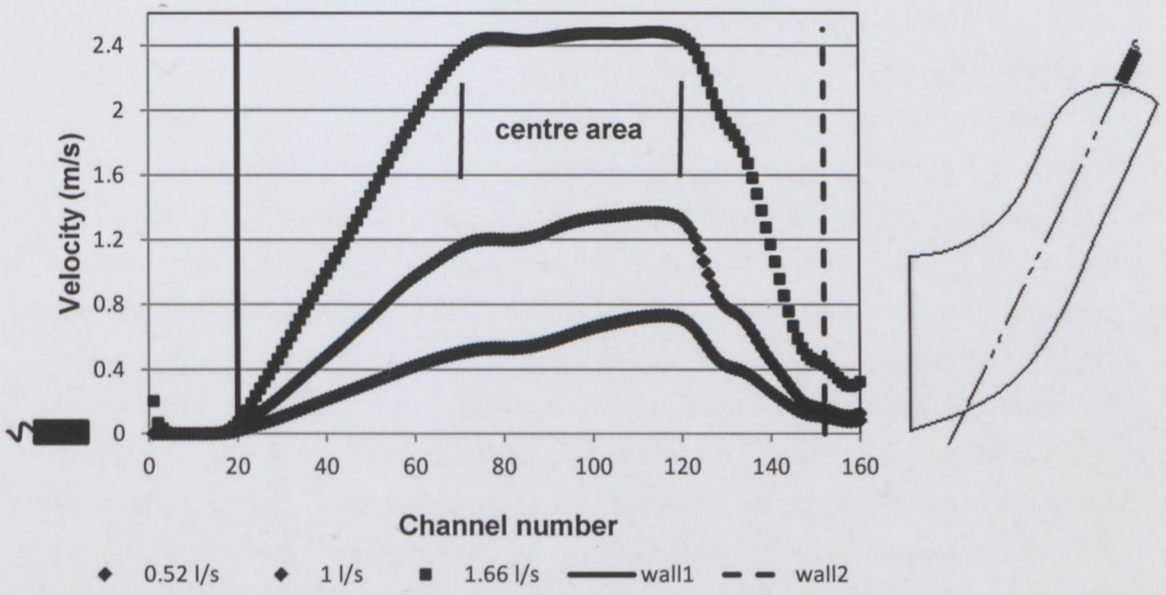

Figure 6.13: Diagonal profiles measured using delay line transducers in valve for CMC 6% w/w

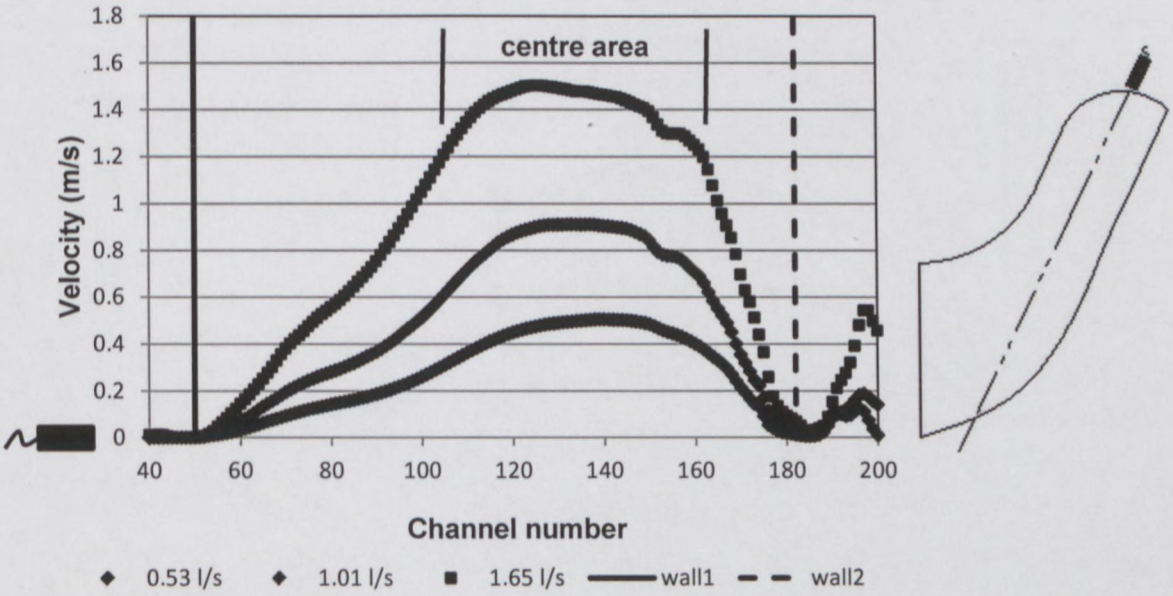

Figure 6.14: Diagonal profiles measured using standard transducers in valve for CMC 6% w/w

It has been shown that the ultrasonic beam generated by the delay line transducer is refracted due to the delay line material and curvature (Section 5.2.2, Chapter 5). Also, in this case the stream lines across the valve centre geometry is unknown and thus even after correcting the Doppler angle parameter not the same velocities are obtained (than that obtained using standard transducers), as the physical stream lines inside the valve could be at different angles with respect to the ultrasonic beam generated by the two transducers. In this particular case and based on the results, the two measurement lines of the delay line and standard transducers were across positions inside the diaphragm valve where physical streamlines or fluid flow were not the same. Furthermore, although the delay line transducer yields good results close to wall interfaces, the beam refraction makes it extremely complicated to accurately determine measurement lines for validation of theoretical predictions, obtained e.g. from CFD models. In a straight pipe this makes no difference (or even for the open channel geometry), however, when measuring in highly complex geometries it is necessary to have an ultrasonic beam parallel to the transducer in order to simplify planning of measurement lines as well as transducer installation.

Results obtained from measurements across TDX Line 4 (Figures 6.15 – 6.16) are symmetrical around the centre position and was expected due to measuring across a symmetrical axis in the valve. However, the velocity gradients measured by the two transducers differed due to the standard transducers measuring actual flow before the wall interface position, shown by the circle in Figure 6.16.

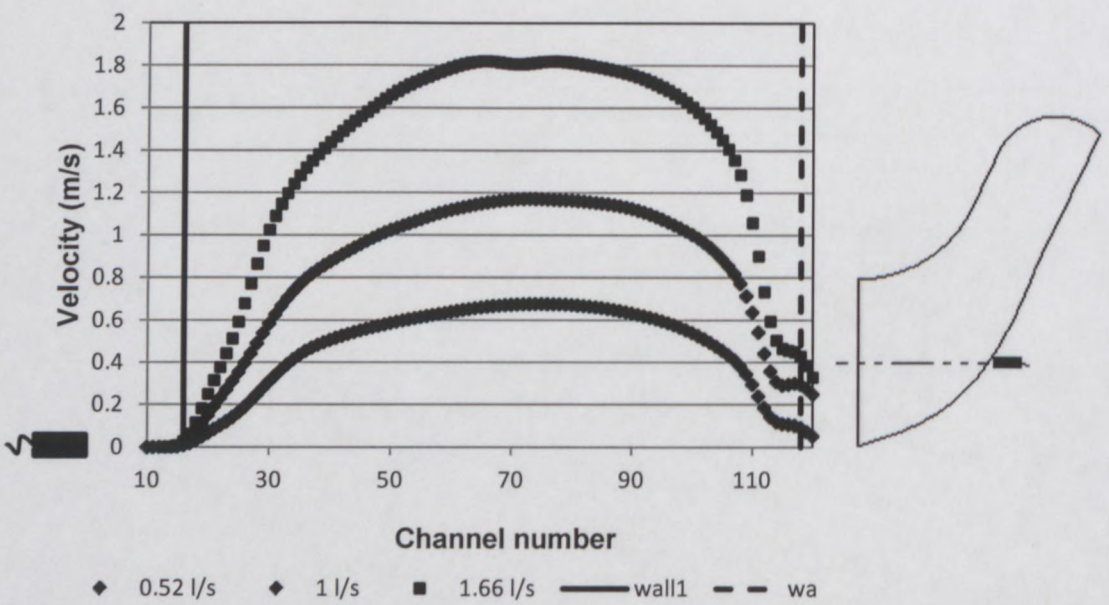

Figure 6.15: Radial profiles measured using delay line transducers in valve for CMC 6% w/w

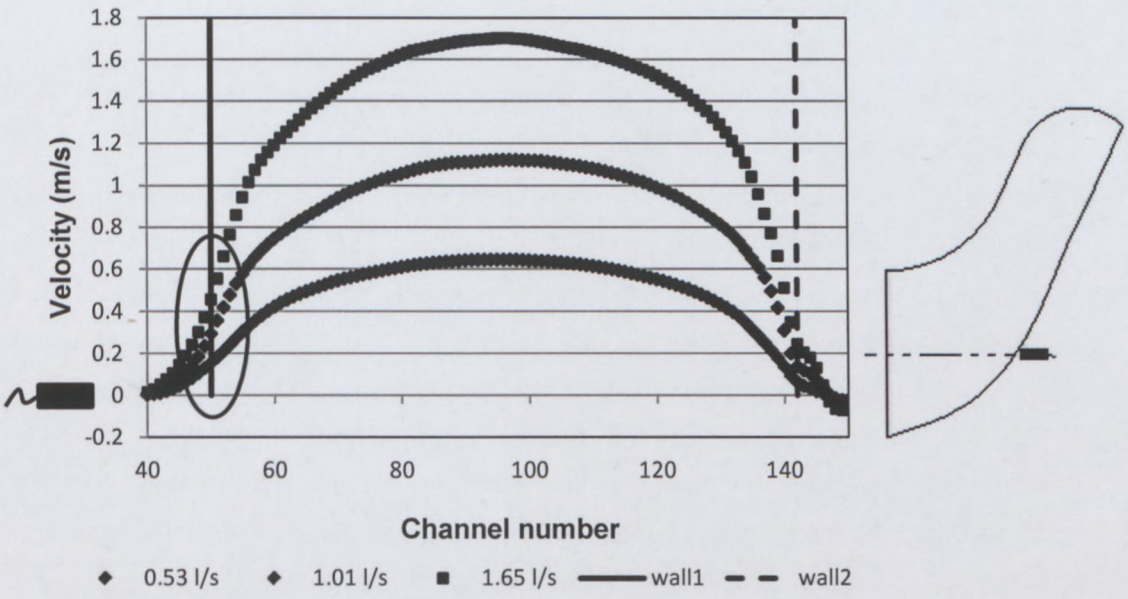

Figure 6.16: Radial profiles measured using standard transducers in valve for CMC 6% w/w

Good quantitative results were measured using the delay line transducer and velocity magnitudes were more or less the same after correcting the Doppler angle when comparing results obtained across TDX Line 4. At the opposite wall the velocity profile seems to lose its symmetry due to multiple reflections from the opposite valve material (Figure 6.15). This can be corrected for by installing an extra transducer at the opposite side of the measurement line in order to obtain accurate velocity data in both directions. This is discussed in more detail in Section 6.3.2. The most important observation that can be made from the presented results is the improvement of velocity data close to wall interfaces when analysing detailed flow behaviour in complex geometries. When actual flow occurs beyond the wall (such as with the cavity setups) the velocity gradients close to the walls are also distorted, which decreases the accuracy of the measured velocity profiles. Based on the results, the combination of using a delay line transducer and signal processing techniques has significant potential for verifying CFD models in highly complex geometries, such as valves or other pipe fittings.

6.3.2 Velocity distributions

Velocity distributions obtained from the combined velocity profile measurements and triangulation algorithm for both delay line and standard transducers are shown in Figures 6.17 – 6.18. Both distributions shown here were obtained from velocity profiles measured at 0.52 – 0.53 l/s. The positions of the transducers are also shown in both Figures 6.17 and 6.18. A 17.3% difference between the calculated (0.43 l/s) and measured (0.52 l/s) volume flow rate was determined from the results obtained using delay line transducers. Even when the extra transducer was added at the centre (see Section 3.3.7, Chapter 3), it still seems that more information is needed to completely determine the total flow throughout the valve centre area. Since the calculated flow rate was lower than the measured flow rate, it can be assumed that more flow information is required. This can also be seen by visual inspection in Figure 6.17, marked by the circles.

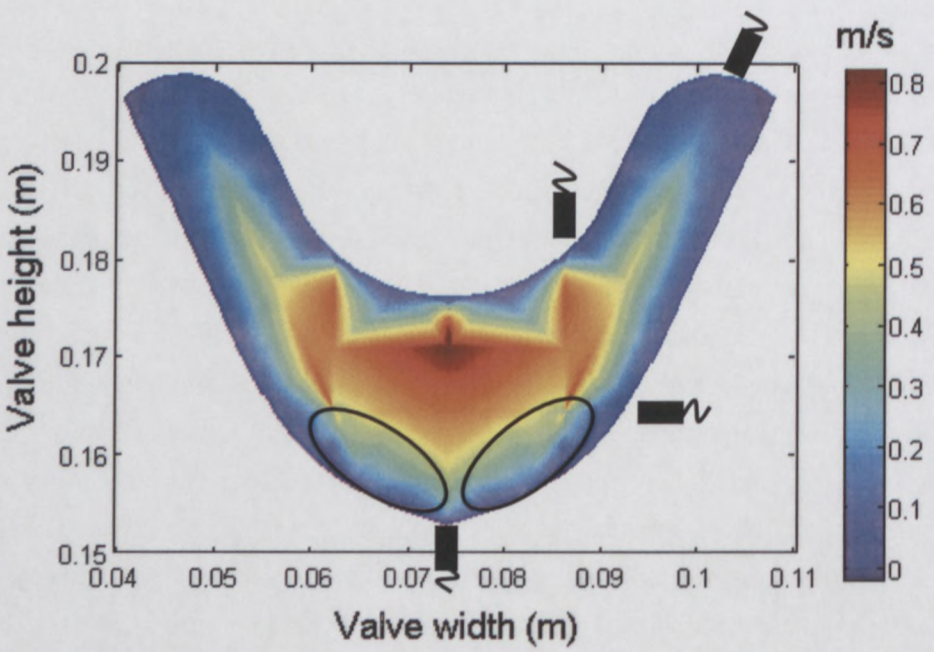

Figure 6.17: Velocity distribution of diaphragm valve centre (delay line transducers, Q = 0.52 l/s)

The flow map obtained using profiles measured with the standard transducers also show a similar qualitative result (same 'missing' flow information, see Figure 6.18 circles). However, quantitatively the error difference between the calculated (0.38) and measured (0.53 l/s) flow rate was 28.4%. This larger error difference could be mainly due to the lower magnitudes of velocity measured in the valve's upper 'ears', as shown

in Figure 6.14. Since the result obtained using delay line transducers has less error difference between the calculated and measured value, it is assumed that it is more accurate than that obtained from standard transducers.

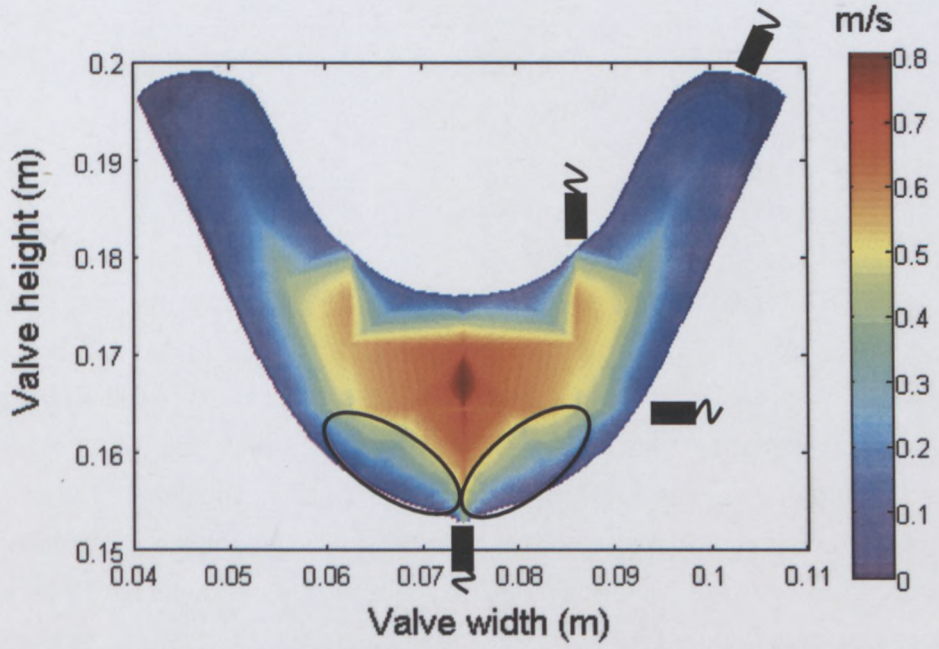

Figure 6.18: Velocity distribution of diaphragm valve centre (standard transducers, Q = 0.53 l/s)

The same observations can be made from the flow maps in Figures 6.17 and 6.18. The majority of the flow seems to be at the centre area of the valve and not at the upper regions. Also, the highest measured magnitudes of velocity appear to be just below the valve diaphragm. Similar results were obtained at different flow rates for both standard and delay line transducers. A comparison of different flow rates obtained by integration of velocity distributions with that measured using the electromagnetic flow meter are shown in Table 6.7 (delay line transducers) and Table 6.8 (standard transducers). For these tests it was assumed that the flow meter results were correct (see Section 3.3).

Table 6.7: Percentage difference between volume flow rates obtained from flow meter and calculation using the velocity distribution of the diaphragm valve for delay line transducers

Reference flow meter (l/s)	Integration of velocity distribution (l/s)	Integration vs. flow meter (%)
0.52	0.43	17.3
0.73	0.6	17.9
1.0	0.82	17.6
1.35	1.12	17.04
1.66	1.35	18.7

Table 6.8: Percentage difference between volume flow rates obtained from flow meter and calculation using the velocity distribution of the diaphragm valve for standard transducers

Reference flow meter (l/s)	Integration of velocity distribution (l/s)	Integration vs. flow meter (%)
0.53	0.38	28.4
0.73	0.5	31.1
1.01	0.68	32.3
1.33	0.89	32.8
1.65	1.12	32.4

From Table 6.8 it can be observed that by increasing flow rates, the error difference percentage between the valve (using UVP) and flow meter (calibrated with weigh tank, see Section 3.4.2) results increased slightly. This was due to more significant distortion of velocity profiles at the wall interfaces as much higher velocities were present with increasing flow rates. Table 6.7 shows more or less a constant error difference percentage, which can be expected due to know significant change in flow conditions with increasing flow rate (when using delay line transducers). Figure 6.19 shows the previous flow map (Figure 6.18), but with added suggestions for transducer positioning and measurement lines in order to increase the accuracy of the bulk flow rate calculation.

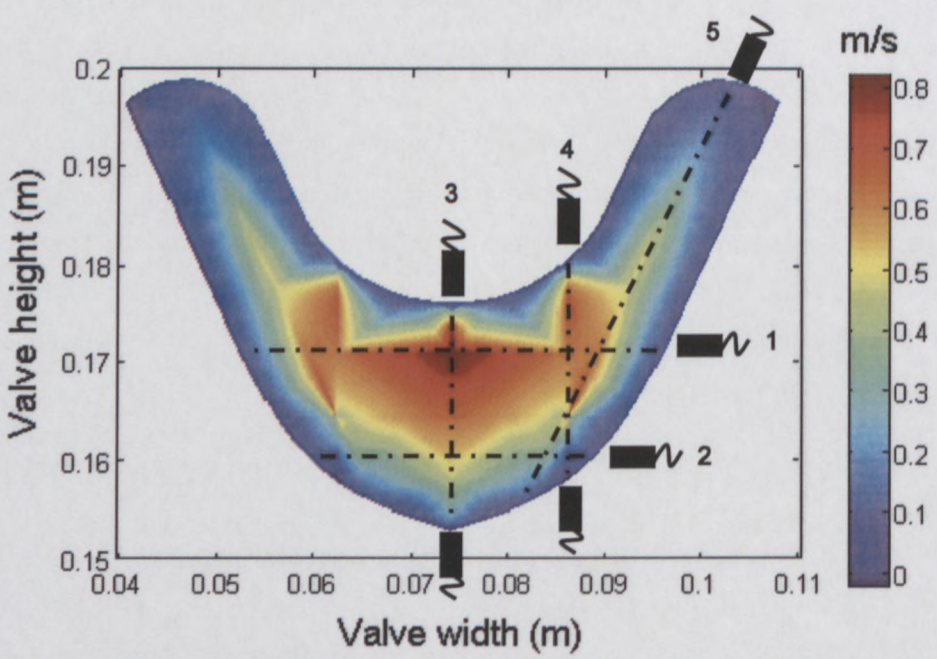

Figure 6.19: New measurement line suggestions for UVP inside diaphragm valve

When measuring across a symmetrical axis inside a particular geometry, only half of the measured profile is needed, as in the case of the radial measurement lines (shown by transducers 1 - 2 in Figure 6.19). Here the effect of multiple ultrasonic reflections is not important as the first half of the experimental profile is assumed to be similar at both sides from the centre position or maximum velocity for a power-law fluid (dotted lines). However, if velocity profiles in complex or asymmetrical geometries are measured, it is essential to acquire accurate velocity data at both wall interfaces, where the velocity gradients are high. One method to compensate for multiple wall reflections is to install another transducer at the opposite wall, thus measuring from both sides (shown by transducers 3 - 4). The extra transducer across the radial measurement line (transducer 2, Figure 6.19) could add the necessary information in order to completely obtain the flow map across the valve centre geometry.

Lastly, it must be stressed again that when measuring non-Newtonian, unknown flows inside complex geometries, the estimation of the wall interface positions are crucial for accurately characterising the flow behaviour. When measuring in fluids exhibiting plug flow, this becomes even more complicated. The delay line transducers reduce this problem by having a fixed and known wall position (after implementing the deconvolution procedure).

6.4 IN-LINE RHEOLOGY USING UVP-PD

This section compares results obtained using the optimised (delay line transducer and deconvolution procedure, presented in Section 5.4, Chapter 5) as well as standard UVP-PD methodology. As before (Section 6.1 – 6.3), all velocity profiles measured using the delay line transducers have been corrected for by implementing the deconvolution procedure. Results are compared to that obtained from conventional rheometric methods, in-line tube viscometry and off-line rotational rheometry. Three UVP-PD flow loops of different diameters (16, 22.5 and 52.8 mm) were constructed for comparison and to test system limitations. The tests were conducted with different concentrations of bentonite and kaolin suspensions as well as CMC (carboxymethyl cellulose) solutions. This yielded a wide range of rheological parameters. This work was conducted at the Material Science and Technology (MST) group at the Cape Peninsula University of Technology (CPUT) in Cape Town.

6.4.1 UVP-PD measurements in 16 mm pipe

6.4.1.1 Comparison of different rheometric methods for CMC 7% w/w

Figure 6.20 and 6.21 compares the experimental data measured using the delay line and standard transducer with a theoretical velocity profile (Equation 2.28) determined from a least-squares fit. The measurements were conducted in CMC 7% w/w at a flow rate of Q = 0.151 *l/s* (Re_2 = 202). Note that in order to calculate rheological parameters all velocity profiles were measured in laminar flow. The wall positions of the power-law profiles measured using standard transducers were calculated by using the maximum velocity as the centre position and subtracting the pipe radius. This method was used for all pipe diameters. Fixed wall positions were used for velocity profiles measured using delay line transducers. By fitting a theoretical velocity profile onto experimental data the parameters K, n and τ_y are solved. A flow curve is constructed and compared to rheological data obtained from tube and rotary viscometry. In this work UVP-PD1 refers to the method where a standard transducer was used and UVP-PD2 to the combined deconvolution and delay line transducer methodology.

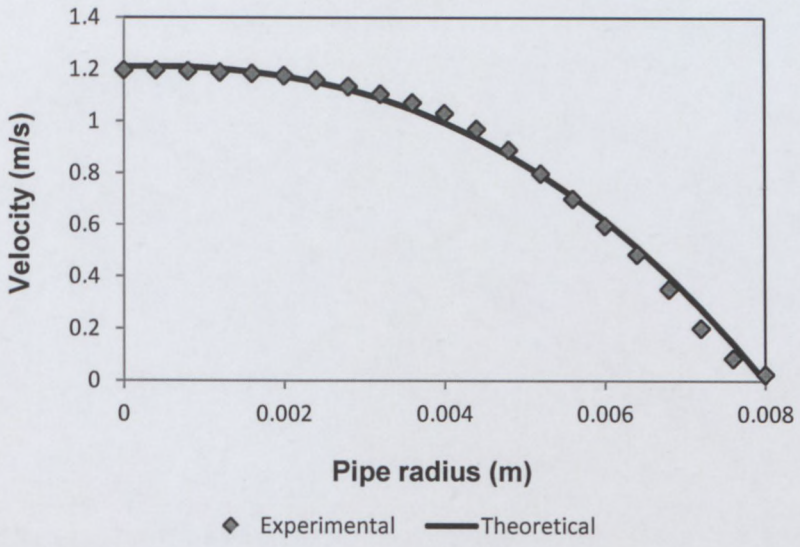

Figure 6.20: Experimental and fitted theoretical velocity profile for delay line transducer (16 mm pipe, CMC 7% w/w)

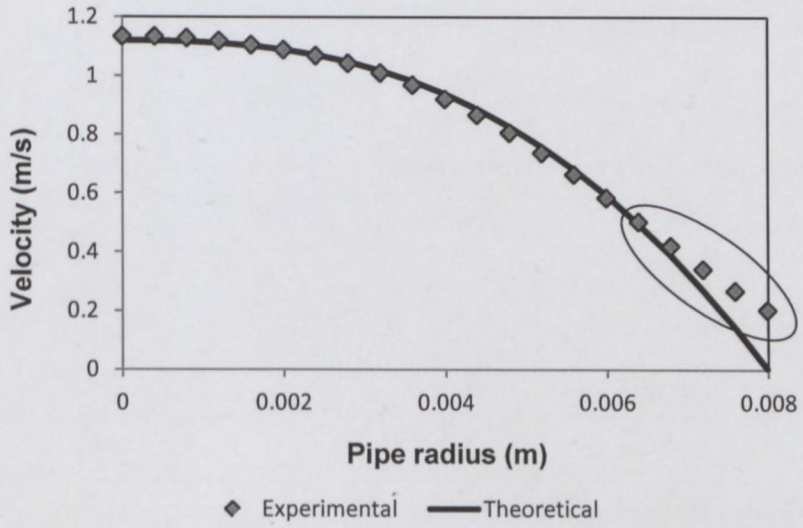

Figure 6.21: Experimental and fitted theoretical velocity profile for standard transducer (16 mm pipe, CMC 7% w/w)

Rheological results are schematically illustrated in Figure 6.22 and the parameters determined from a power-law fit (Equation 2.27) are shown in Table 6.9. It can be observed that non-zero velocities were measured (shown by circle in Figure 6.21) using the standard transducer due to the cavity setup. However, this did not affect the outcome of the final result, as shown by the striped line in Figure 6.22.

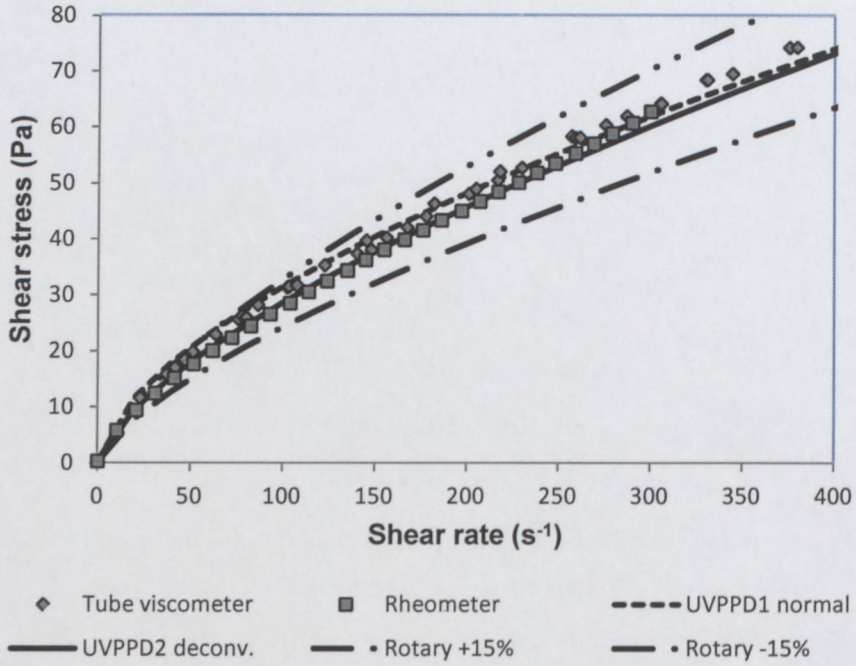

Figure 6.22: Rheogram for CMC 7% w/w (16 mm pipe)

Table 6.9: Rheological parameters measured in 16 mm pipe for CMC 7% w/w

Rheometric method	K (Pa.s)	n -	τ_y (Pa)	R^2
UVPPD1 normal	1.84	0.62	0	0.967
UVP-PD2 deconv.	1.27	0.68	0	0.994
Tube viscometry	1.43	0.67	0	0.999
Rotary viscometry	1.24	0.68	0	0.999

Good agreement of +- 15% was found between all the rheometric methods. According to Table 6.9, the goodness-of-fit was very good for all the power-law curve fittings, except for the UVP-PD1 results, where the cavity affected the fitting of the velocity profile.

6.4.1.2 Comparison of different rheometric methods for bentonite 6.9% w/w

An experimental (delay line) and theoretical velocity profile for bentonite 6.9% w/w is compared in Figure 6.23. Results for the normal transducer and direct fluid contact configuration are displayed in Figure 6.24. Tests were conducted at a flow rate of Q = 0.4 l/s (Re_2 = 1800). Bentonite suspensions showed little attenuation and absorption of ultrasonic energy and thus the acoustic energy could penetrate across the whole pipe diameter. Generally a good echo signal was obtained for all concentrations of bentonite.

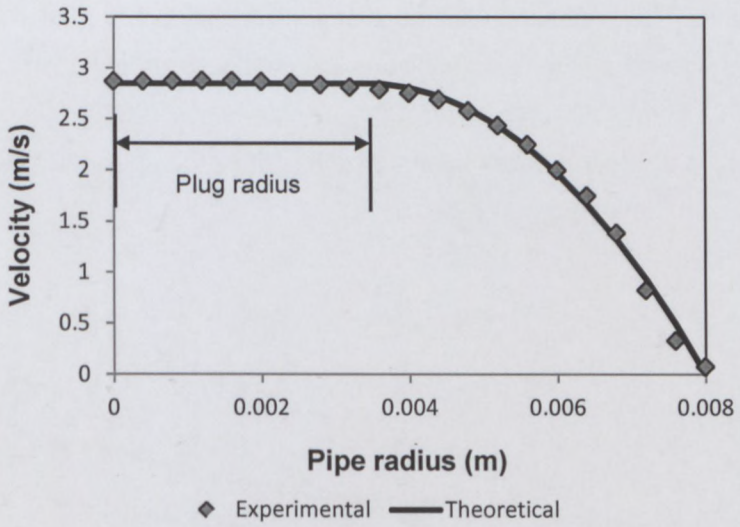

Figure 6.23: Experimental and fitted theoretical velocity profile for delay line transducer (16 mm pipe, bentonite 6.9% w/w)

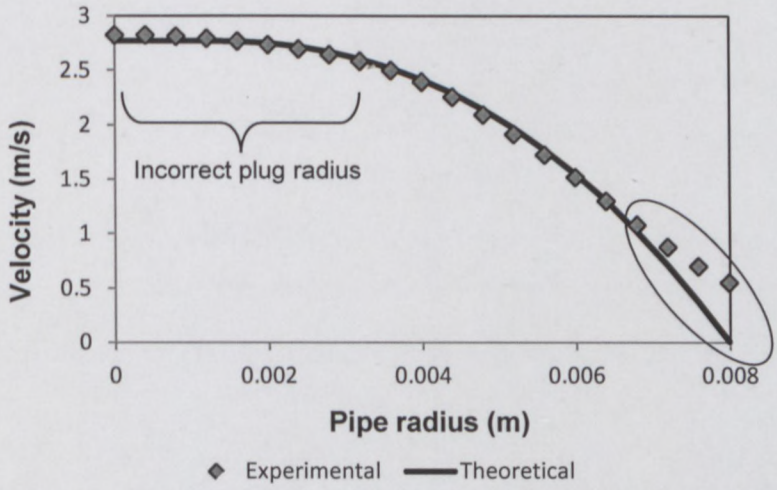

Figure 6.24: Experimental and fitted theoretical velocity profile for standard transducer (16 mm pipe, bentonite 6.9% w/w)

The cavity in front of the standard ultrasonic transducer influences the quality of the measured velocity profile close to the wall interface (shown by circle in Figure 6.24). Also, the gradient of the velocity profile (Figure 6.24) was severely distorted due to the combination of the plug flow present for bentonite suspensions (characterised by Bingham model) and large cavity to pipe diameter ratio (see Section 5.5, Chapter 5). As a result an erroneous plug radius was obtained, which consequently affects the profile fitting and determination of rheological parameters. Non-zero velocities at the wall interface are forced to zero in order to optimise the fitting procedure for calculating rheological parameters. This unfortunately does not improve the overall accuracy of the fit. Furthermore, since there are non-zero velocities at the pipe wall it becomes extremely difficult to estimate wall positions. A significant variation in rheological parameters is observed when wall positions are changed by only one channel distance (less than 0.35 mm) (Wiklund *et al.,* 2007; Kotzé *et al.,* 2008). Calculation of wall positions from plug flow profiles becomes even more complicated due to maximum velocities present, beyond the pipe radius.

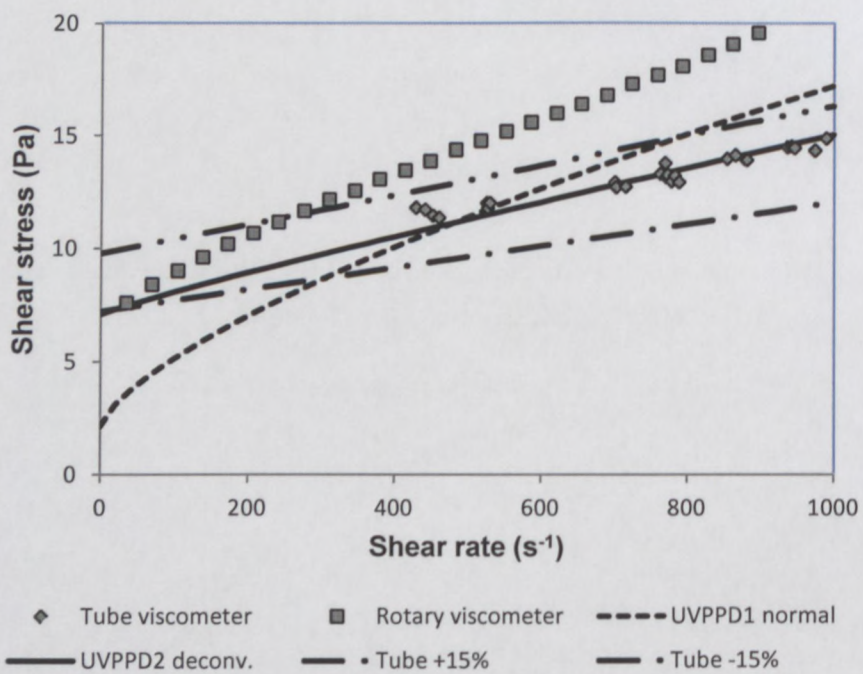

Figure 6.25: Rheogram for bentonite 6.9% w/w (16 mm pipe)

From Figure 6.25 it can be observed that results obtained from tube viscometry and UVP-PD2 are in good agreement (within 15%) with each other across the relevant

shear rate region (400 to 1000 s^{-1}). However, the flow curve obtained from UVP-PD1 suggests a yield pseudoplastic fluid with a low yield stress. When compared to tube and viscometer data this is clearly not the case. The flow curve obtained from the rotary viscometer showed higher apparent viscosities. This could have been due to the time dependant properties of the bentonite suspensions. Although samples were pre-sheared before measuring flow curves, this did not always yield good comparative results. However, other off-line bentonite results showed good comparison (as shown in Sections 6.5.5 – 6.5.6) when tested shortly after in-line experimental measurements. This also illustrates the importance of determining rheological properties in-line during process conditions, as the rheological properties of fluid samples may change with time.

Table 6.10: Rheological parameters measured in 16 mm pipe for bentonite 6.9% w/w

Rheometric method	K (Pa.s)	n -	τ_y (Pa)	R^2
UVP-PD1 normal	0.12	0.71	2.13	0.961
UVP-PD2 deconv.	0.0147	0.91	7.11	0.995
Tube viscometry	0.0057	1	9.01	0.987
Rotary viscometry	0.0133	1	7.81	0.997

An important observation is the yield stress measurements using UVP-PD1 (see Table 6.10). The yield stress is calculated from direct measurements of the plug radius and pressure drop. Due to inaccurate velocity gradients at the pipe wall the plug radius is affected and thus the yield stress measurement. Also, when observing tube viscometry results it can be seen that data were not available at the lower shear rates. This was due to limitations in the pressure drop measurements and in this case the UVP-PD2 methodology was able to characterise the fluid accurately across the relevant shear rate range.

6.4.1.3 Comparison of different rheometric methods for kaolin 17% v/v

Figure 6.26 illustrates experimental and theoretical profiles measured using the delay line transducer for kaolin 17% v/v (Q = 0.2 *l/s*, Re_2 = 330). It was not possible to measure velocity profiles using the standard transducer as the kaolin suspension filled the cavity and absorbed all of the acoustic energy, as discussed in Section 5.4.3, Chapter 5. The theoretical fit showed good correlation with the experimental data, especially close to the wall, where the velocity gradient is high.

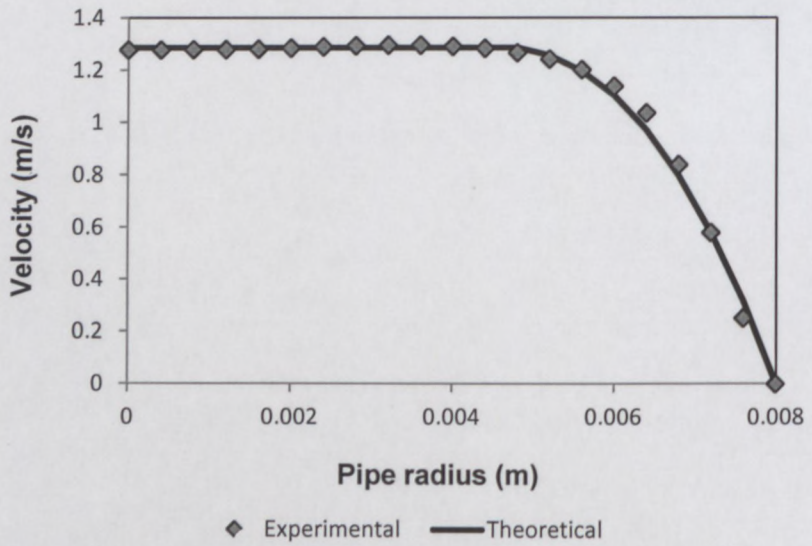

Figure 6.26: Experimental and fitted theoretical velocity profile for delay line transducer (16 mm pipe, kaolin 17% v/v)

Figure 6.27 shows the rheogram obtained from tube (in-line) and rotary (offline) viscometry, as well as using the UVP-PD2 methodology. Table 6.11 shows the rheological parameters determined from a Herschel-Bulkley model fit (see Section 2.3). There is good agreement (less than 15%) between the tube viscometer and UVP-PD2 results. Here the same limitations were found when using the tube viscometer as no apparent viscosities could be measured across the lower shear rate range (< 200 s^{-1}). The rotary viscometer could measure across lower shear rates and therefore showed more curvature (for shear rates lower than 200 s^{-1}) than when compared to the UVP-PD2 method. In this case the user could assume that the UVP-PD2 method is more correct, since the rheology was obtained in-line under true test conditions.

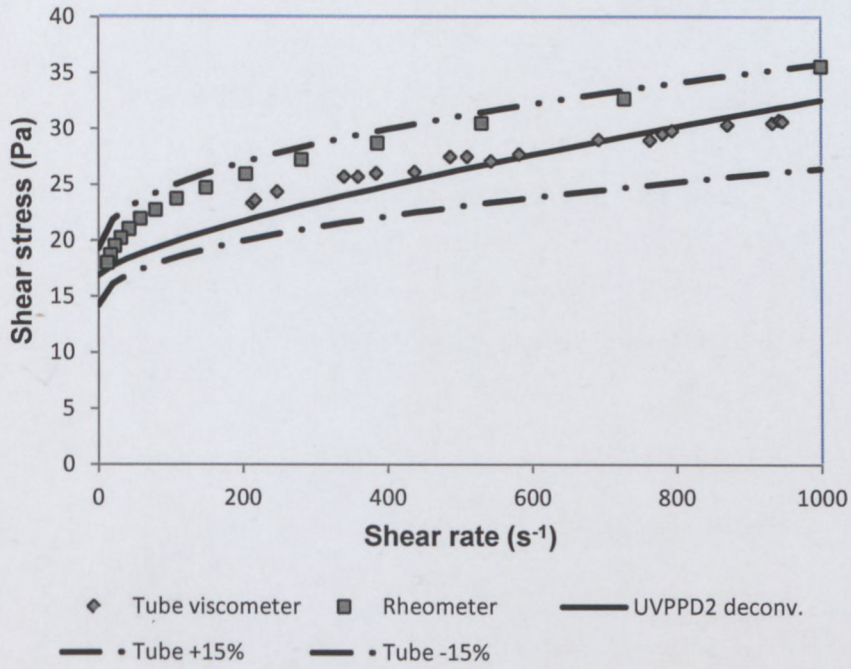

Figure 6.27: Rheogram for kaolin 17% v/v (16 mm pipe)

Table 6.11: Rheological parameters measured in 16 mm pipe for kaolin 17% v/v

Rheometric method	K (Pa.s)	n -	τ_y (Pa)	R^2
UVP-PD2 deconv.	0.096	0.74	16.9	0.988
Tube viscometry	0.54	0.48	16.77	0.998
Rotary viscometry	0.77	0.47	16.4	0.998

From the fitting procedure (using the Herschel-Bulkley model) it can be seen that the yield stress measurements were in very good agreement. It is therefore critical that the plug radius is measured correctly by achieving accurate velocity data at the wall interface in order for the in-line UVP-PD2 method to work.

6.4.2 UVP-PD measurements in 22.5 mm pipe

6.4.2.1 Comparison of different rheometric methods for CMC 6.8% w/w

An experimental (delay line) and theoretical velocity profile for CMC 6.8% w/w is compared in Figure 6.28. Results for the standard transducer and direct fluid contact configuration (see Section 3.2.3.3) are displayed in Figure 6.25. Tests were conducted at a flow rate of Q = 0.55 *l/s* and the calculated Reynolds number was Re_2 = 108.

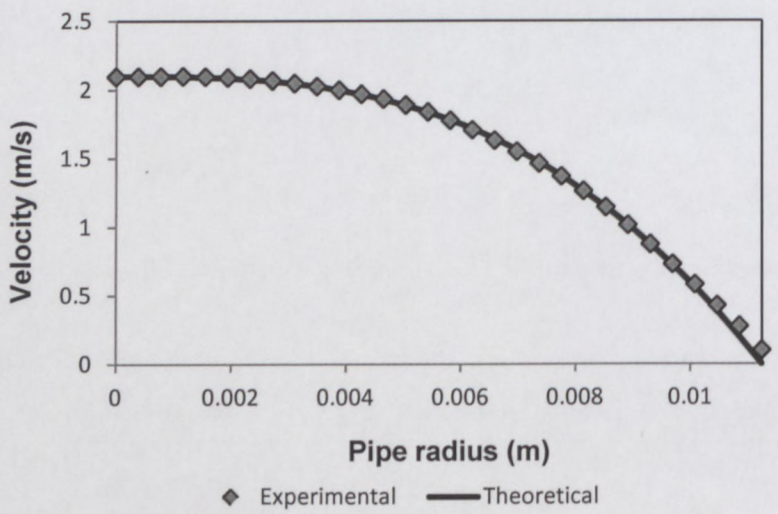

Figure 6.28: Experimental and fitted theoretical velocity profile for delay line transducer (22.5 mm pipe, CMC 6.8% w/w)

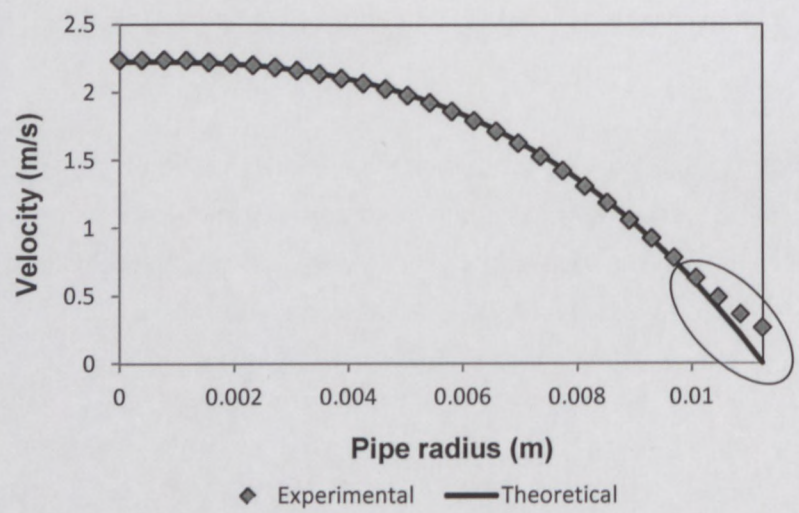

Figure 6.29: Experimental and fitted theoretical velocity profile for standard transducer (22.5 mm pipe, CMC 6.8% w/w)

Similar results as before were observed for the profile measured using the standard transducer (shown with circle in Figure 6.29). This did not affect the accuracy of the determined rheology of the CMC solution (power-law fluid). Based on the rheogram shown in Figure 6.30, very good agreement (15%) was found between all the different rheometric techniques, especially when comparing the in-line rheometric methods (tube viscometry and UVP-PD methods).

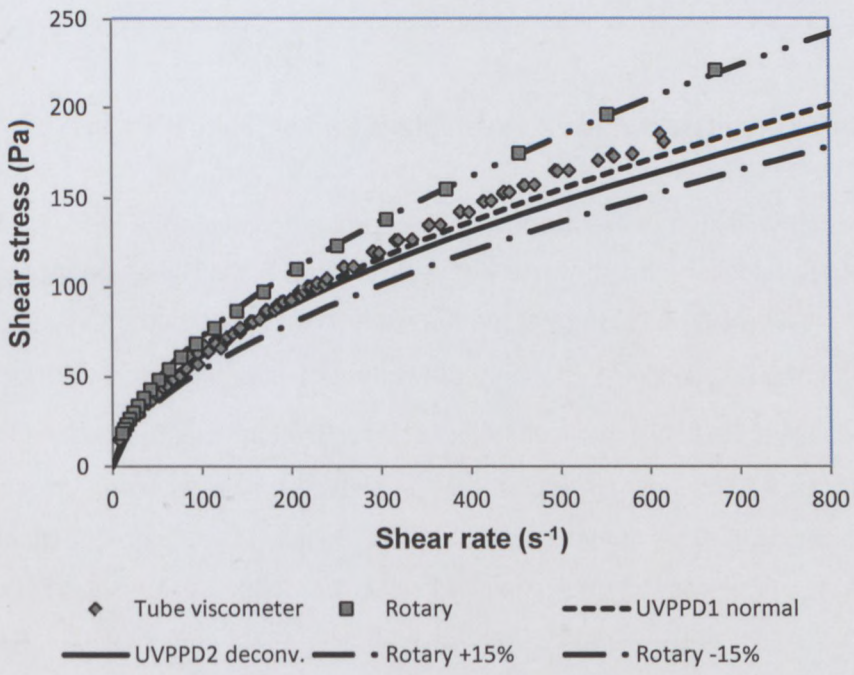

Figure 6.30: Rheogram for CMC 6.8% w/w (22.5 mm pipe)

Table 6.12 also show that the rheological parameters were calculated with confidence (using the power-law model, Equation 2.27), as the R^2 values were almost unity. The presented results inspire confidence in the UVP-PD methodology as accurate rheological parameters could be obtained in both 16 mm and 22.5 mm pipe diameters.

Table 6.12: Rheological parameters measured in 22.5 mm pipe for CMC 6.8% w/w

Rheometric method	K (Pa.s)	n -	τ_y (Pa)	R^2
UVP-PD1 normal	4.82	0.56	0	0.992
UVP-PD2 deconv.	5.22	0.54	0	0.998
Tube viscometry	4.44	0.58	0	0.997
Rotary viscometry	4.41	0.61	0	0.999

6.4.2.2 Comparison of different rheometric methods for bentonite 8% w/w

Experimental velocity profiles along the pipe radius for bentonite 8% w/w measured using both transducers are shown in Figures 6.31 and 6.32. These are represented by the theoretical profile obtained by fitting the experimental data and pressure drop using the Bingham plastic model (Equation 2.30) with the values of K and τ_y listed in Table 6.13. Recall that the flow behaviour index (n) for a Bingham plastic fluid is equal to one. The flow (Q = 1 l/s) is laminar, since the value of the Reynolds number (Re_2) is equal to 1764, validating the use of the theoretical point velocity distribution equations. Similar distortion of the velocity profile measured using the standard transducer were found (Figure 6.32). The velocity gradient was also affected due to the influence of the cavity between the wall and transducer surface, as shown in Figure 6.32.

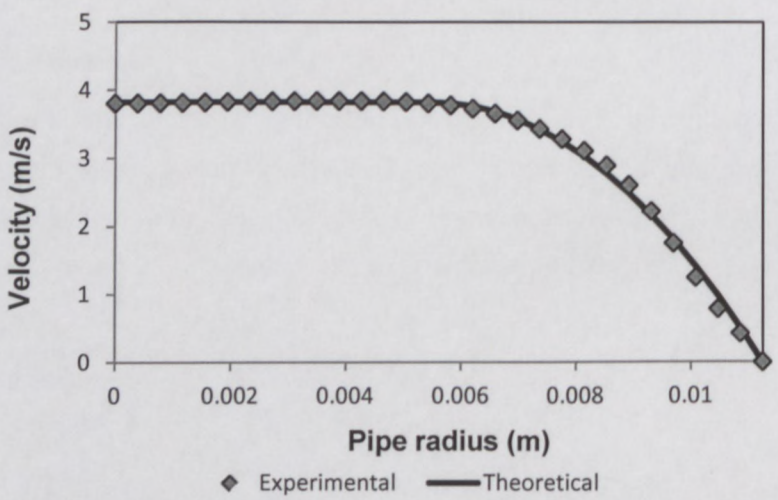

Figure 6.31: Experimental and fitted theoretical velocity profile for delay line transducer (22.5 mm pipe, bentonite 8% w/w)

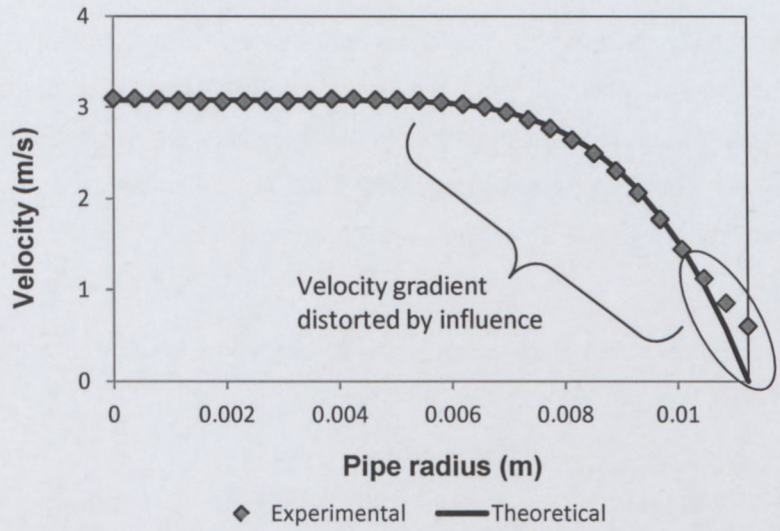

Figure 6.32: Experimental and fitted theoretical velocity profile for standard transducer (22.5 mm pipe, bentonite 8% w/w)

The shape of the velocity profile is critical when determining rheological parameters and this distortion thus influences the accuracy. The result of this can be observed in Figure 6.33. Apparent viscosities along the UVP-PD1 flow curve seems to agree at the higher shear rate range. However in the lower shear rate range a significant difference can be seen. The UVP-PD1 result suggests a yield pseudoplastic fluid (as before) which does not correlate with rheometic data obtained from conventional methods. The flow curve obtained using UVP-PD2 methodology shows a much better agreement with both conventional rheometric methods across the entire shear rate region.

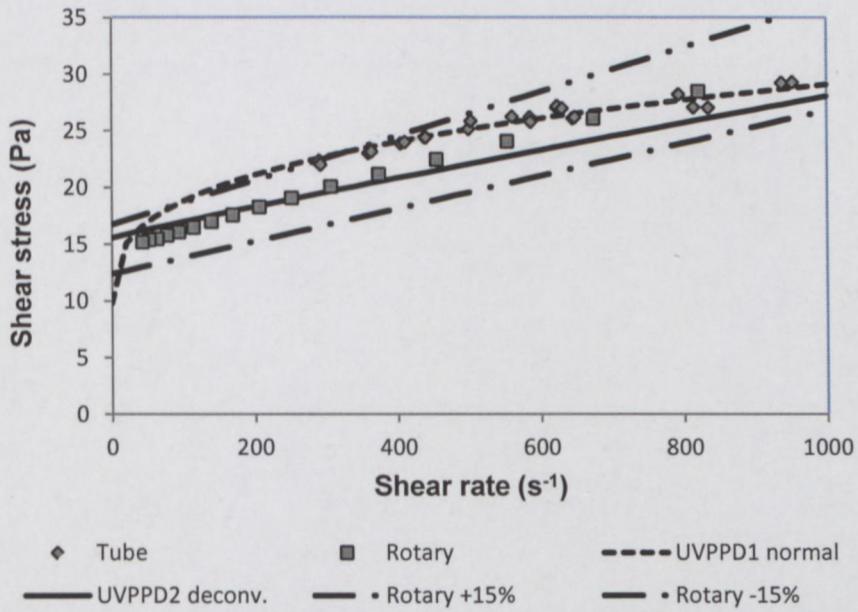

Figure 6.33: Rheogram for bentonite 8% w/w (22.5 mm pipe)

The mathematically determined rheological parameters are depicted in Table 6.13. When comparing conventional rotary viscometry and the UVP-PD2 method, the fluid consistency coefficients and estimated yield stress values are in good agreement with one another. As before apparent viscosities could not be measure at low shear rate ranges due to limitations in the pressure measurements.

Table 6.13: Rheological parameters measured in 22.5 mm pipe for bentonite 8% w/w

Rheometric method	K (Pa.s)	n -	τ_y (Pa)	R^2
UVP-PD1 normal	1.95	0.33	9.84	0.986
UVP-PD2 deconv.	0.019	0.94	15.58	0.997
Tube viscometry	0.0097	1	20.1	0.947
Rotary viscometry	0.017	1	14.59	0.999

6.4.2.3 Comparison of different rheometric methods for kaolin 13% v/v

Figure 6.34 shows a velocity profile measured using the delay line transducer in kaolin 13% v/v at a flow rate of 0.52 l/s (Re_2 = 1521). It was not possible to conduct measurements in kaolin suspensions with the standard transducers (explained in Section 6.4.2).

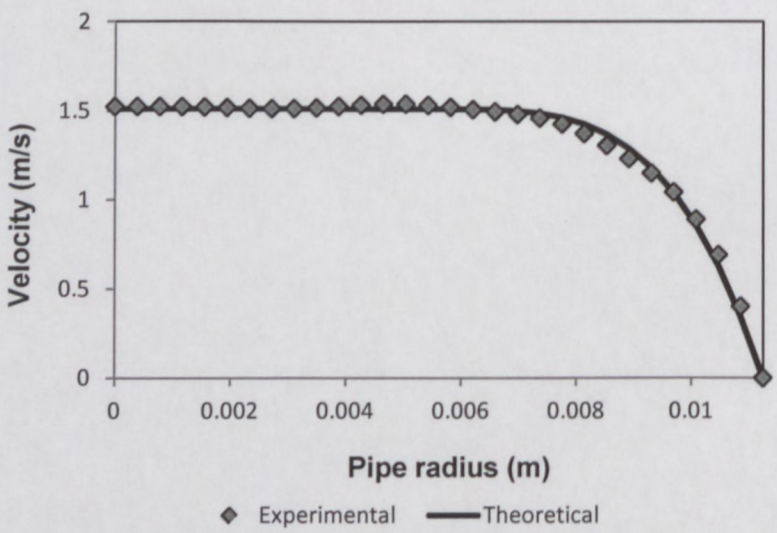

Figure 6.34: Experimental and fitted theoretical velocity profile for delay line transducer (22.5 mm pipe, kaolin 13% v/v)

Figure 6.35 show the summary of rheological results obtained from off-line rheometry, tube viscometry and the UVP-PD1 rheometric method. Experimental data obtained from the tube viscometer and off-line rheometer agree well with that determined by the in-line UVP-PD rheometric method. The error curves illustrate a deviation of +/- 15% from the flow curve determined by the in-line tube viscometry. It can be seen that flow curves obtained from the two in-line methods (UVP-PD method and tube viscometry) show good agreement (less than 10%) when compared with one another across the higher shear rate range (200 s^{-1} – 500 s^{-1}).

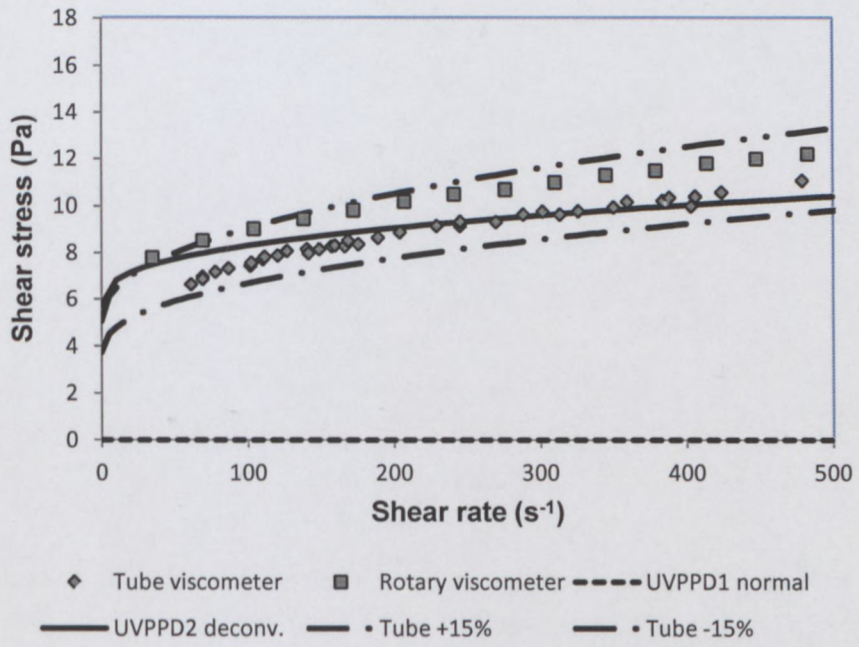

Figure 6.35: Rheogram for kaolin 13% v/v (22.5 mm pipe)

Table 6.14 depicts the rheological parameters used to fit the Herschel-Bulkley model with experimental data. The estimated yield stress values show good agreement when results from all three methods are compared.

Table 6.14: Rheological parameters measured in 22.5 mm pipe for kaolin 13% v/v

Rheometric method	K (Pa.s)	n -	τ_y (Pa)	R^2
UVP-PD2 deconv.	0.48	0.37	5.73	0.966
Tube viscometry	0.41	0.46	4.1	0.995
Rotary viscometry	0.61	0.42	4.5	0.995

6.4.3 UVP-PD measurements in 52.8 mm pipe

6.4.3.1 Comparison of different rheometric methods for CMC 6.15% w/w

Figure 6.36 and 6.37 compares the experimental data measured using the delay line and standard transducer with a theoretical velocity profile (Equation 2.28) determined from a least-squares fit. The measurements were conducted in CMC 6.15% w/w at a flow rate of Q = 2.02 *l/s* (Re_2 = 1440).

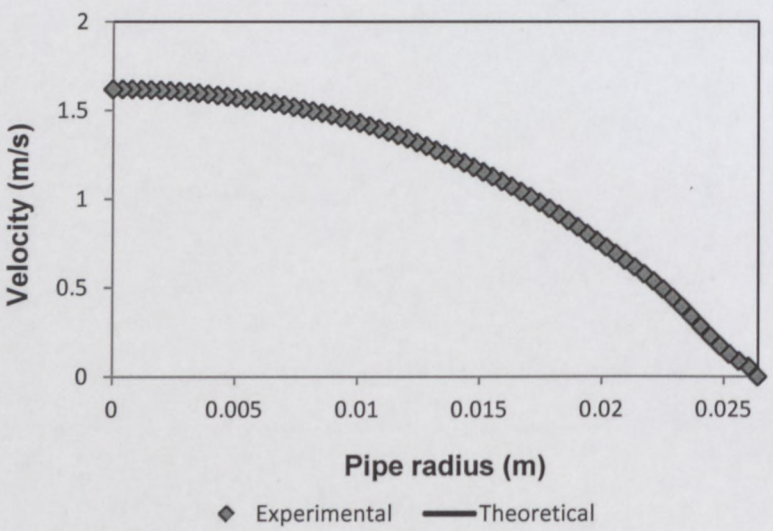

Figure 6.36: Experimental and fitted theoretical velocity profile for delay line transducer (52.8 mm pipe, CMC 6.15% w/w)

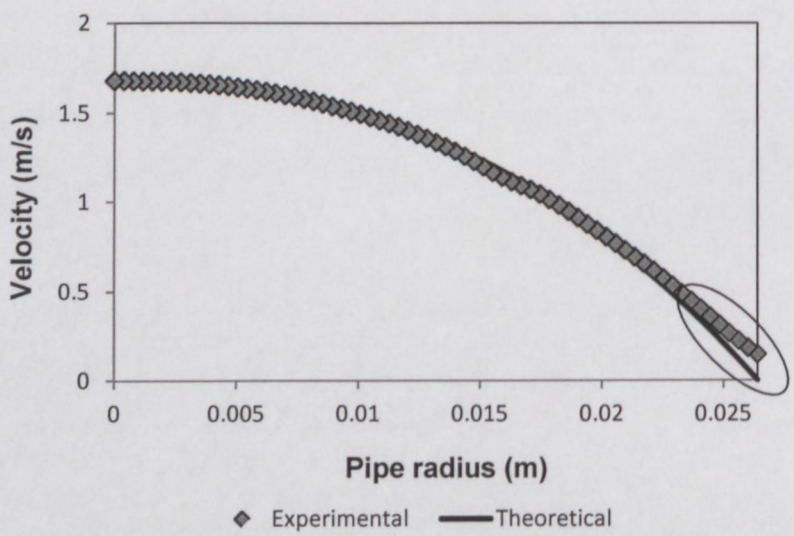

Figure 6.37: Experimental and fitted theoretical velocity profile for standard transducer (52.8 mm pipe, CMC 6.15% w/w)

Similar results (as in Sections 6.4.1 and 6.4.2) were found for the CMC solution in the larger diameter pipe (52.8 mm). The influence of the cavity (shown by circle in Figure 6.37) did not affect the accuracy of rheological parameters, which are illustrated in Figure 6.38 and shown in Table 6.15. All the results are within 15% with the tube viscometer across the entire shear rate range.

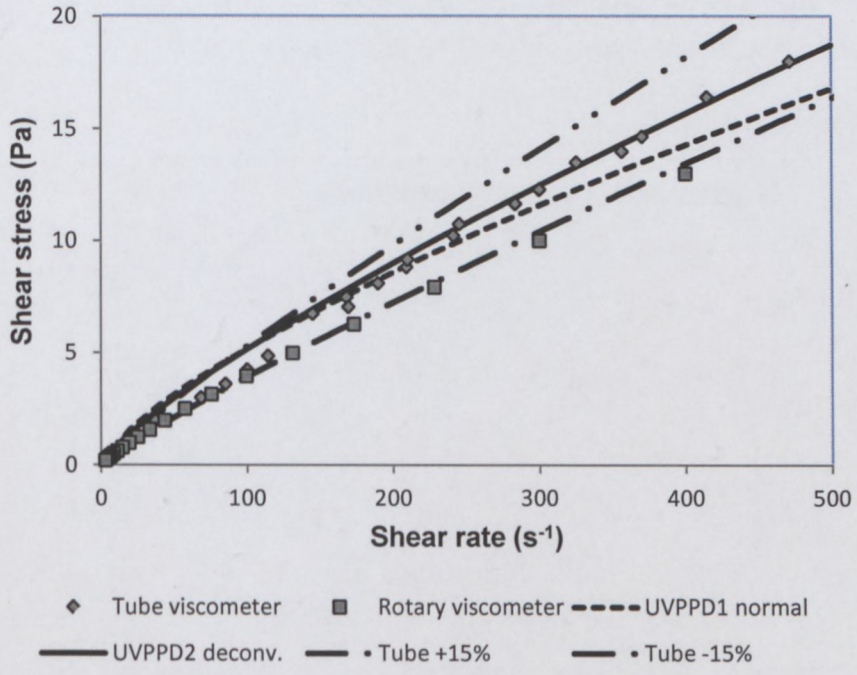

Figure 6.38: Rheogram for CMC 6.15% w/w (52.8 mm pipe)

Table 6.15: Rheological parameters measured in 52.8 mm pipe for CMC 6.15% w/w

Rheometric method	K (Pa.s)	n -	τ_y (Pa)	R^2
UVP-PD1 normal	0.18	0.73	0	0.994
UVP-PD2 deconv.	0.13	0.8	0	0.999
Tube viscometry	0.077	0.89	0	0.996
Rotary viscometry	0.086	0.83	0	0.999

6.4.3.2 Comparison of different rheometric methods for bentonite 8% w/w

As explained before (Sections 6.4.1 – 6.4.2), the cavity influences the quality of the measured velocity profile and thus it becomes difficult to fit theoretical velocity profiles (Equation 2.30) to experimental data without error. An experimental (delay line) and theoretical velocity profile for bentonite 8% w/w (similar fluid used for 22.5 mm pipe tests, see Section 6.4.2) is compared in Figure 6.39. Results obtained using the standard transducer and direct fluid contact configuration is displayed in Figure 6.40. Tests were conducted at a flow rate of Q = 3.25 *l/s* (Re_2 = 1001).

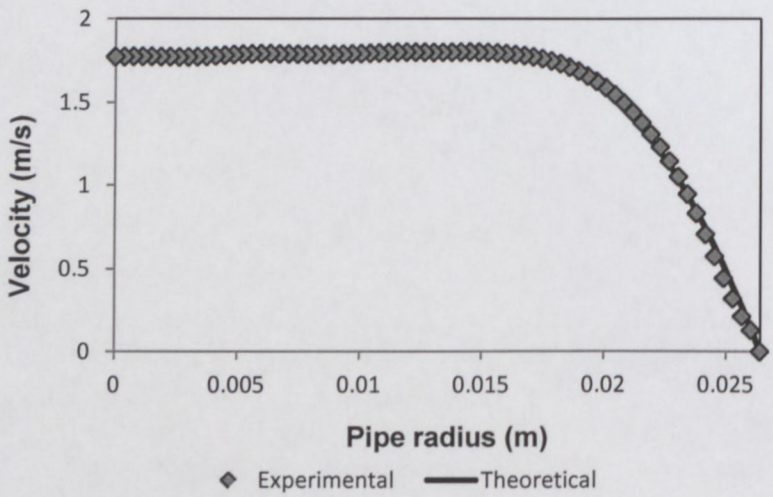

Figure 6.39: Experimental and fitted theoretical velocity profile for delay line transducer (52.8 mm pipe, bentonite 8% w/w)

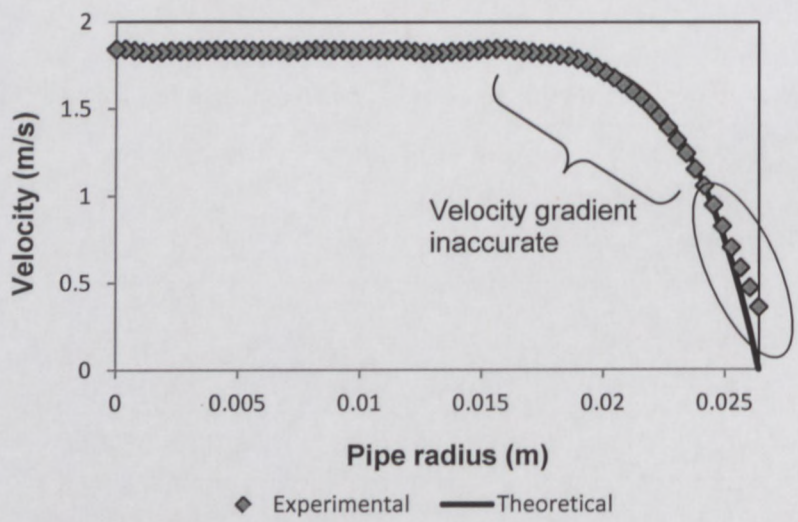

Figure 6.40: Experimental and fitted theoretical velocity profile for standard transducer (52.8 mm pipe, bentonite 8% w/w)

Figure 6.41 and Table 6.16 summarises the rheological results and parameters obtained from conventional rheometric methods and using the two UVP-PD methodologies. Again good agreement was found when comparing the UVP-PD2 method (delay line and deconvolution combination). The results obtained using the standard transducer configuration (UVP-PD1) show a yield-pseudoplastic model with a low yield stress, as previously found for results obtained in 16 and 22.5 mm diameter pipes (bentonite suspensions). It should be, however, mentioned again here that accurate rheological parameters could be obtained from the UVP-PD1 method by using different wall positions, i.e. by shifting the profile so that a larger plug radius can be obtained. Even a margin of 0.5 mm results in similar results as found with the UVP-PD2 method. In this case the user need to have knowledge of the rheology of the fluid beforehand in order to see what wall position is correct (recall that initially the wall positions for standard transducers were calculated from profiles measured in CMC solutions and kept fixed, see Section 6.4.1). By using the delay line transducers no knowledge of the fluid properties are required a priori as fixed wall interface positions are used, no matter what fluid is under investigation.

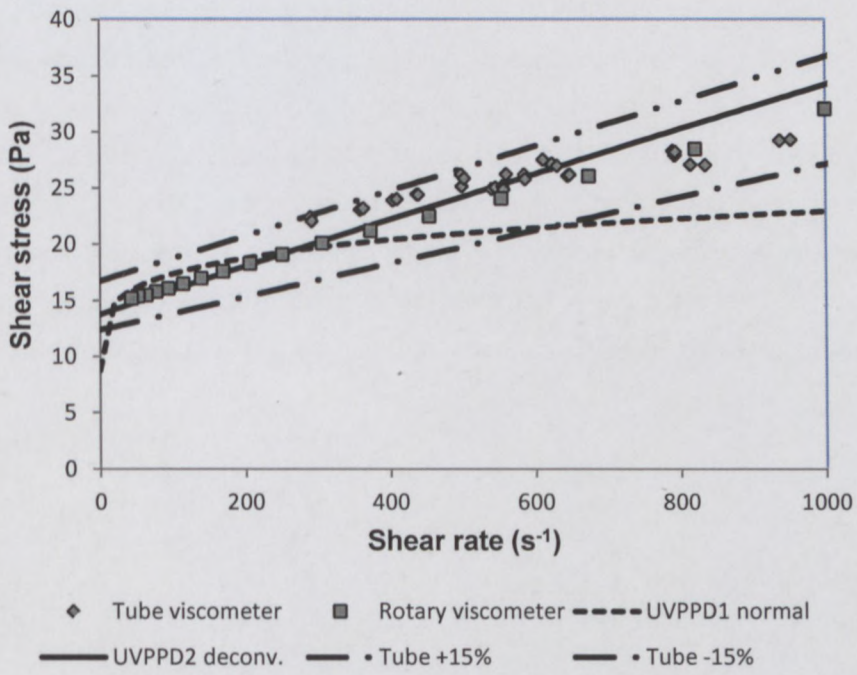

Figure 6.41: Rheogram for bentonite 8% w/w (52.8 mm pipe)

Good correlation was found between the yield stress measurements obtained from the UVP-PD2 method and off-line rheometry (see Table 6.16). The yield stress obtained from the Bingham model fit to the tube viscometry data was higher and since no data could be obtained in the low shear rate region (< 300 s^{-1}), the result obtained from the UVP-PD2 method could be assumed more correct.

Table 6.16: Rheological parameters measured in 52.8 mm pipe for bentonite 8% w/w

Rheometric method	K (Pa.s)	n -	τ_y (Pa)	R^2
UVP-PD1 normal	3.2	0.216	8.73	0.975
UVP-PD2 deconv.	0.026	0.97	13.75	0.998
Tube viscometry	0.0097	1	20.1	0.947
Rotary viscometry	0.017	1	14.59	0.999

Unfortunately it was not possible to measure profiles in kaolin suspensions in the 52.8 mm pipe as the delay line transducers could not penetrate across the pipe radius (R = 26.4 mm), which is the minimum penetration depth required for in-line rheological characterisation (only half of the experimental velocity profile is needed). A transducer with a fixed delay line material which would absorb less acoustic energy could solve the previously mentioned problems. This is discussed in the next chapter. More information on the comparison between the different rheometric methods (standard UVP-PD vs. optimised UVP-PD methodology) can be found in Kotzé and Haldenwang (2011).

6.5 IN-LINE RHEOLOGY USING UVP AND FLUME FLOW DEPTH (FD)

An implication for open channel flow applications

For open channel flow, it is possible just as for pipe flow (Section 6.5, UVP-PD methodology) to establish the rheological parameters by fitting the theoretical equation (in this case Equations 2.19 - 2.20) to the experimental data. Only one velocity profile measurement at the centre of the flume and the corresponding flow depth in laminar flow is required. To test this conjecture, two non-Newtonian fluids were used. The theoretically optimised and the experimental velocity profiles for CMC 5.26% w/w are depicted in Figure 6.42.

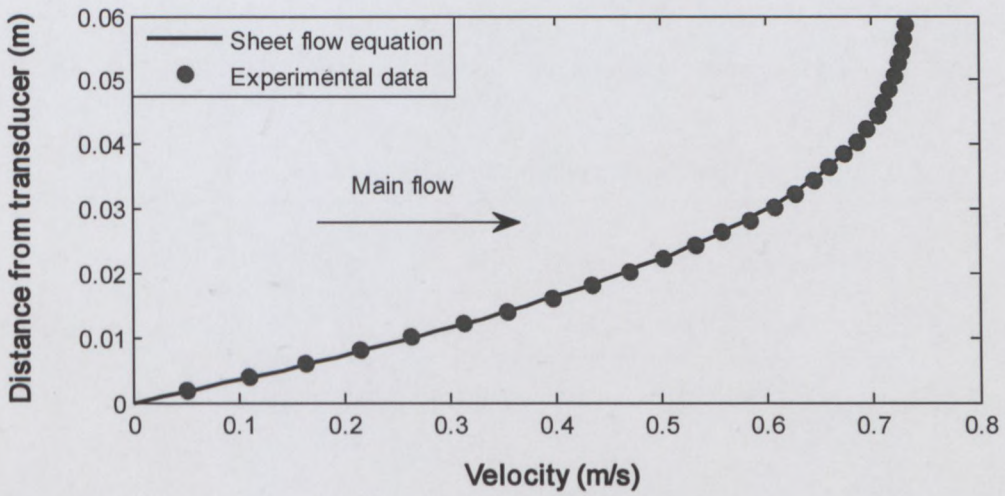

Figure 6.42: Sheet flow experimental vs. theoretical optimised fit for CMC 5.26%

In Figure 6.43 rheograms using the rheological parameters obtained from the flume are compared with those obtained from the tube viscometer. As can be seen, there is excellent agreement (within 15%) between the two flow curves. The rheological parameters as well as goodness of fits (R^2) are shown in Table 6.17.

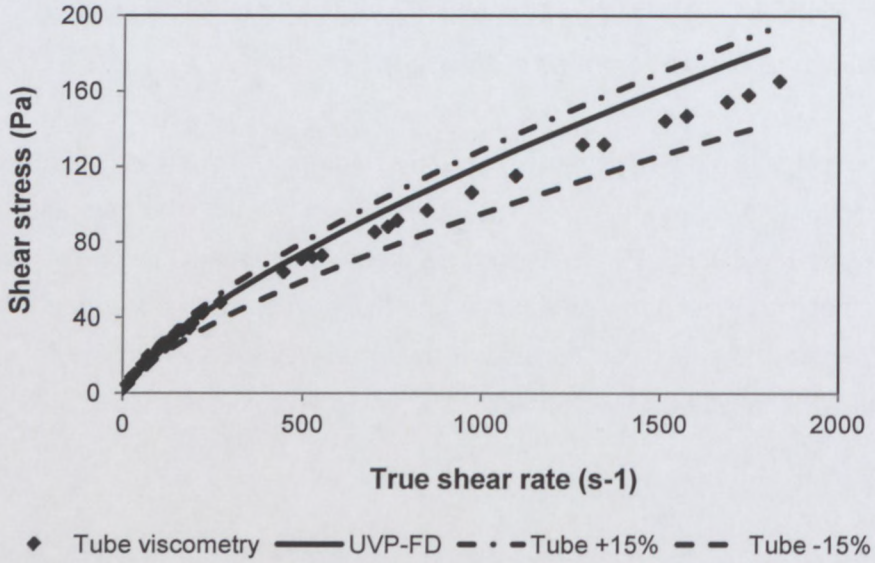

Figure 6.43: Sheet flow versus pipe flow rheology for CMC 5.26%

Table 6.17: Rheological parameters for CMC 5.26% w/w

Rheometric method	K (Pa.s)	n -	τ_y (Pa)	R^2
Tube viscometry	0.97	0.69	0	0.99
UVP-FD	0.94	0.7	0	0.99

In Figure 6.44 and Figure 6.45 a bentonite 5.29% w/w suspension was used and similar results were obtained across the range of shear rates tested. The rheology obtained using the UVP-FD method was found to be within 15% to that obtained from the tube viscometer. Rheological parameters obtained in the bentonite 5.29% w/w suspension are depicted along with the goodness of fit for the two different methods, in Table 6.18. Note that the theoretical fit for the velocity profile was not as good (Table 6.18) when compared to the CMC results (Figure 6.42). This was due to the combination of the low flow depth (22.5 mm), cavity setup (8 mm diameter) and plug flow, which caused an increase in velocity measured beyond the flume surface. As found with the UVP-PD methodology, the estimation of the wall positions (in this case the flume surface position), significantly influences the accuracy of the calculated rheological parameters (see Wiklund *et al.,* 2007 and Kotzé, 2008). More detailed description of obtaining in-line rheology using the UVP-FD method can be found in Haldenwang *et al.* (2011).

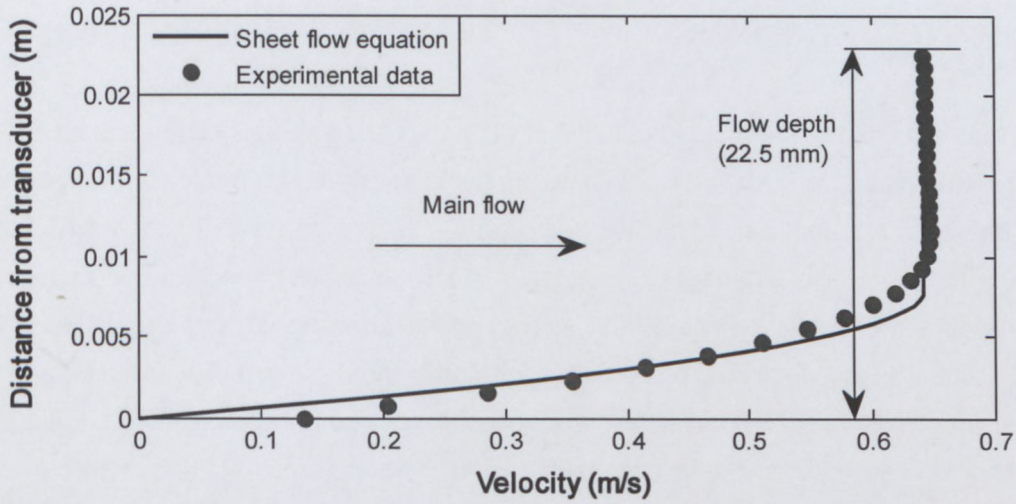

Figure 6.44: Sheet flow experimental vs. theoretical optimised fit for bentonite 5.29%

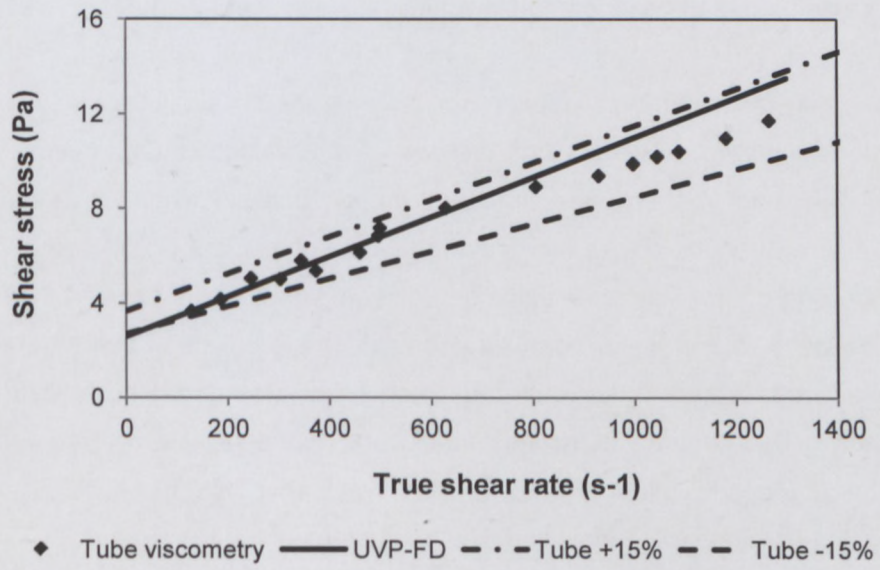

Figure 6.45: Sheet flow versus pipe flow rheology for bentonite 5.29%

Table 6.18: Rheological parameters for bentonite 5.29% w/w

Rheometric method	K (Pa.s)	n -	τ_y (Pa)	R^2
Tube viscometry	0.0068	1	3	0.98
UVP-FD	0.0084	1	2.6	0.95

6.6 SUMMARY OF FINDINGS

Results obtained in the model fluids using both standard and delay line transducers in the rectangular open channel were similar. It has also been shown that UVP is capable of monitoring dynamic flows in-line, e.g. particle settling at the surface which could build up and cause blockages. However, even when similar results were obtained, particles settle inside the cavity which could cause errors in velocity estimation. The delay line transducers would prove useful for monitoring more complex and attenuating industrial fluids due to the cavity being removed. Furthermore, when fluid properties are of concern (Section 5.5) the velocity profile need to be very accurate and therefore any potential causes of errors need to be reduced, such as the cavity setup when using standard transducers. As far as can be ascertained, it is the first time that this technique has been used to measure velocity profiles as well as determine in-line rheological parameters of opaque non-Newtonian fluids in open channels.

The velocity data obtained in the diaphragm valve showed a significant improvement close to the wall interfaces when using the delay line transducers (and deconvolution procedure). However, the change in beam angles between the two transducers produced different results across the diagonal measurement line (TDX Line 3) due to physical direction of flow inside the valve geometry. It was found that when measuring detailed flow behaviour in highly complex geometries, it is crucial to use a transducer with no beam refraction in order to simplify transducer installation and measurement line positioning. Based on the results found using the delay line transducers and combination of deconvolution procedure, UVP will prove to be a useful tool for validating CFD simulations in highly complex geometries.

The temporal behaviour of the flow inside the complex geometries (including hyperbolic contraction; see Section 4.2, Chapter 4) was also investigated. No significant variations of velocity versus time were observed for tests done using standard as well as delay line transducers. For completeness tests conducted for monitoring the temporal flow behaviour in the diaphragm valve, open channel and hyperbolic contraction are depicted in Appendix B.

Rheological parameters obtained from more accurate velocity profile gradients close to pipe walls showed better agreement with conventional rheometric methods. Although results obtained from both transducers were very similar in the larger diameter pipes, the cavity setup still prevented measurements in attenuating fluids as the fluid filled up the entire cavity and absorbed the ultrasonic energy. The delay line transducers reduced this problem and proved that this methodology (combination of new transducer and advanced signal processing techniques) will be useful for accurate monitoring of non-Newtonian fluid behaviour as well as in-line rheology in industrial applications, where fluids with attenuating properties are encountered frequently.

CHAPTER SEVEN

SUMMARY, CONTRIBUTIONS, RECOMMENDATIONS AND CONCLUSIONS

CHAPTER SEVEN

SUMMARY, CONTRIBUTIONS, RECOMMENDATIONS AND CONCLUSIONS

7.1 SUMMARY

According to literature there are many different techniques for studying flows of multiphase and complex fluids. For example, a very well established technique, Laser Doppler Anemometry (LDA) cannot be used in opaque fluids as well as highly concentrated suspensions without considerable effort to match refractive indices of the suspended phase and the liquid (Wiklund *et al.*, 2006; Powell, 2008). Other methods such as Electrical Impedance Tomography (EIT), x-ray radiography and neutron radiography are also available but experimental and cost limitations forces one to consider an alternative approach. MRI is a highly accurate and versatile technique but the experimental apparatus are expensive and requires that the apparatus used to be designed around the particular application, thus making it difficult to implement (Powell, 2008). Also, the requirements for transparent and thin measuring cells, for example made from glass, makes MRI an impractical solution for industrial applications. UVP is an ideal technique since it is non-invasive, works with opaque systems, inexpensive, portable and easy to implement relative to other velocity profile measurement methods (Teufel *et al.*, 1992; Powell, 2008 and Shirai *et al.*, 2008). An instantaneous one-dimensional velocity profile is obtained along the ultrasonic beam axis in liquid flow by using Doppler echography, thus providing detailed flow behaviour in real-time.

Apart from the angle of observation (angle between ultrasonic beam axis and fluid flow - Doppler angle), the dimensions and shape of the measuring or sample volume determine the accuracy of velocity profile measurements (Walker *et al.*, 1982; Flaud *et al.*, 1997). Due to the averaging that takes place over the sample volume the measured velocity profile is distorted. However, when measurements are made non-invasively more negative effects are introduced when the pulse has to propagate through the wall interface. One of the main problems is to accurately calculate the Doppler angle due to its refraction according to Snell's law but also that the shape of the pulse will change when crossing the wall interface leading to a skewed velocity profile. In both cases, the height and position of the peak velocity is shifted, infection points exits as the profile

reaches its extremes and the profile erroneously indicate velocities outside the pipe boundary. One would not observe the same skewed profile with the delay line transducers but one would still have to correct for the data in the near wall region e.g. due to the depletion of scattering particles close to the wall. Jorgensen and Garbini (1974) have shown that the negative effects can be overcome by measuring physical properties of the ultrasonic beam, applying mathematical descriptions to the sound field characteristics and implementing advanced signal processing techniques such as deconvolution and discrete Fourier transforms. The acoustic measurements and signal processing techniques were implemented to improve measurements of velocity distributions in arteries, which are in essence complex geometries, for the biomedical field.

The combination of several transducers measuring along several measurement axis can generate a bi-dimensional flow field (2D) or even a tri-dimensional one (3D). Ouriev (2000) performed two-dimensional time-averaged flow mapping for shear-thinning and dilatant suspensions through a cylindrical contraction using UVP. According to Ouriev (2000) the main disadvantages were that no information could be obtained close to the pipe walls as well as ultrasonic energy loss due to attenuation and absorption. For maximum energy transfer between the ultrasonic transducer and fluid under test the transducer is installed with direct contact to the fluid. This leads to a cavity in front of the transducer (due to the near field distance) and thus influences pipe wall measurements significantly, depending on the ratio between the ultrasonic transducer and pipe radius. This problem was reduced by the introduction of new ultrasonic transducers incorporating a material for beam forming, commonly known as a delay line. The delay line is typically a polymeric or ceramic material optimised for beam forming that contains the near field distance. This delay line was fixed ahead of the piezoelectric crystal of the transducer and in flush with the pipe wall, thus making it possible to have the focal point of the ultrasound beam at the wall interface (see Birkhofer, 2007 and Wiklund, 2007).

Flow through complex geometries such as abrupt contractions and enlargements, as well as valves are important problems in fluid dynamics, because they are integral components and frequently occur in pipeline systems. In order to design pipeline systems efficiently, understanding the energy loss mechanisms in complex geometries is a prerequisite (McNeil & Morris, 1995). In the absence of reliable energy loss estimates the design engineer is forced to make conservative estimates that lead to the

selection of inefficient, oversized pumps (Fester *et al.*, 2007). Energy losses caused by pipe fittings such as contractions and expansions have thus far been analysed using theoretical equations and running simulations using CFD software. In spite of a considerable effort in recent years to resolve difficulties with the simulation of complex flow problems, some outstanding issues remain. The reason for this is that more detailed observations of velocity and pressure fields are experimentally not possible (Binding *et al.*, 2006). Also, equations used for theoretical analysis of complex flows are sometimes dramatically simplified and the implications of these simplifying assumptions need to be quantified (Thompson *et al.*, 1999).

The rheological characterisation of the fluids is an important issue that has a direct effect on the effectiveness of flow predictions. In-line rheological characterisation is often achieved by using some kind of tube viscometer where the volumetric flow rate and the pressure drop are measured and used to calculate the viscosity at a single shear rate, i.e. a point-wise measurement. In-line rheological characterisation can however also be achieved by using UVP in combination with Pressure Difference (PD) measurements to obtain the complete flow curve from a single measurement. Development and adaptation of the UVP-PD technique has given engineers and scientists in the fluid engineering field a new tool to investigate the industrial flow process behaviour of these complex fluids. A complete methodology for UVP-PD in-line measurements have recently been proposed and described e.g. by Birkhofer (2007), Wiklund (2007), Wiklund *et al.* (2007), Birkhofer *et al.* (2008), Wiklund and Stading (2008); and Wiklund *et al.* (2008). In mentioned work, the UVP-PD methodology has been successfully applied to a large number of highly-concentrated non-Newtonian fluids such as foods, cellulose pulp suspensions and drilling fluids. Kotzé *et al.* (2008) investigated the capabilities and limitations of this method for different concentrations of non-transparent, highly concentrated non-Newtonian model mining slurries and found that this methodology can be used effectively for in-line measurement of rheological parameters. However, the accuracy of these parameters is largely dependent on the shape and magnitude of measured velocity profiles and current limitations on transducer designs and installation methods prevent the in-line rheometric method for implementation in industrial applications.

This thesis reports on an investigation into the capabilities and limitations of the UVP system for accurate measurement of non-Newtonian flow behaviour in complex geometries and focuses on improving the accuracy of UVP measurements by using new generation ultrasonic transducers as well as advanced signal processing techniques. Current limitations of the UVP-PD in-line rheometric methodology were identified and were reduced by implementing a transducer incorporating a delay line as well as application based software.

The UVP technique was investigated in Chapter 4 and it was determined that this method is very effective in measuring detailed flow behaviour in complex geometries for opaque non-Newtonian fluids. It was concluded that the main problem is the cavity setup when using standard ultrasonic transducers, which complicates estimation of wall positions and physically distort the flow profile close to the wall interfaces, where the velocity gradients are high (Kotzé *et al.,* 2011).

In Chapter 5 the UVP system was improved for accurate measurement of non-Newtonian flow behaviour by implementing a new ultrasonic transducer with combination of advanced signal processing techniques. Initial results obtained from the delay line transducers proved to be very encouraging for future improvements and new transducer development. Velocity profiles measured by the delay line transducers can be corrected for by using the correct Doppler angle as well as implementing a deconvolution procedure. A significant improvement was obtained for velocity measurements close to wall interfaces in three different pipe diameters (16, 22.5 and 52.8 mm).

The new improved methodology was compared with standard transducers and installation techniques in two complex geometries, 300 mm rectangular flume and 50% open diaphragm valve (Chapter 6). It was found that the main advantages when using delay line transducers are accurate velocity data at the wall and flow measurement setups suitable for industrial applications. This is possible by eliminating the cavity with standard transducer setups, which fill up with fluid particles and prevent measurements in attenuating fluids, which are frequently found in industry.

Rheological parameters were determined using the UVP-PD methodology for non-Newtonian fluids that included pseudoplastic (CMC), yield pseudoplastic (kaolin suspensions) and Bingham fluids (bentonite suspensions). The UVP-PD methodology

was evaluated using delay line transducers and results obtained were compared and verified to results determined by one in-line method, tube viscometry, and one off-line method, conventional rotary rheometry. It was shown that the apparent viscosities obtained with the use of the different methods were within 15% agreement when compared over the measured shear rate range (Kotzé & Haldenwang, 2011).

7.2 SIGNIFICANT CONTRIBUTIONS

The following are the main contributions of this work:

- A number of ultrasonic transducers were acoustically characterised and evaluated. Detailed information about the actual beam shape and intensities of the transducers were gained. This information has lead to more improved next generation delay line transducer designs.

- A deconvolution procedure was developed and tested for correcting erroneous velocity profiles caused by measurement through wall material layers and averaging effects which takes place over the acoustic sample volumes.

- New velocity estimation algorithms (frequency and time domain) were developed. The algorithms are able to measure at lower pulse repetition rates and energy settings, which improved the overall time resolution and penetration depth of the UVP system.

- The combination of the deconvolution process and delay line transducers now provides scientists with a powerful new tool for accurate complex flow behaviour measurements (such as flow in valves and open channels) in order to verify theoretical (CFD) models.

- The UVP-PD methodology has been optimised using a new delay line ultrasonic transducer and advanced signal processing techniques (including custom velocity estimators). The UVP-PD in-line rheometric method is now more versatile (better time resolution), robust (measurements in attenuating fluids) and accurate (no knowledge of rheology initially is required).

- A new non-intrusive method for determining the rheology of a fluid flowing in a flume has also been developed (UVP-FD). The advantage is that only one velocity profile and flow depth measurement is required instead of flow curves over a range of flow rates in at least two tubes.

- Consequently, by using the delay line transducers more accurate velocity of sound measurements are achieved, which is an important parameter in UVP. By eliminating the cavity no fluid particles can build up and cause density changes (e.g. when measuring in concrete suspensions or any particle settling fluid), which results in erroneous time-of-flight and velocity profile measurements.

7.3 RECOMMENDATIONS FOR FUTURE RESEARCH

The following aspects should be investigated in future research.

7.3.1 Penetration depth

Based on the results obtained from the needle hydrophone tests the delay line transducer has less energy output than when compared to the standard transducers. However, the delay line transducers were able to measure in kaolin suspensions where the standard transducers could not. The attenuating test fluid filled the cavities and absorbed the acoustic energy (standard transducer installation). It was established that that the delay line transducer could not penetrate across the radius of the 52.8 mm pipe for the kaolin suspensions, thus preventing in-line rheometric measurements using the UVP-PD methodology. More tests are required in order to fully test this limitation e.g. pipes with diameters between 22.5 and 52.8 mm need to be investigated. The penetration depth can also be improved by introducing next generation transducers that incorporate delay line materials which absorb less acoustic energy.

7.3.2 Next generation delay line transducer

Initial results obtained from the delay line transducers proved to be very encouraging for future improvements and new transducer development. Velocity profiles measured by the delay line transducers can be corrected for by using the correct Doppler angle as well as a deconvolution procedure. However, the refraction of the ultrasonic beam angle could complicate installation procedures and manufacturing of flow adapters for transducer housing. The estimation of pipe wall interface positions (or delay line material surface of the transducer) is still a challenge due to ultrasonic beam refraction through the delay line material. A new 3rd generation transducer with a delay line material at 90 has been developed and is currently being evaluated. This will also enable more accurate measurements in highly complex geometries, such as diaphragm valves. Furthermore, the delay line material should also absorb less energy, which will increase the penetration depth and applicability for industrial purposes.

7.3.3 Velocity estimation algorithms

The velocity profiles were calculated from the acquired DMEA data (in-phase and co-phase data), which was stored in a 3D matrix. As a consequence data blocks can quickly become very large (function of number of pulse repetitions) when measuring successive profiles. This has led to a limitation of +- 10 profiles, where the commercial UVP setup can easily acquire more than a 1000 profiles in short time intervals, which is achieved by using integrated hardware (DSP). The integrity of a measured velocity profile would be significantly increased if more profiles are measured and thus more work is needed on improving the algorithms in order to maximise the potential of using custom velocity estimation algorithms.

7.3.4 RF data access

During this work only DMEA data was acquired, which is the echo data obtained after quadrature demodulation. As explained by Birkhofer (2007) and Wiklund (2007), the direct access to demodulated echo amplitude (DMEA) data or 'raw data' allows for several advantages during velocity profile measurements. Direct access to DMEA data moreover provides the option of implementing alternative algorithms for velocity estimation. There are several advantages, such as increased control of signal quality and gain amplification levels, detection of signal artifacts and DC-offset correction, detection and correction of aliasing phenomena and monitoring the influence of a stationary noise signal on the velocity spectrum. However, it will be more beneficial to obtain the raw echo signal (or RF data) instead of DMEA. If given access to RF data, the user will have more freedom to design more accurate velocity estimation algorithms. Some extra features could include digital demodulation procedures, custom RF filter implementation and more importantly, custom time gain control functions to compensate for energy losses across the acoustic beam propagation. Also, when acquiring RF data, the UVP will be even more versatile, as an experienced user could fully optimise the UVP system around several applications.

7.3.5 Velocity profile measurements in flume

When using the UVP-FD method, the input parameter (in this case the flow depth) needs to be very accurate. It is therefore recommended that ultrasonic distance sensors or other accurate instruments are used for flow depth measurements (accuracy < 0.2 mm). Once the flow depth is known with confidence the velocity of sound in the flume can be measured by installing a transducer at 90 degrees (with respect to the flow direction) and recording the time-of-flight. The sound speed can then be calculated using Equation 3.13).

When using UVP high flow velocities are measured at higher PRF settings, but higher PRF means that lower penetration depths are possible, because effectively the ultrasonic pulse needs to travel twice the measurement distance before another successive pulse is transmitted (Met-Flow SA, 2002). Velocity profiles measured in open channels thus suffer from a double limitation found in UVP, which is due to the fact that as the flow speed increases in the open channel, the flow depth (which is the penetration depth or measuring distance) also increases. These limitations can,

however, be overcome by using DMEA data and implementing software, which can correct erroneous data caused by aliasing (Franca & Lemmin, 2006).

7.3.6 Wall shear stress measurements

The pressure difference measurement is very important due to the sensitivity of this parameter when calculating the fluid consistency index of mineral suspensions. Thus highly accurate pressure transducers must be used for absolute pressure measurements. It is recommended to use pressure sensors with lower ranges at the low flow rates (e.g. 0 - 0.5 bar), especially when dealing with yield stress measurements in tube viscometry. For the higher flow rates the pressures did not exceed more than 2.5 bar and thus transducers with a range of 0 - 3 bar should be installed. These modifications should reduce the combined error in wall shear stress measurements and the limitations of the pipe rig could be reduced.

7.4 CONCLUSIONS

The following final conclusions can be made.

7.4.1 Evaluation of standard UVP system for complex flow measurements

Initial results obtained in the flume proved to be very encouraging for future research in non-Newtonian open channel flow. The error difference between the integrated contour plots ranged from 2% to 6.5%. It was also possible to measure quantitative velocity data at various flow rates for non-Newtonian flow inside a highly complex geometry, such as a diaphragm valve, for the first time. The difference between calculated and measured flow rates varied from 15 to 25%. A range of velocity profiles from developed to contracting flow were also measured by scanning the transducer along a hyperbolic contraction using a high precision robotic arm set-up. Experimental results showed good agreement with theoretical predictions and the maximum error was 10%. Based on the results using standard transducer setups, it was established that the most important remaining problem was the influence of the cavities and wall materials between the transducer surfaces and wall interfaces, which distort flow profiles and complicates the estimation of wall positions. One could measure through material layers to avoid the influence of cavities inside the flow area. However, this is sometimes not possible due to physical material properties, such as significant attenuation of acoustic energy (observed in hyperbolic contraction study) and therefore not suitable for industrial applications.

A newly designed delay line transducer, where the focal point is situated at the wall interface, was evaluated during this work. Knowledge of the acoustic beam properties was essential and transducers were acoustically characterised using advanced needle hydrophone and robotic arm setups. After correcting the beam angle variation of the delay line transducer found from acoustic test results, the profiles agreed well with that measured using standard transducers with no angle refraction. However, noticeable distortion was still present due to the convolution of the finite sample volume size with the actual flow profile. Tests conducted with different UVP system parameter settings showed that the delay line transducer operated well over the entire range of system settings, except for the amplification gain settings. The distortion caused by too high gain settings was very noticeable at the wall region and was easily corrected by adjusting the amplification gain settings.

7.4.2 Optimisation of UVP system for accurate complex flow measurements

A new deconvolution procedure was developed and applied to a range of velocity profiles measured in three different non-Newtonian fluids in three different pipe diameters. Results obtained after implementing a deconvolution procedure on velocity profiles measured using delay line transducers showed significant improvement, especially close to the pipe walls, where the velocity gradients are high.

For larger pipe diameters the standard transducer setup can provide good quality velocity profiles, but the problem with particle sedimentation inside the cavity is still present. When profiles were measured in an attenuating fluid the cavity filled up with the test fluid, which prevented flow measurements even when using a standard transducer with higher acoustic energy output. The delay line transducer reduced both these problems at the same time by eliminating the cavity and providing the focal point of the ultrasonic beam at the delay line material surface, which is installed at the pipe wall interface.

Custom velocity estimation algorithms were developed and could produce profiles at much lower energy inputs as well as low ultrasonic pulse repetition settings, which the commercial algorithm was unable to do. The UVP system can now measure flow profiles in more attenuating fluids and achieve high time resolution (profiles can be measured with a pulse repetition rate as low as 32). Also, having access to both time and frequency domain algorithms, the user can select the best velocity estimator, depending on the signal-to-ratio. This improvement will enable detailed flow behaviour measurements for industrial applications where attenuating fluids are encountered frequently as well as where fast transient flows are of interest.

The UVP system was optimised by using a specially designed delay line transducer, newly developed deconvolution procedure and custom velocity estimation algorithms.

7.4.3 Validation and application of optimised UVP system

Results obtained in the model mining fluids using both standard and delay line transducers in the rectangular open channel were similar. However, the delay line transducers would prove more useful for monitoring more complex and attenuating industrial fluids due to the cavity being removed. A new method for determining in-line rheology in open channel flow was developed and initial rheometric results show good agreement (< 15%) with that obtained from tube viscometry under the same test conditions.

Unfortunately it was not possible to verify and compare results obtained using standard and delay line transducers in the diaphragm valve due to the beam refraction and difference in Doppler angles. However, the velocity data obtained showed a significant improvement close to the wall interfaces when using the delay line transducers (and deconvolution procedure). Based on initial findings and future improvements UVP will prove to be a useful tool for validating CFD simulations in complex geometries. Further verification and improvement of theoretical flow predictions using an ultrasound Doppler based method will contribute to more efficient predictions of energy losses and more efficient pipeline designs.

Rheological parameters obtained from more accurate velocity profile gradients close to pipe walls showed better agreement with conventional rheometric methods (within 15%). More importantly, the fixed delay line material and elimination of cavities provides the user with a fixed wall interface position, which is critical for accurate calculation of rheological parameters. By using the delay line transducers and combined deconvolution methodology, no knowledge of the fluid properties are required *a priori*, no matter what fluid is under investigation. The optimisation and adaptation of the UVP-PD methodology and the development of a non-invasive in-line rheometer will contribute significantly to the manner in which the rheology of complex non-Newtonian fluids is measured and broaden the number of applications in the fluid engineering industry for which the UVP-PD methodology can be used. Furthermore, due to the versatility of the UVP-PD methodology the system can be used for automatic quality control of processes within a wide range of applications, such as explosive emulsion mixing, food quality control, oil and petroleum refining processes and many more.

REFERENCES

REFERENCES

Abdel-Azim, M.S. & Hottinger, C.F. 1982. Distributed Processor for Noninvasive Blood Flow Analysis. *Journal of Medical Systems,* 6(5): 459-472.

Adair, S.P. & Fisher, H.G. 1999. Benchmarking of two-phase flow through safety relief valves and pipes. *Journal of Loss Prevention in the Process Industries,* 12: 269-297.

Alderman, N.J. & Haldenwang, R. 2007. A review of Newtonian and non-Newtonian flow in rectangular open channels. *Hydrotransport,* 17: 87-106.

Alexandrou, A.N., McGilvreay, T.M. & Burgos, G. 2001. Steady Herschel–Bulkley fluid flow in three-dimensional expansions. *Journal of Non-Newtonian Fluid Mechanics,* 100: 77–96.

Alves, M.A., Oliveira, P.J. & Pinho, F.T. 2004. On the effect of contraction ratio in viscoelastic flow through abrupt contractions. *Journal of Non-Newtonian Fluid Mechanics,* 122: 117–130.

Alves, M.A. & Poole, R.J. 2007. Divergent flow in contractions. *Journal of Non-Newtonian Fluid Mechanics,* 144: 140–148.

Aydin, N. & Evans, D.H. 1994. Implementation of directional Doppler techniques using a digital signal processor. *Medical & Biological Engineering & Computing,* 32:157-164.

Aydin, N., Fan, L. & Evans, D.H. 1994. Quadrature-to-directional format conversion of Doppler signals using digital methods. *Physiological Measurement, 15:181-199.*

Balòch, A., Townsend, P. & Webster, M.F. 1996. On vortex development in viscoelastic expansion and contraction flows. *Journal of Non-Newtonian Fluid Mechanics,* 65: 133 149.

Barber, W.D., Eberhard, J.W. & Karr, S.G. 1985. A New Time Domain Technique for Velocity Measurements Using Doppler Ultrasound. *IEEE Transactions on Biomedical Engineering,* BME-32(3): 213-229.

Bergström, J. & Vomhoff, H. 2004. Velocity measurements in a cylindrical hydrocyclone operated with an opaque fiber suspension. *Minerals Engineering*, 17(5): 599-604.

Binding, D.M., Phillips, P.M. & Phillips, T.N. 2006. Contraction/expansion flows: The pressure drop and related issues. *Journal of Non-Newtonian Fluid Mechanics,* 137:31-38.

Birkhofer, B. H. 2007. *Ultrasonic In-Line Characterization of Suspensions.* Laboratory of Food Process Engineering, Institute of Food Science and Nutrition, Swiss Federal Institute of Technology (ETH), Zurich, Switzerland. ISBN 978-3-905609-34-7.

Birkhofer, B.H., Shaik, J.A.K., Windhab, E.J., Ouriev, B., Lisner, K., Braun, P. & Zeng, Y. 2008a. Monitoring of fat crystallization process using UVP-PD technique. *Flow Measurement and Instrumentation,* 19(3-4): 163-169.

Birkhofer, B., Wiklund, J.A., Stading, M.T., Jeelani, S.A.K. & Windhab, E.W. 2008b. In-line Ultrasound Doppler based Rheology of Particulate Suspensions. *Applied Rheology*. (Submitted)

Black, R.A. & How, T.V. 1989. Pulsed Doppler ultrasound system for the measurement of velocity distributions and flow disturbances in arterial prostheses. *Journal of Biomedical Engineering,* 11:35-42.

Bouillard, J., Alban, B., Jacques, P. & Xuereb, C. 2001. Liquid flow velocity measurements in stirred tanks by ultra-sound Doppler velocimetry. *Chemical Engineering Science*, 56: 747-754.

Brinkworth, B.J. 1968. *An Introduction to experimentation.* London: English University Press.

Cheng, N-S. 2007. Power-law index for velocity profiles in open channel flows. *Advances in Water Resources,* 30: 1775-1784.

Chhabra, R.P. & Richardson, J.F. 1999. *Non-Newtonian Flow in the Process Industries.* Oxford, Great Britain: Butterworth-Heinemann.

Chow, V.T. 1959. *Open Channel Hydraulics.* New York: McGraw-Hill.

Cooke, R. 2002. Laminar Flow Settling: The Potential for Unexpected Problems, *Proc. 15th International Conference on Hydrotransport*, Banff.

De Kee, D., Chhabra, R.P., Powley, M.B. & Roy, S. 1990. Flow of Viscoplastic Fluids on an Inclined Plane: Evaluation of Yield Stress. *Chemical Engineering Communication,* 96: 229-239.

Ein-Mozaffari, F. & Upreti, S.R. 2009. Using ultrasonic Doppler velocimetry and CFD modeling to investigate the mixing of non-Newtonian fluids possessing yield stress. *Chemical Engineering Research and Design,* 87: 515-523.

Etuke, E.O. & Bonnecaze, R.T. 1998. Measurement of angular velocities using electrical impedance tomography. *Flow Measurement and Instrumentation,* 9: 159-169.

Feng, N., Zhang, J. & Wang, W. 2006. A quadrature demodulation method based on tracking the ultrasound echo frequency. *Ultrasonics,* 44: 47-50.

Fester, V., Mbiya, B. & Slatter, P. 2008. Energy losses of non-Newtonian fluids in sudden pipe contractions. *Chemical Engineering Journal,* 145: 57-63.

Fester, V.G., Kazadi, D.M., Mbiya, B.M. & Slatter, P.T. 2007. Loss Coefficients for Flow of Newtonian and Non-Newtonian Fluids Through Diaphragm Valves. *Chemical Engineering Research and Design,* 85(9):1314-1324.

Flaud, P., Bensalah, A. & Peronneau, P. 1997. Deconvolution process in measurement of arterial velocity profiles via an ultrasonic pulsed Doppler velocimeter for evaluation of the wall shear rate. *Ultrasound in Medicine & Biology,* 23(3):425-436.

Floyd, T.L. 2003. *Digital Fundamentals.* 8th ed. USA: Von Hoffman Press. ISBN 0-13-046411-2.

Franca, M.J. & Lemmin, U. 2006. Eliminating velocity aliasing in acoustic Doppler velocity profiler data. *Measurements in Science and Technology,* 17: 313-322.

Frank, S., Heilmann, C. & Siekmann, H.E. 1996. Point-velocity methods for flow-rate measurements in asymmetric pipe flow. *Flow Measurement and Instrumentation,* 7(3/4): 201-209.

Fu, W-S. & Ger, J-S. 1999. A consice method for determining a valve flow coefficient oof a valve under compressible gas flow. *Experimental Thermal and Fluid Science,* 18: 307-313.

Ganvir, V., Lele, A., Thaokar, R. & Gautham, B.P. 2007. Simulation of viscoelastic flows of polymer solutions in abrupt contractions using an arbitrary Lagrangian Eulerian (ALE) based finite element method. *Journal of Non-Newtonian Fluid Mechanics,* 143: 157–169.

Guidi, G. Corti, L. & Tortoli, P. 2000. Application of Autoregressive Methods to Multigate Spectral Analysis. *Ultrasound in Medicine & Biology,* 26(4): 585-592.

Haldenwang, R. & Slatter, P.T. 2006. Experimental procedure and database for non-Newtonian open channel flow. *Journal of Hydraulic Research,* 44(2): 283-287.

Haldenwang, R. 2003. Flow of Non-Newtonian fluids in Open Channels. Unpublished D. Tech Thesis. Cape Technikon.

Haldenwang, R., Kotze, R. & Chhabra, R.P. 2011. Determining the rheology of non-Newtonian fluids using a laminar sheet flow model and ultrasound velocity profile system. *Chemical Engineering Communications.* (Submitted)

Haldenwang, R., Slatter, P., Alderman, N., Kotzé, R., Sery, G. & George, N. 2006. Balanced Beam Tube Viscometry vs Rotary Viscometry: A Comparison. *12th International Conference on Transport and Sedimentation of Solid Particles,* Tbilisi, Georgia. 12:145-156.

Haldenwang, R., Slatter, P.T. & Chhabra, R.P. 2002. Laminar and transitional flow in open channels for non-Newtonian fluids. *Hydrotransport,* 15: 755-768.

Halliday, D., Resnick R. & Walker, J. 1993. *Fundamentals of Physics.* 4th Edition (Extended). John Wiley & Sons, New York.

Holmbom, M. 2011. Evaluation and optimization of velocity estimators for pulsed ultrasound Doppler based velocity profile measurements. Uppsala University School of Engineering, Sweden, Uppsala. Report no: UPTEC X 11 024.

Hong, S.B., Eliaz, N., Sachs, E.M., Allen, S.M. & Latanision, R.M. 2001. Corrosion behaviour of advanced titanium-based alloys made by three-dimensional printing (3DP™) for biomedical applications. *Corrosion Science,* 43: 1789-1791.

Hughes, P.E. & How, T.V. 1994. Pulsatile Velocity Distribution and Wall Shear Rate Measurement using Pulsed Doppler Ultrasound. *Journal of Biomechanics,* 27(1): 103-110.

Humphreys, P., Erfort, E., Fester, V., Chhiba, M., Kotze, R., Philander, O. & Sam, M. 2011. Development of an Experimental Diaphragm Valve used for Velocity Profiling of such Devices. *Journal for New Generation Sciences,* 8(2): 32-45.

Jacobs, P., 1996. *Stereolithography and Other RP&M Technologies*. ASME Press, New York, NY.

Jensen, J.A. 1996. *Estimation of Blood Velocities Using Ultrasound: A Signal Processing Approach*, Great Britain, Cambridge University Press.

Jorgensen, J.E. & Garbini, J.L. 1974. An Analytical Procedure of Calibration for the Pulsed Ultrasonic Doppler Flow meter. *Journal of Fluids Engineering,* 96: 158-167.

Jorgensen, J.E., Campau, D.N. & Baker, D.W. 1973. Physical characteristics and mathematical modelling of the pulsed ultrasonic flowmeter. *Medical and Biological Engineering,* 11(4): 404-421.

Kasai, C., Namekawa, K., Koyano, A. & Omoto, R. 1985. Real-Time Two-Dimensional Blood Flow Imaging Using an Autocorrelation Technique. *IEEE Transactions on Sonics and Ultrasonics,* SU-32(3): 458-464.

Keunings, R. 1990. Progress and challenges in computational rheology. *Rheologica Acta,* 29: 556-570.

Kotzé, R. & Haldenwang, R. 2011. Development of an ultrasonic in-line rheometer: Evaluation, optimisation and verification. *15th International Conference Transport and Sedimentation of Solid Particles,* 15: 49-61.

Kotzé, R. 2008. Rheological Characterisation of Highly Concentrated Mineral Suspensions using an Ultrasonic Velocity Profiler. Unpublished M. Tech thesis, Cape Peninsula University of Technology, Cape Town. http://dk.cput.ac.za/td_cput/39/

Kotzé, R., Haldenwang, R. & Slatter, P. 2008. Rheological characterisation of highly concentrated mineral suspensions using an Ultrasonic Velocity Profiling with combined Pressure Difference method. *Applied Rheology,* 18(6):62114.

Kotzé, R., Wiklund, J., Haldenwang, R. & Fester, V. 2011. Measurement and analysis of flow behaviour in complex geometries using the Ultrasonic Velocity Profiling (UVP) technique. *Flow Measurement and Instrumentation*, 22: 110-119.

Kra, E.Y. & Merkley, G.P. 2004. Mathematical; modelling of open-channel velocity profiles for float method calibration. *Agricultural Water Management,* 70: 229-244.

Kristoffersen, K. 1988. Time-Domain Estimation of the Center Frequency and Spread of Doppler Spectra in Diagnostic Ultrasound. *IEEE Transactions on Ultrasonics, Ferroelectrics and Frequency Control,* 35(6): 685-700.

Kukura, H., Yamanaka, G. & Aritomi, M. 2004. Effect of measuring volume size on turbulent flow measurement using ultrasonic Doppler method. *Experiments in fluids,* 36(1): 187-196.

Kuttruff, H. 1991. *Ultrasonics: Fundamentals and Applications.* Elsevier Applied Science, London and New York.

Larrarte, F. 2006. Velocity fields within sewers: An experimental study. *Flow Measurement and Instrumentation,* 17: 282-290.

Lemmin, U. & Rolland, T. 1997. Acoustic Velocity Profiler for Laboratory and Field Studies. *Journal of Hydraulic Engineering,* 123(12): 1089-1098.

Lubansky, A.S., Boger, D.V., Servais, C., Burbidge, A.S. & Cooper-White, J.J. 2007. An approximate solution to flow through a contraction for high Trouton ratio fluids. *Journal of Non-Newtonian Fluid Mechanics*, 144: 87-97.

Manica, R. & De Bortoli, A.L. 2004. Simulation of sudden expansion flows for power-law fluids. *Journal of Non-Newtonian Fluid Mechanics,* 121: 35–40.

Mao, W. & Khayat, R.E. 1995. Numerical simulation of transient planar flow of a viscoelastic material with two moving free surfaces. *International Journal for Numerical Methods in Fluids,* 21: 1137-1151.

Markou, C.P. & Ku, D.N. 1991. Accuracy of Velocity and Shear Rate Measurements using Pulsed Doppler Ultrasound: A Comparison of Signal Analysis Techniques. *Ultrasound in Medicine & Biology,* 17(8): 803-814.

Mbiya, B.M., Pienaar, V.G. & Slatter, P.T. 2007. Prediction of pressure losses in straight-through diaphragm valves. *Hydrotransport,* 17: 121-134.

McNeil, D.A. & Morris, S.D. 1995. A Mechanistic Investigation of Laminar Flow Through an Abrupt Enlargement and a Nozzle and its Application to Other Pipe Fittings. Technical Report No. Report EUR 16348 EN, European commission, Institute for Safety Technology, Ispra.

Mei, C.C. & Yuhi, M. 2001. Slow flow of a Bingham fluid in a shallow channel of finite width. *Journal of Fluid Mechanics,* 431: 135-159.

Meile, T., De Cesare, G., Blanckaert, K. & Schleiss, A.J. 2008. Improvement of Acoustic Doppler Velocimetry in steady and unsteady turbulent open-channel flows by means of seeding with hydrogen bubbles. *Flow Measurement and Instrumentation,* 19: 215–221.

Messer, M. & Aidun, C. K. 2009. Main effects on the accuracy of Pulsed-Ultrasound-Doppler-Velocimetry in the presence of rigid impermeable walls. *Flow Measurement and Instrumentation,* 20: 85-94.

Met-Flow SA. 2002. UVP Monitor – Model UVP-DUO User's Guide. Software version 3. Met-Flow SA, Lausanne, Switzerland.

Mezger, T.G. 2002. *The Rheology Handbook: For users of rotational & oscillation rheometers.* Hannover: Curt R. Vincentz Verlag.

Mitsoulis, E. & Huilgol, R.R. 2004. Entry flows of Bingham plastics in expansions. *Journal of Non-Newtonian Fluid Mechanics*, 122: 45–54.

Mo, L.Y.L., Yun, L.C.M. & Cobbold, R.S.C. 1988. Comparison of Four Digital Maximum Frequency Estimators for Doppler Ultrasound. *Ultrasound in Medicine & Biology,* 14(5): 355-363.

Mondy, L.A., Graham, A.L., Majumdar, A. & Bryant, L.E. 1986. Techniques of measuring particle motions in concentrated suspensions. *International Journal of Multiphase Flow,* 12: 497-502.

Morris, A. 2001. *Measurements & Instrumentation Principles.* Butterworth-Heinemann. Oxford.

Morris, S.D. 1996. Liquid flow through safety valves: Diameter ratio effects on discharge coefficients, sizing and stability. *Journal of Loss Prevention in the Process Industries,* 9(3): 217-224.

Muller, M. 1998. Neue Methoden Der Prozessviskosimetrie: Kugelschüttungsströmung Und Gradienten – Ultraschall – Puls – Doppler – Verfahren Vol. Doctoral thesis, University of Erlangen, Germany.

Müller, M., Brunn, P.O. & Wunderlich, T. 1997. New Rheometric Technique: the Gradient-Ultrasound Pulse Doppler Method. *Applied Rheology,* 7:204-210.

Nigen, S. & Walters, K. 2002. Viscoelastic contraction flows: comparison of axisymmetric and planar configurations. *Journal of Non-Newtonian Fluid Mechanics,* 102: 343–359.

Norton, I. 2011. *Practical Food Rheology: An Interpretive Approach*. Wiley-Blackwell. ISBN-10: 1405199784.

Nowak, M. 2002. Wall shear stress measurement in a turbulent pipe flow using ultrasound Doppler velocimetry. *Experiments in Fluids,* 33: 249-255.

Nowicki, A., Karlowicz, P., Piechocki, M. & Secomski, W. 1985. Method for the Measurement of the Maximum Doppler Frequency. *Ultrasound in Medicine & Biology,* 11(3): 479-486.

Obayashi, H., Tasaka, Y., Kon, S. & Takeda, Y. 2007. Velocity vector profile measurement using multiple ultrasonic transducers. *Flow Measurement and Instrumentation*, 19(3-4): 189-195.

Oliveira, M.S.N., Oliveira, P.J., Pinho, F.T. & Alves, M.A. 2007. Effect of contraction ratio upon viscoelastic flow in contractions: The axisymmetric case. *Journal of Non-Newtonian Fluid Mechanics*, 147: 92–108.

Ouriev, B. & Windhab, E.J. 2002. Rheological study of concentrated suspensions in pressure-driven shear flow using a novel in-line ultrasound Doppler method. *Experiments in fluids,* 32: 204-211.

Ouriev, B. 2000. *Ultrasound Doppler Based In-Line Rheometry of Highly Concentrated Suspensions*. ETH dissertation No. 13523, ISBN 3-905609-11-8. Zurich. Switzerland.

Ouriev, B. & Windhab, E. 2003. Novel ultrasound based time averaged flow mapping method for die entry visualization in flow of highly concentrated shear-thinning and shear-thickening suspensions. *Measurement Science and Technology,* 14: 140-147.

Park, J.Y. & Chung, M.K. 2006. Study on Hydrodynamic Torque of a Butterfly Valve. *Journal of Fluids Engineering,* 128: 190-195.

Paterson, A.J.C. 2004. High density slurry and paste tailings, transport systems. *International Platinum Conference 'Platinum Adding Value',* The South African Institute of Mining and Metallurgy.

Peters, F., Lobry, L. & Lemaire, E. 2010. Pressure-driven flow of a micro-polar fluid: Measurement of the velocity profile. *Journal of Rheology,* 54(2): 311-325.

Poole, R.J., Alves, M.A. Oliveira, P.J. & Pinho, F.T. 2007. Plane sudden expansion flows of viscoelastic liquids. *Journal of Non-Newtonian Fluid Mechanics,* 146: 79–91.

Powell, R.L. 2008. Experimental techniques for multiphase flows. *Physics of Fluids,* 20(4): 605-627.

Powell, R.L., Maneval, J.E. & Seymour, J.D. 1994. Note: Nuclear magnetic resonance imaging for viscosity measurements. *Journal of Rheology,* 38(5): 1465-1470.

Povey, M.J.W. 1997. *Ultrasound Techniques For Fluids Characterization.* Academic Press. San Diego, California, USA: Harcourt Brace & Company (Publishers). ISBN 0-12-563730-6.

Rothstein, J.P. & McKinley, G.H. 2001. The axisymmetric contraction–expansion: the role of extensional rheology on vortex growth dynamics and the enhanced pressure drop. *Journal of Non-Newtonian Fluid Mechanics*, 98: 33–63.

Sachs, E., Haggerty, J., Williams, P. & Cima, M. 1993. Three-Dimensional Printing Techniques, US Patent 5,204,055, April 20.

Sato, T. & Richardson, S.M. 1994. Numerical simulation method for viscoplastic flows with free surfaces – fringe element generation method. *Internation Journal of Meth. Fluids,* 19: 555-574.

Shandas, R., Gharib, M. Sahn, D.J. & Facc. M.D. 1995. Nature of Flow Acceleration Into a Finte-Sized Orifce: Steady and Pulsatile Flow Studies on the Flow Convergence Region Using Simultaneous Ultrasound Doppler Flow Mapping and Laser Doppler Velocimetry. *Journal of the American Colloge of Cardiology,* 25: 1199-1212.

Shekarriz A. & Sheen D.M. 1998. Slurry Pipe Flow Measurements using Tomographic Ultrasonic Velocimetry and Densitometry. *Proceedings of FEDSM, ASME Fluids Engineering Division Summer Meeting*, Washington, D.C., USA, 21-25 June 1998, FEDSM98-5076.

Shirai, K., Bayer, C., Voigt, A., Pfister, T., Büttner, L. & Czarske, J. 2008. Near-wall measurements of turbulent statistics in a fully developed channel flow with a novel laser Doppler velocity profile sensor. *European Journal of Mechanics B/Fluids*, doi:10.1016/j.euromechflu.2007.12.001.

Shutilov, V.A. 1980. *Fundamental Physics of Ultrasound – English Translation by Michael E. Alferieff, 1988.* Amsterdam, Netherlands: Gordon and Breach Science Publishers.

Signal Processing SA. 2007. *Transducers ultrasonic field.* http://www.signal-processing.com/transducers/transducers_theory_frame.htm [06 June 2011].

Slatter, P.T. & Lazarus, J.H. 1993. Critical flow in slurry pipelines. British Hydromechanics Research Group, *12th International Conference on Slurry Handling and Pipeline Transport, HYDROTRANSPORT 12*; Brugge, Belgium: 28-30 September 1993. ISBN 0 85298 874 5. pp 639-654.

Slatter, P.T. 1994. Transitional and Turbulent flow of non-Newtonian slurries in pipes. Unpublished PhD thesis. Cape Town: University of Cape Town.

Stading, M. 2008. Determination of Extensional Rheological Properties by Hyperbolic Contraction Flow. *AIP Conference Proceedings*, 1027: 1114-1116.

Steger, R. 1994. OptischUnd Akustische Metoden in Der Rheometrie. Erlangen: University of Erlangen: 1-100.

Stickel, J.J. & Powell, R.L. 2005. Fluid Mechanics and Rheology of Dense Suspensions. *Annual Review of Fluid Mechanics,* 37: 129-149.

Stickel, J.J., Phillips, R.J. & Powell, R.L. 2006. A constitutive model for microstructure and total stress in particulate suspensions. *Journal of Rheology,* 50(4): 379-413.

Takeda, Y. 1986. Velocity Profile Measurement by Ultrasound Doppler Shift Method. *International Journal of Heat and Fluid Flow,* 7: 313-318.

Takeda, Y. 1991. Development of an ultrasound velocity profile monitor. *Nuclear Engineering and Design,* 126: 277-284.

Takeda, Y. 1995. Velocity Profile Measurement by Ultrasonic Doppler Method. *Experimental Thermal and Fluid Science,* 10: 444-453.

Takeda, Y. 1999. Ultrasonic Doppler Method for Velocity Profile Measurement in Fluid Dynamics and Fluid Engineering. *Experiments in Fluids,* 26: 177-178.

Takeda, Y. & Kikura, H. 2002. Flow mapping of the mercury flow. *Experiments in Fluids*, 32: 161-169.

Teufel, M., Trimis, D., Lohmüller, A., Takeda, Y. & Durst, F. 1992. Determination of velocity profiles in oscillating pipe-flows by using laser Doppler velocimetry and ultrasonic measuring devices. *Flow Measurement and Instrumentation*, 3(2): 95-101.

Thompson, R.L., Mendes, P.R.S. & Naccache, M.F. 1999. A new constitutive equation and its performance in contraction flows. *Journal of Non-Newtonian Fluid Mechanics,* 86: 375-388.

Tortoli, P., Guidi, F., Guidi, G. & Atzeni, C. 1996. Spectral Velocity Profiles for Detailed Ultrasound Flow Analysis. *IEEE Transactions on Ultrasonics, Ferroelectrics, and Frequency Control,* 43(4): 654-659.

Turian, R.M., Ma, T.W., Hsu, F.L.G., Sung, M.D.J. & Plackmann, G.W. 1998. Flow of concentrated slurries. 2. Friction losses in bends, fittings, valves and venturi meters. *International Journal of Multiphase Flow,* 24: 243–269.

Vaitkus, P.J. & Cobbold, R.S.C. 1988. A Comparitive study and Assessment of Doppler Ultrasound Spectral Estimation Techniques Part 1: Estimation Methods. *Ultrasound in Medicine & Biology,* 14(8): 661-672.

Walker, A.R., Phillips, D.J. & Powers, J.E. 1982. Evaluating Doppler Devices Using a Moving String Test Target. *Journal of Clinical Ultrasound,* 10: 25-30.

Wallace, M.S., Dempster, W.M., Scanlon, T., Peters, J. & McCulloch, S. 2004. Prediction of impact erosion in valve geometries. *Wear,* 256: 927-936.

Wang, Y-H. & Yu, G-H. 2007. Velocity and concentration profiles of particle movement in sheet flows. *Advances in Water Resources,* 30: 1355-1359.

Wassell P., Wiklund, J., Stading, M., Bonwick, G., Smith, C., Almiron-Roig, E. & Young, N.W.G. 2010. Ultrasound Doppler based in-line viscosity and solid fat profile measurement of fat blends. *International Journal of Food Science and Technology*, 45: 877–883.

Wiklund, J. & Stading, M. 2008. Application of in-line ultrasound Doppler based UVP-PD rheometry method to concentrated model and industrial suspensions. *Flow Measurement and Instrumentation*, 19:171-179.

Wiklund, J. 2003. *Rheological in-line techniques based on ultrasound Doppler methods for the food industry: A literature survey.* LUND University & The Swedish Institute for Food and Biotechnology. SIK-Report SR-710, ISBN 91-7290-225-X. Sweden.

Wiklund, J. 2007. *Ultrasound Doppler Based In-Line Rheometry: Development, Validation and Application.* SIK – The Swedish Institute for Food and Biotechnology, Lund University, Sweden. ISBN 978-91-628-7025-6.

Wiklund, J. A., Stading, M., Pettersson, A. J. & Rasmuson, A. 2006. A comparative study of UVP and LDA techniques for pulp suspensions in pipe flow. *AIChE Journal*, 52(2): 484-495.

Wiklund, J., Shahram, I. & Stading, M. 2007. Methodology for in-line rheology by ultrasound Doppler velocity profiling- and pressure difference techniques. *Chemical Engineering Science*, 62: 4277-4293.

Wiklund, J., Stading, M. & Trägårdh, C. 2010. Monitoring liquid displacement of model and industrial fluids in pipes by in-line ultrasonic rheometry. *Journal of Food Engineering*, 99: 330-337.

Wunderlich, T.H. & Brunn, P.O. 2000. A wall layer correction for ultrasound measurement in tube flow: comparison between theory and experiment. *Flow measurement and Instrumentation,* 11: 63-69.

Xu, H. & Aidun, C.K. 2005. Measuring velocity profile of wood fiber suspension flow by pulsed ultrasonic Doppler velocimetry. *International Journal of Multiphase Flow*, 31: 318-36.

Xue, S.C., Phan-Thien, N. & Tanner, R.I. 1998. Three dimensional numerical simulations of viscoelastic flows trhough planer contractions. *Journal of Non-Newtonian Fluid Mechanics,* 74: 195-245.

Young, N.W.G., Wasell, P., Wiklund, J. & Stading, M. 2008. Monitoring struturants of fat blends with ultrasound based in-line rheometry (ultrasonic velocity profiling with pressure difference). *International Journal of Food Science and Technology,* 43: 2083-2089.

Zatti, D., Wiklund, J., Vignali, G. & Stading, M. 2009. Determination of Velocities Profiles in Hyperbolic Contraction using Ultrasound Velocity Profiling. *Annual Transactions of the Nordic Rheology Society*, 17: 277-280.

APPENDICES

APPENDIX A

EXPERIMENTAL RESULTS

The following is depicted in this appendix:

- The flow curves that were measured using the off-line Paar Physica MCR300 rheometer are depicted in the form of rheograms in Section A.1.

- Experimental pipe data and flow curves that were measured using the tube viscometers at the MST are presented in Section A.2.

The following materials were used:

CMC 2.63 – 6.15 % by weight

Bentonite 5.29 – 8 % by weight

Kaolin 13 – 17 % by volume

Note: Not all fluid concentrations were rheologically characterised using both in-line tube and off-line rotary viscometry.

A.1 ROTARY VISCOMETER DATA

CMC 2.63%

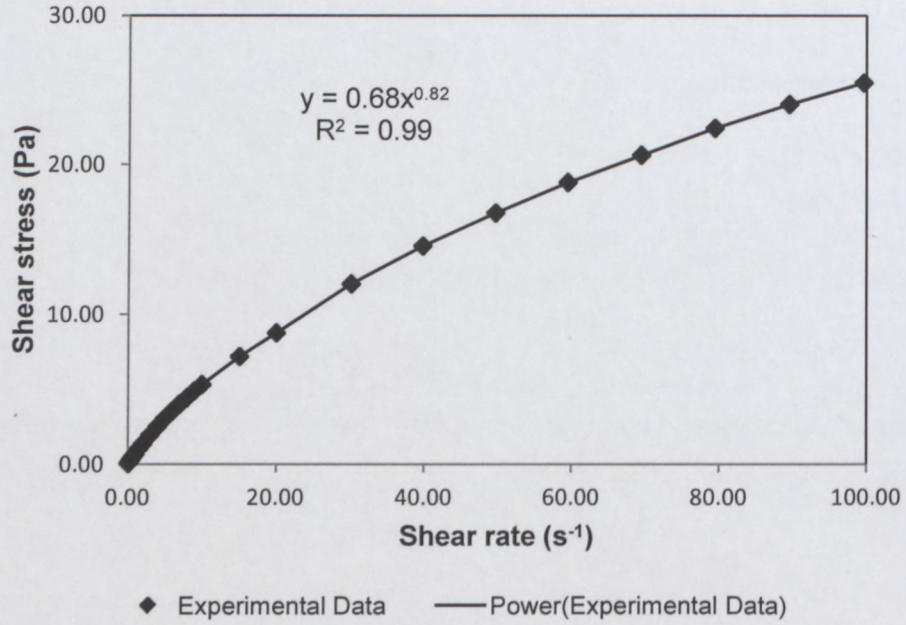

CMC 6.15%

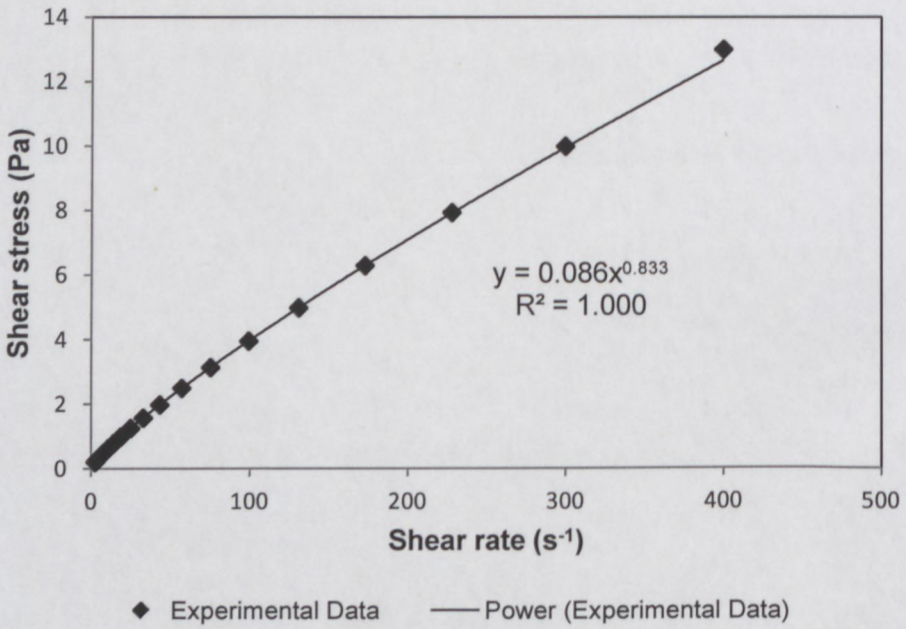

CMC 6.8%

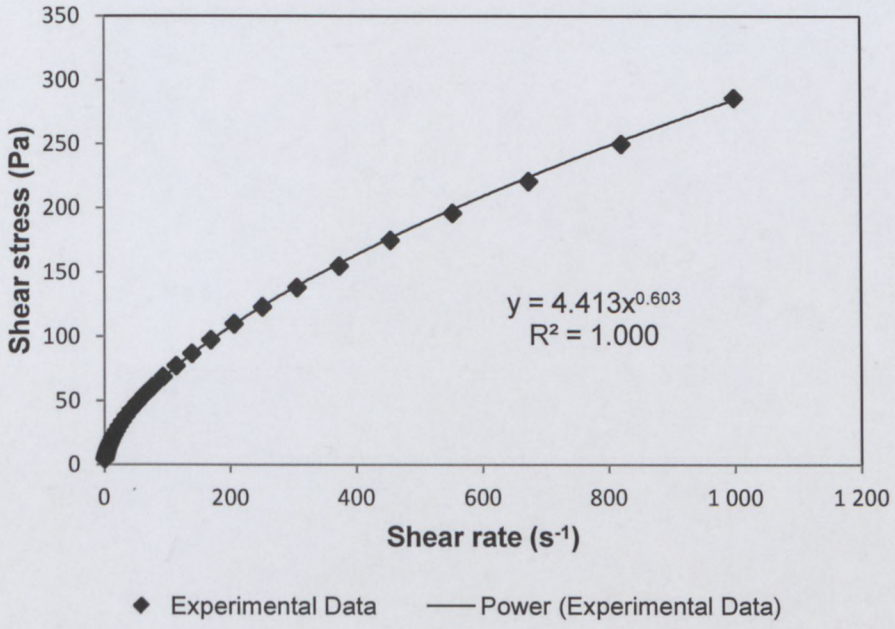
Shear stress (Pa)
Shear rate (s-1)
y = 4.413x0.603
R² = 1.000
Experimental Data
Power (Experimental Data)

CMC 7%

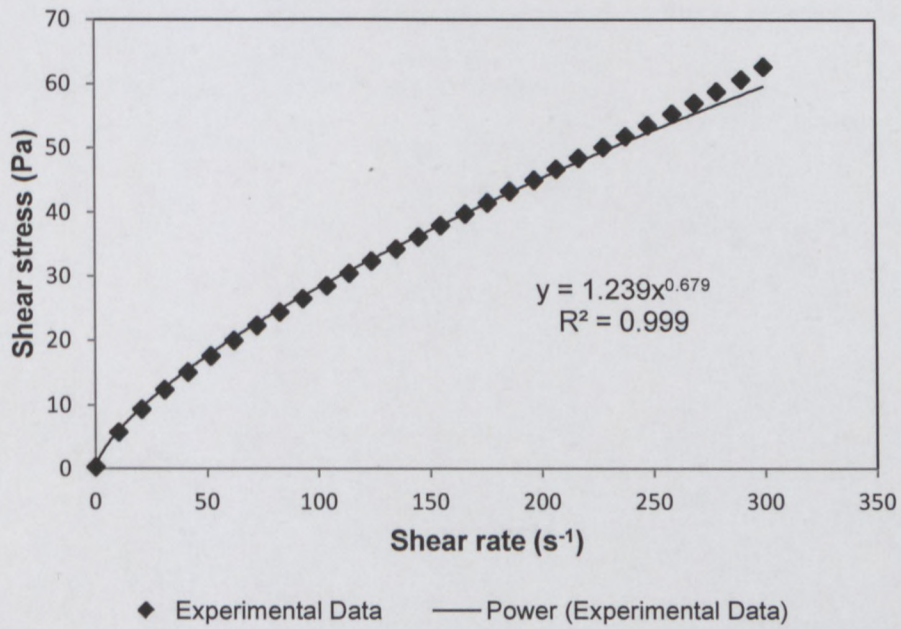
Shear stress (Pa)
Shear rate (s-1)
y = 1.239x0.679
R² = 0.999
Experimental Data
Power (Experimental Data)

BENTONITE 6.9%

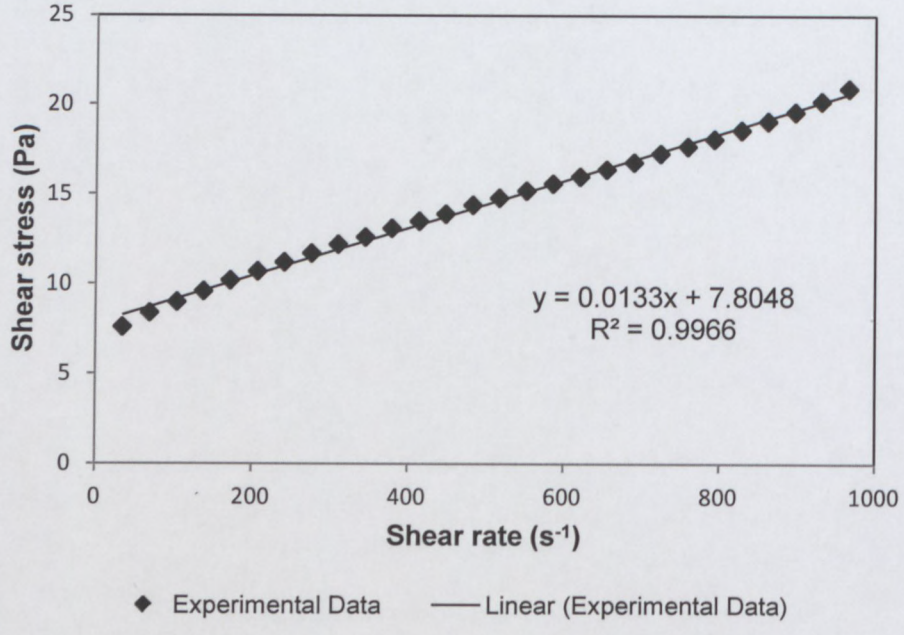

BENTONITE 8%

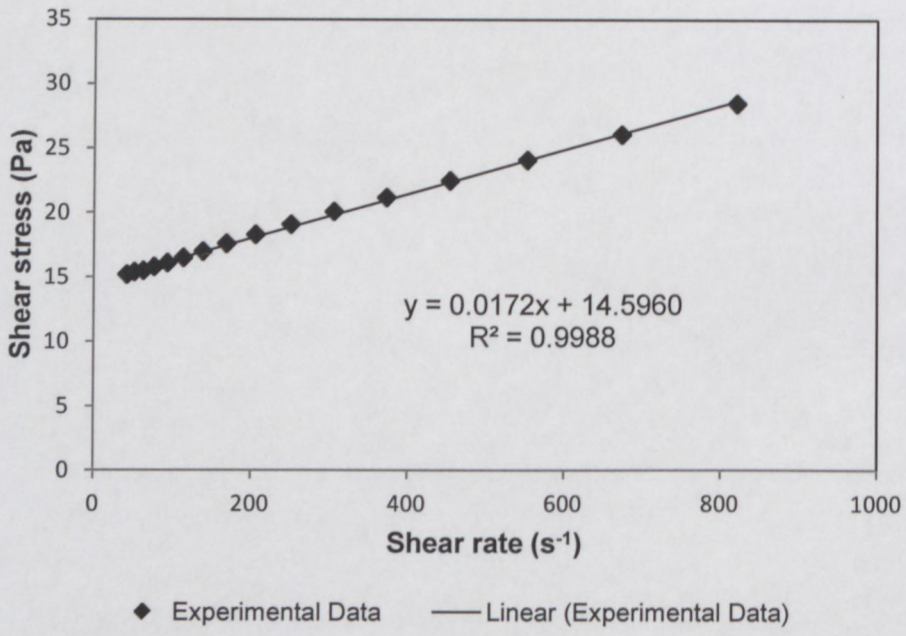

KAOLIN 13%

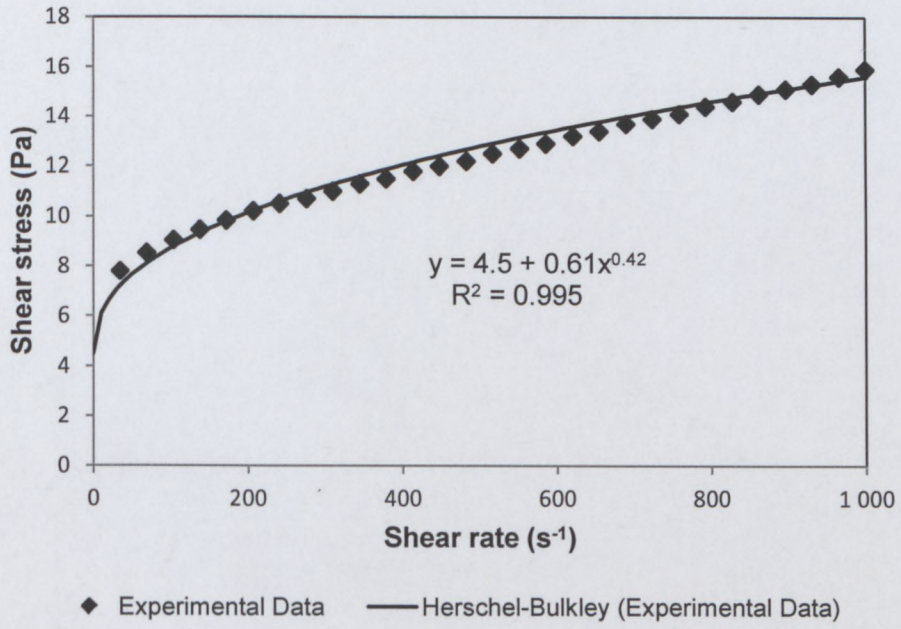

KAOLIN 17%

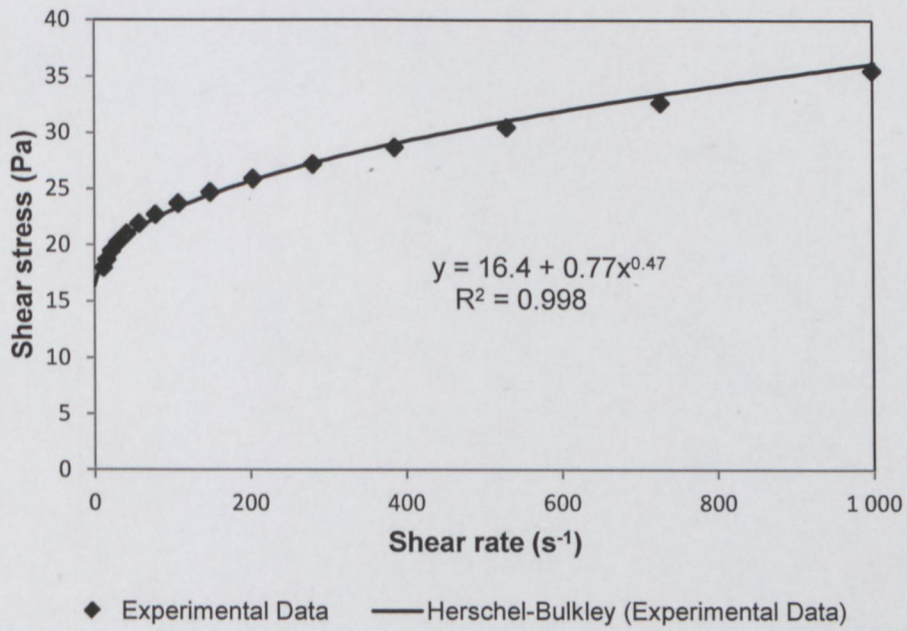

A.2 TUBE VISCOMETER DATA

CMC 3.25%

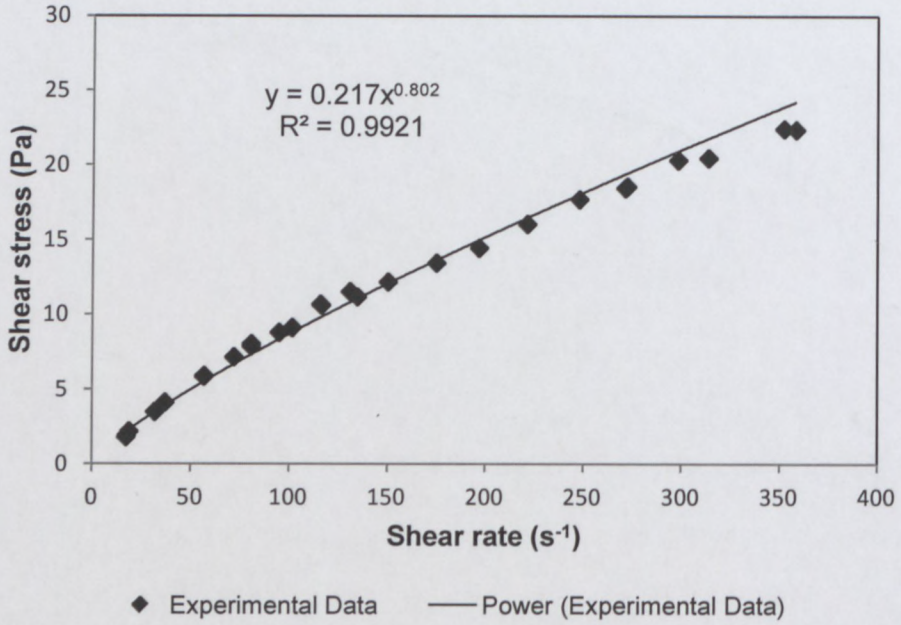

CMC 4.5%

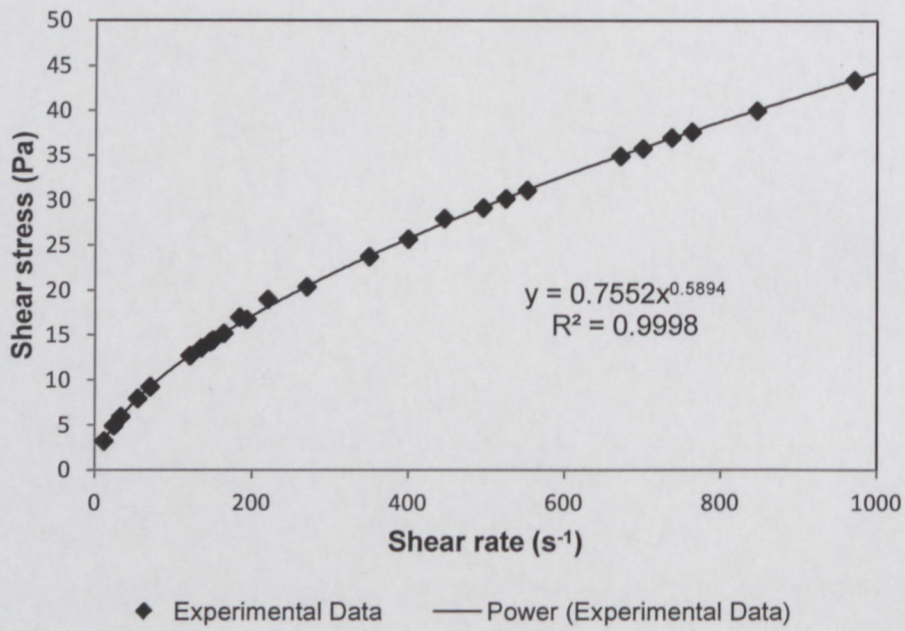

CMC 5.26%

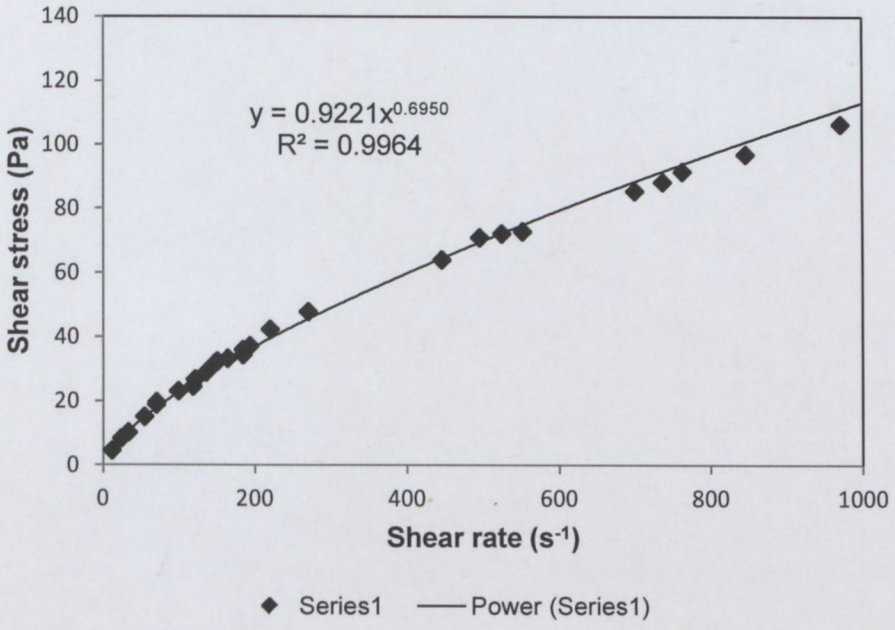
y = 0.9221x^0.6950
R² = 0.9964
Shear stress (Pa)
Shear rate (s-1)
0
20
40
60
80
100
120
140
0
200
400
600
800
1000
Series1
Power (Series1)

CMC 6%

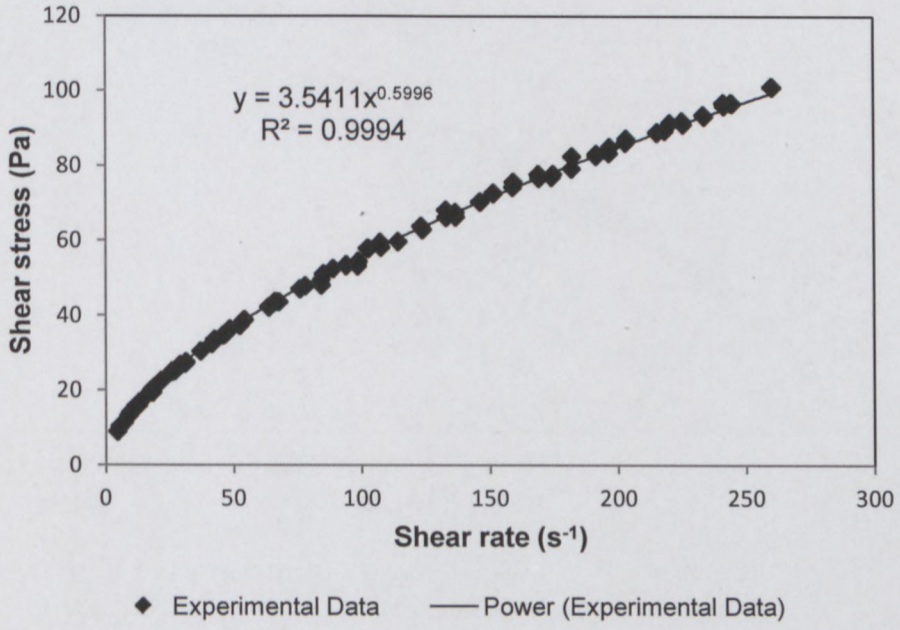
y = 3.5411x^0.5996
R² = 0.9994
Shear stress (Pa)
Shear rate (s-1)
0
20
40
60
80
100
120
0
50
100
150
200
250
300
Experimental Data
Power (Experimental Data)

CMC 6.15%

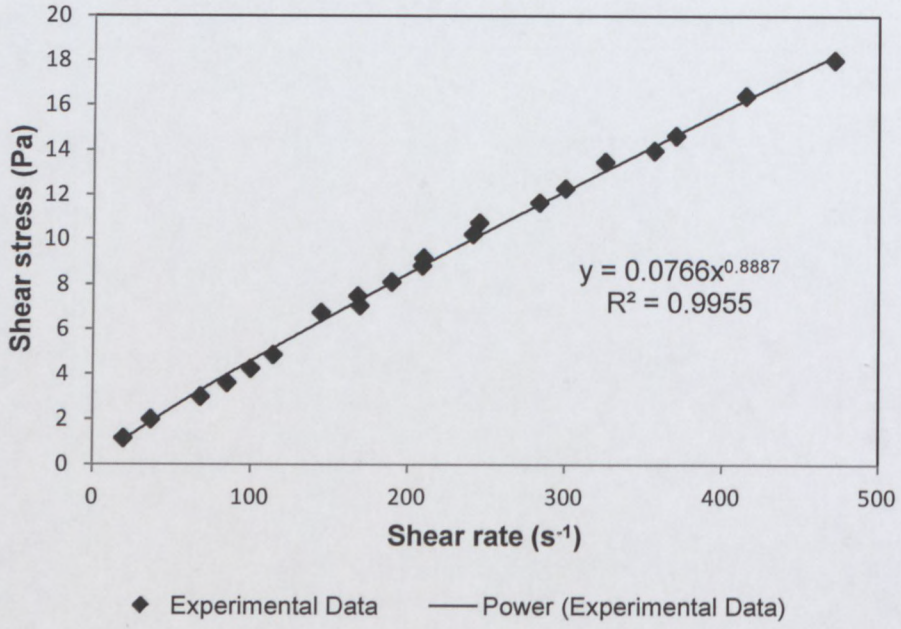

CMC 6.8%

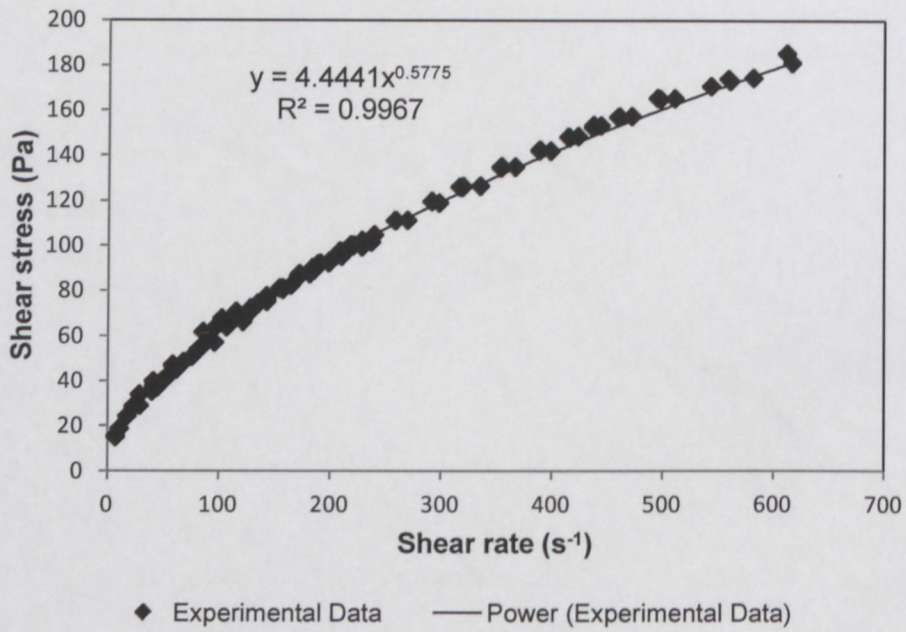

CMC 7%

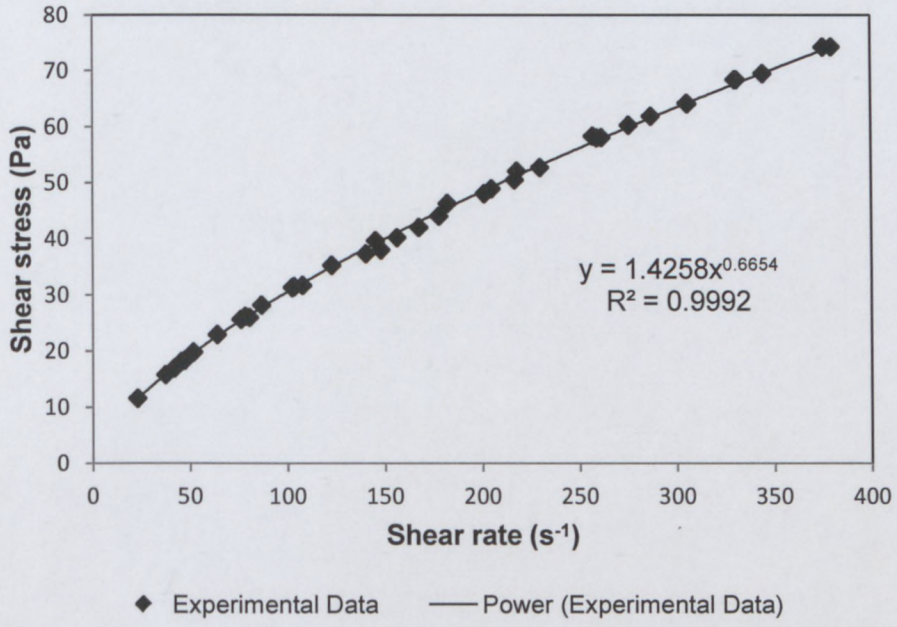

BENTONITE 5.29%

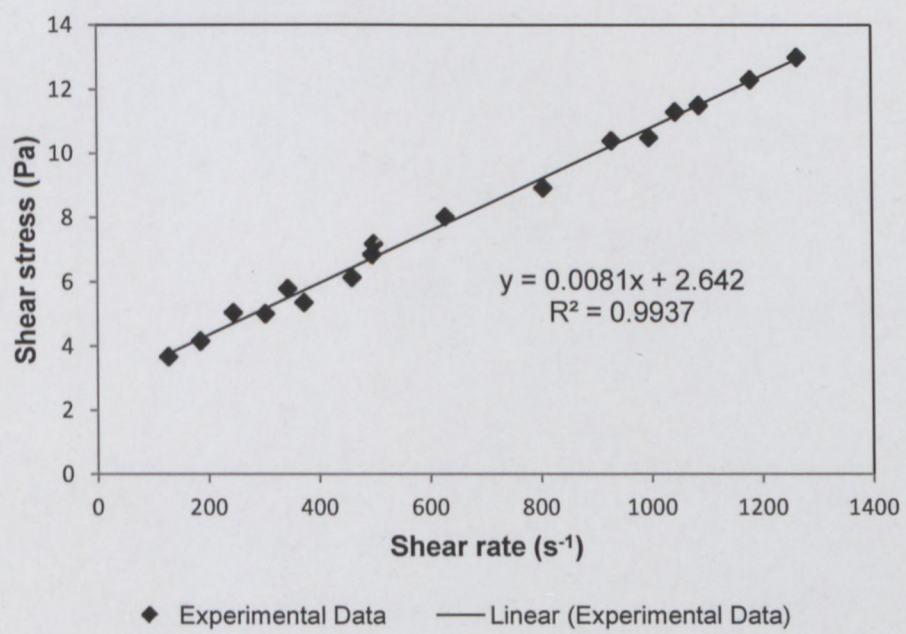

BENTONITE 6.5%

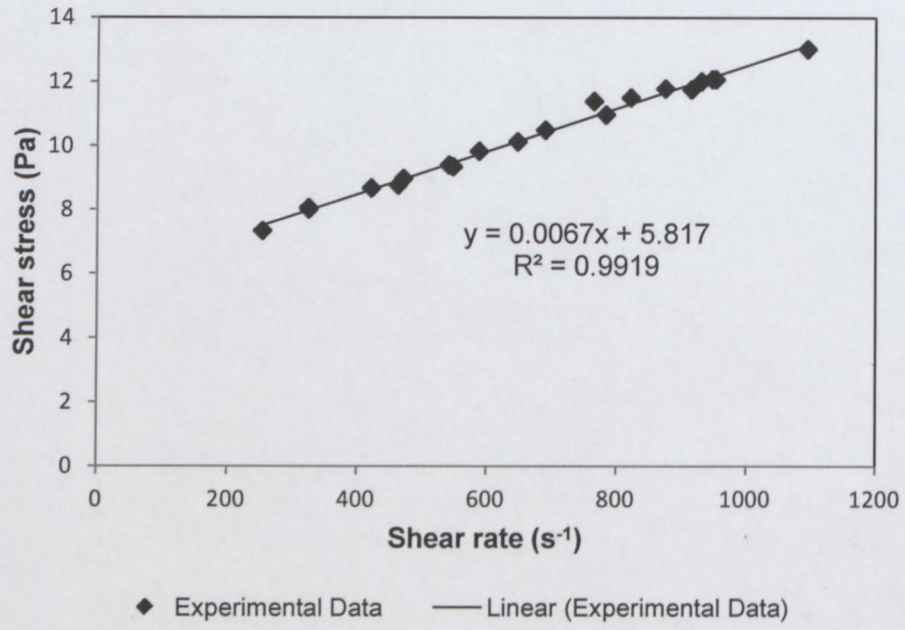

BENTONITE 6.7%

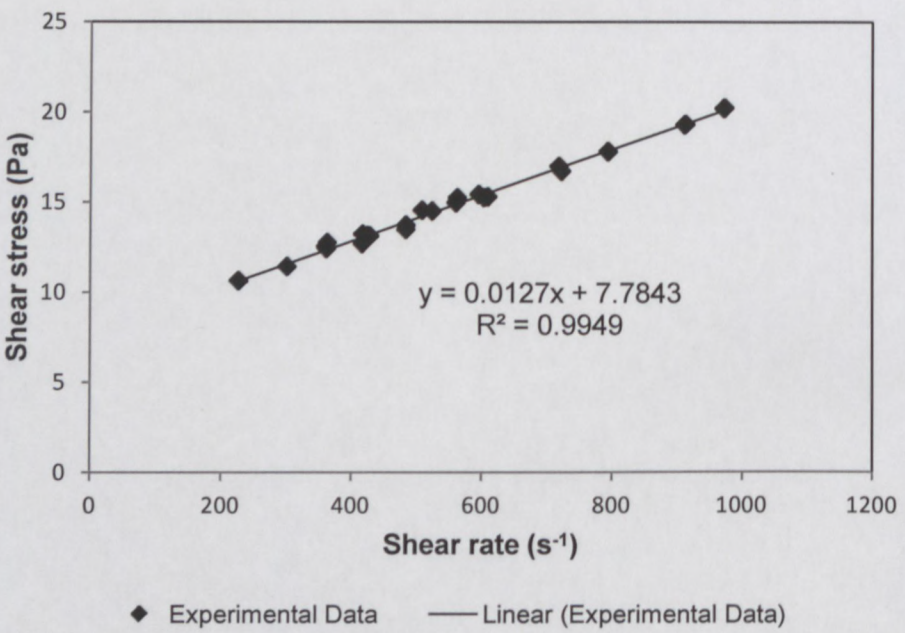

BENTONITE 6.9%

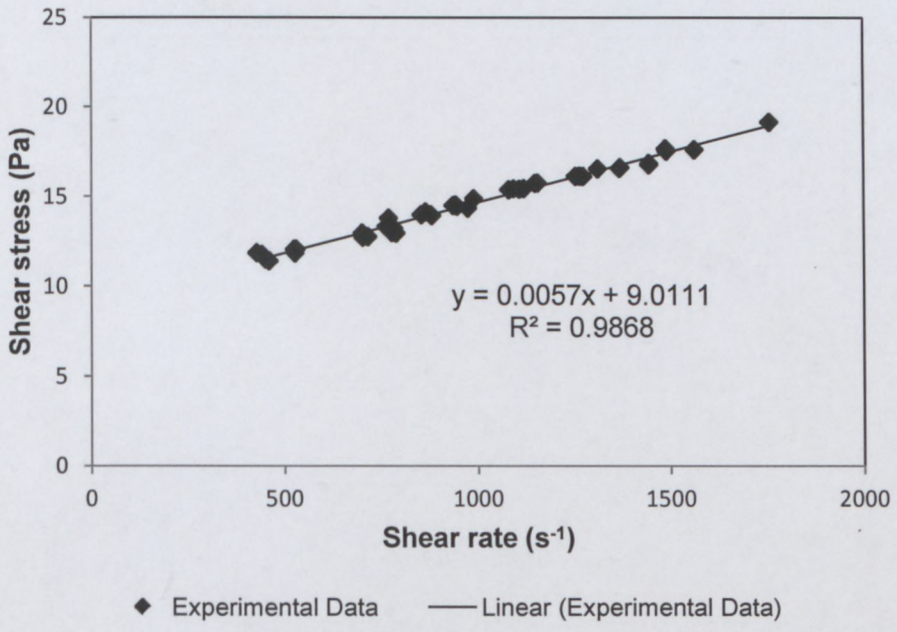

BENTONITE 8%

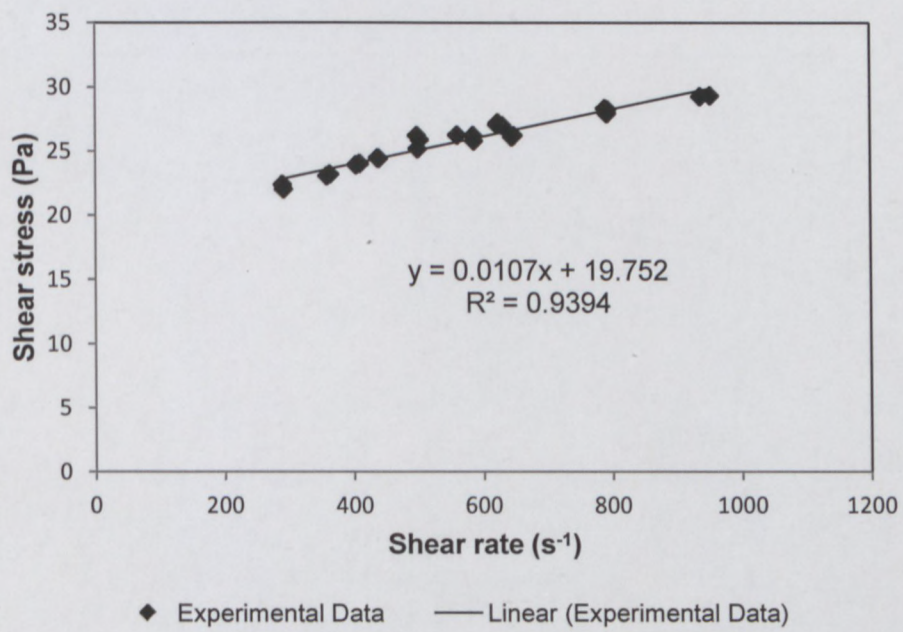

KAOLIN 13%

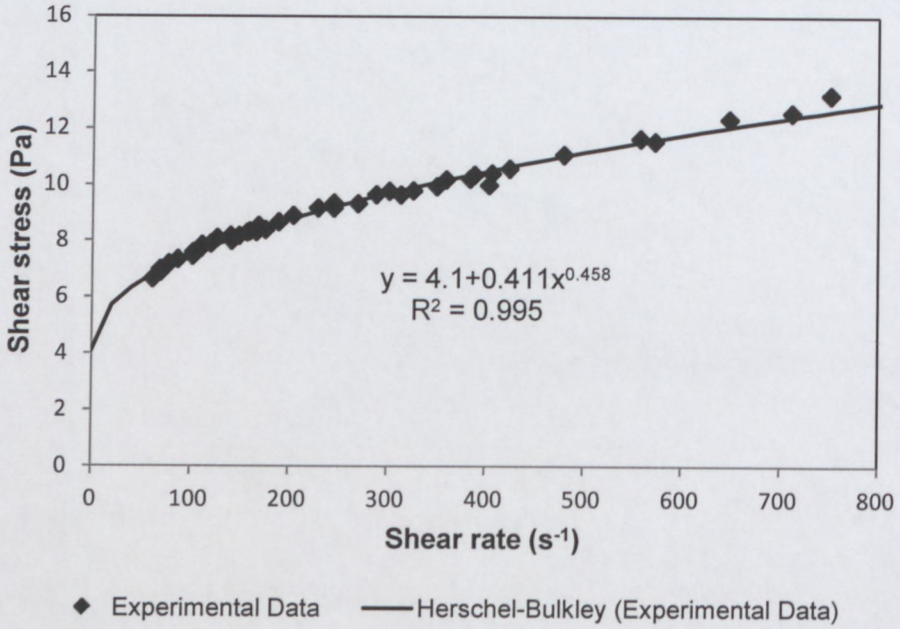

KAOLIN 17%

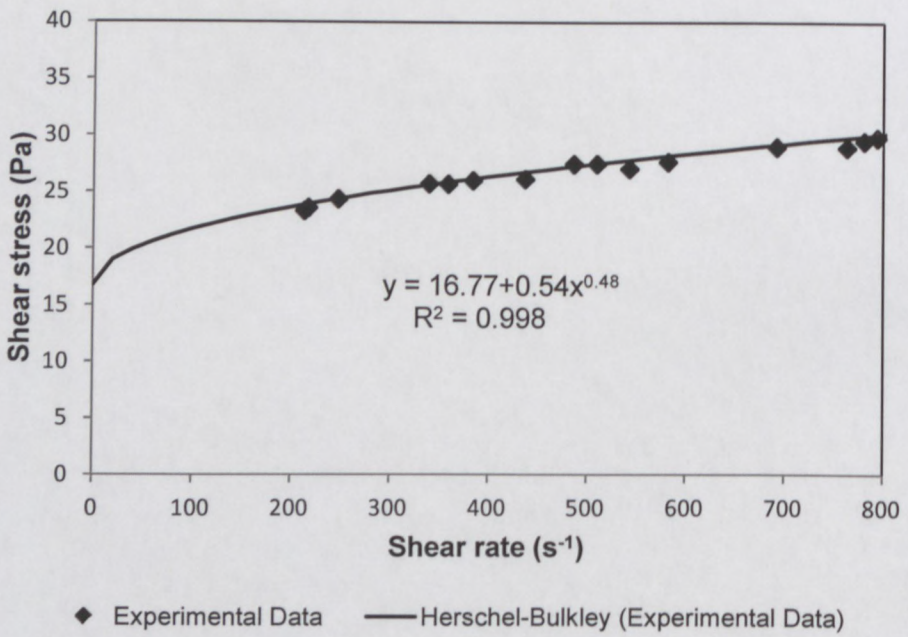

APPENDIX B

TEMPORAL FLOW BEHAVIOUR IN COMPLEX GEOMETRIES

The following is depicted in this appendix:

- The temporal behaviour of the flow in the hyperbolic contraction is depicted in Section B.1. Three positions were chosen for display as similar results were found for profiles measured along the contraction length.

- Time series plots of velocity profiles measured in the 300 mm rectangular open channel are presented in Section B.2. Only results obtained in a CMC suspension using delay line transducers are shown.

- The temporal behaviour of the flow measurements in the 50% open diaphragm valve measured using UVP are shown in Section B.3. Only results obtained using delay line transducers are shown.

Tests were done at various flow rates in laminar flow only using delay line and standard transducers. For illustrative purposes time series plots for only one flow rate and results obtained using one ultrasonic transducer (delay line transducer for valve and open channel study; standard transducer for hyperbolic contraction study) are presented in this appendix. Similar results were found for different flow rates and when using both standard and delay line transducers. Results obtained in the bentonite suspensions during the open channel study are also not included as no significant velocity variations with respect to time were observed. Therefore only results obtained in CMC fluid suspensions for all complex geometries are shown in Appendix B.1 – B.3:

Hyperbolic contraction	CMC 2.63% w/w
Open channel	CMC 4.5% w/w
Diaphragm valve	CMC 6% w/w

B.1 HYPERBOLIC CONTRACTION

POSITION *R1*

UVP PARAMETER SETTINGS AND TEST CONDITIONS

Doppler Angle (°)	PRF (kHz)	US Voltage (V)	Number of cycles/pulse	Number of pulse repetitions	Sound speed (m/s)	Gain	Flow (l/s)
15	7.024	150	2	1024	1548	7-9	0.6

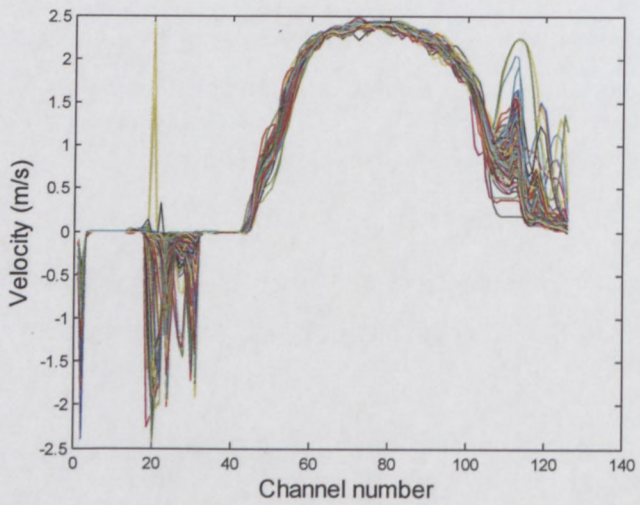

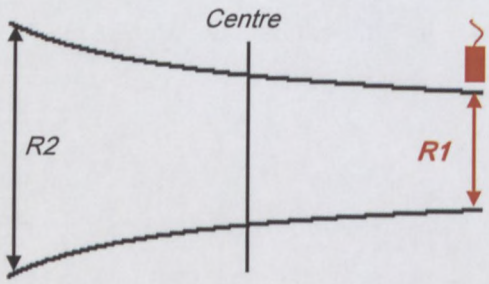

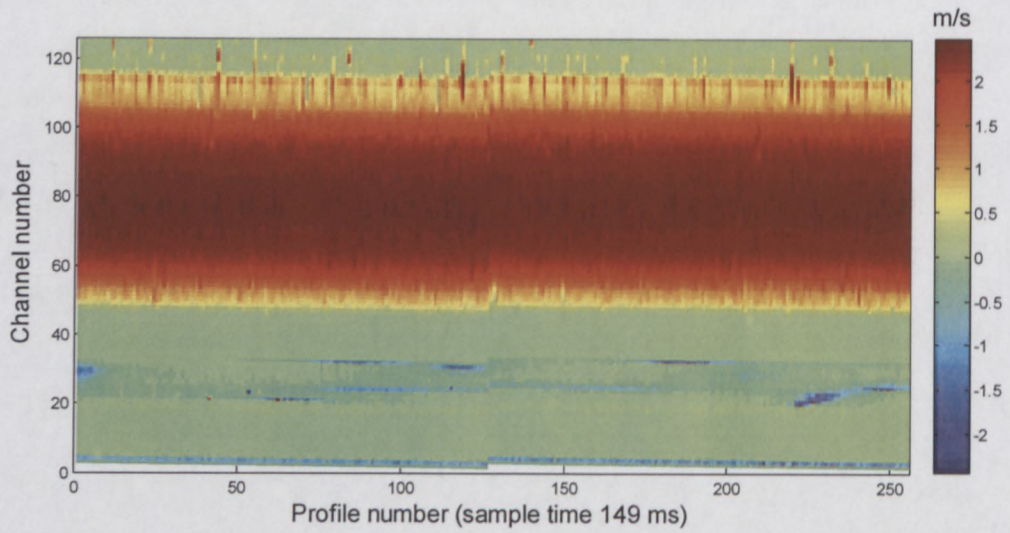

POSITION *CENTRE*

UVP PARAMETER SETTINGS AND TEST CONDITIONS

Doppler Angle (°)	PRF (kHz)	US Voltage (V)	Number of cycles/pulse	Number of pulse repetitions	Sound speed (m/s)	Gain	Flow (l/s)
15	8.12	150	2	1024	1548	7-9	0.68

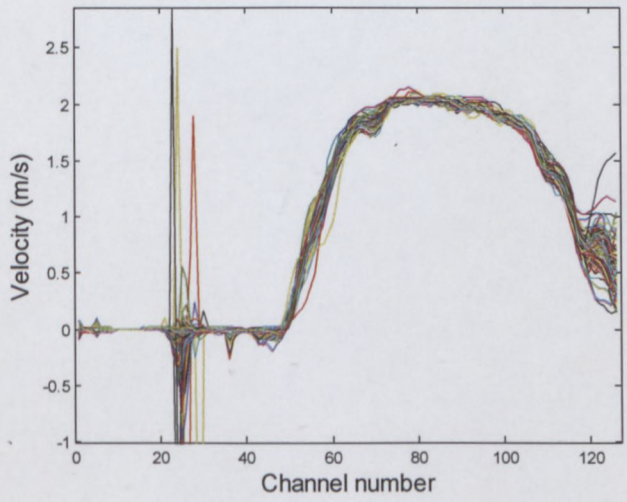

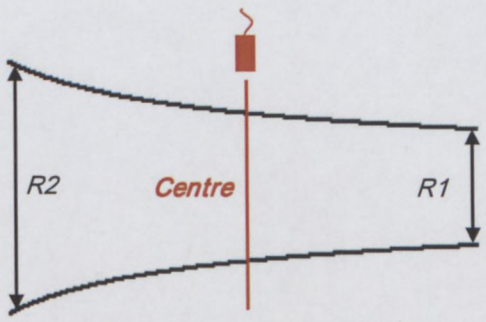

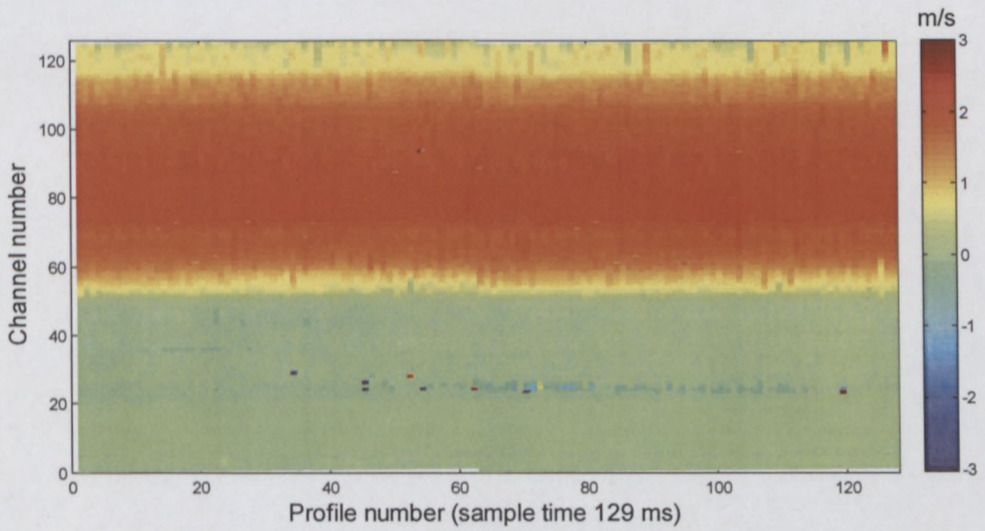

POSITION *R2*

UVP PARAMETER SETTINGS AND TEST CONDITIONS

Doppler angle (°)	PRF (kHz)	US Voltage (V)	Number of cycles/pulse	Number of pulse repetitions	Sound speed (m/s)	Gain	Flow (l/s)
15	4.58	150	2	2048	1548	7-9	0.7

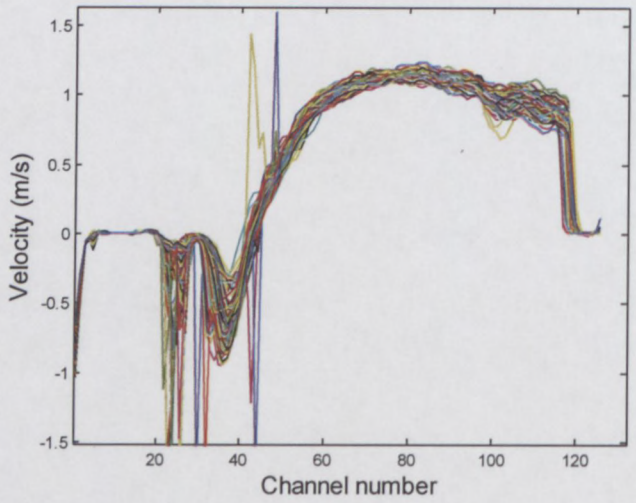

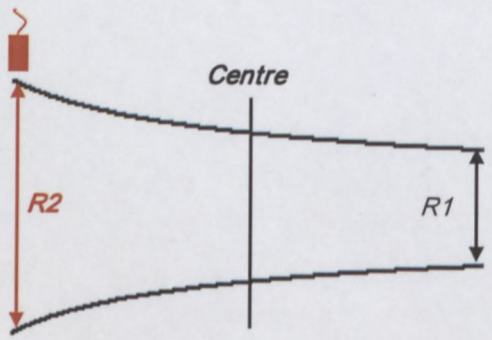

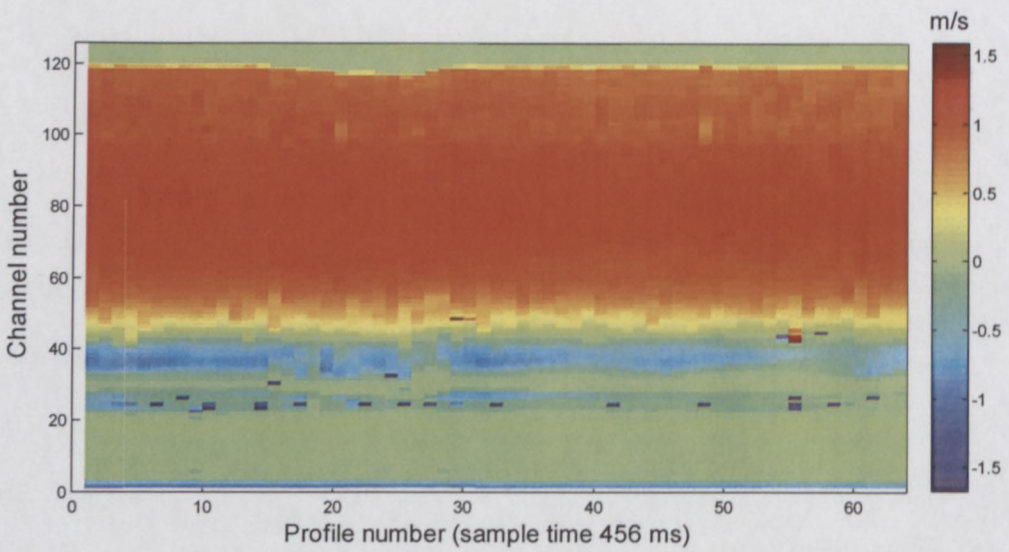

B.2 OPEN CHANNEL

POSITION *B1*

UVP PARAMETER SETTINGS AND TEST CONDITIONS

Doppler angle (°)	PRF (kHz)	US Voltage (V)	Number of cycles/pulse	Number of pulse repetitions	Sound speed (m/s)	Gain	Flow (l/s)
77.4	4.31	90	2	256	1490	5-7	10.5

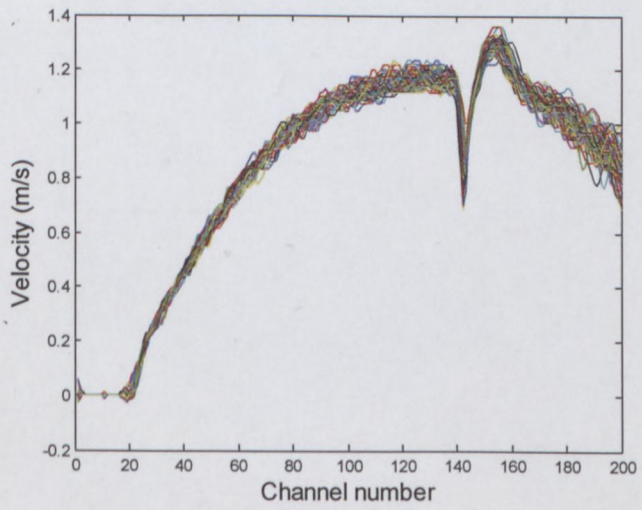

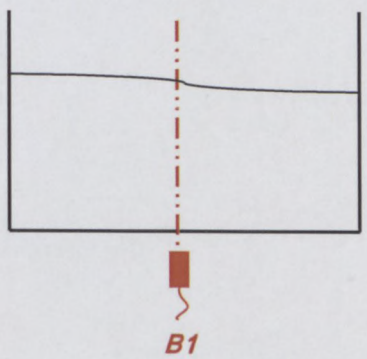

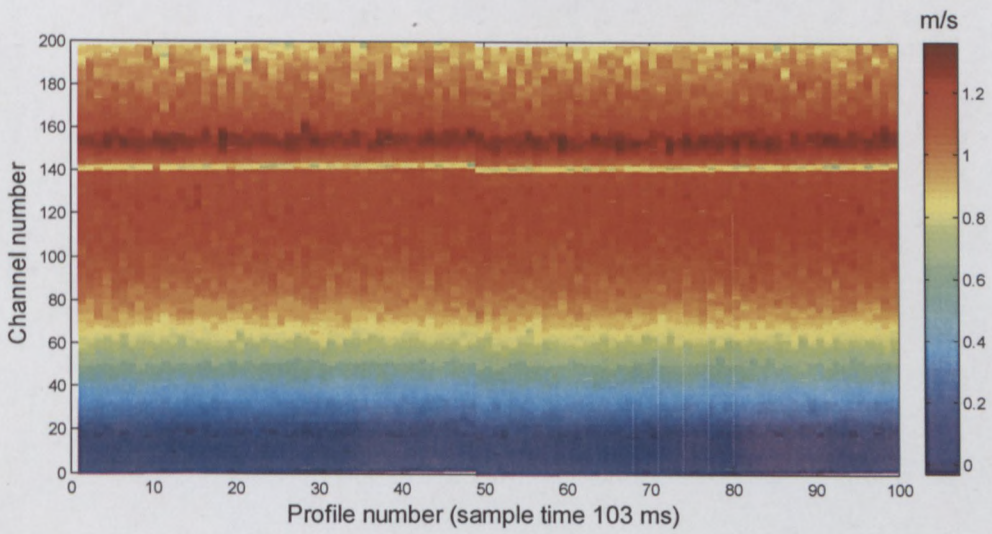

POSITION *B2*

UVP PARAMETER SETTINGS AND TEST CONDITIONS

Doppler angle (°)	PRF (kHz)	US Voltage (V)	Number of cycles/pulse	Number of pulse repetitions	Sound speed (m/s)	Gain	Flow (l/s)
77.4	4.31	90	2	256	1490	5-7	10.5

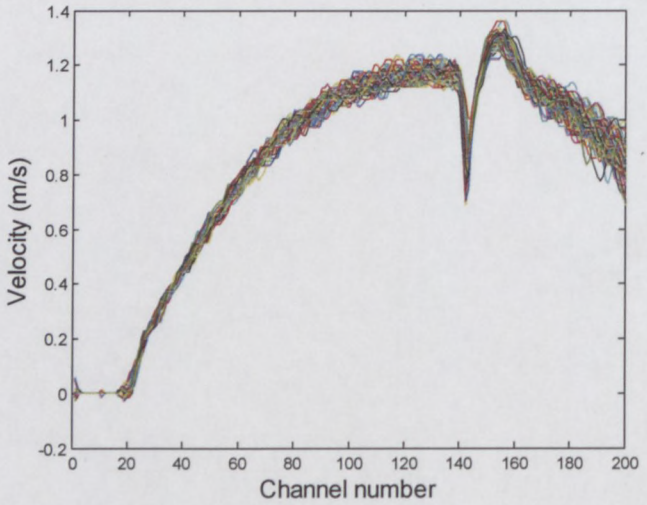

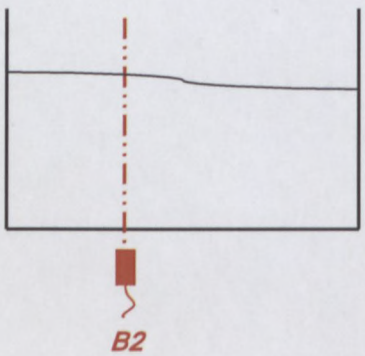

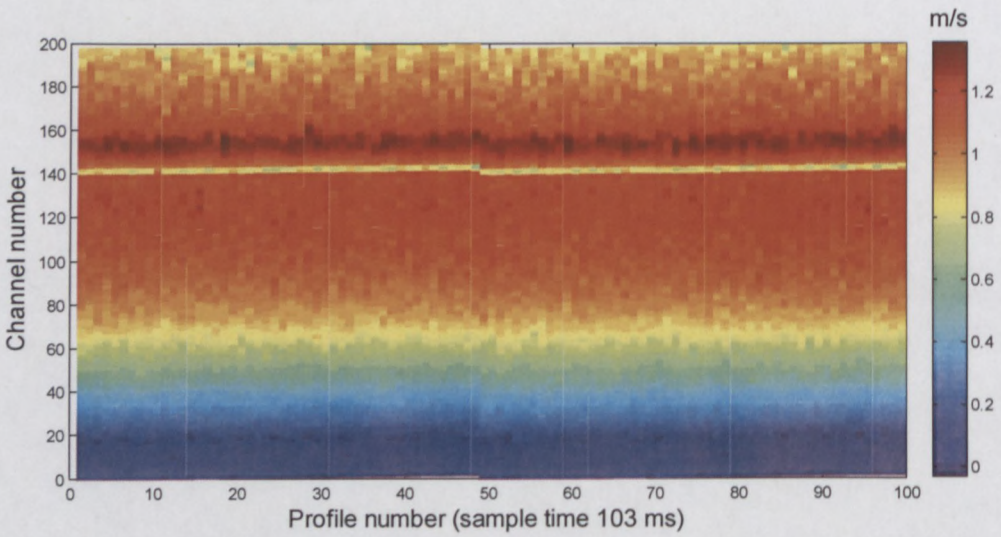

POSITION *B3*

UVP PARAMETER SETTINGS AND TEST CONDITIONS

Doppler angle (°)	PRF (kHz)	US Voltage (V)	Number of cycles/pulse	Number of pulse repetitions	Sound speed (m/s)	Gain	Flow (l/s)
77.4	4.31	150	2	256	1490	5-7	10.5

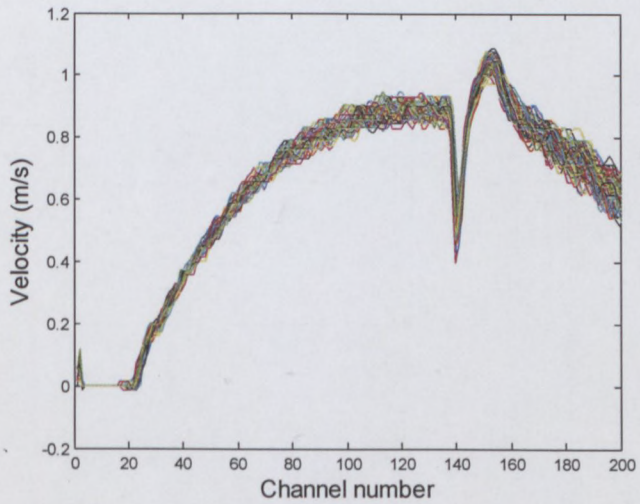

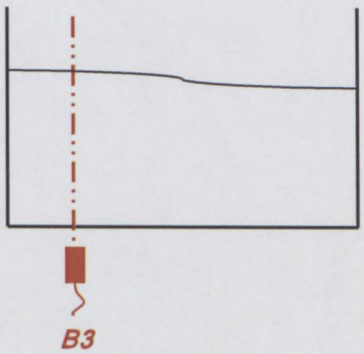

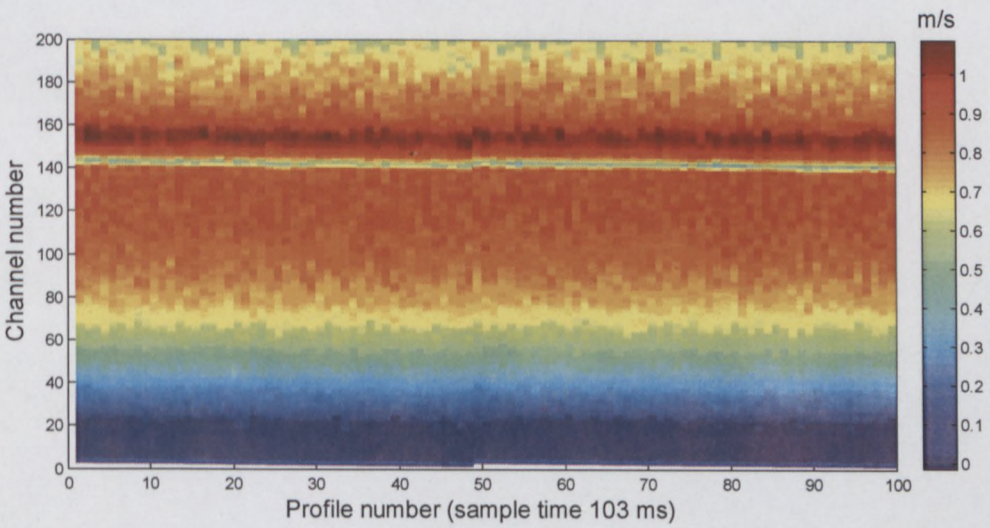

POSITION *B4*

UVP PARAMETER SETTINGS AND TEST CONDITIONS

Doppler angle (°)	PRF (kHz)	US Voltage (V)	Number of cycles/pulse	Number of pulse repetitions	Sound speed (m/s)	Gain	Flow (l/s)
77.4	2.68	150	2	256	1490	5-7	10.5

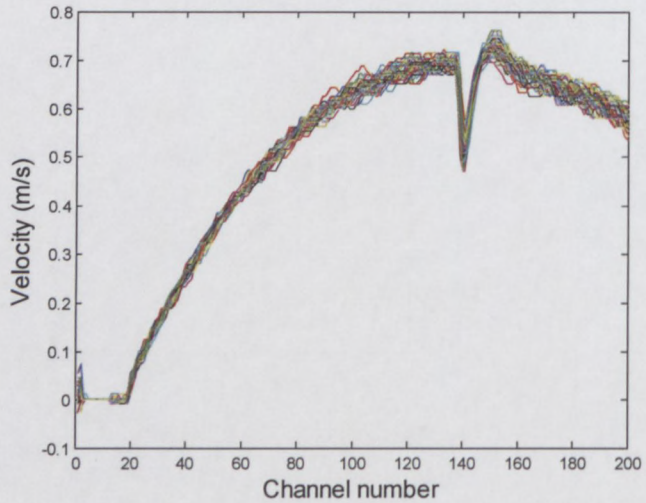

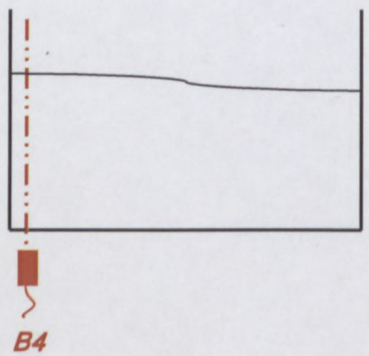

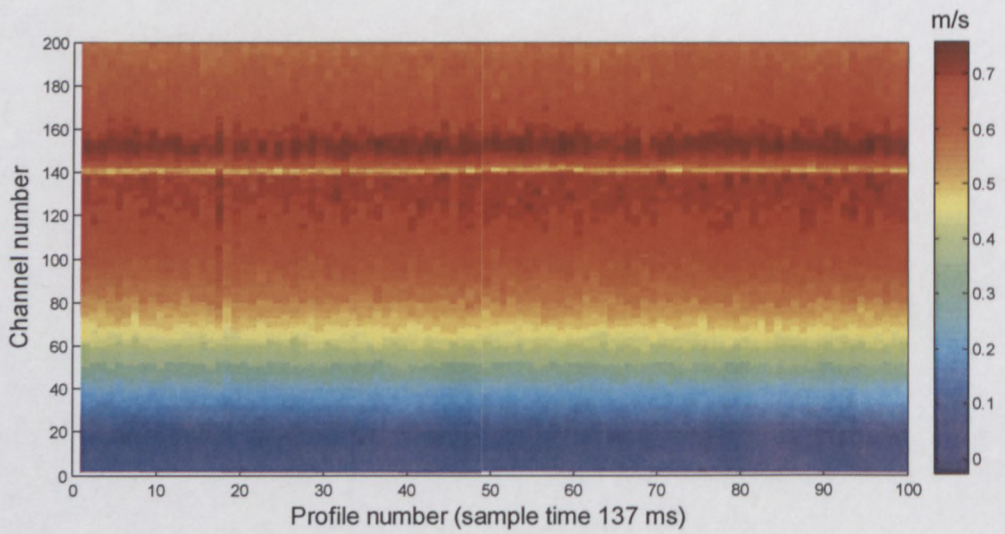

POSITION *S1*

UVP PARAMETER SETTINGS AND TEST CONDITIONS

Doppler angle (°)	PRF (kHz)	US Voltage (V)	Number of cycles/pulse	Number of pulse repetitions	Sound speed (m/s)	Gain	Flow (l/s)
77.4	2.16	150	2	256	1490	7-9	10.5

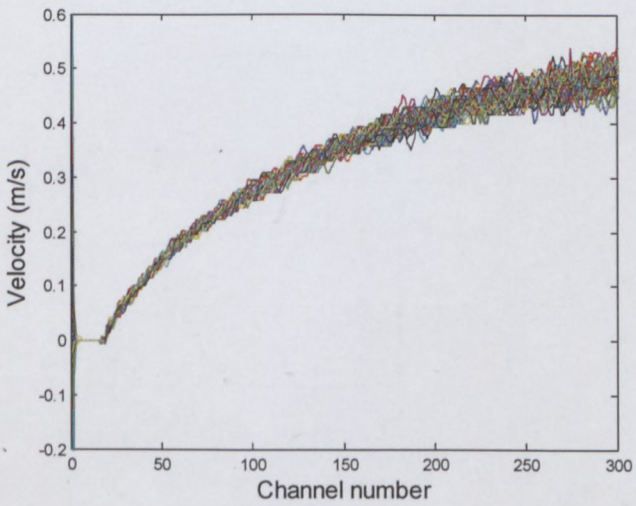

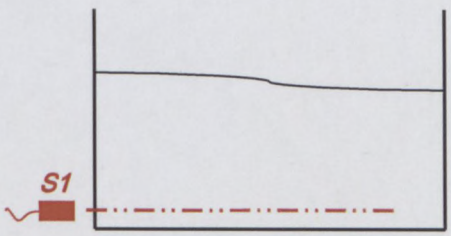

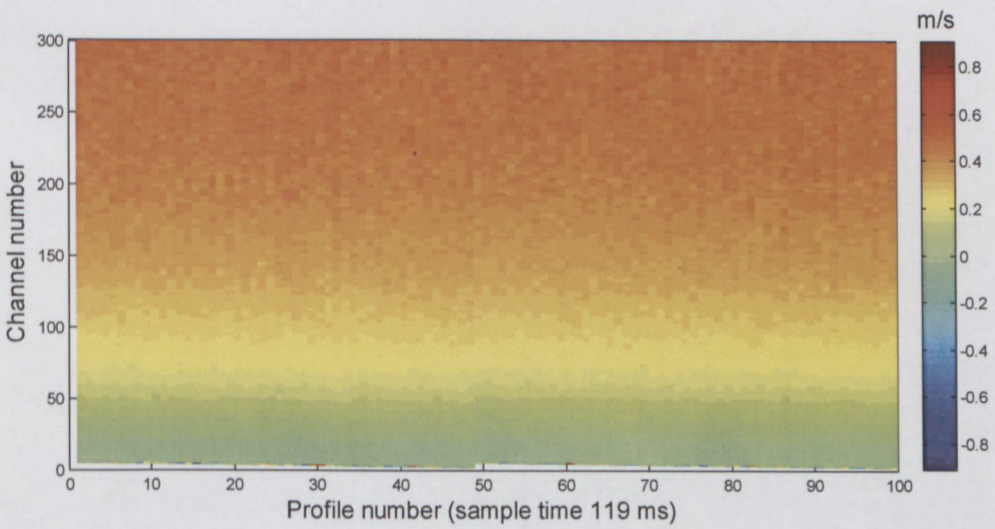

POSITION *S2*

UVP PARAMETER SETTINGS AND TEST CONDITIONS

Doppler angle (°)	PRF (kHz)	US Voltage (V)	Number of cycles/pulse	Number of pulse repetitions	Sound speed (m/s)	Gain	Flow (l/s)
77.4	3.24	150	2	256	1490	5-7	10.5

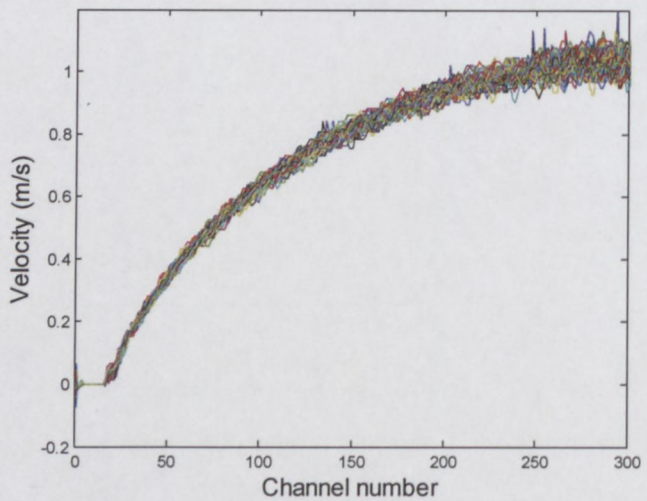

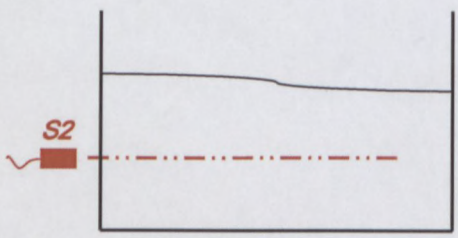

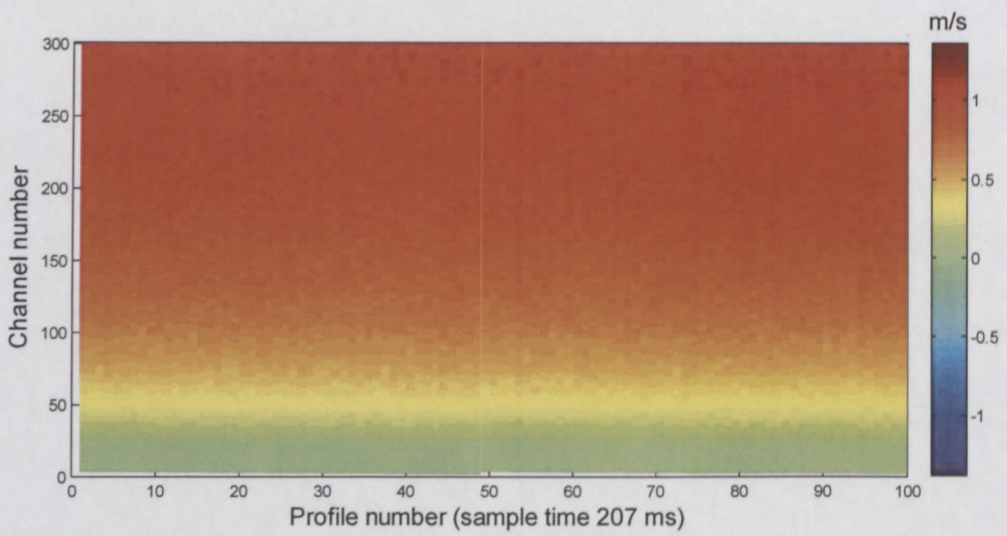

B.3 DIAPHRAGM VALVE

LATERAL POSITION

UVP PARAMETER SETTINGS AND TEST CONDITIONS

Doppler angle (°)	PRF (kHz)	US Voltage (V)	Number of cycles/pulse	Number of pulse repetitions	Sound speed (m/s)	Gain	Flow (l/s)
77.4	4.26	150	2	256	1504	5-7	1.34

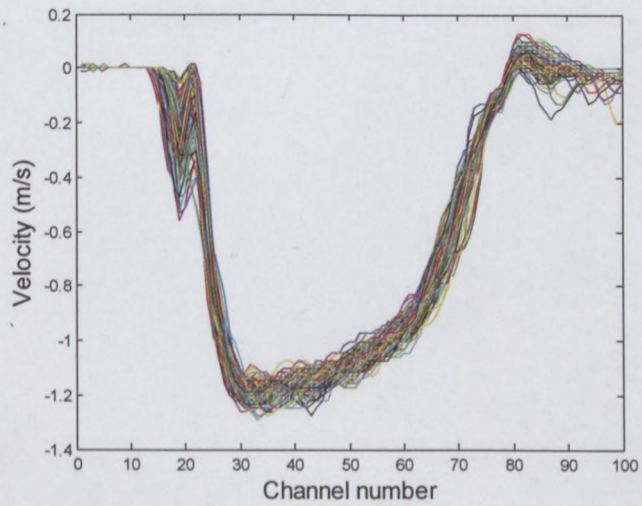

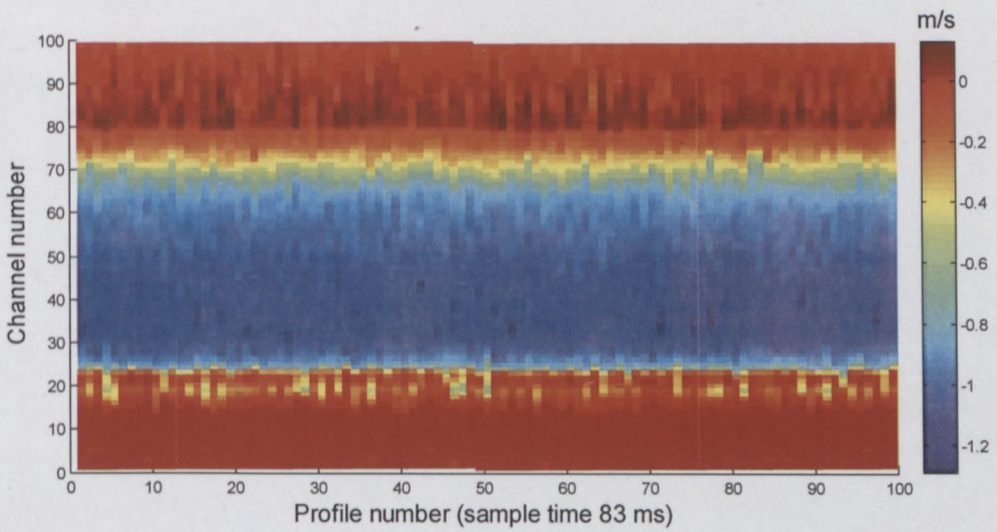

DIAGONAL POSITION

UVP PARAMETER SETTINGS AND TEST CONDITIONS

Doppler angle (°)	PRF (kHz)	US Voltage (V)	Number of cycles/pulse	Number of pulse repetitions	Sound speed (m/s)	Gain	Flow (l/s)
77.4	5.88	150	2	512	1504	7-9	1.34

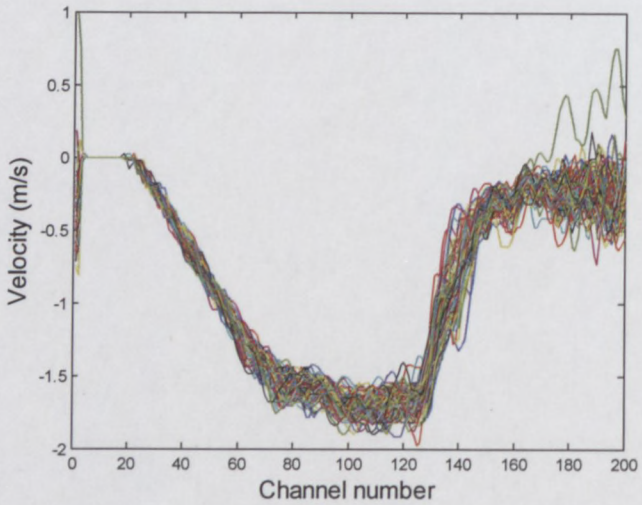

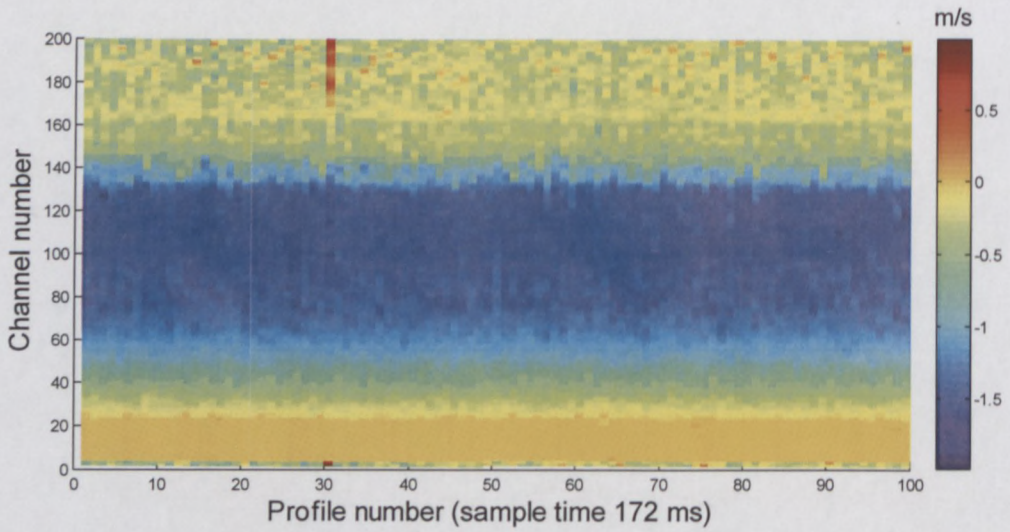

RADIAL POSITION

UVP PARAMETER SETTINGS AND TEST CONDITIONS

Doppler angle (°)	PRF (kHz)	US Voltage (V)	Number of cycles/pulse	Number of pulse repetitions	Sound speed (m/s)	Gain	Flow (l/s)
77.4	4.26	150	2	256	1504	5-7	1.34

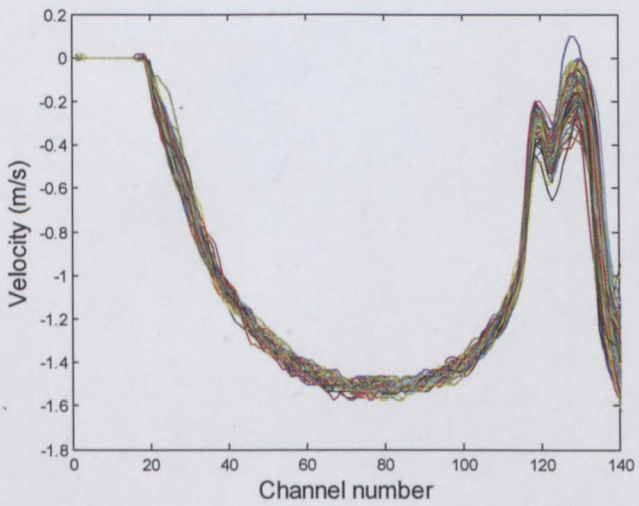

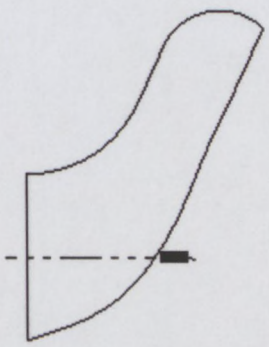

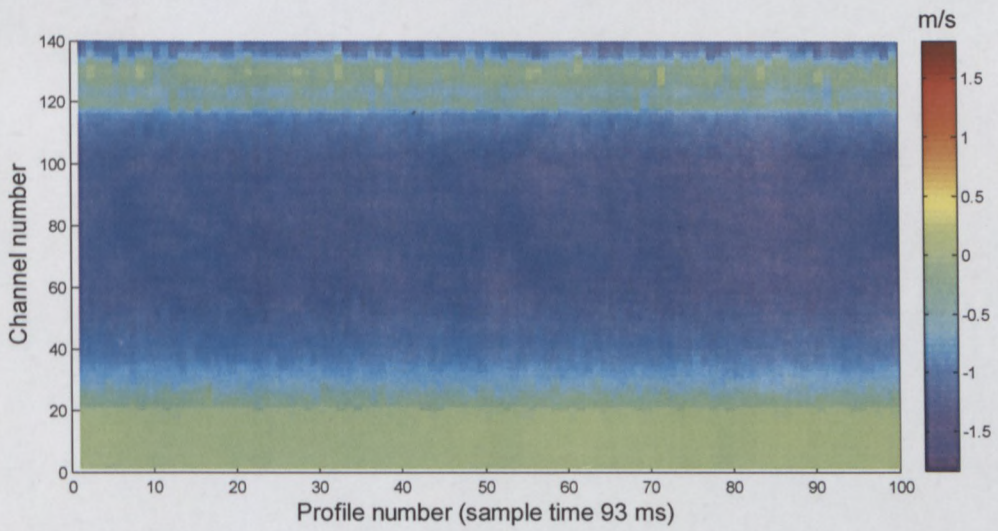

CENTRE POSITION

UVP PARAMETER SETTINGS AND TEST CONDITIONS

Doppler angle (°)	PRF (kHz)	US Voltage (V)	Number of cycles/pulse	Number of pulse repetitions	Sound speed (m/s)	Gain	Flow (l/s)
77.4	5.32	150	2	256	1504	5-7	1.34